Application of Hydrophilic Interaction Chromatography and High Resolution Mass Spectrometry in an Investigation of the LNCaP prostate cancer cell metabolome

A thesis presented by

Manal A. M. Al-ossaimi

For the degree of Doctor of Philosophy

of

University of Strathclyde

February 2015

Institute of Pharmacy and Biomedical Sciences

Department of Pharmaceutical Analysis

University of Strathclyde, Glasgow, UK.

Author's declaration

Abstract

Metabolomics can be used as an aid to functional genomics in order to investigate the functions of genes or enzymes. In the current study metabolomics was employed in the study of the response of LNCaP prostate cancer cells to sphingosine kinase inhibitors. Cell culture conditions, metabolite extraction and the LC/MS settings were optimized aiming at a reliable, unbiased, sensitive, and high throughput metabolomic protocol. Three different sphingosine kinase inhibitors were studied and reported in this work. A global metabolic profiling method based on electrospray ionisation mass spectrometry was developed for prostate cancer cells metabolites. The method involved optimizing the extraction of LNCaP cells metabolites followed by analysis using liquid chromatography coupled with high-resolution mass spectrometry (HRMS). Extraction repeatability and storage were studied and 480 metabolites were putatively identified. In the study protocol ~ 180 standard compounds from different chemical classes were also run. Five different columns were compared in terms of their performance using these metabolites in combination with MS operated in both positive and negative electrospray ionization modes. The ZIC-pHILIC column showed the best performance and the highest number of metabolites separated. An effect of storage conditions on metabolite profiles was assessed using multivariate statistics (PCA). The treatment of LNCaP and LNCaP-AI cells with 2-(p-hydroxyanilino)- 4-(p-chlorophenyl)thiazole (Ski) modulated the metabolome, with marked changes in glutathione, NADPH, pentose phosphate shunt and glycolytic metabolite levels which were indicative of a pronounced oxidative stress response and modulation of the Warburg effect. Diadenosine triphosphate (Ap3A) was not detected in LNCaP-AI but was present in LNCaP. Ap3A and diadenosine tetraphosphate (Ap4A) are novel apoptotic markers and were quantified by using tandem mass spectrometry.(R)-FTY720 methyl ether (ROME), which is a SK2-selective inhibitor, did not affect produce oxidative stress or affect the pentose phosphate pathway but increased in the levels of several lysophosphatidylinositols (Lyso PI). However, increases in phosphatidylserine (PS), sphingosine and sphinganine, hydroxysphingosine and hydroxysphinganine were marked when the cells treated with (S)-FTY720 Vinylphosphonate. In addition, it caused a fall in hypoxanthine, guanine and uridine which which may be linked with purine nucleoside phosphorylase (PNP). Cell based metabolomics provides a method for exploring the mechanism of drug action.

Publications

Papers

1- Tonelli, F., Alossaimi, M., Williamson, L., Tate, R. J., Watson, D. G., Chan, E., Bittman, R., Pyne, N. J. and Pyne, S. (2013), The sphingosine kinase inhibitor 2-(*p*-hyroxyanilino)-4-(*p*-chlorophenyl) thiazole reduces androgen receptor expression via an oxidative stress-dependent mechanism. British Journal of Pharmacology, 168: 1497–1505.

2- David G. Watson, Francesca Tonelli, Manal Alossaimi, Leon Williamson, Edmond Chan,Irina Gorshkova, Evgeny Berdyshev, Robert Bittman, Nigel J. Pyne, Susan Pyne, (2013). "The roles of sphingosine kinases 1 and 2 in regulating the Warburg effect in prostate cancer cells." Cellular Signalling 25(4): 1011-1017.

3- Tonelli, F.; Alossaimi, M.; Natarajan, V.; Gorshkova, I.; Berdyshev, E.; Bittman, R.; Watson, D.G.; Pyne, S.; Pyne, N.J. The Roles of Sphingosine Kinase 1 and 2 in Regulating the Metabolome and Survival of Prostate Cancer Cells. *Biomolecules* 2013, *3*, 316-333.

Poster

Optimization of a metabolomic method for analysis of LNCaP cell cultures using Exactive-Orbitrap mass spectrometer. Manal Alossaimi, Susan Pyne, Muhammed Alwasheh, Gavin Blackburn, Tong Zhang, Liang Zheng , David G. Watson . In Metabolomics 2013 9th Annual International Conference of the Metabolomics Society, Glasgow ,Scotland, UK.

Acknowledgement

In the name of Allah, the most gracious, the most merciful. I would like to thank following people for their contribution during my PhD:

I would like to express my sincerest gratitude to my supervisors, Dr. Dave Watson for allowing me to undertake this exciting research project under his supervision. He has provided invaluable guidance, advice and support throughout the duration of this study with his patience and knowledge for which I will always be truly grateful.

I definitely want to thank Prof. Nigel Pyne and Prof. Sue Pyne for their help and collaboration on this project and for providing the samples.

I would also like to thank all student members of the lab, past and present for their friendship, advice and grateful help that they provide to me.

My greatest appreciation also goes to my fellow friends, Dr. Haya and Dr. Sana for their invaluable advice and words of encouragement, also I will not forget my loyal friends Dr. Latefa, Reem, Seren, Tahani, Najla and Athari for their caring and especially the joy and laughter they brought to my life.

I am indebted to the Ministry of Higher Education of Saudi Arabia and Saudi Cultural Bureau in UK for the financial support and their unlimited support, encouragement and help.

I extend my warmest thanks to my parents, brothers and sisters for their encouragement and love. Finally yet importantly, a special thanks to my beloved husband, Salman for his encouragement, understanding, sacrifice and devotion to our family, and my lovely kids, Leen and Yousif, for making this and everything worthwhile.

Thanks to everyone else who I've not mentioned but who have also contributed to the completion of this thesis.

Abbreviations

AMP	adenosine monophosphate
ACN	Acetonitrile
AIPC	androgen-independent prostate cancer
API	atmospheric pressure ion source
API	atmospheric pressure ionization
Ap3A	Diadenosine triphosphate
Ap4A	Diadenosine tetraphosphate
AR	androgen receptors
ATP	adenosine triphosphate
cAMP	cyclic adenosine monophosphate
CE	capillary electrophoresis
Cer	ceramide
cGMP	cyclic guanosine monophosphate
CID	collision-induced dissociation
DHAP	dihydroxyacetone phosphate
DIMS	direct infusion mass spectrometry
BEH	Ethylene bridged hybrid
EDTA	ethylenediamine tetra acetic acid
ESI	Electrospray ionization
FTIR	Fourier transform infrared spectroscopy
GC	Gas chromatography
GC-MS	Gas chromatography Mass Spectrometry
GMP	guanosine monophosphate
GPCR	G-protein-coupled receptor
G-protein	guanine nucleotide-binding protein
GSH	glutathione
GSSG	oxidized glutathione
GTP	guanosine-5'-triphosphate
GPCRs	five specific G protein coupled-receptors
HILIC	Hydrophilic Interaction Chromatography
KEGG	Kyoto Encyclopaedia Of Genes And Genomes
LC-MS	Liquid chromatography MS
LTQ	linear ion trap
LC-MS	Liquid chromatography mass spectrometry
LOD	Limite of detection
m/z	mass-to-charge ratio
MALDI	Matrix assisted laser desorption ionization
MeOH	methanol
mg	milligram
min	minutes
ml	millilitre
mM	millimolar
MRM	multiple reaction monitoring
MSI	The Metabolomics Standards Initiative
MS2	mass spectrometry
MS/MS	tandem mass spectrometry

MVA	multivariate (data) analysis
NaCl	sodium chloride
NAD+	Nicotinamide Adenine Dinucleotide
NADH	Nicotinamide Adenine Dinucleotide reduced
NADPH	Nicotinamide adenine dinucleotide phosphate
NaHCO3	Sodium bicarbonate
NAC	N-acetyl cysteine
NP	non-aqueous normal phase liquid chromatography
NMR	nuclear magnetic resonance
PBS	phosphate buffered saline
PCA	principal component analysis
PC	Prostate cancer
ROME	(R)-FTY720 methyl ether
ROS	Reactive oxygen species
RPC	reversed phase liquid chromatography
Rt	Retention time
PNP	purine nucleoside phosphorylase
PS	phosphatidylserine
PSA	prostate-specific antigen
RSD	relative standard deviation
PZ	peripheral zone
Si OH	silanol groups
Ski	2-(p-hydroxyanilino)- 4-(p-chlorophenyl)thiazole
Sph	sphingosine
S1P	sphingosine-1-phosphate
SK	Sphingosine kinase
TOF	Time of flight
QQQ	triple quadrupole
UPLC	ultra performance liquid chromatography

Table of Content

List of tables

List of figures

Chapter1: Introduction

Introduction

1.1 Metabolomics

In the last two decades, great progress has been made in biological sciences in the various omics approaches. For instance, genomics identifies genes, transcriptomics shows the conversion of genes into RNA, proteomics indicates whether or not RNA translates to protein as well as the protein modifications taking place after translation, and finally the changes in metabolites due to the protein expression is an indication for metabolomics. Metabolomics was defined by Dunn as “the non- biased quantification and identification of all metabolites present in a biological system”. The term metabonomics is defined as the “quantitative measurement of time-related multi-parametric metabolic responses of multicellular systems to pathological stimuli or genetic modification” with some scientists arguing that the terms metabonomic and metabolomic are interchangeable (Kamleh et al., 2009) (Dunn, 2008). The samples used for studying metabolomics include microorganisms, tissues, cell culture, and biological fluids such as serum and urine (Kell, 2004). Metabolomics has been applied in many fields including agriculture, drug discovery, drug development, drug efficacy, toxicity analysis, biomarker detection and the pathophysiology of diseases (Kell, 2006). The biological chemistry variations in plant metabolomics are caused by the difficulty in managing the environment of plants such as shade and light, geographical variations and harvesting procedures. In microbial metabolomics, it is easy to control the environment and the sample repetitions but variability still exists due to the cell counts. The differences in sex, lifestyle, diet, disease state and sampling time make human metabolites the most variable. Hence, the biological variations are greater than the analytical ones (Dunn et al., 2005).

1.1.1 Analytical techniques used in metabolomic studies

Nuclear magnetic resonance spectroscopy (NMR) is a relatively insensitive and less specific technique compared to mass spectrometry. However, it is widely used in metabolomics providing complementary information to mass spectrometry. The combination of chromatographic methods with high resolution mass spectrometry is a powerful invention due to its ability to detect, under optimal conditions, the majority of metabolites predicted from the genome, at least in the case of simple organisms. The chromatography – mass spectrometry platforms, such as gas chromatography, liquid chromatography or capillary electrophoresis combined with mass spectrometry, have played a major role in the progression of metabolomics due to their high sensitivities and specificities. Chromatography-mass spectrometry platforms provide powerful techniques for the detection, quantification and identification of many metabolites. However, sample throughput tends to be slow due to long analysis times (30 – 60 min/run) (Kamleh et al., 2009, Dunn, 2008). In contrast, direct infusion mass spectrometry (DIMS) is a high throughput technique providing rapid screening of samples introduced directly into the electrospray mass spectrometer. However, it is less satisfactory for quantification and identification because of the occurrence of ion suppression and its inability to distinguish between isomers (Watson, 2010).

1.1.2 Separation methods used in metabolomics studies

The advantages of using chromatography in combination with mass spectrometry are in decreasing ion suppression effects and the ability to differentiate between isomers. GC-MS is one of the main techniques contributing to the development of metabolomics. The high resolution separation is produced by the capillary GC column. The main advantages of GC are the controlled temperature programme, which can be used to improve the peak resolution, and the fact that the electron impact spectra produced in the GC-MS mode can be matched against a wide range of libraries with the ability to recognise unknowns. Also, in GC-MS there is no solvent background as in LC–MS because the mobile phase in GC–MS is an inert gas. On the other hand, the sample introduced into the capillary GC has to be volatile which is a disadvantage of GC since not all metabolites are volatile (Kamleh et al., 2009). Another method for separation involves the coupling of capillary electrophoresis (CE) and mass spectrometry, which has been recently applied for metabolomic analysis. It is able to separate isomeric compounds and although the sample volume introduced is very small leading to lower sensitivity.

Direct analysis of amino acids, acylcarnitines, and their stereoisomers eas carried out by using a CE-MS method in an analysis of dried blood spot extracts without chemical derivatization. Detection of low-abundance metabolites in complex biological samples without ionization suppression or isomeric/isobaric interferences was shown. Also a CE-MS method was used to quantify 19 aminoacids in urinary bladder cancer patients, comparing the results with healthy subjects indicated that the concentrations of three amino acids (methionine, cysteine, and valine) were significantly lower in the urine of bladder cancer patients (Ramautar et al, 2011).

The most commonly used technique in metabolomics is liquid chromatography–mass spectrometry, which is able to analyse low molecular weight compounds in a similar way to GC-MS but also has the ability to analyse high molecular weight compounds (>600 Da) such as phospholipids, glycosides and sugars. Reversed phase chromatography (RPC) is a suitable technique for the analysis of metabolomic samples especially lipophilic compounds, because they are eluted in order of their lipophilicity, as well as most drugs in biological systems. The drawback of (RPC), however, is the presence of ion suppression and interference caused by phospholipids which are strongly retained in this mode. This problem can be solved by washing the column with a high level of organic solvent following the run. In addition, polar compounds, such as glycine and alanine, which are polar amino acids, have little retention in the RPC column, may elute at the void volume of the column, and are thus not subjected to chromatographic separation. One way to solve these problems is to use hydrophilic interaction chromatography (HILIC). The HILIC mechanism of retention depends on a water surface layer (pseudo–stationary phase) associated with a zwitterionic or polar surface coating on the column. The main advantage of the zwitterionic coating present in popular columns, such as ZICIHLIC, is its overall neutral charge and its ability to separate both positive and negatively charged molecules through charge interaction with the analyte in order to neutralize it. HILIC columns tend to be efficient because they can operate with a high percentage of organic solvent in the mobile phase leading to a decrease in the diffusion contribution to the mass transfer terms in the van Deemter equation. The ZICHILIC column can separate some compounds with good peak shapes such as AMP and NAD, whereas ATP is not eluted from the ZICHILIC phase due to its highly polar nature and probably the need for a high concentration of a counter ion such as ammonium to reduce association with sodium ions. The changes in the retention time of compounds between instruments and different fragmentation routines used in LC-MS analysis makes the building of universal LC–MS libraries very difficult, which is why such libraries have yet to become available, (Dunn, 2008, Watson, 2010).

1.1.3 Description of Some Different HILIC Columns

Reversed phase liquid chromatography (RPC) has been used since 1970, while non-aqueous normal phase (NP) liquid chromatography was used mainly in thin-layer and low-pressure column liquid chromatographic techniques. The increase of retention in the normal phase depends on an increase in the polarity of the solute and of the stationary phase and a decrease in the polarity of the mobile phase. In addition, the retention mechanism in NP using non-aqueous mobile phases is based on the competition between the compound and the mobile phase for defined polar adsorption centres on the adsorbent surface such as Si-OH groups on silica gel (Nawrocki, 1997, Snyder et al., 2011).

The term "Hydrophilic Interaction Liquid Chromatography" (HILIC) was introduced by Alpert. The term "hydrophilic" means having an affinity to water. The HILIC chromatography technique uses an NP stationary phase with an RPC mobile phase, which is more than 50% organic solvent in water. There are two reasons which have made HILIC chromatography increasingly popular: the better separation efficiency for strongly polar solutes compared to reversed-phase LC due to a less viscous organic-rich mobile phases, and the suitability of HILIC chromatography for mass spectrometry (LC/MS) where ionisation efficiency is better. Furthermore, to facilitate retention in HILIC a true mixed mode retention mechanism is used in the interaction between the analyte, the stationary phase and the mobile phase (Jandera, 2011). This is summarised in figure 1.1. The high requirement for the analysis of polar metabolites in proteomics, glycomics and in drug analysis during the last years has led to increased development of the HILIC technique (Jandera, 2011). Publication rate for applications of HILIC technique has increased between 2002 and 2010 more than 10 times with 250 papers being published up to 2010 according to a SciFinder Scholar search results (figure 1.2) (Buszewski and Noga, 2012) and the publication continues to increase, based on the numbers of publications per year, which was 1.7% higher in 2013 than in 2010[(1)].

[(1)]http://pubs.acs.org/

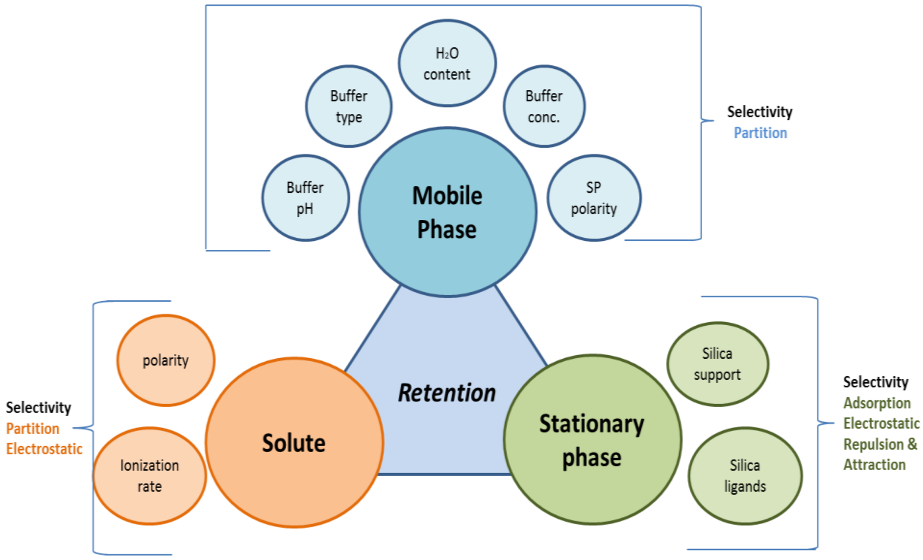

Figure1.1 Liquid Chromatography mixed mode retention on HILIC.

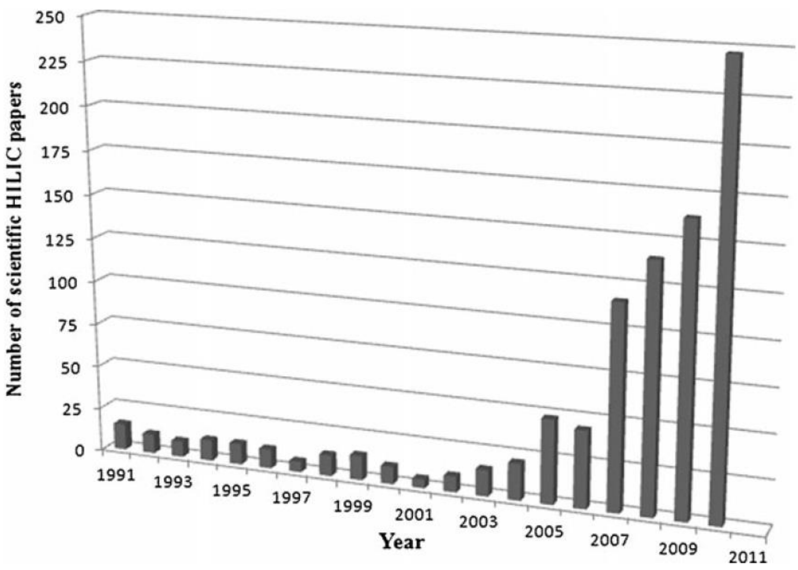

Figure 1.2 SciFinder Scholar search results documenting the continuously growing research area of HILIC, (Buszewski and Noga, 2012).

The silicon hydride stationary phase

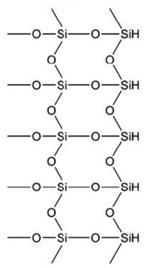

Figure 1.3 The silicon hydride stationary phase.

The use of silicon hydride (figure 1.3) as a separation material began around 1990 (Pesek and Matyska, 2012). It was assumed that the silica hydride (Si-H) functional groups were unstable but after 20 years of development it is apparent that the Si-H bond on the modified surface is stable. The TYPE-C columns surface is occupied with non-polar silica hydride (Si-H) functional groups instead of silanols, which makes the surface of silica hydride slightly hydrophobic with less attraction for water than silica, thus improved reproducibility of retention and gives some selectivity properties for HILIC separations of less polar solutes (Jandera, 2011). The free silanol groups on the surface of this phase are <2% so it does not behave like silica gel which has Si-OH groups and which has property of ion exchange interactions (Bawazeer et al., 2012).

HILIC & pHILIC Stationary Phases

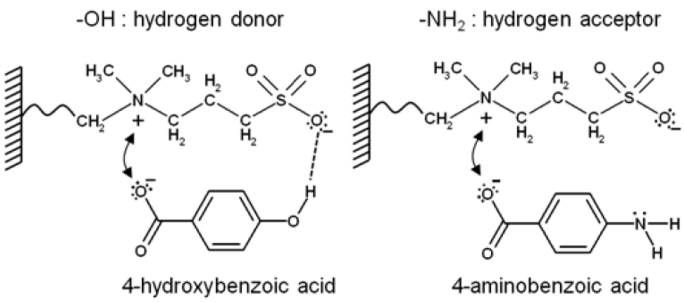

Figure 1.4 The surface ligand on ZICHILIC phases.

Zwitterionic sulfoalkylbetaine stationary phases contain equal amounts of oppositely charged groups bonded to the surface of the stationary phase in order to promote HILIC separations (figure 1.4). The active layer is comprised of both strongly acidic sulfonic acid groups and strongly basic quaternary ammonium groups separated by a short alkyl spacer. This is attached onto wide-pore silica gel (as on ZIC-HILIC) or a polymer support (as on ZIC-pHILIC) (Greco and Letzel, 2013). Ion-exchange interactions of the zwitterionic stationary phase are expected in addition to the possibility of partitioning between the water layer on the surface and nonpolar interactions with the carbon chain. In comparative studies for metabolomic applications a zwitterionic phases, particularly ZIC-HILIC, is the most commonly the column which, when evaluated, gives the best results. In previous applications ZIC-HILIC was used for targeted and non-targeted studies of fermentation broths and optimized the analytical conditions for studying the leishmaniasis parasitic disease (Buszewski and Noga, 2012, Rojo et al., 2012).

BEH-Amide Stationary Phase

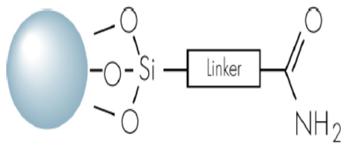

Figure 1.5 The BEH amide stationary phase chemistry.

The silica gel surface is linked via a short alkyl spacer to a carbamoyl or an amide group in these stationary phases (figure 1.5). Ion-exchange interactions do not have much effect on the retention of ionizable samples because these phases do not have basic properties. Ionic mobile phases are not essential in amide columns that thus introduce less salt into the mass spectrometer; however this might decrease the sample ionization process. Carbamoyl-silica HILIC (TSK-gel Amide-80) columns show good HILIC separations of mono- and oligosaccharides, sugar derivatives, peptides and amino acids (Jandera, 2011). The ethylene bridged hybrid (BEH) Amide column at high pH shows strong retention of polar basic pteridine derivatives under HILIC UHPLC conditions (Nováková et al., 2010). A study using some nucleutides evaluated the selectivity of three of Waters BEH stationary phases: BEH Amide, BEH Diol and BEH HILIC (uncoated silica). The BEH Amide phase was the most hydrophilic and its elution pattern was similar to the diol phase but not to the BEH HILIC phase (Guo and Gaiki, 2011).

1.1.4 Mass spectrometric Ionization Methods

There are many types of ionization techniques that can be combined with chromatography depending on the purpose of the analysis. Over the 60 years since electron impact ionisation (EI) was first invented. However, EI can only be used along with GC separation. In contrast, EI analysis in conjunction with LC–MS is not satisfactory because it is impossible to introduce solvent into the instrument and maintain high vacuum. EI produces many fragments leading to a fingerprint of the analyte which can be matched with EIMS libraries. This is the main advantage of the EI technique. Electrospray Ionisation (ESI) is the most commonly used technique with liquid chromatography. There are two ion modes of ESI; negative ion electrospray ionisation (NIESI) and positive ion electrospray ionisation (PIESI). In general, NIESI is less sensitive than PIESI. Among the compounds that can be detected in both modes are amino acids which can have a positive or negative charge. PIESI provides highly sensitive analysis of compounds containing amine groups while being unable to ionise polar acid groups such as Krebs cycle acids and neutral sugars. Such compounds, however, can be easily detected by NIESI. Many molecular ions appear with adducts of components in the mobile phase and with other abundant components in the metabolite mixture. For instance, the most common adducts in positive mode are formed with acetonitrile, methanol, ammonia and sodium, while negative mode adducts are formed with formic acid, acetic acid and chloride. Furthermore, when using a high percentage of organic solvent in the mobile phase, droplet evaporation will be enhanced and consequently gas phase ion formation, thus promoting more efficient ionisation of compounds in ESI (Kamleh et al., 2009). In contrast, the ionisation efficiency can be suppressed by environmental contamination or by the content of an abundant matrix component such as when the sample is directly infused into the instrument. In order to solve this problem it is best to combine mass spectrometry with a chromatographic system. Phosphorylated compounds including ATP, NADP and acetyl CoA are difficult to ionise by ESI. Since these compounds form strong ion pairs with ions present in biological systems, they can be suppressed under ESI although they can be ionized very well with matrix assisted laser desorption ionisation (MALDI) combined with chromatography. The disadvantage of MALDI is that it is used as a static technique and is not readily interfaced with a separation technique. This technique will become important for mapping biomarkers in tissues (Watson, 2010).

1.1.5 Ion Separation and Detection Methods

There are four steps for sample analysis by mass spectrometry. After sample introduction in the liquid or gas phase, ions are produced by the ion source. The ions have then to be separated according to their mass to charge ratio (m/z) using a mass analyser. The fourth step follows, in which the physical detection of ions takes place based on the ion current striking a photo or electron multiplier or by orbital frequencies being detected as an image current (figure 1.6). The first two steps have already been discussed and the rest will be discussed below.

Mass spectrometry has two ways of identifying metabolites via the measurement of molecular mass, which at high mass accuracy (< 1 ppm) can give a molecular formula or through the fragmentation mass spectra collection where the fragments are indicative of the molecular structure. Various different types of ion separation (mass analyser) techniques are employed in metabolomics.

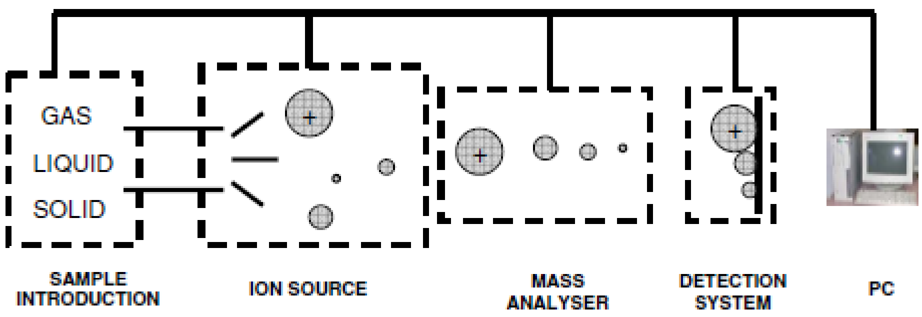

Figure 1.6 Diagram representing the mass spectrometer operating process, (Dunn, 2008).

A single quadrupole instrument gives complex data if combined with a good chromatographic system and provides a basic LC-MS system with a reasonable cost but does not deliver accurate mass measurement or fragmentation. The highest sensitivity is delivered by triple quadrupole (Tandem MS) instruments, which are extensively used to analyse drugs and their metabolites and can produce fragments. The main disadvantage of quadrupole instruments is their limited resolution which is usually around 0.5 amu. Ion trap instruments have less sensitivity than quadrupole instruments but provide multiple fragmentations and can give more details of the compound structure.

In the case of time of flight (TOF) instruments, variations in the kinetic energy of a population of ions with the same m/z led to poor resolution in early TOF instruments. The introduction of a reflectron improved the focusing of these ions. Quadrupole time of flight (QTOF) instruments deliver accurate mass data thus are recommended in metabolomic analysis. This instrument has a limitation in resolving power because resolution depends on the length of the flight tubes. TOF can also be combined with matrix assisted laser desorption ionization (MALDI) to produce a very sensitive method for the detection of proteins although it is not widely used in metabolomics. FT–ICR provides the highest mass resolution (>100,000) and mass accuracy (<1 ppm). It has a high sensitivity but ion-to-ion interaction in

FT–ICR reduces the dynamic range of the measurements, which depend on the frequency of the oscillating ions. This device is a very expensive mass analyser.

In an Orbitrap, ions are trapped due to their electrostatic attraction to the inner electrode which is balanced by centrifugal forces. Then the ions rotate around the inner electrode on oval paths. The ions also move backward and forward along the axis of the central electrode so their paths in space are like helices. First, the field between electrodes is reduced and then ions are injected from an external ion source while the electric field is increased when ion packets are injected tangentially into the field. Ions are squeezed towards the inner electrode until they reach the trap and at this time ramping is stopped and the field becomes static and detection starts. Each packet contains many ions of different velocities thus ions move with different rotational frequencies but with the same axial frequency. This means that ions of a specific mass-to-charge ratio spread into rings which oscillate along the inner spindle. Axial oscillations of the ion rings are detected by their image current induced on the outer electrode which is divided in two symmetrical pick-up sensors. The ions are detected simultaneously over a given period of time (Perry et al., 2008).

The Orbitrap was invented by Makarov (Makarov, 2000), and first introduced in 2005 by Thermo Finnegan. The mechanism of action is based on electrostatic trapping of the ions injected into the trap between an outer barrel-like electrode and an inner spindle-like electrode. The Orbitrap analyser is fed with a population of ions by a C–trap which stores the ions before injecting them in a short pulse. When the ions are exposed to axial oscillation, they generate a current image which can measure the m/z ratio following a Fourier transformation. This process is independent of energy. The Orbitrap is able to measure very low concentrations of ions (≈1 ng/ml) due to its capability to detect small changes in the current image. The trapping is independent of m/z ratio leading to a large space charge capacity at higher masses and large trapping volume, unlike FTICR instruments and Paul's trap, as well as the high mass resolution (up to 100,000). There are currently three generations of the Orbitrap in the market: the Exactive (figure 1.7) is able to measure the accurate masses but no fragmentation is produced, the Discovery measures accurate masses and produces fragmentation, while accurate masses and high/low energy fragmentations can be produced by the Orbitrap XL, (Makarov, 2000, Makarov and Scigelova, 2010). Recently a Q Exactive was introduced which is similar to the Exactive but has fragmentation capability.

The Exactive Mass Analyser is a bench-top Orbitrap instrument combined with linear ion trap technology. It has high resolution of up to 100 000, accurate mass better than 2 ppm in full scan. These specifications plus wide dynamic range and fast scanning capabilities, it can be ideally used in research, identification and quantification analysis. Moreover, this system has fast polarity switching without sacrificing mass accuracy, as one scan is gained in positive and one in negative ion modes within one second. Samples are introduced into the atmospheric pressure ion source (API) by direct infusion or via U-HPLC (Exactive PDF on World Wide Web URL).

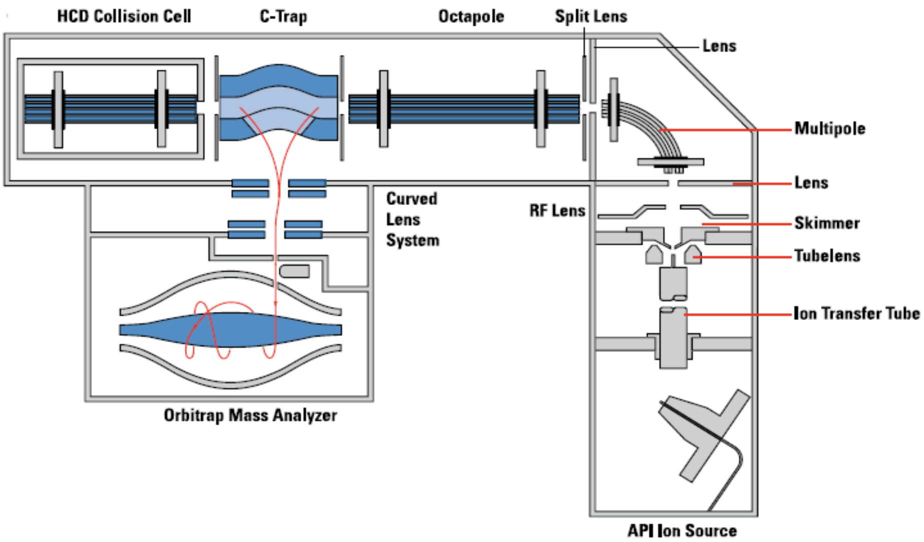

Figure 1.7 Diagram of the composition of an Orbitrap Exactive Instrument (Exactive PDF on World Wide Web URL, 2008)

1.2 Data Extraction and Processing

After LC/MS data collection, the raw data (which are often signals from different metabolites) were converted to appropriate format for data analysis (Hendriks et al., 2011). The LC/MS data of a single sample are in the form of a 3D-matrix (m/z .retention time. intensity), which is processed using a range of software to deconvolve into a matrix of detected peaks plus sample identification (ID), with peak response for metabolites determined. This strategy assists in aligning retention time and accurate mass drift due to the order in injections; similarly, every chromatographic peak in each sample has the same parameter for identification (Dunn et al., 2011). Several types of software can used for data preprocessing, e.g., Waters MarkerLynx, ThermoFisher SIEVE, Agilent MassHunter, Shimadzu Profiler AM, ThermoScintific ToxID and LECO ChromaTOF, which are available from instrument companies (Dunn et al., 2011) or XCMS (Smith et al., 2006), MZmine (Katajamaa et al., 2006), mzMatch (Scheltema et al., 2011) and IDEOM (Creek et al., 2012), which are freely available software. We used Sieve and Sieve extractor, XCMS, mzMatch, IDEOM and ThermoScintific ToxID softwares in our projects.

1.2.1 Sieve and mzMatch

Metabolomic approaches produce massive quantities of data and these data should be processed using commercial or non-commercial software in order to have clear metabolite identification which is followed by interpretation. SIEVE is one of the commercial software programmes. It is automated software package which carries out comparative analyses of sample populations. It compares the raw data from LC/MS of control and treatment samples to detect the changes in two sample sets, which may indicate differential protein expression. In a single experiment, Sieve can analyze about 100 LC/MS data files and as a minimum four in which half sample files are controls and the other half are treatments. It depends on the MS intensity to calculate the statistical differences (SIEVE User Guide pdf, 2007). It uses ChromAlign for chromatographic alignment (Katajamaa and Orešič, 2007). The drawbacks of Sieve are that it analyses only two sets comparing control and treatment and it is expensive software, not free online. In addition, the volume of redundant data which SIEVE generates takes a long time to sort out and remove the background noise. MzMatch is an open source and platform software. Raw LC-MS data are processed with conversion of instrument-specific data format to XCMS Centwave for peak picking and mzMatch is used for noise filtering, peak detection and alignment, then identification is done by IDEOM. mzMatch is applied in R statistical language (Katajamaa and Orešič, 2007). In a single experiment mzMatch can analyze more than 100 LC/MS data files with many groups of experiments to compare more than two sets. Database retention time updated in each experiment by RT calculater uses the Quantitative Structure Retention Relationships (QSRR) approach to predict retention times based on the known retention times of authentic standards and the physicochemical nature of the interactions of analyte with columns that determine retention (Creek et al., 2012).

Quantitative structure–retention relationship (QSRR) is a technique capable of improving the identification of a compound by predicting its retention time and when it is analyzed by liquid chromatography. It is aims to predict the retention for solutes by identifying the most important structural descriptors relevant to the retention behavior of the solute coupled with an understanding of the molecular mechanism of separation operating in a given chromatographic system (Goryński et al., 2013). The molecular descriptor is the final result of a logical and mathematical procedure which transforms chemical information encoded within a symbolic representation of a molecule into a useful number (theoretical descriptor), or as the result of some standardized experiment (experimental descriptor). The simplest classification of molecular descriptors into groups is based on the nature of the descriptor (whether it is theoretical or experimental). Theoretical molecular descriptors are further classified; the first class is derived from the chemical formula and the information considered is the number and type of atoms, the molecular mass, any function of atomic properties. A second class representation of a molecule consists of a list of molecular fragments (functional groups, substituents, etc.) and counts descriptors of functional groups, rings and bonds. A third class contains topological information which describes how the atoms are bonded in a molecule. Other groups of theoretical descriptors are calculated which are geometrical. Finally the fifth class descriptors are derived from a stereo-electronic or lattice representation of the molecule (Du et al., 2009).

1.2.2 Simca P

A chemometric method for supervised classification of data as soft independent modeling of class analogy (SIMCA) Software is useful in metabolomics studies and for mathematical purposes (Umetrics, SIMCA-P). It is user-friendly and it was developed by Umetrics. SIMCA-P is particularly designed for chemometrics, which focuses on principal components Analysis and partial least square (PLS) regression. The operation of models in this software is very easy to work on and the result simply elucidated by plot and list, which explain the reading of the model in forms. SIMCA-P is a popular tool used by many researchers in many scientific fields (Wu et al., 2010). Its aim is to reduce dimensionality of datasets and provide better visualization and it reveals relationships between datasets (Cubbon et al., 2010). It can be simply used by uploading Excel spreadsheets derived from the output of mzMatch or Sieve.

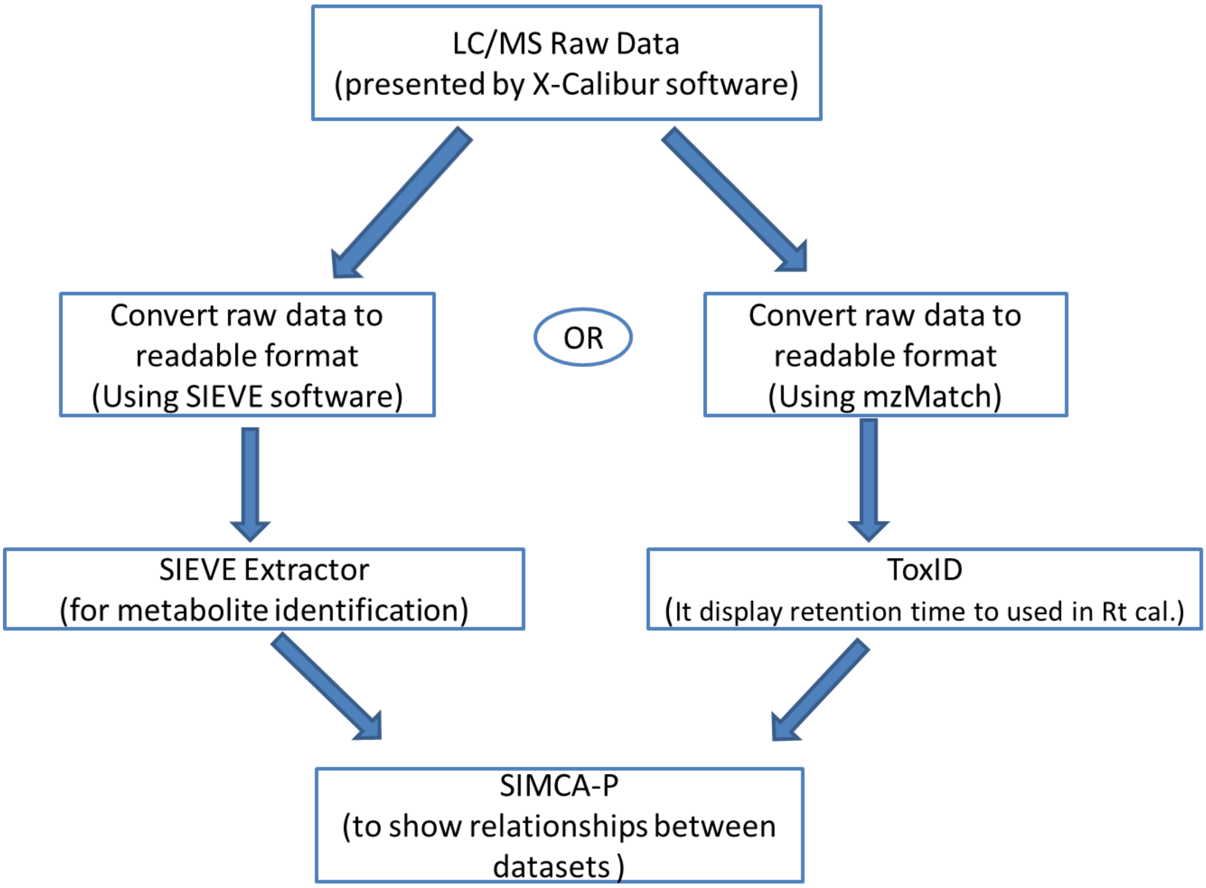

Figure 1.8 Flow chart of data analysis.

1.3 Applications of metabolomics in cancer research

1.3.1 Using metabolomics in oncology

The early stage detection of cancers plays a key role in improving survival rates and reducing mortality rates. For instance, an improvement of up to five years can be achieved in the survival rates of ovarian cancer patients if diagnosed early enough (Rein et al., 2011). In order to decrease the morbidity and mortality associated with various cancers, a novel technology for early diagnosis of the disease or tumour stage was used. A variety of tumour biomarkers were determined through the use of genomic, proteomic and metabolomic technologies (Tainsky, 2009). Expanding the use of metabolomics is continually supported by academics, the National Cancer Institute, field specialists and industry. In addition, more consideration is being given to Magnetic resonance spectroscopy imaging (MRSI) to evaluate the therapeutic response (Evelhoch et al., 2005). A combination of analytical techniques is used in chemical profiling for metabolomics which analyses small molecule metabolites (Tainsky, 2009). Variations in the glycolytic pathways, apoptosis, and phosphometabolic changes provide a good visualisation of the cancer progression (Mazurek and Eigenbrodt, 2002). As well as detection of alterations in the metabolic profile, metabolomics can find more specific biomarkers related to the carcinogenic stage, grade, response to the treatment, and prognosis which are integrated by metabolomics and other omics technologies (Tomlins et al., 2006). Glunde and Serkova stated that choline phospholipid metabolism intermediates might be considered as possible biomarkers for monitoring the treatment efficacy of different cancer cases (Glunde and Serkova, 2006). As a response to the chemotherapy or radiation, a reduction in the signal of the total choline on ^{1}H-NMR was discovered in breast and prostate cancers, brain tumours, and non–Hodgkin's lymphoma as an early marker (Spratlin et al., 2009). This could also provide a good assessment of the prostate cancer stage and aggressiveness that can be determined after prostatectomy (Cheng et al., 2005). Ultrasound, tumour markers, or both can be used as early diagnosis and for production of an effective plan of treatment for cancer cases (Jacobs et al., 1999).

In cancer cell metabolomics cells, fluids, and tissues, either *in vitro* or *in vivo*, have been used to analyse the metabolites. The easiest sample preparation in the biochemical analysis is biofluids (serum, plasma, urine, ascitic fluid, saliva, prostatic secretions, or fecal water). The most commonly used samples in tumour biochemistry are serum and urine samples which are easy to prepare. On the other hand, direct use of malignant tissue in metabolomics trials is difficult in the preparation due to tissue heterogeneity and contamination from adjacent stromal and epithelial cells. This plus the difficulty associated with sample-to-sample variation and sensitivity, mostly for extraction-dependent MS-based techniques (Spratlin et al., 2009). The challenges in the metabolomics study are metabolite normalisation, data interpretation, and statistical analysis of the whole batch of trial. If any of these parameters is altered, the results will change even though the raw data remains the same (Roberts et al., 2011).

1.3.2 Cancer diagnosis and treatment.

Many kinds of experimental plans for the omics technologies have been used to detect tumours and diagnose different types of cancer. In the analysis of breast biopsy trials, more than thirty endogenous metabolites were found in breast tumours using NMR. A comparison between breast cancer and benign tumours or healthy tissues showed an increase in the total choline levels and a decrease in both glycerophosphocholine and glucose levels. These make the application of metabolomics most suitable in breast cancer diagnosis as opposed to other cancers (Bathen et al., 2007, Glunde et al., 2004). When the MRSI of the breast was carried out on patients, the differentiation between malignant and benign tissue was 100% sensitive *in vivo* based on choline detection (Spratlin et al., 2009). The metabolic profile of prostate cancer showed distinctive metabolites, which were marked with high levels of total choline and phosphocholine accompanied by an increase in lactate and alanine (Swanson et al., 2006). An elevation in spermine and a decline in citrate levels, when compared the prostatic fluid of prostatic cancer patients with non-cancer men, was shown using ^{1}H-NMR (Serkova NJ, 2007). The low molecular weight metabolites, which are created by the cell, can be identified and quantified by metabolomics (Roberts et al., 2011). Prominently, total choline (tCho) was determined in breast, prostate, and brain tumours via MRSI, (Howe et al., 2003, Stanwell et al., 2005). Furthermore, lipid metabolic profiles differentiate between cancer patients and controls with an 83% accuracy via the analysis of blood samples using NMR-based metabolomics, (Spratlin et al., 2009). In prostate cancer, sarcosine is a potential biomarker that has been detected with the increase in amino acid and nitrogen breakdown, (Burton et al., 2010). Despite these achievements, there is a lack in knowledge of the metabolomes in tumours. Moreover, it is difficult to generalise the result across tumour types due to the wide variety of metabolite profiles which includes alanine, citrate, glycine, lactate, nucleotides, and lipids (Griffin and Shockcor, 2004).

1.3.3 The Warburg Effect

In 1956 Otto Warburg demonstrated metabolism changes in cancer cells and then he described his observations which were high rates of glucose uptake and lactic acid production in cancer cells. Also he found that cancer cells preferred aerobic glycolysis to oxidative phosphorylation because cancer cells did not consume more oxygen than normal tissue cells. Normal cells depend on mitochondrial oxidative phosphorylation to generate the energy needed for cellular processes while most cancer cells rely on aerobic glycolysis which is an inefficient way of generating adenosine 5-triphosphate (ATP). In the presence of oxygen, most differentiated cells primarily metabolize glucose to carbon dioxide by oxidation of pyruvate in the mitochondrial tricarboxylic acid (TCA) cycle. This reaction produces NADH which then fuels oxidative phosphorylation to maximize ATP production, with minimal production of lactate. It is only under anaerobic conditions that differentiated cells produce large amounts of lactate. In contrast, most cancer cells produce large amounts of lactate regardless of the availability of oxygen and hence their metabolism is often referred to as "aerobic glycolysis." Warburg originally hypothesized that cancer cells develop a defect in their mitochondria that leads to impaired aerobic respiration and a subsequent reliance on glycolytic metabolism (Wu et al., 2013).

1.3.4 Applications of metabolomics in prostate cancer

1.3.4.1 Prostate cancer

Burton and his colleagues defined prostate as "a male accessory sex gland situated at the base of the bladder surrounding the urethra. Its function is to produce several components of semen that aid sperm survival, function and motility". Prostate cancer is the second important cause of cancer death in American men and an estimated 33,720 deaths and 240,890 new cases occured in the US during 2011. About 97% of all prostate cancer cases are diagnosed in men 50 years of age and older. It accounts for an estimated 29% of all new cancer cases (Cancer Facts & Figures, 2011). According to Cancer Research UK incidence statistics used 2008 data; there has been a huge rise in prostate cancer incidence over the last 20 years. It is the most common cancer in men and it accounts for nearly a quarter (24%) of all new male cancer diagnoses in the UK. There were 37,051 new cases diagnosed in the UK, which is around 101 men every day or one man every 15 minutes[2]. An increase in the rate of mortality is associated with obesity and smoking (Cancer Facts & Figures, 2011).

The treatments of prostate cancer vary depending on age, stage, and grade of the cancer. For those with metastatic disease, androgen blockade therapy is the most effective form of systemic therapy, and it produces an ideal response in 80% of patients which results in cancer cells dying. However, these cures are temporary because the surviving cells can transform into androgen-independent (AIPC) prostate cancer within 6–18 months and deaths occur in the majority of these cases (McGarvey et al., 2001). Increasing cell proliferation and decreasing apoptosis of prostate cancer cells were associated with androgen independent progression (Zhou et al., 2004). The mechanisms for transformation of androgen-dependent prostate into androgen-independent prostate cancer (AIPC) are not completely understood. The mechanisms leading to androgen-independent prostate cancer (AIPC) may include 1) Pre-existing genetic changes in prostate cancer stem cells; (2) oncogenes and the inhibition of apoptosis; (3) ligand-independent AR activation; (4) AR hypersensitivity;(5) AR mutations that lead to a change in the specificity of AR; (6) gene fusions; and (7) androgen synthesis in androgen-independent prostate cancer (AIPC) tissues. Extensive research will be required in order to understand the characterization of signalling pathways and their molecular mechanisms. That will clarify the prostate cancer pathology and will be useful to develop effective therapies and to find out new drug targets (Schröder, 2008).

1.3.4.2 Factors affect prostate cancer progression

There are many studies proving that the advancement and aggressiveness of prostate cancer is affected by several environmental factors. There is a link between the metabolic sequels of a Western lifestyle, such as obesity, insulin resistance and abnormal hormone production, and prostate cancer progression through several overlapping pathways (Burton et al., 2010). Age is the most important factor in prostate cancerous progression as the risk of developing prostate cancer increases sharply after middle age. Another major factor that affects the prostate cancer progression significantly is ethnicity. Around 2 out of 3 prostate cancer cases in the USA and UK are expected to be black as opposed to white (Ben-Shlomo et al., 2008). A relation between body mass and the advancement, aggressiveness and/or fatality of the prostate cancer was investigated in many studies (Wallström et al., 2009).

1.3.4.3 Detection of prostate cancer via metabolomics

Metabolomics has been used as a novel method in the early detection of prostate cancer in order to enable early intervention and treatment due to its capability to monitor the alteration in metabolic characters, which imitate the modifications in phenotype and its functions, (Roberts et al., 2011). Physiologically, the peripheral zone (PZ) of the prostate is considered to have the main function with a volume of (70%) and has a major tumor rate of 85%, (Costello and Franklin, 2008). The prostatic fluid is produced, stored, and secreted by the PZ epithelium and contains citrate, polyamines (spermine & myoinositol), and prostate-specific antigen PSA, (Teahan et al., 2011). The citrate in normal cells is converted to isocitrate via the m-aconitase enzyme in the Krebs cycle. In prostate cells the m-aconitase activity is inhibited by the extremely high zinc level which allows the accumulation of citrate in the peripheral zone (PZ). As a result, the uncompleted Krebs cycle leads to a decrease in the production of ATP and an increase in the level of glucose and aspartate required by PZ cells. In contrast, when the PZ epithelial cell fails to accumulate zinc, i.e. there is a decline in the zinc concentration, the m-aconitase enzyme converts the citrate to isocitrate and the Krebs cycle concludes by producing 24 molecules of ATP during the oxidation of glucose and oxidative phosphorylation as shown in figure 1.8. Therefore, normal PZ epithelial cells are not capable of producing bioenergy as well as prostate cancer cells (Roberts et al., 2011). Prostate cancer shows an increase in choline and creatine levels due to the rise in cell proliferation, which increases the membraneogenesis and choline metabolites,

---

(2) http://info.cancerresearchuk.org/cancerstats/types/prostate/incidence/

(Noworolski et al, 2008). A further reduction in citrate levels was detected as a result of its utilization in the membraneogenesis of malignant cell proliferation (Costello and Franklin, 2008). The levels of zinc and citrate determine the aggressiveness of the prostate cancer because they are normally too insignificant to detect in weakly discriminated prostate cancer tumours, (Roberts et al., 2011).

Sarcosine is considered as a potential biomarker for prostate cancer. It was detected in urine samples using LC-MS/GC-MS as a method for the diagnosis of prostate cancer (Sreekumar et al., 2009). The elevation of the sarcosine level in 42% of prostate cancer samples and 79% of metastatic samples was observed in a study by Burton which indicated its possible role in the progression of prostate cancer (Burton et al., 2010). In Sreekumar's research, sarcosine was found in a tissue associated with prostate malignancy and metastatic potential. When sarcosine was introduced to a prostate epithelial cell culture, a malignant modification was induced. The differentiation between PC-positive and PC-negative biopsy patients was shown using sarcosine/alanine ratios in the sediment of urine and sarcosine/creatinine ratios in the supernatants of urine. However, the level of sarcosine/alanine ratios in urinary supernatants or serum is not correlated with the biopsy grade (Sreekumar et al., 2009).

In conclusion, the comparison of healthy prostate, benign prostatic hyperplasia BPH tissue, and prostate-specific biofluids, resulted in the marking of the prostate cancer with high levels of lactate, choline, and creatine and the low levels of citrate and polyamines (Spermine, myo-inositol) levels (Roberts et al., 2011). Metabolomics has recently emerged as a valuable tool in the early detection of prostate cancer, (Sreekumar et al., 2009). Research work is continuing with the aim of discovering more markers for the accurate localisation and grading of prostate cancers, (Roberts et al., 2011).

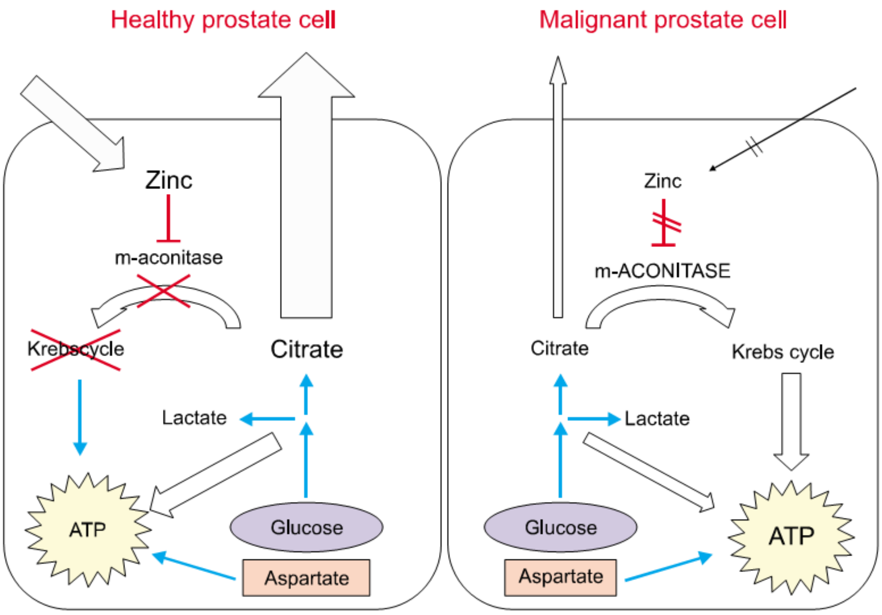

Figure1.9 The physiology of peripheral prostate in healthy (left) and diseased (right) (Roberts, *et al*, 2011).

1.3.4.4 LNCap and LNCap-AI cells are used as a biological module to study prostate cancer

LNCaP cells are a cell line of human prostate cancer cells commonly used in oncology research. The presence of highly sensitive androgen receptors in the cytosol of LNCaP makes this cell line highly androgen-sensitive (Horoszewicz et al., 1983). LNCaP cells are a good model for studying transcriptional regulation in genes of the prostate because they are androgen sensitive, and functionally differentiated; i.e. they express Prostate Specific Antigen (PSA), and Human Prostatic Acid Phosphatase (hPAP)[3].LNCaP-AI is an LNCaP derivative while it is androgen independent in terms of cell growth and proliferation, it is expresses the androgen receptors (AR) more than LNCaP cells and is able to express androgen-regulated genes such as the PSA (Prostatic Specific Antigen) gene (Halkidou et al., 2003, Lu et al., 1999). Lu and his colleague reported that LNCaP-AI cells expressed a much higher level of anti-apoptotic gene bcl-2 when they were treated by 12-O-tetradecanoylphorbol-13-acetate that may improve the antiapoptosis phenotype. McDonnell and his group thought that androgen independence may due to expression of bcl-2 because it is not expressed in the normal secretary of prostate epithelial cells whereas, is expressed in prostate cancer specimens (McDonnell et al., 1992, Zhou et al., 2004). In the Shan's study, LNCaP-AI cells treated with a protein kinase activator (TPA), which is used as an apoptosis inducer showed a high rate of cell viability and a low rate of cell death was detected. Moreover, analyzing of DNA fragmentation (a marker of apoptosis) showed an increase of fragmented DNA in LNCaP cells, while LNCaP-AI cell's DNA was undamaged. This information demonstrates that LNCaP-AI cells have got antiapoptotic properties (Shan *et al*, 1999). The increase in prostatic cancer stage and grade associated with p53 gene alterations and p53 protein accumulation, mutation and finally change from AD to AI growth in metastatic and hormone-refractory tumours (Apakama et al., 1996). In the studying of biochemistry of androgen-independent cells reported that the alteration to androgen-independent might be occur with contribution of P53, HSP27, and the MAPK pathways. So blocking MAPK signalling pathway may be a useful as a way to treat androgen-independent prostate cancer (Wang et al., 2010).

---

(3) http://www.lncap.com/

1.4 Sphingolipids

Sphingolipids are part of all eukaryotic cell membranes. Chemically, a sphingolipid (SL) consists of a ceramide (Cer) part linked with any number of lipids via the 1-OH position. Ceramides, the backbone of all sphingolipids, consist of a sphingoid base (a long chain base (LCB)). Palmitoyl CoA condenses with serine to form 3-ketosphinganine in the first step of the de novo synthesis of sphingolipids. The reduction of this compound gives a sphinganine (dihydrosphingosine). The hydrolysis of N-acyl chains in dihydrosphingosine to dihydroceramide then 4– 5 trans double bond is introduced to form ceramide. Sphingosine is not produced by this process, only by deacylation of ceramide. Synthesis of sphingomyelin occurs by adding a phosphocholine to the primary hydroxyl of ceramide. The phosphorylation of sphingosine is carried out by the two isoforms of sphingosine kinase (SKl or SK2) yielding a sphingosine 1-phosphate (S1P) (figure 1.9) (Maceyka et al., 2005). It has been clearly shown that sphingolipids and their metabolites have an important signalling role. The sphingolipid metabolites: ceramide (Cer), sphingosine (Sph), and sphingosine-1-phosphate (S1P) have an opposite physiological function.

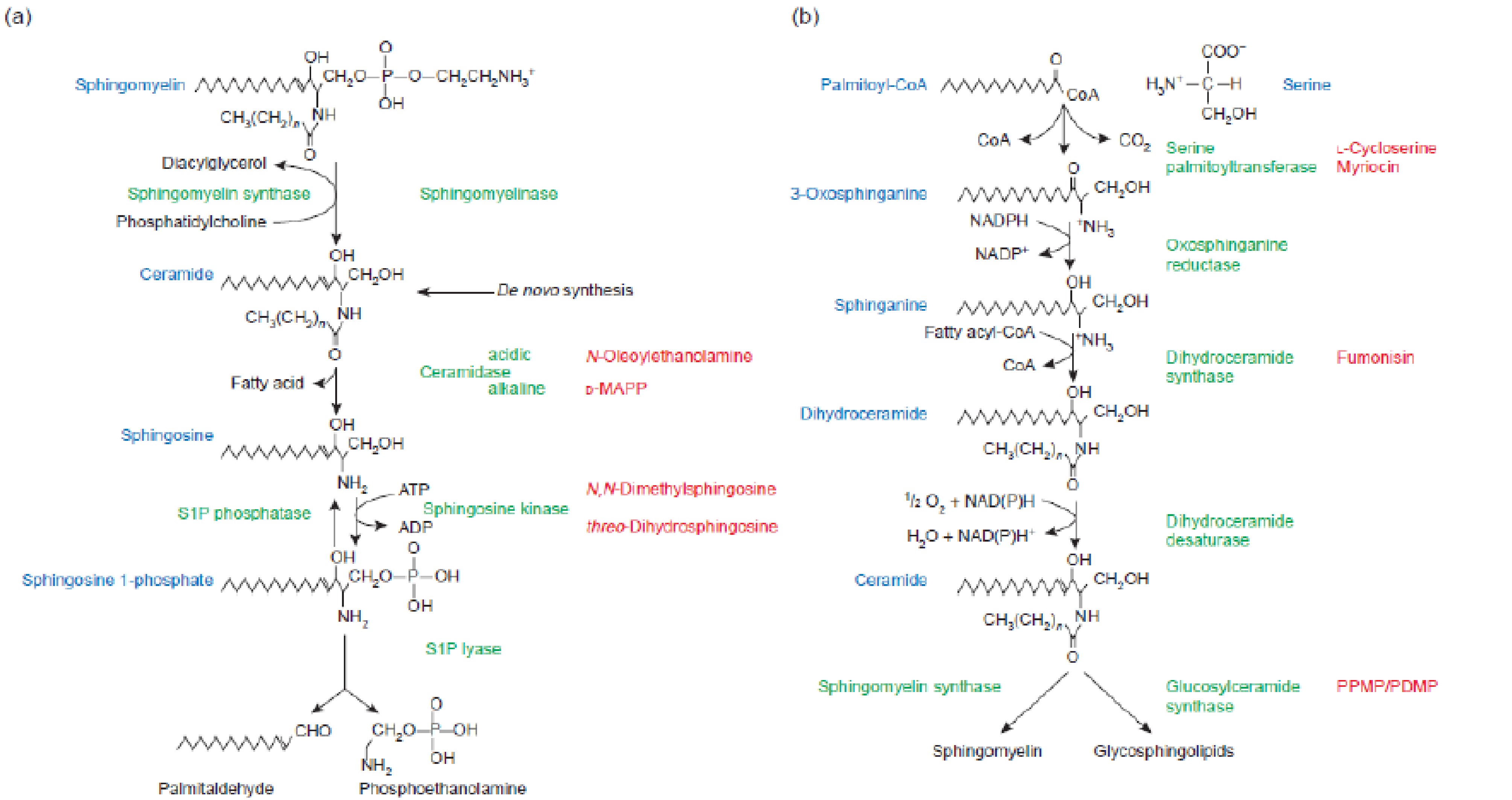

Figure 1.10 Sphingolipid metabolism.(Pyne and Pyne, 2000)

1.4.1 Sphingolipid Metabolism

The dynamic balance between intracellular sphingosine-1-phosphate versus ceramide and sphingosine is called the “sphingolipid rheostat”. This dynamic balance is a main feature that determines cell fate (Cuvillier et al., 1996). The opposing signalling pathway in sphingolipid metabolism is that ceramide and sphingosine are associated with growth arrest and apoptosis. In contrast, increased intracellular levels of sphingosine-1-phosphate lead to cellular proliferation and survival. Many stress stimuli increase levels of ceramide and sphingosine such as cytokines, irradiation and anti-cancer drugs (Spiegel and Milstien, 2002). The above results suggesting that the transformation of ceramide to sphingosine-1-phosphate by sphingosine kinase will convert the apoptotic action on the cell to cellular growth. So the inhibition of sphingosine kinase action induces apoptosis and may help in the treatment of disease states such as cancer (Pyne and Pyne, 2000).

1.4.2 Sphingosine 1-phosphate

The phosphorylation of sphingosine on the primary hydroxyl by sphingosine kinases (SK1 or SK2), produces sphingosine -1-phosphate (S1P), which is a polar lipid metabolite and it can be cleaved by S1P lyase. Sphingosine -1-phosphate (S1P) degradation using lyase is an irreversible step; so it is converted back to sphingosine by S1P phosphohydrolases (SPPs) (Maceyka et al., 2005). These reactions regulate cellular S1P. On the one hand, it is to minimize unneeded biosynthesis of ceramide by forming of cytosolic S1P using sphingosine kinase 1 (Maceyka et al., 2005), on the other hand, the excess S1P is degraded by S1P lyase in the cytoplasm producing hexadecenal (palmitaldehyde) and ethanolamine phosphate, the end point of metabolism of sphingolipids (Futerman and Riezman, 2005). The platelets considered as storage and releasing sites, when their activation, for sphingosine -1-phosphate. S1P acts as both an extracellular mediator and as an intracellular second messenger (Pyne and Pyne, 2000, Olivera and Spiegel, 2001). Moreover, the extracellular sphingosine -1-

phosphate controls cellular processes through binding with five specific G protein coupled-receptors (GPCRs) (Pyne and Pyne, 2000).

1.4.3 Sphingosine kinase

Sphingosine kinase (SK) is a conserved lipid kinase that catalyzes the formation of the mitogenic second messenger sphingosine-1-phosphate (French et al., 2006). The first mammalian SK, murine or mSK1 was originally purified from rat kidney as a 49-kDa protein. Two isoforms were cloned, named mSK1a and mSK1b with expected molecular mass 42.2 and 43.2 kDa respectively and the differences between them are only in a small number of amino acids at their amino-termini. Afterwards, human SK1 was also cloned. A broad similarity in the tissue distributions between mSK1 and hSK1 was detected (Kohama et al., 1998). There are two types of Sphingosine kinase that differ in sequence, catalytic properties, localization, and in their functions, SK1 and SK2 (Maceyka et al., 2005). SK1 has pro-survival functions and it is found in the cytosol of eukaryotic cells, due to its lack of hydrophobic properties, and migrates to the plasma membrane upon activation. SK2 is localized to the nucleus and SK2 is a putative BH3-only protein, inhibits cell growth and enhances apoptosis (Kohama et al., 1998).

The plasma membrane is the site for generation of sphingolipids. While SK1 is mainly located in the cytosol, it needs activation to translocate to the membrane (Hait, et al, 2006). SK is activated by a several types of agonist such as ligands for G-protein coupled receptors (GPCR), including acetylcholine, prosaposin, lysophosphatidic acid, formylmethionine peptide, and others. Also, the activation of SK through a specific GPCR by S1P itself was detected (Maceyka et al., 2005). In addition, agonists of growth factor receptors (PDGF, VEGF, NGF, and EGF), transforming growth factor beta and the pro-inflammatory cytokine TNF-alpha were shown to stimulate SK (Spiegel and Milstien, 2003). These stimulations led to an increase in intracellular levels of S1P as a result ceramide-dependent apoptosis is arrested by S1P and concluded in survival and proliferation of the cell (French et al., 2006). Since SK regulates the balance between ceramide level and S1P, which decides whether a cell proliferates or undergoes apoptosis, this has made SK an attractive target for cancer therapy (Maceyka et al., 2005).

1.5 Cell line (culture) analysis in metabolomic studies

Serum, plasma, urine, lymph fluid, cerebrospinal fluid, bile, feces, saliva, cells and tissues are various types of human samples all of which have different methods for collection, extraction and analysis. Recent studies show that metabolomic analyses of cell culture extracts performed on LC/MS instruments are robust and reliable, generating highly reproducible results (Pandher *et al*., 2009, Sreekumar *et al*., 2009, Putluri *et al*., 2011).

1.6 Experimental design

In human metabolomics studies there are two different strategies. *In vitro* which uses tissue culture systems, or *in vivo,* which is study of the general population and animal models. In an *in vitro* study the experiment takes place in a well-controlled environment and the treatment is the only variable. This reflects on the results obtained for the metabolome, which is clearly changed and easily quantified so that a small sample size can still provide statistical confidence in the results. However, an *in vivo* study needs to take into account the fundamental variety found in physiology, metabolic status and lifestyle in the general human population that makes the results relatively sensitive and therefore large-scale epidemiological studies are required to provide statistical confidence (Dunn *et al*., 2011).

1.7 Cell culture and quenching

The application of cell culture in metabolomics has been associated with some challenges (Čuperlović-Culf *et al*., 2010). The 'quenching' of cell cultures (stopping the cellular metabolism), harvesting and preparation of samples to avoid changes in metabolic profiles during the extraction procedures are some of the challenges.

The extraction method for intracellular metabolites is critical as it should be reproducible and stable for most compounds, particularly those of high interest. In addition, as many metabolites as possible should be extracted without causing chemical or physical degradation (Dunn *et al.*, 2011, Dietmair *et al.*, 2010). Some methods affect the metabolites by using heating, high or low pH or aggressive chemicals to deteriorate the cell wall (Danielsson *et al*., 2010). Generally, extraction methods are one-phase liquid or two-phase liquid-liquid extraction of the organic phase and the aqueous phase, which are suitable for both hydrophilic and lipophilic compounds. The advantage of two-phase extraction is the possibility of analyzing both polar and non-polar metabolites individually, but it is a time consuming and tedious method. On the other hand, in a one-phase system precipitated proteins, DNA, and RNA are removed (Gullberg *et al*., 2004) and the extract will contain both polar and non-polar compounds. A combination of several miscible solvents can be used to improve the selectivity of the one-phase system. Ditemair and his group used a very low volume of extraction as 5×10^6 cells were extracted with 100-1000µl solution, but achieving significantly higher concentrations of nucleotides than lower volumes of extraction solution did not result in significantly higher concentrations of amino acids. The maximal cell extractions from the comparison of 12 methods of extraction were cold 50% MeOH, MeOH with freezing, MeOH/Chloroform, and ACN because of their minimal degradation. In the same study, it was concluded that acetonitrile is the most suitable extraction solvent for metabolomics analysis because its recovery of standards was excellent and the extraction efficiency from cells was better than with other methods (Dietmair *et al*., 2010). Although acetonitrile is highly polar and may be less suitable for nonpolar substances, it has been shown to extract lipids. The addition of organic solvent or solvent mixtures to precipitate high molecular weight molecules is followed by a centrifugation step to separate the supernatant containing the metabolites from the precipitate.

1.8 Aims

1. To evaluate the performance of five different columns with regard to the analysis of a range of metabolite standards.

2. To validate the extraction of metabolites from LNCaP cells.

3. To evaluate the stability of LNCaP cell extracts.

4. To carry out a metabolomic study on the the effect of sphingosine kinase inhibitors on LNCaP cells and androgen independent LNCaP cells.

5. To develop a quantitative method for diadenosine phosphates in LNCaP cells.

6. To develop methods for the characterisation and quantification of sphingosine bases in LNCaP cells.

Chapter 2: Materials and Methods

Materials and Methods

2.1 Chemicals and Solvents

HPLC grade acetonitrile (ACN), chloroform and methanol were purchased from Fisher Scientific, UK. HPLC grade water was produced by a Direct-Q 3 Ultrapure Water System from Millipore, UK. AnalaR grade formic acid (98%) was obtained from Fisher Sceintific, UK. Ammonium carbonate, ammonium acetate, ammonium hydroxide solution (30-33%) and all standard compounds used to evaluate the column or develop the methods were purchased from Sigma-Aldrich, UK. Sodium chloride (NaCl; Sigma-Aldrich, UK, cat. no. S7653).Di-sodium hydrogen phosphate dihydrate ($Na_2HPO_4.2H_2O$; Fluka Analytical, UK, cat. no 71633).

Potassium dihydrogen phosphate (KH_2PO_4; Sigma-Aldrich, UK, cat. no. P5655).

RPMI 1640 medium was from Sigma-Aldrich (Poole, UK, cat. no. R0883)

Penicillin-streptomycin (10000 U/ml penicillin and 10000 μg/ml streptomycin) was from Sigma-Aldrich (Poole, UK, cat. no. P4333). L-glutamine was from Invitrogen (Paisley, UK, cat. no. 25030-081). European fetal calf serum (EFCS) was from Sera Laboratories (Haywards Heath, UK, cat. no. EU-145-F).

Human androgen-sensitive LNCaP cells - LNCaP cells were gifts from Professor Hing Leung (Beatson Institute, Glasgow) to Susan Pyne.

2.2 Preparation of Solutions of Metabolite Standards

Each metabolite standard was prepared at 1 mg/ml with HPLC grade methanol and water (1:1, v/v) as the stock solution and stored at -20°C. 100 µl was taken from each stock solution, about 52 metabolites were mixed and then the solution was made up to 10 ml with acetonitrile. Consequently, the final concentration for each metabolite standard was 10 µg/ml and 180 metabolite standards were distributed into four mixed metabolite standard solutions (detailed in Table 2.1). In order to avoid identity confusion, isomers were distributed into different standard solutions and in-source fragments were also carefully verified since they could be mistaken for another metabolite.

For linearity, a stock solution of 1mg/ml diluted to prepare the concentrations 15 and 20 µg/ml. Serial concentrations (1 - 5000 ng/ml) were prepared by dilution of stock solution 10 µg/ml by acetonitrile.

Table 2.1 The distribution of metabolite standards into four mixed metabolite standard solutions.

Standard mixture 1	**Standard mixture 2**	**Standard mixture 3**	**Standard mixture 4**
3-(2-Aminoethyl)-1H-indol-5-ol*	Inosine	L-Kynurenine	Biopterin
3-Phenylpropionylglycine*	IMP	O-Acetylcarnitine	dADP*
Adenosine	Guanosine	Pantothenate	DL-4-aminobutyrate
AMP	dAMP	L-Metanephrine	D-Mannose
GMP	Glutathione	L-Tryptophan	L-Arabinose**
ATP*	Ectoine	Maltose	L-Cysteine-N15*
GTP*	Glutethimide***	Melatonin**	L-Leucine
5-Hydroxyindoleacetate**	Folate*	S-Adenosyl-L-homocysteine	L-Threonine
Antipyrine**	Fluorescein*	Riboflavin	Malonyl-CoA*

5'-Methylthioadenosine	Glycine	NAD^{+}	N-Acetyl-D-mannosamine
1,10-Phenanthroline***	Ethanolamine phosphate	$NADP^{+}$*	Phosphocreatine*
β-Alanine	L-Alanine	Oxalate	Picolinic acid
Allantoin	L-Cysteine	Putrescine*	S-Adenosyl-L-methionine
(R)-Malate	Guanidine* LMw	Methylglyoxal*	Sarcosine
β-alanine-methyl-ester	Fumarate	Pyruvate	Sepiapterin
Betaine	Homoserine lactone**	Malonate	Spermidine*
Citraconate**	L-Aspartate	L-Serine	Spermine*
2-Oxoglutarate	2-Hydroxybutanoic acid	Maleic acid	Succinate
5-Oxoproline	Creatine	Oxaloacetate*	Sucrose**
Citramalate	L-Glutamine	Methylmalonate	Taurine
5-Aminolevulinate	Deoxyribose*	DL-3-aminobutyrate	Thymidine
beta;-L-fucose**	D-Xylose	L-Homocysteine	trans-4-Hydroxy-L-proline
D-Glucose	Hypoxanthine	L-Homoserine	Triethanolamine
Cis-Aconitate	Isonicotinic acid	L-Valine	UDP-N-acetyl-D-glucosamine*
Benzenesulfonate	Guanine	L-Methionine	UMP
Ascorbate	Itaconate	L-Ornithine	Xanthine
AcetylCholine	Cis-4-Hydroxy-D-Proline	Alloxanthine	Urate*
4-Nitrobenzoate***	L-Glutamate	Mesaconate	Xanthosine*
1,7-DimethylXanthine	D-Galactono-1,4-lactone**	L-Proline	N-Acetyl-L-glutamate
1-Phenylethylamine	D-Galacturonate**	O-Acetyl-L-serine	6-Phospho-D-gluconate**
1-(4-Hydroxyphenyl)-2-aminoethanol	Galactarate*	D-Glucuronate	N-Formyl-L-methionine*
4-hydroxylphenylacetate	Creatinine**	D-Galactose	3-Deoxy-2-keto-6-phosphogluconic acid**
Adenine	L-Cystine	L-isoleucine	S-Lactoylglutathione

2-Phenylglycine	D-Fructose	D- Glucosamine	
Amphetamine***	D-Gluconic acid**	L-Lysine	
CMP	D-Glucosamine	Mannitol	
2-Indolecarboxylicacid	D-Glucose6-phosphate	Nicotinate**	
2-phenyl Imidazole**	L-Arginine	Nicotinamide**	
4-Coumarate	D-Glucosamine6-Phosphate	L-Histidine	
Caffeate	Cytosine	N-Acetyl-L-aspartate	
Glycine-C13*	D-Isoascorbic acid**	N(pi)-Methyl-L-histidine	
Glycolate*	Isocitrate	Theophylline**	
	Diethyl2-oxoglutarate	L-Noradrenaline	
	Cystathionine	Pyridoxamine	
	Gallate	N-Acetyl-D-Glucosamine	
	Theobromine*	N6-Acetyl-L-Lysine	
	Dopamine*	N-Acetyl-D-glucosamine6-phosphate	
	4-Hydroxyphenylacetaldoxime	Phthalate	
	Cytidine	Pyridoxal**	
	Dihydrobiopterin	L-Phenylalanine	
	L-Adrenaline	L-Tyrosine	
	Aspirin**	Phenylephrine*	

I EXCLUDED THIESE METABOLITES FROM MY STUDY AS FOLLOWS:

* no signal (low limit of detection or the method is not suitable)

** Chromatographic separation is not good

*** It is not metabolite (drug), substances foreign to an entire biological system.

2.3 HPLC conditions

2.3.1 Mobile phase solutions for ZIC-HILIC Chromatography

All mobile phase solutions were freshly prepared and were stored at room temperature for up to 48 hours.

Mobile phase A: (0.1% formic acid in water pH 3) was prepared by addition of 1ml of formic acid to 800 ml of HPLC-grade water followed by mixing then was completed the volume to 1L.

Mobile phase B: (0.1% formic acid in acetonitrile pH 3) was prepared by addition of 1ml of formic acid to 800 ml of HPLC-grade acetonitrile, followed by mixing then completing the volume to 1L.

The column used was a ZIC-HILIC column (L150 * I.d. 4.6 mm, 5µm, silica support) from Hichrom Ltd, Reading UK.

2.3.2 Mobile phase solutions for ZIC-pHILIC chromatography

All mobile phase solutions were freshly prepared and were stored at room temperature for up to 48 hours.

Mobile phase A: (20mM Ammonium carbonate buffer pH 9.2) was prepared by addition of 1.92g of ammonium carbonate to 800 ml of HPLC-grade water followed then adjustment to pH 9.2 with ammonia solution and then was completed to a volume of 1L.

Mobile phase B: it was HPLC-grade Acetonitrile only.

The column used was a ZIC-pHILIC column (L150 * I.d. 4.6 mm, 5µm, polymeric bead support) from Hichrom Ltd, Reading, UK.

2.3.3 Mobile Phase for C18 Chromatography

All solutions were freshly prepared and were stored at room temperature for up to 48 hours.

Mobile phase A: (0.1% formic acid in water pH 3) was prepared by addition of 1ml of formic acid to 800 ml of HPLC-grade water followed by mixing then was completed to a volume to 1L.

Mobile phase B: (0.1% formic acid in Acetonitrile pH 3) was prepared by addition of 1ml of formic acid to 800 ml of HPLC-grade Acetonitrile followed mixing then was completed to a volume of 1L.

The column used was an ACE C18-AR (150 × 4.6mm, particle size 5 µm, pore size 100A˚) from Hichrom Ltd., Reading UK.

2.3.4 Mobile Phase for Silica-C Chromatography

All solutions were freshly prepared and were stored at room temperature for up to 48 hours.

Mobile phase A: (10mM Ammonium acetate buffer pH 6.5) was prepared by addition of 0.77g of ammonium acetate to 800 ml of HPLC-grade water followed mixing until it dissolved and then was completed to a volume to 1L.

Mobile phase B: It was HPLC-grade Acetonitrile only.

The column used was a Cogent Type C silica column (250 mm × 4.6 mm × 4 µm, base silica surface area 350 m^2 g^{-1}, pore size 100A˚) from Hichrom Ltd., Reading UK.

2.3.5 Mobile Phase for BEH Amide Chromatography

All solutions were freshly prepared and were stored at room temperature for up to 48 hours.

Mobile phase A: (20mM Ammonium carbonate buffer pH 9.2) was prepared by addition of 1.92g of ammonium carbonate to 800 ml of HPLC-grade water followed by mixing until it dissolved then adjustment of the pH to 9.2 with ammonia solution and was completed to a volume of 1L.

Mobile phase B: was HPLC-grade Acetonitrile only.

The column used was an XBridge BEH Amide Column, 130Å, 3.5 µm, 4.6 mm x 150 mm from Waters, Manchester, UK.

2.4 HPLC setup

The HPLC was fitted with the appropriate mobile phase components. The auto-sampler needle and sample syringe were flushed with the syringe wash solution (Methanol: Water 1:1). The system was flushed with the mobile phase components by opening the drain valve then operating with 100% mobile phase B with a flow at 5 ml/min for 5 min and next, 100% mobile phase A with a flow at 5 ml/min for another 5 min. Then the drain valve was closed.

The selected HPLC column was conditioned by operating with 50% mobile phase B at a flow rate of 0.3 ml/min and leaving for 10 min (outlet tube not connected with the mass spectrometer). The operating pressure was monitored, should be < 2,000 p.s.i. Then the outlet tube was connected with the mass spectrometer. Chromatographic separations were performed on different columns applying a linear gradient over 30 min between nonorganic/organic mobile phase systems. Same gradient elutions were performed for the ESI interface which was operated in a positive/negative polarity switching mode. Positive and negative ion mode detection, as described in table 2.2 for the four HILIC columns (ZICHILIC, ZICpHILIC, Silica C and BEHamide), with flow rates of 0.3 ml/min. Samples were kept in a vial tray which was set at constant temperature of 4 ˚C to avoid any possible degradation of samples.

Table 2.2 linear gradient elution program applied for HPLC-MS analysis for ESI positive and ESI negative modes.

Time (min)	flow rate (ml/min)	Mobile phase A%	Mobile phase B%
0	0.3	20	80
30	0.3	80	20
31	0.3	92	8
36	0.3	92	8
37	0.3	20	80
46	0.3	20	80

2.5 Orbitrap Exactive MS setup:

LC-MS was carried out with an Accela HPLC pump coupled to an Exactive (Orbitrap) mass spectrometer from Thermo Fisher Scientific. The data acquired from an instrument is a representative indication of the quality of data. The quality of data in one set run while standard mixtures which were run with each set can assess the quality of acquired data through the study by checking the peak widths, heights, retention times and chromatographic resolution do not vary significantly (by > 20%). If the retention time shifts from the data acquired at the beginning and the end of the set varies significantly (by > 0.3 min) the HPLC system was checked for leaks or using a new column were considered.

The vacuum pressures and all voltages were set as in the Tune page of LTQ Tune. If any errors are found, analysis was postponed until the instrument is serviced.

Every week the source was cleaned to remove residues that can reduce the instrument sensitivity. This involves sonication of the sample cone and transfer lens in a 50:50 (vol/vol) methanol/water solution for 15 min.

The mass spectrometer was tuned according to the manufacturer's specifications.

The MS system was calibrated according to the manufacturer's instructions, using the standard Thermo Calmix solution with addition of compounds to cover the low mass range. The signals of acetonitrile dimer (2xACN+H) m/z 83.0604 and m/z 195.03765 for caffeine were used as lock masses for positive (PIESI) mode and m/z 91.0037 (2 x formate-H) was used as a lock mass for negative (NIESI) mode, during each analytical run. The intensities of all calibrant peaks should be between 10^4 and 10^7. The error for all calibrant peaks should be within 3 p.p.m. If the mass error is greater, perform a second mass calibration. If the mass calibration error is still > 3 p.p.m., either rectified immediately or analysis was deferred until the instrument was serviced. The spray voltage used was 4.5 kV for positive mode and 4.0 kV for negative mode. The temperature of the ion transfer capillary was 275 °C and the sheath and auxiliary gases were set at 50 and 17 arbitrary units, respectively. The full scan range was 75 to 1200 m/z for both positive and negative modes with settings of AGC target and resolution as Balanced and High ($1E^6$ and 50,000), respectively.

2.6 GC–MS method used for the Analysis of Methylglyoxal

Both samples and reference materials were prepared in the same manner. 500µL of sample was blown to dryness with nitrogen gas. The residue was then derivatized with 100 µL of the pyridine methoxyl amine HCl solution (2% w/v) and allowed to react at 80°C for 30min. Then the pyridine was blown away and 200 µL of methanol was added to the residue. Then it was injected into the GC/MS system. Methylglyoxal standard diluted with acetonitrile to 4% w/v. Then 50 µL of standard was derivatized with 100 µL of the pyridine methoxylamine HCl solution (2% w/v) and allowed to react at 80°C for 30min. Then the pyridine was blown away and 200 µL of methanol was added to the residue. Then it was injected into the GC/MS system. Analysis was performed with a FOCUS GC and DSQ II single quadrupole MS (ThermoElectron, Hemel Hempstead, UK) operated in electron impact mode. The following conditions were used: an RTX-1 30 m × 0.25 mm (i.d) capillary column coated with 100% dimethylpolysiloxane (film thickness, 0.25µm) from Thames Restek, UK was used. The following program was used switch on the filament at 3 minutes. The oven temperature was programmed from 60°C (held for 1min) then to 150 °C at 5°C min-1. Carrier gas (He) pressure was maintained at 100KPa until the end of the run. The GC inlet temperature was 200°C and MS transfer lines were maintained at 200 °C.; electron energy, 70eV; Ion source temperature, 200°C; mass range, 50-1200; cycle time, 0.8170 scans per second. Sample injection volumes were 1 µl injected with a splitless mode.

2.7 Cell Culture Methods

2.7.1 Reagents preparation

Culturing medium: RPMI 1640 medium supplemented with 10% EFCS, 100 U/ml penicillin, 100 µg/ml streptomycin and 1% L-glutamine. Divide into 50ml aliquots and keep at -25 °C until use.

Phosphate buffer (500 mM): phosphate buffer (500 mM) containing 500 mM $Na_2HPO_4.3H_2O$ + 500 mM KH_2PO_4 was prepared. Then pH 7.4 was adjusted. This solution is stable several weeks at 4 °C.

Phosphate buffer saline (PBS): PBS buffer was prepared by dissolving 140 mM NaCl in 10 mM phosphate buffer. This solution is stable for several weeks at room temperature (20 – 25 °C).

2.7.2 Culture Conditions

Human androgen-sensitive LNCaP cells were maintained in complete medium which is RPMI 1640 medium supplemented with 10% EFCS, 100 U/ml penicillin, 100 µg/ml streptomycin and 1% L-glutamine. All cells were maintained in a humidified atmosphere at 37°C with 5% CO_2. Stocks were grown in 75cm^2 flasks using 10 ml of complete medium per flask. For experiments 750,000 cells were plated in T-25 cell culture flasks and grown until the cell number doubled (48 h) before being extracted; each flask was one metabolomics sample.

2.7.3 Quenching and extraction of samples

Cell extracts were prepared by removing the medium and the cells were swiftly washed with 3 ml 37°C of phosphate-buffered saline (PBS) twice. Quenching of metabolites was performed by putting the flasks on ice then adding the calculated volume of pre-cooled extraction solution [methanol: acetonitrile: water –all HPLC grade – 50:30:20; pre-cooled by keeping on a dry ice/methanol mixture].

The cells were subsequently scraped off using a cell scraper. The volume of extraction solution to be added was calculated according to 1ml per $2x10^6$ of cells. Cell lysates were transferred into the Eppendorf tubes. The samples were rotated on Thermo mixer at 4°C for 12 minutes then centrifuged at 0 °C and 25,885 x g for 15mins. The supernatants were collected and transferred into the HPLC-vials which were then ready for LC-MS analysis. Figure 2.1 shows full steps of cell line metabolomics preparation (quenching and extraction, LC/MS analysis, data collection and analysis). To remove the variables that might be introduced from preparing samples separately, all six samples for analysis were prepared at the same time so that potential errors observed in replicate sample preparation procedures reduced. After preparation, aliquots (0.5 ml) of extracted cells should be rapidly frozen and stored at -80 °C until analysed, as they can be stored for no longer than two weeks. Each sample should be labelled with a unique identifier. To ensure that analysis order does not correlate with sample preparation order and to ensure that no systematic biases are present, the sample preparation order should be randomized from sample picking and re-randomized from sample analysis order in an LC/MS auto injector.

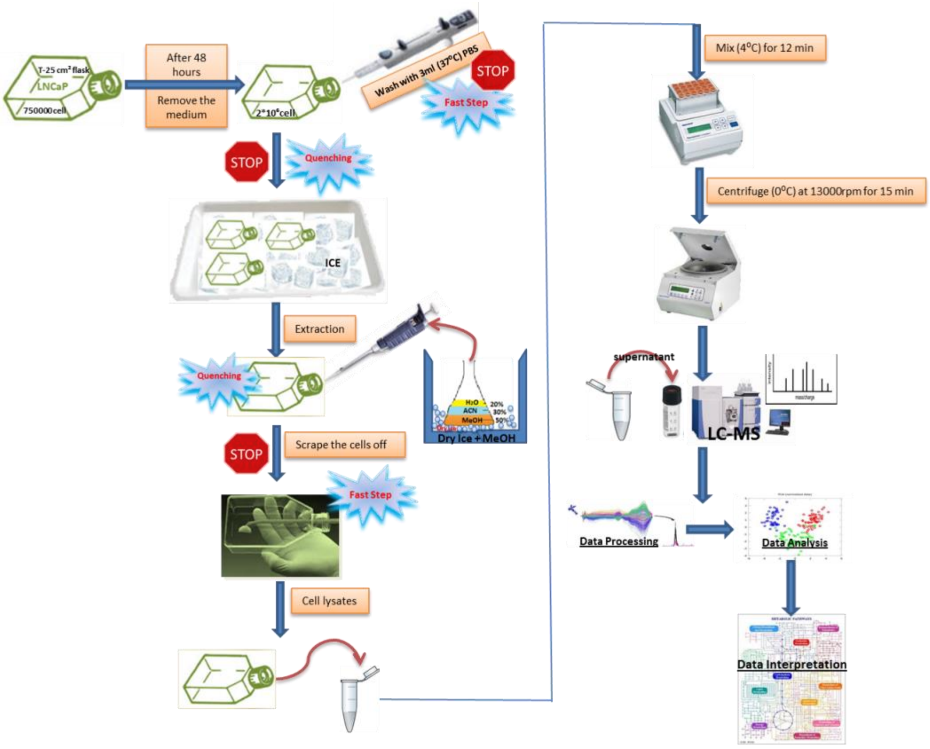

Figure 2.1 Details of steps involved in the extraction of a cell line prior metabolomics analysis.

2.7.4 Assessment of Extract Stability

According to conference report II was as it is important to assess: "the chemical stability of an analyte in a given matrix under specific conditions for given time intervals". The reliability of quantitative analytical procedure needs stability of the analyte over the whole analytical procedure (Tiwari, 2010). A stability method should estimate the analytes persistence over the period of the experiment. The stability study include after long-term (frozen at the specific storage temperature) and short-term (instrument auto injector, room temperature) storage, and after going through freeze and thaw cycles and the analytical process (FDA, 2001). The samples storage stability was investigated using a freshly made LNCaP cell extract.

2.7.4.1. Freeze and Thaw Stability

Analyte stability was evaluated after three freeze and thaw cycles. Thaw cycle stability was assessed by analyzing six samples which were stored at the required storage temperature (-20°C) for 24 hours and thawed unassisted at room temperature. When the samples had completely thawed they were refrozen again for 24 hours under the same conditions. The freeze–thaw cycle was repeated two more times and then the sample was analyzed on the third cycle.

2.7.4.2. Short-Term Temperature Stability

Four aliquots of the LNCaP cell extract were thawed at room temperature and kept at this temperature for 0, 4 and 24 hours (based on the expected duration that samples would be kept at room temperature in the study procedure) and analyzed.

2.7.4.3. Long-Term Stability

The long term stability test was performed by analyzing six prepared samples from the same LNCaP cell extractions each sample divided into 10 aliquots (one kept at -20°C and the other one at -80°C) analyzed every week for five weeks. The stability samples were then compared to the mean of calculated peak response values for the set run in the first day (fresh samples).

2.8. Data Extraction Methods Used in Processing the Files Obtained from LC-MS analysis of Cell Culture Extracts

2.8.1 Sieve and Sieve Extractor

To start a Sieve experiment select create a new experiment. Then, data obtained from Xcalibur software were exported into Sieve Software 1.3 (Thermo Fisher Co.) to be converted into a readable format. The Sieve program deals with two sets the control samples and the treatment samples. The software then searches for metabolites according to this categorization after sifting the parameters (threshold, m/z start, m/z stop, frame time width, retention time start and retention time stop). Sieve software aligns (an automatic aligning process aligns the chromatograms of the sample files with the first control file, correcting chromatographic shifts, or with the sample chosen) and frames chromatograms. The data outputted are retention time, exact mass, ratio for the mean peak areas, mass intensity and P-value based on a two tailed T-test.

Sieve Extractor (SE) program was designed in-house and written as an Excel Macro (Microsoft 2007). It helps automate the identification of metabolites by exact masses through comparing exact masses obtained experimentally from Sieve with the exact masses of metabolites from databases (Metlin, Kegg, HMDB and LipidMaps). A window for mass deviation was set at ± 3 ppm. The Sieve data in the form of a frames table are copied and pasted into Sieve Extractor then compared against the database and the putative identities for the metabolites produce. In addition, manual checking for extracted ion chromatograms from the Xcalibur files is necessary. Using mass of the ion m/z determined from the Sieve software which entered into Xcalibur in order to find its chromatographic peak which should be symmetric and sharp peak, and a possible elemental compositions for the ion chromatogram are generated with < 2 ppm mass accuracy.

2.8.2 mzMatch and IDEOM

All raw data files (Thermo-Xcalibur format) were manually sorted into folders according to study groups. Then they were converted to mzXML files and split polarity using mzMatch split function to separate Exactive files that contain both positive and negative polarity. After this, XCMS was run through R, using the centwave function, peaks were picked and each individual file converted to peakml format, i.e., peaks were found and a list of peaks created, as shown in figure 4. Settings for the centwave function were employed as mass deviation from scan to scan (< 2) ppm, range for baseline peak width (minimum 5 seconds and maximum 100 seconds), Signal to Noise ratio (3), prefilter intensity (1000), Mzdiff (0.001). This was followed by running mzMatch to match peaks from each sample to produce a single dataset and group individual peakml files, as shown in Figure 2.2 and 2.3. Furthermore, the noise filter, RSD filter, intensity filter and detection filter were run to remove irreproducible signals in either biological or technical replicates (Scheltema et al., 2011). Parameter settings for the mzMatch filters were mass deviation from sample to sample (5 ppm) and RT deviation from sample to sample (0.5 min). If there is a large shift in retention time, the signal intensity will not be comparable and the datasets will not make sense. mzMatch filtrations are [1] RSD filter (0.5), where peak reproducibility is assessed by the RSD of peak intensities for each group of replicates; [2] noise filter (0.8), where peak shape is assessed by CoDA-DW score (0-1); [3] intensity filter (3000), where features are removed if no sample has a peak above the intensity threshold; and, [4] detection filter (3), where peaks must be present in a minimum number of samples. In addition, mzMatch fills the gap for peaks which may fall off during the process. Finally, IDEOM is used to filter the data further, and then the metabolites are compared and identified.

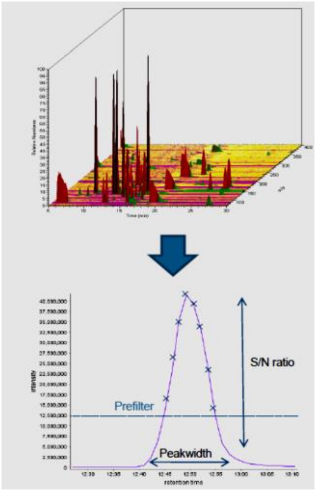

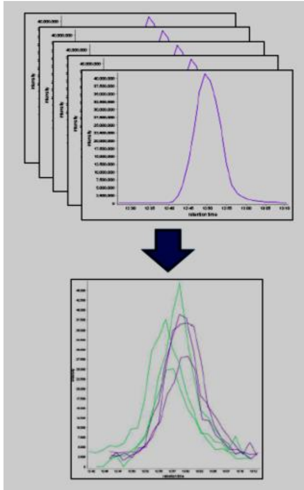

Figure 2.2 peaks picking and peak list. **Figure 2.3** grouping the individual peakml files.

IDEOM is a Microsoft Excel template enabled for automated data processing of high-resolution LC-MS data from untargeted metabolomics studies (Creek et al., 2012).

In IDEOM, more noise filtration is done and the authentic chemical standard is matched with a sample metabolite. It is necessary to update DB with retention times using a list of retention times from authentic standards (≈180 standards) run with each experiment is required; this list is created using Toxid (which is an automated compound identification tool that dramatically simplifies LC/MS data and identifies compounds according to retention time and chemical formula). The retention time calculator also uses physiochemical properties (depending on the functional group and chemical formula of compounds) in the DB sheet to predict retention times based on a multiple linear regression model with the authentic standards. The retention time calculator uses the Quantitative Structure Retention Relationships (QSRR) approach to predict retention times based on the known retention times of authentic standards and the physicochemical nature of the interactions of analyte with columns that determine retention (Creek et al., 2011). Identification of more accurate putative metabolite requires more filtration of mzMatch files. The blank run with the study group to filter all intensities in a study group must be greater than that in the solvent blanks to remove contaminants. Other filters for noise, such as RSD, intensity and detection filters, are repeated. Chromatography filters, shoulder peak filter and duplicate peak filter, are also applied in IDEOM. Identification of metabolites is performed by matching the accurate mass (accurate mass error for mass identification with DB < 3ppm is suitable for formula identification from a biochemical database with unique entries in DB of 97%) and retention time (RT for identification of authentic standards is 5%) of detected metabolite peak to metabolites in the database. Final lists of identified and rejected peaks are annotated with confidence level from 0 to 10 (10 = most confident) according to the identification of each metabolite; confidence < 5 is rejected as false identification and metabolites matched with authentic standards are identified metabolites and highlighted yellow.

2.8.3 Simca P

These were the basic features required from the macros which would generate a matrix of feature rows (variables) which are the metabolites intensities and sample columns (observations) which are the time of stability or repeatability compatible with exporting to SIMCA-P for multivariate analysis.

1. To start a new SIMCA-P project need to import the primary dataset.
2. Quick look into the dataset information (variables or observation).
3. Prepare a workset variables and observation.
4. Select the model type (PCX) principal component score for X.
5. Fit the model analysis (autofit or fast button).
6. Plot results analysis (scatter, line, column, 3d scatter and histogram).

2.8.4 Statistical analysis

According to ICH (International Conference on Harmonisation of Technical Requirements for Registration of Pharmaceuticals for Human Use), limit of detection is the lowest concentration of an analyte in a sample which can be detected but not necessarily quantified as an exact value. This value is a semi-quantitative or a qualitative determination (Tiwari, 2010). LOD were estimated Based on the Calibration Curve. The LOD can be estimated from the slope and standard deviation (SD) of the linearity curve and according to ICH the standard deviation of y-intercepts of regression lines can be used as the standard deviation.

$$\text{Detection Limit, LOD} = 3.3 \times SD\ /\text{slope}$$

$$\text{Quantification Limit, LOQ} = 10 \times SD\ /\text{slope}$$

Where: SD = standard deviation of y-intercepts; Slope = slope of the linearity curve obtained by regression analysis.

Statistical comparisons are provided by Sieve software in Study the effect of sphingosine kinase inhibitors on the metabolome of LNCaP cells. Comparative data analysis was carried out according to the fold change that identified metabolite ratios between the treatment and control groups. This ratio values were considered significant if $0.5 > \text{ratio} > 1.5$ with Student's two-tailed t-test < 0.05 (p-value).

Chapter 3: Column Selection and Method optimization

Column Selection and Method Optimization

3.1 Introduction

Reversed-phase (RPC) chromatography is by far the most popular chromatography technique for pharmaceutical analysis. The technique is characterised by the use of a non-polar stationary phase and a polar mobile phase, retention increases with decreasing polarity of the analytes or stationary phase or with increasing mobile phase polarity. The most hydrophilic (polar) compounds elute first, and the most hydrophobic (non-polar) last. The main disadvantage of reversed-phase column is the insufficient retention of very polar compounds (Dejaegher and Vander Heyden, 2010).

Drugs and their metabolites are often polar and these compounds are often insufficiently retained on a classical reversed-phase column, and elute near the solvent front so to increase their retention the use of a mobile phase with a low organic modifier percentage is required in reversed-phase mode, or to switch to normal phase chromatography, ion-pairing chromatography, or HILIC. If mass spectrometry is used as a detector for liquid chromatography, the reversed-phase condition is less suitable at the LC-MS interface because the high water content. The normal phase column has the advantage that retention for polar compounds is better, but it uses toxic and environmental unfriendly MP solvents. The ion-pairing chromatographic methods has the drawbacks that the column can not be used later for other purposes and it may take time to reach an equilibrium (Dejaegher and Vander Heyden, 2010) and is not compatible with MS. HILIC with a high percentage of organic solvent in the mobile phase retains (very) polar compounds and provides good conditions for the LC-MS interface, high signals and a good sensitivity. To obtain retention for the polar compounds in HILIC, a MP with high organic percentage should be used but does not retain hydrophobic compounds strongly (Dejaegher and Vander Heyden, 2010).

Classical bare silica or silica gels modified with polar functional groups can be used as HILIC stationary phases also polymer-based stationary phases can be used. The design of chromatographic columns is growing especially the HILIC column because the wide variety of different types of stationary phase for HILIC which have different retention characteristics (Buszewski and Noga, 2012).

Cogent TYPE-C silica based columns can operate with a wide range of HPLC solvents due to MicroSolv's bonding technology and the silica hydride surface. As a result, all TYPE-C columns can be operated in 3 modes of chromatography: reversed-phase, normal- phase and aqueous normal phase (ANP). In 2012, a study of metabolomic profiling of urine shows that the retention properties of a type C silica (silicon hydride) column for bases, sugars and polar acids were greater than on a silica gel column. In the same study the unmodified type C silica column gave the strongest retention of the many polar metabolites in urine (Bawazeer et al., 2012).

3.2Results

3.2.1 Overview of the results

The objective of the work described in this section was to select the chromatography column which would give the best performance for the greatest number of metabolites. In order to do this four mixtures containing about 180 metabolites which range of representative types were run on five different columns. The results are summarized in table 3.1 for the standard mixtures and LNCaP cell culture extracts. The table gives the retention times for the metabolites and comments on the quality of the peaks generated for each metabolite. It is difficult to find a single column which gives good performance for every metabolite type. A very complex and extensive set of data was generated in this way and table 3.2 summarizes the overall performance of each column. The data is also summarized in the form of pie charts in figure 3.1 where it can be clearly seen that overall the best performance was on the ZIC-pHILIC column.

Table 3.1 Evaluation of Some Different Columns for Metabolomic Profiling of Cell cultures. The running conditions for the different columns are shown in section 2.3. The retention times of the peaks for the standards and LNCaP cell extract are shown along with comments on the quality of the peak.

		ZICHILIC			ZIC-pHILIC			C18			Cogent Silica-C			BEH Amide		
Compound Name	Polarity	Comment STD/sample	Intensity of sample	RT STD/sample	Comment STD/sample	Intensity of sample	RT STD/sample	Comment STD/sample	Intensity of sample	RT STD/sample	Comment STD/sample	Intensity of sample	RT STD/sample	Comment STD/sample	Intensity of sample	RT STD/sample
Amino acids																
2-Phenylglycine	+	good peak	ND	13.25/ND	good peak	ND	10.67/ ND	good peak	ND	6.85/ ND	good peak	ND	18.49/ ND	good peak	ND	10.88/ ND
beta-Alanine	+	not separated (Alanine and sarcosine)	36607	17.33/17.41	good peak	12599	14.79/14.93	not separated (Alanine,beta-Alanine and sarcosine)	59500	5/4.99	not separated(Alanine,beta-Alanine and sarcosine)	27308	24.53/25.17	not separated(Alanine,beta-Alanine and sarcosine)	307801	15.72/15.6
cis-4-Hydroxy-D-proline	+	good peak	2806382	17.27/16.26	good peak	394075	14.37/ 13.92	good peak	124065	5.13/5.26	good peak	89100	23.5/22.94	good peak	2660000	16.41/15.33
Creatine	+	good peak	3059784	15.07/15.43	good peak	13062836	14.13/14.26	good peak	735269	5.41/5.51	good peak	40727	24.6/24.85	good peak	4129485	15.9/15.6
Ectoine	+	bad-low intensity	2125	14.4/14.7	bad peak-low intensity	19152	13.9/14.06	good peak	ND	5.53/ ND	good peak	ND	27.48/ ND	good peak	4606	15.5/15.01
Gamma-Aminobutyric acid	+	good peak	46883	16.64/15.98	good peak	172500	14.86/14.91	low intensity	9379	5.19/5.12	low intensity	2624	27.25/27.5	good peak	50121	16.7/16.4

		ZICHILIC			ZIC-pHILIC			C18			Cogent Silica-C			BEH Amide		
Compound Name	Polarity	Comment STD/sample	Intensity of sample	RT STD/sample	Comment STD/sample	Intensity of sample	RT STD/sample	Comment STD/sample	Intensity of sample	RT STD/sample	Comment STD/sample	Intensity of sample	RT STD/sample	Comment STD/sample	Intensity of sample	RT STD/sample
Glycine	+	good peak	1175748	18.51/18.27	good peak	253622	15.06/15.2	good peak	20243	5.02/5.12	good peak	7610	22.4/22.78	good peak	48502	16.3/15.91
L-Alanine	+	not separated (Alanine and sarcosine)	241428	15.94/15.92	good peak	545171	14.20/14.28	not separated (Alanine,beta-Alanine and sarcosine)	59786	5.21/5.12	not separated(Alanine,beta-Alanine and sarcosine)	27308	24.85/25.17	not separated(Alanine,beta-Alanine and sarcosine)	307801	15.72/15.6
L-Arginine	+	good peak	2060000	26.88/27.37	good peak	1269097	24.6/25.3	good peak	90621	4.8/4.9	too broad	252000	28.19/29.19	good peak	797509	23.99/23.94
L-Aspartate	+	good peak	2630394	17.44/17.23	good peak	4026190	14.6/14.64	good peak	10054	5.12/4.8	tailing	12644	17.4/17.7	good peak	4859	15.64/15.23
L-Cystathionine	-	good peak	151614	22.84/22.8	good peak	216233	16.2/16.6	good peak	ND	4.95/ ND	tailing	ND	25.5/ ND	low intensity	1058	18.77/18.16
L-Cysteine	-	good peak	320477	15.28/15.25	bad peak	15504	15.53/15.05	2 peaks	ND	4.95-5.44/ ND	not good peak	ND	24.7/ ND	multipeaks	ND	7.01-10.85-11.7-17.38/ ND
L-Cystine	-	good peak	12468	22.46/22.3	good peak	25165	15.56/15.74	good peak	ND	4.95/ ND	tailing	ND	25.0/ ND	low intensity	3070	17.33/16.8
L-Glutamic acid	+	good peak	8960000	16.89/16.65	good peak	9000	10.54/10.47	good peak	28385	5.48/5.29	multipeaks	1350000	18.25-20.6-20.9/18.73	good peak	6190000	15.33/14.92
O-Acetyl-L-serine	+	multipeaks	ND	6.6-8.3-14.6-16.6/ ND	multipeaks-not good separation	ND	10.48/ ND	multipeaks-not good separation	ND	5.2-5.4-5.8-9.93/ ND	multipeaks	ND	9.5-11.6-17.5-20.5-21.6/ ND	multipeaks	ND	7.28-10.15-12.03/ ND
L-Glutamine	+	good peak	5763853	18.1/17.92	good peak	19086221	14.47/14.63	low intensity	1045	5.05/5.29	not good peak	40683	22.4/21.8	low intensity	7467	16.2/15.87
L-Histidine	+	good peak	152000	25.84/26.02	tailing	629028	13.98/14.18	good peak	10002	4.74/4.9	ND	ND	ND	bad peak	28262	16.6/16.46

		ZICHILIC			ZIC-pHILIC			C18			Cogent Silica-C			BEH Amide		
Compound Name	Polarity	Comment STD/sample	Intensity of sample	RT STD/sample	Comment STD/sample	Intensity of sample	RT STD/sample	Comment STD/sample	Intensity of sample	RT STD/sample	Comment STD/sample	Intensity of sample	RT STD/sample	Comment STD/sample	Intensity of sample	RT STD/sample
L-Homoserine	+	good peak	1481689	18.1/17.38	good peak	874252	14.39/14.03	good peak	44128	5.07/5.23	good peak	1686186	22.3/21.71	good peak	748234	16.0/15.07
L-Isoleucine	+	not separated (leucine and isoleucine)	1430000	13.38/13	good peak	1863105	10.81/10.9	bad peak- but STD is good	19630	8.25/8.2	good peak	642368	20.16/20.64	good peak	407057	12.3/12.26
L-Kynurenine	+	good peak	ND	12.64/ ND	good peak	ND	10.32/ ND	not good peak	ND	11.27/ ND	good peak	ND	17.40/ ND	good peak	ND	11.08/ ND
L-Leucine	+	not separated (leucine and isoleucine)	1763173	13.08/13.14	good peak	1213105	10.33/10.39	bad peak- but STD is good	19630	6.94/7.54	good peak	777022	19.52/19.94	2 peaks	536221	9.69-11.71/11.73
L-Lysine	+	good peak	128000	27.16/27.55	good peak	46449	23.21/24.02	good peak	30006	4.6/4.42	good peak	ND	26.95/ ND	2 peaks	36000	17.1-24.16/24.15
L-Methionine	+	good peak	1272766	13.85/13.77	good peak	840145	10.98/11.1	not good peak	90236	6.9/6.6	good peak	1495641	19.4/19.6	good peak	599613	12.21/12.14
L-Ornithine	+	good peak	124000	27.13/27.53	good peak	48146	21.32/22.18	good peak	23311	4.67/4.78	bad separation	ND	ND	good peak - tailing	34489	22.52/22.3
L-Phenylalanine	+	good peak	511000	12.45/12.6	good peak	461620	9.64/9.78	not good peak	71001	10.44/10.32	bad peak	279807	17.98/18.2	good peak	241782	10.6/10.6
L-Proline	+	good peak	5110000	15.7/15.03	good peak	21412889	12.31/12.4	good peak	547718	5.4/5.54	good peak	38324	24.91/24.99	good peak	3925722	14.72/14.5
L-Serine	+	good peak	2527943	18.8/18.42	good peak	1020000	15.13/15.32	good peak	34043	5.01/4.75	good peak	769596	21.85/21.82	2 peaks	371439	10.15-16.45/16.07
L-Threonine	+	good peak	1481689	17.55/17.18	good peak	713973	13.8/13.95	good peak	37196	5.09/4.84	good peak	1686186	21.53/21.71	good peak	655240	15.23/15.07
L-Tryptophan	+	good peak	144734	12.86/13.14	good peak	62925	11.1/11.19	good peak	10986	12.6/12.47	good peak	53847	16.81/16.82	good peak	35941	10.89/10.88

		ZICHILIC			ZIC-pHILIC			C18			Cogent Silica-C			BEH Amide		
Compound Name	Polarity	Comment STD/sample	Intensity of sample	RT STD/sample	Comment STD/sample	Intensity of sample	RT STD/sample	Comment STD/sample	Intensity of sample	RT STD/sample	Comment STD/sample	Intensity of sample	RT STD/sample	Comment STD/sample	Intensity of sample	RT STD/sample
L-Tyrosine	+	good peak	ND	12.5/ ND	bad peak	ND	5.52/ ND	multi peaks	ND	7.0-9.7-9.9-11.3/ ND	multi peaks	ND	11.4-14.6-17.9/ ND	good peak	ND	7.19/ ND
L-Valine	+	good peak	1890000	15/14.99	good peak	554217	11.98/12.1	good peak	540488	5.78/5.48	good peak	358557	21.42/21.84	not separated(Betaine and Valine)	1355741	13.51/13.27
Nα-Acetyl-L-lysine	+	2 peaks	ND	16.48-18.46/ ND	good peak	ND	14.51/ ND	good peak	ND	5.41/ ND	good peak	ND	26.95/ ND	good peak	ND	17.1/ ND
O-Acetylcarnitine	+	good peak	87953	14.26/13.85	good peak	48116	10.55/10.46	not good peak	13337	5.99/6.11	good peak	32493	33.9/34.52	good peak	121861	14.02/13.79
Pantothenate	+	not good peak	73057	6.76/6.86	not good peak	158910	8.46/8.43	not good peak	3148	10.44/10.59	not good peak	15154	12.77/12.78	good peak	23776	8.83/9.12
Picolinic acid	+	bad peak	ND	6.83/ ND	good peak	ND	8.40/ ND	bad peak	ND	5.9/ ND	bad separation	ND	ND	bad peak	ND	8.5/ ND
Taurine	-	good peak	731535	15.84/15.82	good peak	205654	14.39/14.44	good peak	45353	5.13/5.22	good peak	108920	17.56/17.75	good peak	625044	12.69/12.74
5-Aminolevulinate	+	good peak	2810000	18.5/16.03	good peak	5476412	13.13/13.95	good peak	178494	5.26/5.26	good peak	ND	26.7/ ND	good peak	2260000	14.13/15.33
Saccharopine	-	good peak	5129	22.15/22.93	good peak	96974	15.22/15.21	good peak	ND	5.02/ ND	good peak	56552	20.87/20.97	good peak	15969	17.6/17.06
N-Acetyl-L-aspartate	+	good peak	830357	7.74/7.95	good peak	447632	14.27/14.23	not good peak	3307	6.72/6.74	multi peaks-v. low int	515	14.6-14.8-15.8/14.59	good peak	14713	13.9/13.73
N-Acetyl-L-glutamate	+	not good peak	1168383	7.41/7.67	good peak	228473	13.8/13.85	good peak	18931	17.0/16.95	2 peaks-v. low int	421	7.5-15.08/15.07	2 peaks	140997	4.38-13.36/13.32
S-Adenosyl-L-homocysteine	+	2 peaks/ v.low int	573	20.58-22.2/20.15	v.low int	673	12.91/12.96	good peak	ND	5.8/ ND	low intensity	1280	22.53/22.58	good peak	ND	16.12/ ND

		ZICHILIC			ZIC-pHILIC			C18			Cogent Silica-C			BEH Amide		
Compound Name	Polarity	Comment STD/sample	Intensity of sample	RT STD/sample	Comment STD/sample	Intensity of sample	RT STD/sample	Comment STD/sample	Intensity of sample	RT STD/sample	Comment STD/sample	Intensity of sample	RT STD/sample	Comment STD/sample	Intensity of sample	RT STD/sample
Betaine	+	good peak	2103205	15.87/15.21	good peak	1855883	10.83/10.91	good peak	432525	5.37/5.06	good peak	790431	27.9/28.46	not separated (Betaine and Valine)	1355741	13.4/13.27
Sarcosine	+	not separated (Alanine and sarcosine)	241428	16.33/16.12	good peak	5978	13.49/13.61	not separated (Alanine,beta-Alanine and sarcosine)	27318	5.41/5.29	not separated(Alanine,beta-Alanine and sarcosine)	27308	24.85/25.17	not separated(Alanine,beta-Alanine and sarcosine)	307801	15.36/15.6
B-alanine-methyl-ester	+	good peak	20764	15.29/15.22	not good peak	136214	12.38/13.7	not good peak	9379	5.6/5.12	bad separation	ND	ND	high noise	ND	6.45-11.29
2-Indolecarboxylicacid	-	not good peak	ND	5.58-6.10/ ND	good peak	ND	7.01/ ND	good peak	ND	22.04/ ND	good peak	ND	6.6/ ND	bad peak	ND	5.45/ ND
DL-3-aminobutyrate	+	multi peaks	ND	15.9-17.41/ ND	good peak	ND	13.50/ ND	2 peaks	ND	5.26-5.6/ ND	good peak	ND	25.11/ ND	good peak	ND	15.30/ ND
N(pi)-Methyl-L-histidine	+	good peak	ND	26.24/ ND	v.low int	3818	12.17/12.04	good peak	ND	4.8/ ND	tailing	ND	35.78/ ND	good peak	ND	15.96/ ND
trans-4-Hydroxy-L-proline	+	good peak	2806382	16.31/16.03	good peak	5476412	13.94/13.95	good peak	178494	5.14/5.26	good peak	88704	22.45/22.94	good peak	3134329	15.65/15.33
(R)-S-Lactoylglutathione	+	good peak	ND	14.64/ ND	good peak	ND	12.98/ ND	good peak	ND	6.9/ ND	good peak	ND	17.14/ ND	good peak	ND	14.5/ ND
Glutathione	-	good peak	7396764	15.71/15.02	good peak	5719604	ND /13.94	good peak	128539	ND /5.86	good peak	173662	17.5/17.71	good peak	37800	ND /14.8

		ZICHILIC			ZIC-pHILIC			C18			Cogent Silica-C			BEH Amide		
Compound Name	Polarity	Comment STD/sample	Intensity of sample	RT STD/sample	Comment STD/sample	Intensity of sample	RT STD/sample	Comment STD/sample	Intensity of sample	RT STD/sample	Comment STD/sample	Intensity of sample	RT STD/sample	Comment STD/sample	Intensity of sample	RT STD/sample
Sugars																
D-Fructose	-	multi peaks	83313	12.75/13.79	multi peaks	303715	13.42/13.84	not good peak	3289	5.28/4.85	2 peaks	189387	12.3-15.5/15.99	2 peaks	87294	13.77/14.65
D-Galactose	-	multi peaks	122000	14.36/14.33	multi peaks	643000	14.36/14.65	not good peak	3289	5.22/4.85	2 peaks	159000	16.3-17.63/18.94	2 peaks	481253	15.04-17.79/17.76
D-Mannose	-	multi peaks	73751	13.23/13.77	multi peaks	303715	13.50/13.84	not good peak	3289	5.28/4.85	good peak	189387	15.67/15.99	2 peaks	87294	13.77-14.12-14.79/14.65
Maltose	-	bad-low intensity	6350	15.47-16.04/15.04	bad-low intensity	2819	15.43/14.61	not good peak	ND	5.19/ ND	2 peaks	ND	12.6-17.65/ ND	bad-low intensity	3916	17.79/16.94
D-Xylose	-	not good peak	11300	11.83-12.78/10.36	multi peaks	9528	12.44/12.43	bad peak-low int	ND	15.36/ ND	multi peaks	ND	12.8-14.33-15.1/ ND	bad-low intensity	ND	12.43/ ND
D-Glucosamine	+	binary peak	ND	23.45-23.86	binary peaks	ND	13.86-14.20/ ND	ND	ND	ND	too brode	ND	32.77	2 peaks	ND	11.21-15.17/ ND
N-Acetyl-D-glucosamine	+	2 peaks-low int	1919	11.71/11.87	good peak-low int	2378	11.34/11.36	ND	ND	ND	good peak	ND	16.16/ ND	forked peak	ND	12.93-13.16/ ND
D-Glucose	-	multi peaks	86386	13.93-14.44/14.34	multi peaks	303715	14.23/13.84	not good peak	3289	5.2/4.85	good peak	189387	15.88/15.99	2 peaks	87294	14.8/14.65
Cis-Aconitate(Dehydro ascorbic acid)	-	not good peak	41276	6.8-7.5-10.8/7.47	multi peaks	70703	11.3-13.8-17.7-18.5/17.49	ND	ND	ND	2 peaks-bad peak	ND	10.63-13.58	multi peaks	ND	9.03-13.01-16.02-16.57
N-Acetyl-D-mannosamine	+	2 peaks	ND	11.9-13.09	low int-good peak	2378	11.64/11.36	ND	ND	ND	good peak	ND	16.4/ ND	good peak	ND	12.89/ ND

		ZICHILIC			ZIC-pHILIC			C18			Cogent Silica-C			BEH Amide		
Compound Name	Polarity	Comment STD/sample	Intensity of sample	RT STD/sample	Comment STD/sample	Intensity of sample	RT STD/sample	Comment STD/sample	Intensity of sample	RT STD/sample	Comment STD/sample	Intensity of sample	RT STD/sample	Comment STD/sample	Intensity of sample	RT STD/sample
Carboxylic Acids																
(R)-Malate (Malic acid)	-	too broad-multi peaks	107047	8.8-9.5-10.8/10.42	good peak	1615866	15.64/15.62	good peak	ND	5.94/ ND	too brode-tailing	ND	13.6/ ND	bad peak	49182	14.57/14.27
Phthalate	+	tailing	ND	6.48/ ND	good peak	ND	13.4/ ND	good peak	ND	14.85/ ND	not good peak	ND	6.51/ ND	bad peak	ND	10.58/ ND
2-Hydroxybutanoic acid	-	not good peak	2918	6.26/6.96	good peak	ND	7.78/ ND	forked peak	ND	9.4/ ND	good peak	ND	9.13/ ND	2 peaks	ND	7.65-17.33/ ND
2-Oxoglutarate	-	multi peaks- bad separation	30258	6.9-7.7-10.8/8.9-9.9	good peak	573641	15.26/15.24	bad peak	ND	5.83/ ND	not good peak	ND	11.12/ ND	binary peak	45575	12.34-12.42/12.21
4-Coumarate	-	ND	ND	ND	good peak	ND	8.68/ ND	2 peaks	ND	17.1-17.6/ ND	good peak	ND	7.99/ ND	good peak	ND	6.8/ ND
4-hydroxylphenylacetate	-	ND	ND	ND	good peak	ND	8.78/ ND	good peak	ND	15.69/ ND	good peak	ND	8.22/ ND	good peak	ND	6.8/ ND
Ascorbate	-	not good peak	ND	10.84/ ND	good peak	71653	14.26/14	ND	ND	ND	not good peak	4296	10.5/9.62	not good peak	ND	9.09/ ND
Caffeate	-	ND	ND	ND	tailing	ND	11.16/ ND	2 peaks	ND	14.9-15.5/ ND	multi peaks-bad separation	ND	7.6-8-8.7/ ND	tailing	ND	7.2
Citramalate	-	multi peaks	6222	7.7-8.2-9.1-10.8-12.1/8.26	good peak	3004334	14.74/14.82	good peak	3392	6.8/6.4	too brode-bad peak	89660	7.8-9.7-11.3-12.6/13.57	good peak	275272	13.86/13.62
Diethyl 2-oxoglutarate	-	bad- low intensity	1469	5.38/5.73	tailing-multi peaks	ND	3.95-4.55/ ND	ND	ND	ND	good peak	ND	8.10/ ND	good peak	7388	4.46/4.8

		ZICHILIC			ZIC-pHILIC			C18			Cogent Silica-C			BEH Amide		
Compound Name	Polarity	Comment STD/sample	Intensity of sample	RT STD/sample	Comment STD/sample	Intensity of sample	RT STD/sample	Comment STD/sample	Intensity of sample	RT STD/sample	Comment STD/sample	Intensity of sample	RT STD/sample	Comment STD/sample	Intensity of sample	RT STD/sample
Fumarate	-	multi peaks	139656	6.43/7.94	good peak	288461	15.64/15.65	2 peaks	ND	7.06-8.3/ ND	good peak	ND	12.09/ ND	good peak	108506	12.73/13.72
Gallate	-	ND	ND	ND	tailing	ND	17.77/ ND	bad peak	ND	9.8/ ND	tailing	ND	8.2/ ND	bad peak	ND	9.7/ ND
Isocitrate	-	multi peaks- bad separation	124724	10.5-11.9-12.1-12.7-14.21/12.24	good peak	2016184	18.02/17.55	bad peak-low int	18284	5.88/6.3	multi peaks-bad separation	ND	15.13-15.5-18.09/ ND	taling	396964	17.33/17.54
Isonicotinic acid	+	ND	ND	ND	good peak	ND	7.5/ ND	good peak	74958	5.69/5.2	too broad	ND	9.5/ ND	not good peak	ND	7.69/ ND
Itaconate	-	multi peaks- bad separation	111240	5.6-6.5-9.9/8.24	good peak	382439	14.7/14.8	multi peaks	ND	5.75-11.11-13.92/ ND	multi peaks-bad separation	ND	7.6-8.5-11.3/ ND	multi peaks-bad separation	ND	5.1-6.3-9.1-12.3-13.1-17.3
Maleic acid	-	ND	ND	ND	not good peak	ND	12.36/ ND	not good peak	ND	6.99/ ND	2 peaks	ND	5.8-14.7/ ND	multi peaks-bad separation	108506	6.19-13.96/13.72
Malonate	-	ND	ND	ND	good peak/ not good peak	18845	15.35/14.94	bad peak	ND	6.13/ ND	taling	ND	7.94/ ND	binary peak/too bad peak	8469	13.7-14.15/12.78
Mesaconate	-	bad peak	ND	6.2/ ND	multi peaks	ND	7.5-12.04-15.09/ ND	multi peaks	ND	9.8-10.6-11.2-13.8/ ND	multi peaks	ND	9.21-9.59-12.34/ ND	multi peaks-bad separation	ND	6.9-12.07-12.7/ ND
Methylmalonate	-	not good peak	17046	6.6/6.8	good peak	51070	14.5/14.7	bad peak	ND	9.3-10.4/ ND	taling	ND	7.5/ ND	binary peak	ND	12.89/ ND
Oxalate	-	ND	ND	ND	good peak/ not good peak	41121	17.26/16.8	bad peak	ND	5.4/ ND	bad peak	ND	16.6/ ND	good peak/multi and bad peaks	55422	15.26/15.8

		ZICHILIC			ZIC-pHILIC			C18			Cogent Silica-C			BEH Amide		
Compound Name	Polarity	Comment STD/sample	Intensity of sample	RT STD/sample	Comment STD/sample	Intensity of sample	RT STD/sample	Comment STD/sample	Intensity of sample	RT STD/sample	Comment STD/sample	Intensity of sample	RT STD/sample	Comment STD/sample	Intensity of sample	RT STD/sample
Pyruvate	-	multi peak-bad separation	27100	6.8-8.7-9.4-14.9/6.7	good peak	100623	16.9/17.4	multi peaks	ND	7.01-11-12.5/ ND	not good peak	ND	9.5/ ND	multi and bad peaks	19005	6.9-11.4-14.3/14.75
Succinate	-	good peak	273993	6.8/6.8	good peak	58827	14.8/14.8	2 peaks	ND	6.9-8.9/ ND	bad peak	14878	12.52/12.41	good peak/multi and bad peaks	ND	13.6/ ND
D-Glucuronate	-	ND	ND	ND	2 peaks	ND	9.8-15.79/ ND	good peak	ND	5.16/ ND	multi peaks	ND	8.5-9.6-10.9-11.9/ ND	good peak/multi and bad peaks	ND	15.04/ ND
Nucleosides & Nucleotides																
5'-Methylthioadenosine	+	good peak	95078	10.85/11.02	good peak	43175	7.02/7.10	not good peak	10499	11.74/11.71	good peak	30112	12.10/12.06	good peak	18476	7.02/7.39
Adenosine	+	good peak	1456	13.39/13.45	good peak	1425	8.4/8.5	ND	ND	ND	good peak	983975	14.8/14.26	good peak	ND	9.87/ ND
Cytidine	+	good peak	ND	19.92/ ND	good peak	1011	11.34/11.45	ND	ND	ND	good peak	58306	16.28/15.75	good peak	ND	12.15/ ND
Guanosine	+	ND	ND	ND	ND	ND	ND	ND	ND	ND	ND	ND	ND	ND	ND	ND
Inosine	+	good peak	ND	10.52/ ND	good peak	ND	10.35/ ND	ND	ND	ND	good peak	ND	14.85/ ND	good peak	ND	11.14/ ND
Thymidine	-	good peak	ND	7.33/ ND	good peak	1141	7.04/7.16	multi peaks	ND	9.7-10.08/ ND	good peak	ND	11.9/ ND	good peak	ND	7.83/ ND
IMP (inosine monophosphate)	-	good peak	3250	14.8/14.82	good peak	1120	15.02/15.09	good peak	7676	5.7/5.85	good peak	ND	17.69/ ND	good peak	3893	16.83/16.18
Allantoin	-	good peak	ND	12.67/ ND	good peak	ND	13.45/ ND	good peak	ND	5.52/ ND	good peak	ND	12.74/ ND	good peak	ND	10.62/ ND
CMP	-	good peak	ND	19.82/ ND	good peak	ND	15.34/ ND	good peak	ND	5.3/ ND	good peak	ND	18.85/ ND	good peak	ND	17.42/ ND

		ZICHILIC			ZIC-pHILIC			C18			Cogent Silica-C			BEH Amide		
Compound Name	Polarity	Comment STD/sample	Intensity of sample	RT STD/sample	Comment STD/sample	Intensity of sample	RT STD/sample	Comment STD/sample	Intensity of sample	RT STD/sample	Comment STD/sample	Intensity of sample	RT STD/sample	Comment STD/sample	Intensity of sample	RT STD/sample
UMP	-	good peak	2234	14.52/14.75	good peak	18349	14.75/14.76	good peak	3655	5.52/5.22	good peak	66934	16.9/16.94	good peak	ND	16.49/ ND
AMP	+	good peak	7846	17.63/17.28	good peak	9664	13.3/13.17	good peak	3553	5.6/5.6	good peak	108749	18.13/18.37	good peak/low int	6597	15.95/15.41
dAMP	+	good peak	ND	17.14/ ND	good peak	ND	12.31/ ND	good peak	ND	5.81/ ND	good peak	ND	18.43/ ND	good peak	ND	15.36/ ND
GMP	+	good peak	1611	16.95/16.95	good peak	5342	16.15/ 16.17	good peak	3309	5.77/5.42	tailing	2614	17.8/17.9	good peak/low int	6058	17.7/18.3
NAD+	+	not good peak	34081	20.4/20.12	good peak	196762	13.68/13.67	good peak	25179	5.69/5.76	good peak	125905	18.75/18.86	good peak	57059	17.08/16.48
Purines & Pyrimidines																
Adenine	-	2 peaks	10027	15.43/14.75	multi peaks	1853	7.01-8.9-9.10/7.07-9.16	good peak	ND	5.78/ ND	multi peaks	ND	12.16-15.8-16.01/ ND	multi peaks	ND	7.03-9.59-9.86/ ND
Guanine	+	2 peaks	ND	12.5-14.6/ ND	good peak/low int	1894	11.79/11.9	multi peaks	ND	5.7-7.02-8.8/ ND	binary peak	ND	15.4/ ND	2 peaks	ND	11.4-12.5/ ND
Hypoxanthine	-	good peak	3935	9.6/9.8	good peak	ND	9.68/ ND	not good peak	ND	6.04/ ND	good peak	ND	14.69/ ND	good peak/low int	6269	9.8-11.13/10.07
1,7-DimethylXanthine (Paraxanthine)	-	ND	ND	ND	good peak	ND	6.9/ ND	ND	ND	ND	good peak	ND	11.92/ ND	good peak	ND	6.8/ ND

		ZICHILIC			ZIC-pHILIC			C18			Cogent Silica-C			BEH Amide		
Compound Name	Polarity	Comment STD/sample	Intensity of sample	RT STD/sample	Comment STD/sample	Intensity of sample	RT STD/sample	Comment STD/sample	Intensity of sample	RT STD/sample	Comment STD/sample	Intensity of sample	RT STD/sample	Comment STD/sample	Intensity of sample	RT STD/sample
Xanthine	-	ND	ND	ND	good peak/low intensity	2611	11.08/11.09	2 peaks	ND	6.9-8.5/ ND	good peak	ND	12.82/ ND	good peak	ND	10.30/ ND
Pyridoxamine	+	good peak	ND	29.02/ ND	bad peak	ND	10.48/ ND	good peak	ND	4.88/ ND	bad peak	ND	19.6/ ND	bad peak	ND	14.56/ ND
Cytosine	+	2 peaks	ND	18.4-19.9/ ND	good peak	9920	10.7/10.03	2 peaks	ND	5.2-5.6/ ND	binary peak	22149	16.2-16.8/15.75	2 peaks	ND	10.7-12.13/ ND
Alloxanthine	-	good peak	ND	8.44/ ND	good peak/low intensity	2611	10.12/11	good peak	ND	7.01/ ND	not good peak	ND	11.4/ ND	bad peak	ND	8.77/ ND
Pterins																
Biopterin	-	good peak	ND	12.12/ ND	good peak	ND	11.01/ ND	good peak	ND	6.9/ ND	good peak	ND	15.18/ ND	good peak	ND	11.27/ ND
Dihydrobiopterin	+	ND	ND	ND	good peak	ND	8.33/ ND	ND	ND	ND	good peak	ND	13.54/ ND	good peak	ND	8.59/ ND
Riboflavin	+	good peak	ND	8.09/ ND	binary peaks	ND	7.20-7.79/ ND	multi peaks	ND	14.03-16.99/ ND	multi peaks	ND	9.5-13.4/ ND	multi peaks	ND	7.3-7.6-8.3-10.06/ ND
Sepiapterin	+	good peak	ND	7.86/ ND	good peak	ND	7.04/ ND	good peak	ND	11.8/ ND	good peak	ND	12.6/ ND	good peak	ND	7.62/ ND
Amines																
Acetylcholine	+	good peak	20678	14.95/14.8	good peak	1027	14.93/14.90	good peak	6222	5.64/5.77	ND	ND	ND	good peak	7910	15.59/16.6
4-Hydroxyphenylacetaldoxime	-	good peak	ND	6.68/ ND	good peak	2499	7.19/7.79	good peak	ND	11.4/ ND	tailing	ND	11.4/ ND	not good peak	ND	6.7/ ND
Triethanolamine	+	good peak	12607	19.39/18.84	good peak	10528	8.6/8.9	good peak	1951	5.14/5.23	ND	ND	ND	good peak	ND	9.69/ ND

		ZICHILIC			ZIC-pHILIC			C18			Cogent Silica-C			BEH Amide		
Compound Name	Polarity	Comment STD/sample	Intensity of sample	RT STD/sample	Comment STD/sample	Intensity of sample	RT STD/sample	Comment STD/sample	Intensity of sample	RT STD/sample	Comment STD/sample	Intensity of sample	RT STD/sample	Comment STD/sample	Intensity of sample	RT STD/sample
1-Phenylethylamine	+	good peak	4555	12.9/13.4	too broad	ND	19.22/ ND	bad peak	ND	12.08/ ND	ND	ND	ND	tailing	ND	11.14/ ND
1-(4-Hydroxyphenyl)-2-aminoethanol	+	2 peaks	ND	17.14-17.8/ ND	good peak	ND	18.02/ ND	good peak	ND	5.8/ ND	tailing	ND	5.8/ ND	good peak	ND	12.57/ ND
Sugar Phosphates																
D-Glucosamine 6-phosphate	-	tailing	ND	21.55/ ND	good peak	ND	15.79/ ND	good peak	ND	4.95/ ND	good peak with tailing	ND	19.6/ ND	good peak	ND	18.29/ ND
N-Acetyl-D-Glucosamine6-Phosphate	+	multi peaks	ND	14.6-15.5-16.2/ ND	good peak	ND	14.71/ ND	good peak	ND	5.12/ ND	good peak	ND	18.25/ ND	2 peaks	ND	16.5-17.10/ ND
D-Glucose 6-phosphate	-	binary peak	16441	17.4/17.6	good peak	11610	16.35/16.31	tailing	ND	5.01/ ND	tailing	31314	18.09/18.8	good peak	11686	18.40/17.7
Miscellaneous																
Ethanolamine phosphate	-	good peak	39956	19.43/19.39	good peak	6288	15.45/15.21	good peak	41972	5.01/5.1	good peak	126823	25.6/25.8	good peak	272285	18.3/17.6
L-Metanephrine	+	good peak	ND	15.16/ ND	good peak	ND	16.7/ ND	2 peaks	ND	7.02-8.5/ ND	too broad	ND	15.2/ ND	good peak	ND	14.6/ ND
L-Adrenaline	+	not good peak	ND	16.9/ ND	too broad	ND	23.6/ ND	good peak	ND	5.79/ ND	ND	ND	ND	too broad and bad sep	ND	18.4/ ND
L-Noradrenaline	+	not good peak	ND	15.9/ ND	good peak	178922	7.96/7.7	multi peaks-bad sep	ND	6.1-6.4-7.7-10.5-11.02-12.2/ ND	multi peaks-bad sep	5878	11.3-13.5-15.97/16.2	not good peak	ND	8.6/ ND

Key to comments in table 3.1

2 peaks: there are 2 peaks in the cell extract sample chromatogram with good separation and symmetry.

Bad peak: low intensity of multiple not separated well peaks.

Binary peak: there are 2 peaks in the cell extract sample chromatogram but not separated or splitted peak.

Good peak: narrow and symmetric peak shapes with high intensity.

Multi peaks: more than 3 peaks in the cell extract sample chromatogram with not good separation.

ND: not detected cell extract.

Not good peak: fronting, forked or broad (its width more than 1 and less than 2.5 minutes) peaks.

Not separated: the isomers not separated.

Taling: the peak has tailing.

Too broad: the peak is too broad, its width more than 2.5 minutes.

Table 3.2 Summary of the five different columns performance through metabolites detected by their classifications.

	ZIC-HILIC	ZIC-pHILIC	C18	Cogent Silica-C	BEH Amide
Amino acids	Most of amino acids (76%) had excellent shape and symmetric peaks under HILIC conditions and gave higher intensity in positive ionization mode due to positive charging of their amino group. Pantothenate, Picolinic acid, N-Acetyl-L-glutamate and 2-Indolecarboxylic acid had less retention (< 8 min) in the column so they did not give a good peak shape because acidic metabolites are only partially ionized under the conditions of ZIC-HILIC+FA (mobile phase A pH=2.8) . These conditions also did not separate the isomers of beta-	Most of amino acids (90%) had excellent shape and symmetrical peaks under pHILIC condition and gave higher intensity in positive ionization mode due to positive charging of their amino group. The hydrophilic amino acids Lys and Arg eluted much later at significantly higher water contents and eluted in slightly broader peaks. Ectoine and tyrosine had additional weakly acidic groups so they may be partially ionized under the conditions of ZIC-pHILIC+AC (mobile phase A pH=9.2) and that may be the reason behind their bad peak shapes. In addition the high pH may be responsible for cysteine oxidation and dimerization behavior which happens under more basic conditions the -SH group is more capable of being oxidized and replaced by -SR, where R is anything except for hydrogen leading to bad peak shape with ZIC-pHILIC+AC condition on the other hand at low pH the	About 90% of amino acids eluted early as sharp spikes in reversed phase column (before 7 minutes). Additionally the column did not separate any of the isomers as in pHILIC condition.	About 50% of amino acids are separated by the silica-C column and ammonium acetate mobile phase with good shape and symmetric peaks. The hydrophilic amino acids cystathionine, cysteine, cystine, glutamine, aspartate, N (pi)-methyl-L-histidine and arginine eluted much later at significantly higher water contents and eluted in slightly broader peaks with significant tailing. Pantothenate showed fronting and too broad a peak. The amino acids isomers (isoleucine/ leucine) and (4-aminobutyric acid/ 3-aminobutyric acid) and (Cis-4-hydroxy D-proline/Trans-4-hydroxy	About 65% of amino acids separated by the BEH Amide column and ammonium carbonate mobile phase with good shape and symmetric peaks. The amino acids isomers (isoleucine/ leucine) and (4-aminobutyric acid/ 3-aminobutyric acid) and (Cis-4-hydroxy D-proline/Trans-4-hydroxy D-proline) separated while (beta-alanine/ alanine/ sarcosine) and valine/betaine were not.Cysteine and acetyl-L-serine showed multiple peaks. Histidine, picolinic acid, β-alanine-methyl-ester and 2-indolecarboxylicacid showed bad peaks which are too broad (more than 3 minutes) and multiple peaks. Leucine, lysine,

	alanine, alanine and sarcosine very well or the isomers of isoleucine and leucine.	equilibrium is shifted to the reduced, -SH form as in ZIC-HILIC+FA which shows a good peak for cysteine. However, this condition was very good in separation of isomers (beta-Alanine/ Alanine/ sarcosine), and (Isoleucine/ Leucine) and (4-aminobutyric acid/ 3- aminobutyric acid) and (Cis-4-hydroxy D-proline/Trans-4-hydroxy D-proline) and, (Valine/Betaine).Pantothenate and β-alanine-methyl-ester showed poor peaks. Malonate and oxalate showed good peaks with the standards but not good in the cell extracts.		D-proline) and (valine/betaine) separated while (beta-alanine/ alanine/ sarcosine) are not.Glutamic acid, O-acetyl-L-serine, tyrosine, N-acetyl-L-aspartate and N-acetyl-L-glutamate showed multiple peaks. Histidine, ornithine, phenylalanine, picolinic acid and β-alanine-methyl-ester showed bad separation and the peaks could not be detected.	serine and N-Acetyl-L-glutamate showed good peaks.

	ZIC-HILIC	ZIC-pHILIC	C18	Cogent Silica-C	BEH Amide
Sugars	ZICHILIC conditions were not good for sugar separation. All sugars gave multiple peaks. Amino sugars (Glucosamine, N-Acetyl-D-glucosamine, N-Acetyl-D-mannosamine) showed two peaks for each compound. D-Fructose and D-Mannose eluted at the same retention time. D-Galactose and D-Glucose eluted at the same retention time. D-Xylose, N-Acetyl-D-glucosamine and N-Acetyl-D-mannosamine eluted at the same retention time. Separation is complicated by the presence of alpha and beta anomers of the sugars.	ZIC-pHILIC conditions were not good for sugar separation. All the reducing sugars and maltose, fructose, glucose, galactose and mannose gave multiple peaks. Amino sugars (Glucosamine, N-Acetyl-D-glucosamine, N-Acetyl-D-mannosamine) showed good peaks. D-Fructose and D-mannose eluted at the same retention time. D-Galactose and D-glucose eluted at the same retention time. N-Acetyl-D-glucosamine and N-Acetyl-D-mannosamine eluted at the same retention time.	All reducing sugars eluted early as sharp spikes in reversed phase column (at the same retention time of 5.2 minutes). Amino sugars (Glucosamine, N-Acetyl-D-glucosamine, N-Acetyl-D-mannosamine) were not detected. Elution at the void volume makes it more likely that analytes will not be detected as a result of ion suppression effects.	About 40% of the sugars have good peaks with silica-C conditions (Mannose, N-acetyl-D-glucosamine, D-glucose, N-acetyl-D-mannosamine) which were not separated by ZICHILIC or C18 conditions. While D-Fructose, D-Galactose, Maltose, and Cis-Aconitate showed two peaks for each compound. However, D-Xylose gave multipl peaks and D-Glucosamine showed too broad a peak. D-Fructose and D-mannose eluted in the same retention time. D-Galactose and D-glucose eluted in the same retention time. D-Xylose, N-Acetyl-D-glucosamine and N-Acetyl-D-mannosamine eluted in the same retention time.	About 50% of sugars gave two peaks for each compound. Amino sugars (N-Acetyl-D-glucosamine, N-Acetyl-D-mannosamine) had good peaks under these conditions. While Maltose and D-Xylose had bad separation. D-Fructose and D-mannose eluted in the same retention time. D-Galactose and D-glucose eluted in the same retention time. D-Xylose, N-Acetyl-D-glucosamine and N-Acetyl-D-mannosamine eluted in the same retention time.

	ZIC-HILIC	ZIC-pHILIC	C18	Cogent Silica-C	BEH Amide
Carboxylic Acids	Only Succinate had excellent shape and a symmetric peak under ZIC HILIC conditions. 30% of acids poor peaks and 26% gave multiple peaks due to the partially ionized of acid at pH 2.8 of 0.1% formic acid mobile phase while the other 39% were not detected by HILIC condition : 4-Coumarate, 4-hydroxylphenylacetate , caffeate, gallate, isonicotinic acid, maleic acid, malonate, oxalate and D-Glucuronate which might be due to incomplete ionisation these conditions.	Most of carboxylic acids (82%) had excellent shape and symmetric peaks under pHILIC conditions and gave higher intensity in negative ionization mode due to negative charging of their carboxylic group since they are completely ionized at pH9.2. D-Glucuronate has two peaks and maleic acid, mesaconate and Diethyl 2-oxoglutarate gave multiple peaks. This condition was very good for separation of isomers (Methylmalonate/ succinate) and Fumarate/ Maleic acid.	26% of carboxylic acids (Malate, phthalate, 4-hydroxylphenylacetate, citramalate, isonicotinic acid, and D-glucuronate) had good peaks in RPC condition while the others gave bad separation and multiple peaks. Ascorbate and Diethyl 2-oxoglutarate were not detected.	About 22% of carboxylic acids (2-Hydroxybutanoic acid, 4-coumarate, 4-hydroxylphenylacetate, diethyl 2-oxoglutarate, fumarate) had good peaks under Silica-C conditions while the others gave too broad, tailing) or multiple peaks. Maleic acid showed two peaks.	About 35% of carboxylic acids (4-Coumarate, 4-hydroxylphenylacetate, Citramalate, Diethyl 2-oxoglutarate, Fumarate, Oxalate, Succinate, D-Glucuronate) had good peaks under the BEH-amide conditions while the others gave poor (too broad and tailing) and multiple peaks. 2-Hydroxybutanoic acid and 2-Oxoglutarate showed two peaks for each compound.

	ZIC-HILIC	ZIC-pHILIC	C18	Cogent Silica-C	BEH Amide
Nucleoside & Nucleotide	All nucleosides and nucleotides had excellent shape and symmetrical peaks under ZICHILIC conditions and gave higher intensity in positive ionization mode apart from thymidine, IMP, Allantoin, CMP, and UMP which had higher response in negative ionization mode. Except NAD+ did not give a good peak.	All nucleosides and nucleotides had excellent shapes and symmetric peaks under pHILIC conditions and gave higher intensity in positive ionization mode (Thymidine, IMP, Allantoin, CMP, and UMP gave greater response in negative ionization mode).	Most of Nucleosides were not separate by the RP column and all the nucleotides eluted early as sharp spikes peaks (at the same retention time 5.5 minutes).	All nucleosides and nucleotides had excellent shape and symmetric peaks under Silica-C conditions and gave higher intensity in positive ionization mode (Thymidine, IMP, Allantoin, CMP, and UMP had higher response in negative ionization mode). Except GMP had tailing.	All nucleosides and nucleotides had excellent shape and symmetric peaks under BEH-amide conditions and gave higher intensity in positive ionization mode (Thymidine, IMP, Allantoin, CMP, and UMP in gave greater response in negative ionization mode). Under these conditions the best separation of nucleosides and nucleotides were achieved and there was no overlap in retention time.

	ZIC-HILIC	ZIC-pHILIC	C18	Cogent Silica-C	BEH Amide
Purines & Pyrimidins	Hypoxanthine, Pyridoxamine and Alloxanthine had excellent shape and symmetric peaks on HILIC condition. Adenine, Guanine and Cytosine showed two peaks under these this conditions. 1,7-DimethylXanthine and Xanthine were not detected.	Most of Purines and Pyrimidins had excellent shape and symmetric peaks on pHILIC condition. However, Adenine and Pyridoxamine had bad separation.	Adenine, Pyridoxamine and Alloxanthine eluted early as sharp spikes under RPC conditions. Guanine, Hypoxanthine gave not good peaks. Xanthine and Cytosine showed two peaks in this condition. 1,7-DimethylXanthine did not detected. All of them eluted before 7 minutes).	Hypoxanthine, 1,7-DimethylXanthine and Xanthine had excellent shape and symmetric peaks under Silica-C conditions. However, Adenine, Pyridoxamine and Alloxanthine had bad separation. Guanine and Cytosine showed binary peaks.	Hypoxanthine, 1,7-DimethylXanthine and Xanthine had excellent shape and symmetric peaks under BEH-amide conditions. However, Adenine, Pyridoxamine and Alloxanthine had bad separation. Guanine and Cytosine showed two peaks.

	ZIC-HILIC	ZIC-pHILIC	C18	Cogent Silica-C	BEH Amide
Pterins	All the pterins had excellent peak shapes and symmetric peaks under ZICHILIC conditions and gave higher intensity in positive ionization mode. But dihydrobiopterin was not detected under these conditions. Riboflavin showed a good peak in these conditions only. The isomers (Biopterin/ Sepiapterin) were separated.	All Pterins had excellent shape and symmetric peaks under pHILIC conditions and gave higher intensity in positive ionization mode. But riboflavin showed binary peaks under these conditions. This condition was very good for the separation of isomers (Biopetrin /Sepapetrin).	Biopterin and sepiapterin had excellent shapes and symmetric peaks under RPC conditions. But riboflavin showed multiple peaks and Dihydrobiopterin was not detected under these conditions.	All Pterins had excellent shapes and symmetric peaks under Silica-C conditions and gave higher intensity in positive ionization mode. But riboflavin showed multiple peaks under these conditions. The isomers (Biopterin/ Sepiapterin) were separated.	All Pterins had excellent shape and symmetric peaks under BEH-amide conditions and gave higher intensity in positive ionization mode. But riboflavin showed multiple peaks under these conditions. The isomers (Biopterin/ Sepiapterin) were separated.

	ZIC-HILIC	ZIC-pHILIC	C18	Cogent Silica-C	BEH Amide
Amines	All the amines gave excellent shapes and symmetric peaks under ZIC HILIC conditions and gave higher intensity in positive ionization mode due to positive charging of their amino group. However, 1-(4-Hydroxyphenyl)-2-aminoethanol showed two peaks under these conditions.	All the amines gave excellent shapes and symmetric peaks under pHILIC conditions and gave higher intensity in positive ionization mode due to positive charging of their amino group. However, 1-phenylethylamine showed a broad peak under pHILIC conditions.	All the amines gave excellent shape and symmetric peaks under C18 conditions and eluted early. However, 1-phenylethylamine showed a bad peak shape under RPC conditions.	Only 4-Hydroxyphenylacetaldoxime and 1-(4-Hydroxyphenyl)-2-aminoethanol showed tailing peaks under Silica-C conditions while the others were not detected.	All the amines gave excellent shape and symmetric peaks under BEH-amide conditions. However, 1-phenylethylamine and 4-hydroxyphenylacetaldoxime did not show good peaks.
Sugar Phosphates	All the sugar Phosphates did not have good separation under ZICHILIC conditions.	pHILIC condition is the best condition to separate Sugar Phosphates. All Sugar Phosphates gave good peaks under pHILIC conditions. This condition was very good in separation of the isomers DL-glyceraldehyde 3-phosphate and dihydroxy-acetone phosphate.	All Sugar Phosphates eluted early as sharp spikes under RPC condition (before 5 minutes).	All Sugar Phosphates had good peak on Silica-C conditions, apart from D-Glucose 6-phosphate which had tailing.	All Sugar Phosphates had good peaks under BEH-amide conditions apart from N-Acetyl-D-Glucosamine 6-Phosphate which showed two peaks.
Miscellaneous	Ethanolamine phosphate and L-Metanephrine had good separation under ZICHILIC conditions. L-Adrenaline and L-oradrenaline showed broad and multiple peaks probably due to their instability.	Ethanolamine phosphate, L-metanephrine and L-Noradrenaline had good separation under pHILIC conditions. L-Adrenaline gave broad peaks.	Ethanolamine phosphate and L-noradrenaline eluted early as sharp spikes under RPC conditions (before 6 minutes). L-Adrenaline and L-metanephrine showed multiple peaks.	Only Ethanolamine phosphate had a good peak under Silica-C conditions. L-Noradrenaline and metanephrine showed broad and multiple peaks. L-Adrenaline was not detected.	Ethanolamine phosphate and L-metanephrine had good separation under BEH-amide conditions. L-Adrenaline and and L-Noradrenaline showed broad and multiple peaks.

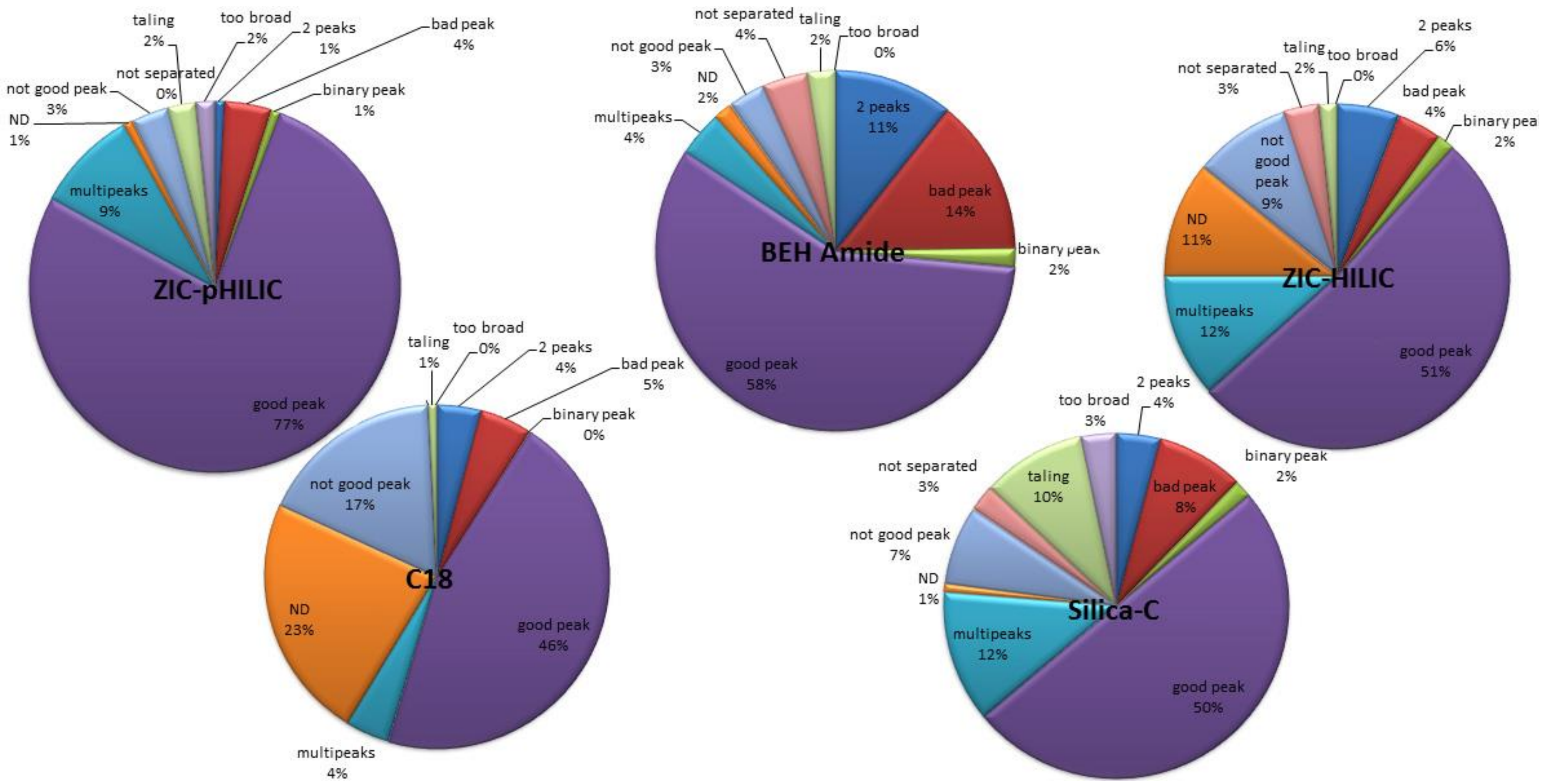

Figure 3.1 Pie chart for the evaluation of five columns for the chromatography of polar compounds.

3.2.2 Examples of Chromatographic Performance

Figures 3.2-3.6 show some of the chromatographic traces obtained from the five columns. Figure 3.2 shows examples of good chromatography on the ZIC-pHILIC column. It can be seen that the efficiencies obtained under HILIC conditions were very good which in part results from a favorable mass transfer term where in part the stationary phase is composed of a liquid and diffusion in the low viscosity high organic mobile phase is rapid. High efficiencies were also obtained on the ZICHILIC column although not far as great number of analytes as with the ZIC-pHILIC column. Figure 3.3 shows some examples of good chromatography on the ZICHILIC column. The C18 AR column produced sharp peaks for many analytes (figure 3.4) but this is largely as a result of a lack of chromatographic retention. The lack of chromatographic retention brings with it the risk of ion suppression effects in biological extracts. The silica C column was also capable of producing good chromatographic performance (figure 3.5) albeit for a more limited range of analytes than the ZIC-pHILIC column. Finally the BEH amide column also produced good chromatographic performance (figure 3.6) and was second in overall high quality coverage to the ZIC-pHILIC column although the ZICHILIC column complements the ZIC-pHILIC column in terms of its separation abilities.

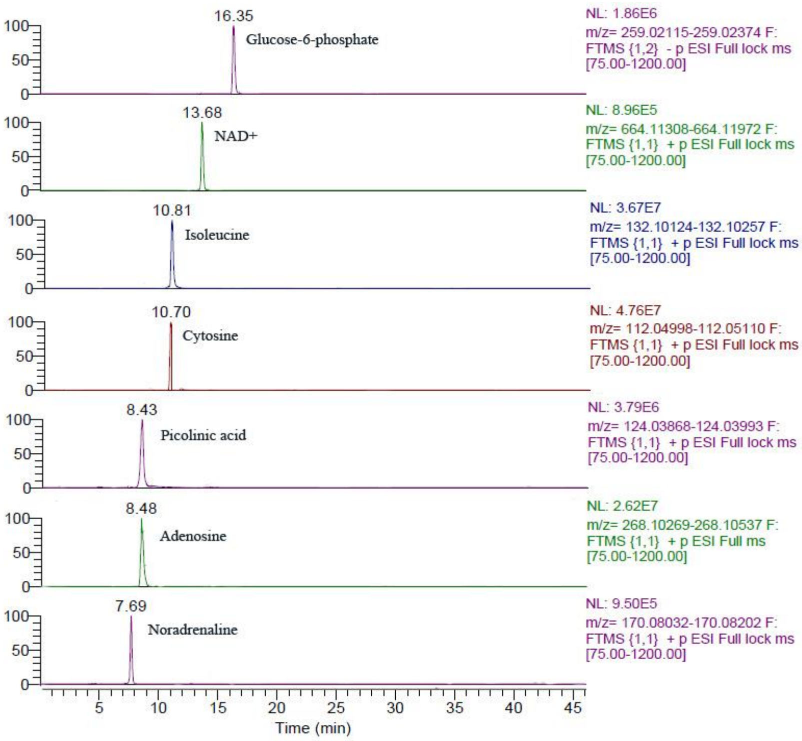

Figure 3.2 examples of good peaks on a ZIC-pHILIC column. Conditions as in section 2.3.2.

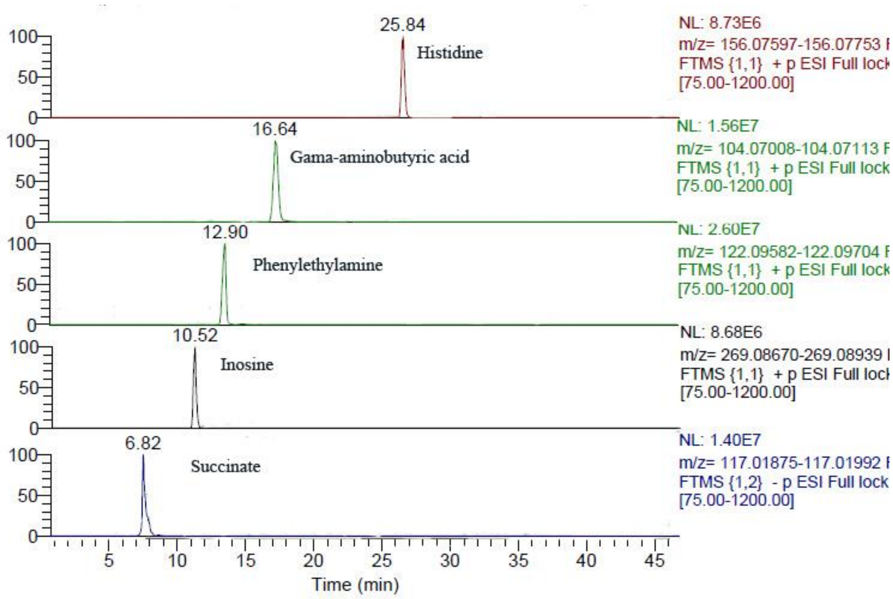

Figure 3.3 examples of good peaks on a ZIC-HILIC column. Conditions as in section 2.3.1.

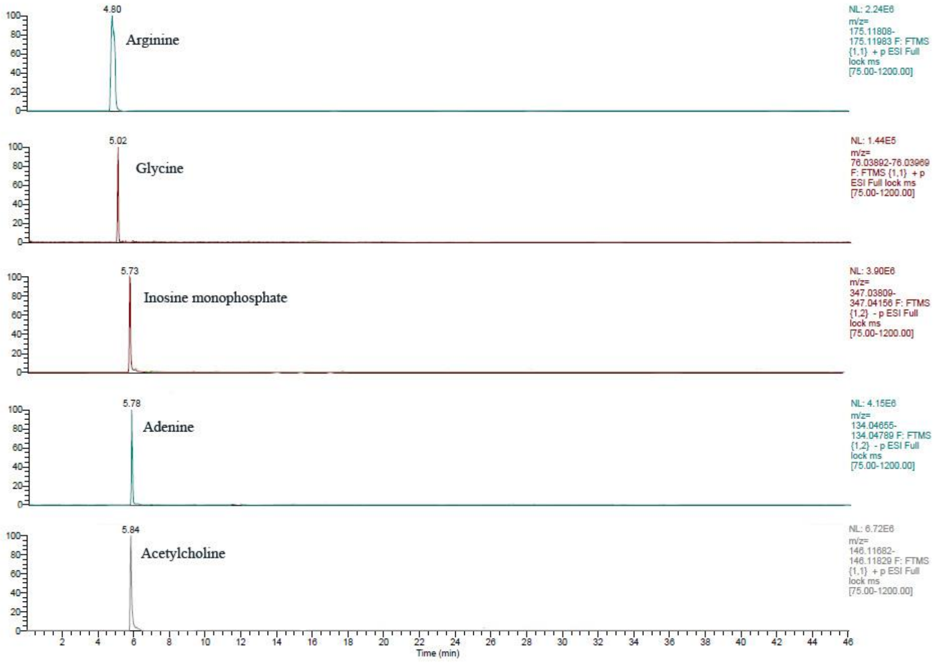

Figure 3.4 Examples of sharp spikes peaks on a C18-AR column. Conditions as in section 2.3.3.

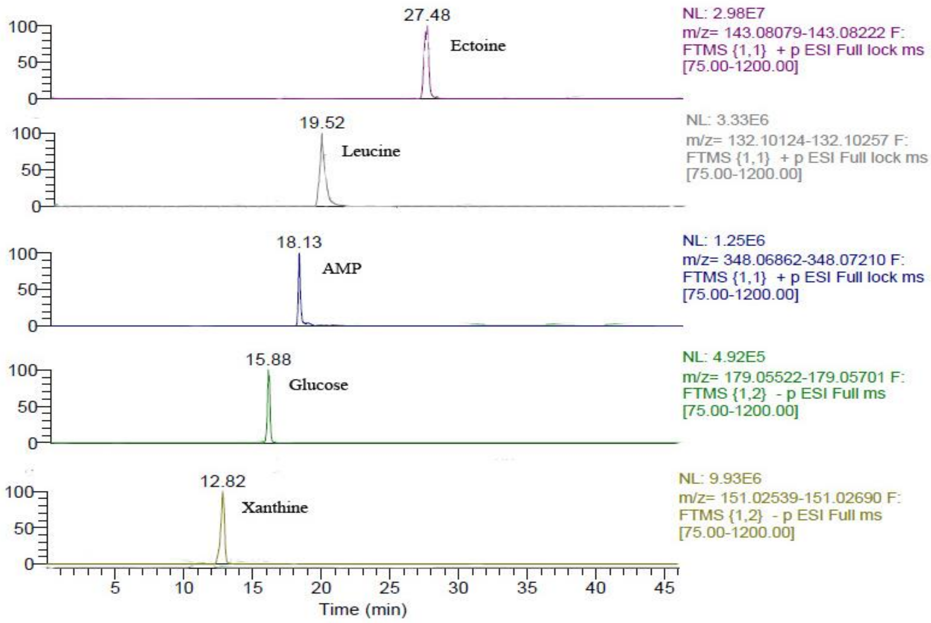

Figure 3.5 Examples of good peaks on a Silica-C column. Chromatographic conditions as in section 2.3.4.

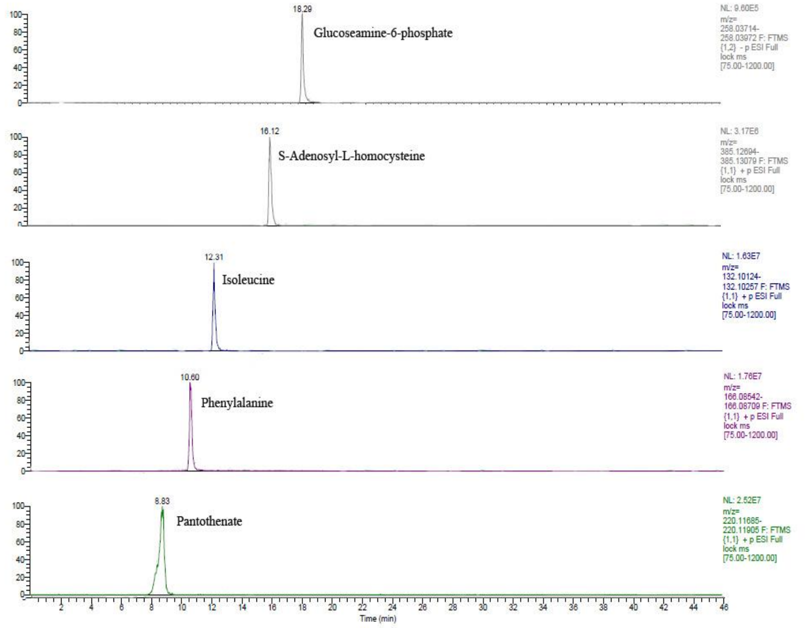

Figure 3.6 Examples of good peaks on a BEH Amide column. Conditions as in section 2.3.5

The clearest superiority of performance of the ZIC-pHILIC column can be seen in the separations produced for acids. Figure 3.7 compared the chromatography of four acids on the five columns and as can be seen from the chromatograms no column comes close to matching the performance of the ZIC-pHILIC column.

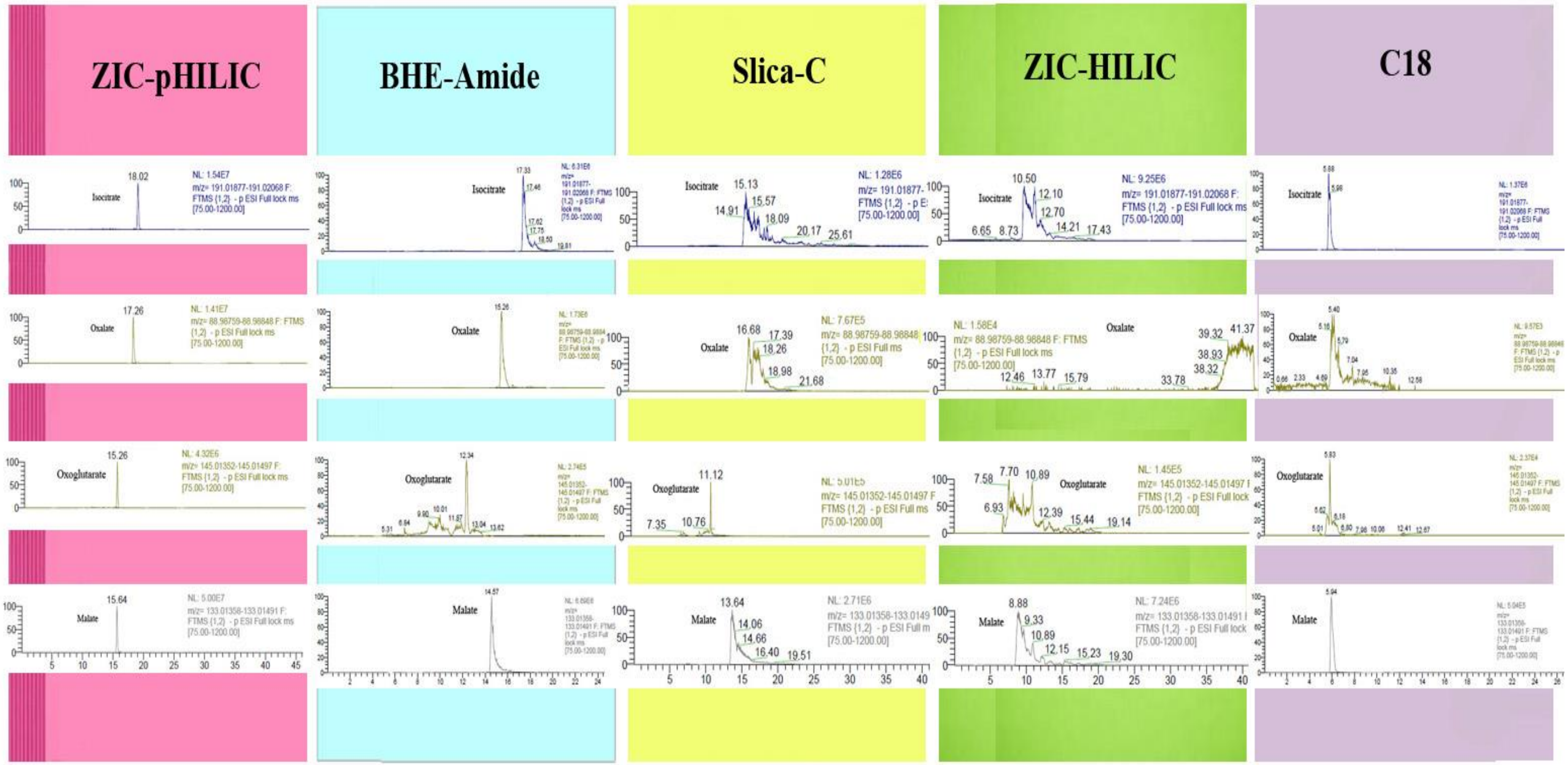

Figure 3.7: Separation of acids on five columns. Conditions as in section 2.3

3.2.3 The elution ranges for the compounds

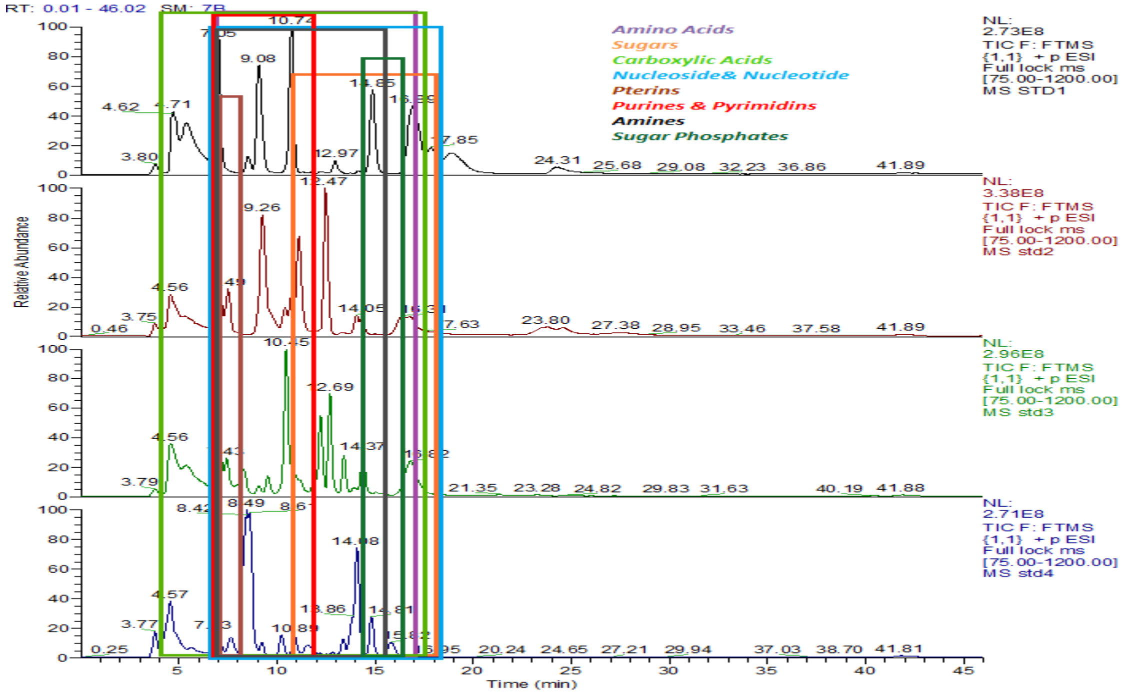

Figure 3.8 outlines where the groups of compounds elute within the ZIC-pHILIC chromatogram.

The ZIC-pHILIC method can be used for profiling analytes of interest, such as amino acids, sugars, carboxylic acids, nucleosides, nucleotides, petrins, purines, amines and sugar phosphates. The elution of polar metabolites using the ZIC-pHILIC column can be divided according to their physicochemical properties, as seen in figure 3-8. The carboxylic acids region starts at 4 min, finishes at 18 min. The nucleosides and nucleotides region starts at 6.5 min and finishes at 18.5 min. Purines and pyrimidines region starts at 6.5 min and finishes at 12 min. The amino acids region starts at about 7 min, finishes around 17 min. The amines region starts at 7 min and finishes at 15.5 min. The pterins region starts at 7 min and finishes at 8 min. The sugars region starts at about 11 min, finishes around 18 min. The sugar phosphates region starts at 14.5 min and finishes at 16.5 min. Such retention data can be used to assist in the identification of metabolites that come from the LNCaP cell culture extract identified to (Metabolomics Standards Initiative) MSI level 1 according to accurate mass and comparison of retention times with standards[(4)]. The chromatographic methodology should also be able to discriminate between isomeric metabolites as far as possible.

3.2.4 Isomer separation

Although when making measurements using high resolution mass spectrometry it is important to be confident of the elemental composition of a metabolite where two compounds are isomers and have the same elemental composition chromatographic separation is required to distinguish them. The five columns can be compared for their ability to separate isomers. α- alanine, β- alanine and sarcosine which have the same accurate masses (m/z 90.0549) were separated by the ZIC-pHILIC and ZIC-HILIC columns but not by the other columns. Figure 3.8 shows the separation of the standards on ZIC-pHILIC and figure 3.9 shows the separation of these compounds in a sample extract from a cell culture by the ZIC-pHILIC column. Methylmalonate and succinate have the same accurate masses (m/z 117.01889) and on the ZIC-pHILIC column which they were nearly separated and might be separable with more optimisation of the HPLC parameters while in the other columns they were not separated at all. Figure 3.10 shows the partial separation of these standards by the ZIC-pHILIC column. Isoleucine and leucine have the same accurate masses (m/z 132.10188) and they were well separated by the ZIC-pHILIC, Silica-C and BEH-amide columns but not by ZIC-HILIC. Figure 3.11 shows the separation of isoleucine and leucine standards on ZIC-pHILIC and figure 3.12 shows their separation in the sample extracts by a ZIC-pHILIC column. 4-aminobutyric acid and 3- aminobutyric acid have the same accurate masses (m/z 104.0706) and were separated by ZIC-pHILIC, Silica-C and BEH-amide but not by ZIC-HILIC. Figure 3.13 shows the separation of 4-aminobutyric acid and 3- aminobutyric acid

---

[(4)]MSI = http://cosmos-fp7.eu/msi

standards by a ZIC-pHILIC column. Cis-4-hydroxy D-proline and Trans-4-hydroxy D-proline have the same accurate masses (m/z 132.0655) and were separated by ZIC-pHILIC, Silica-C and BEH-amide columns but not by a ZIC-HILIC column. Figure 3.14 shows the separation of cis-4-hydroxy D-proline and trans-4-hydroxy D-proline standards by a ZIC-pHILIC column. Biopetrin and sepiapetrin have the same accurate masses (m/z 238.09348) and were separated by ZIC-pHILIC, Silica-C, BEH-amide and ZIC-HILIC columns. Figure 3.15 shows the separation of biopetrin and sepiapetrin standards by a ZIC-pHILIC column. DL-glyceraldehyde 3-phosphate and dihydroxy-acetone phosphate have the same accurate masses (m/z 168.9909) and were separated well only by a ZIC-pHILIC column, the Silica-C column shows one broad peak and BEH-amide shows multiple unseparated peaks and ZIC-HILIC shows a partially separated peak. Figure 3.16 shows the separation of DL-glyceraldehyde 3-phosphate and dihydroxy-acetone phosphate standards by a ZIC-pHILIC column. Betaine and valine have the same accurate masses (m/z 118.0863) and were separated by ZIC-pHILIC, Silica-C and ZIC-HILIC columns but not a BEH-amide column. Figure 3.17 shows the separation of the standards for betaine and valine and figure 3.18 shows their separation in a sample extract by the ZIC-pHILIC column. Fumarate and maleic acid have the same accurate masses (m/z 115.0038) and were separated only by the ZIC-pHILIC column while Silica-C shows two peaks for maleic acid and BEH-amide shows multiple peaks and bad separation for maleic acid and it was not detected by ZIC-HILIC. Figure 3.19 shows the separation of the standards for fumaric and maleic acid and figure 3.20 shows the separation of these compounds in a sample extract by a ZIC-pHILIC column. None of these sets of isomers could be separated on the C18 AR column.

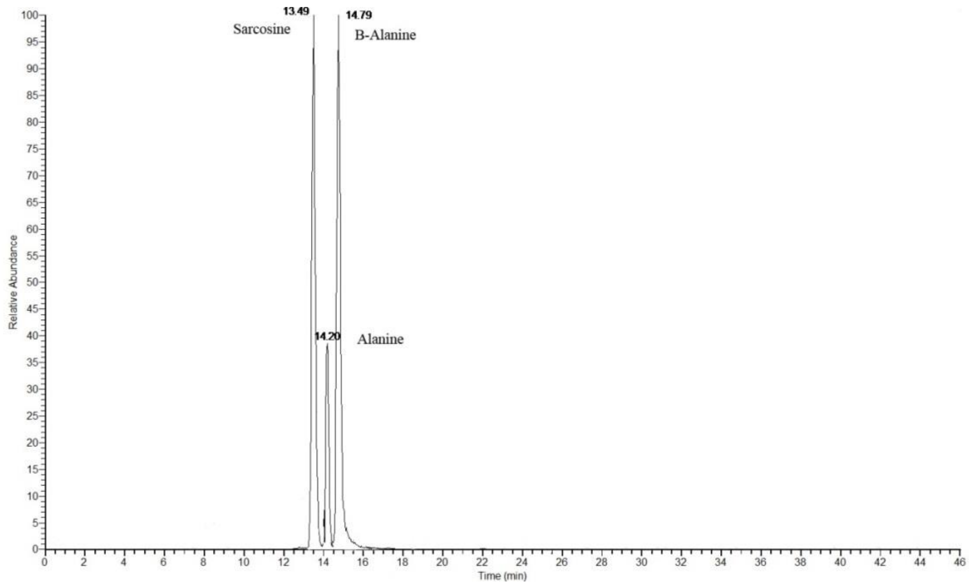

Figure 3.9 β-alanine, α-alanine and sarcosine standards separated on a ZICpHILIC. Conditions as in section 2.3.2.

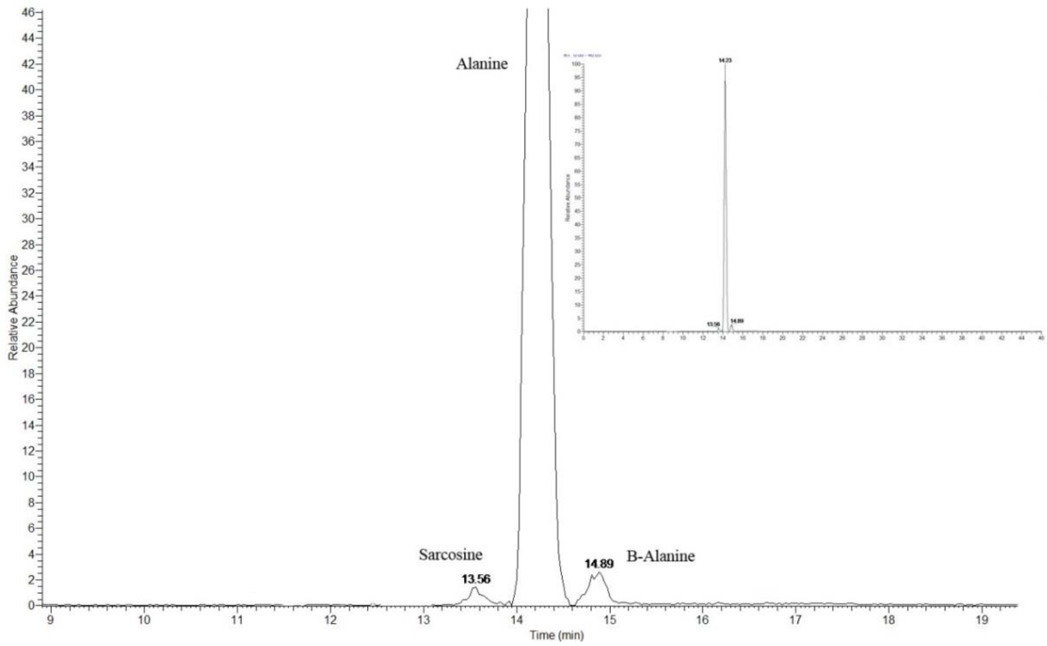

Figure 3.10 β-alanine, α-alanine and sarcosine in an LNCaP cell extract sample separated on a ZICpHILIC column. Conditions as in section 2.3.2.

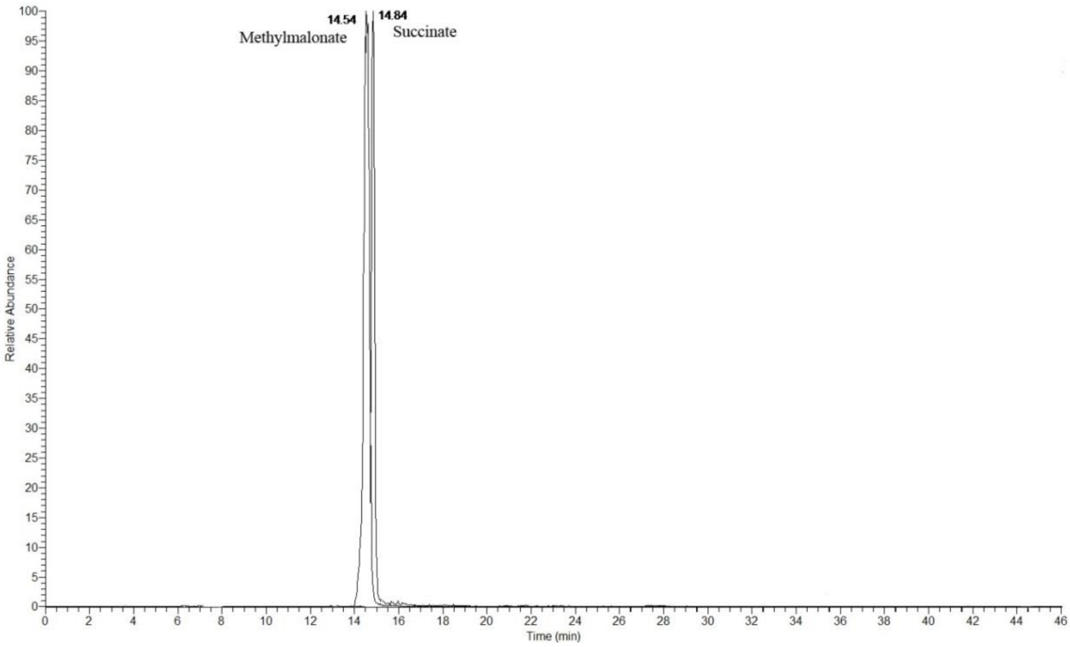

Figure 3.11 Partial separation of methylmalonate and succinate on a ZICpHILIC column. Conditions as in section 2.3.2.

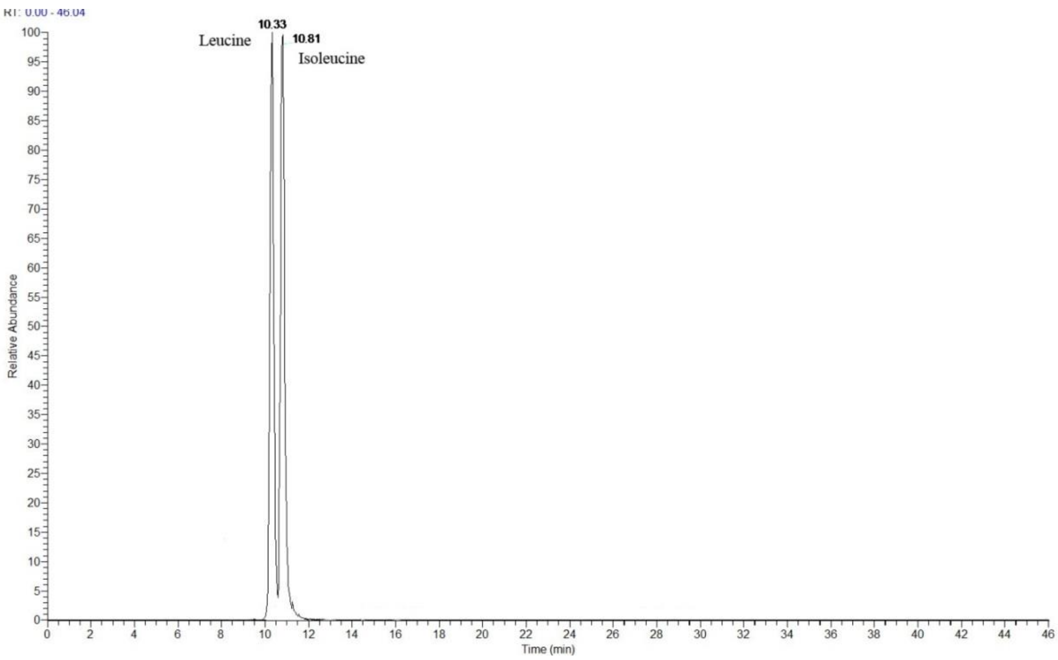

Figure 3.12 Isoleucine and Leucine standards on a ZICpHILIC column. Conditions as in section 2.3.2.

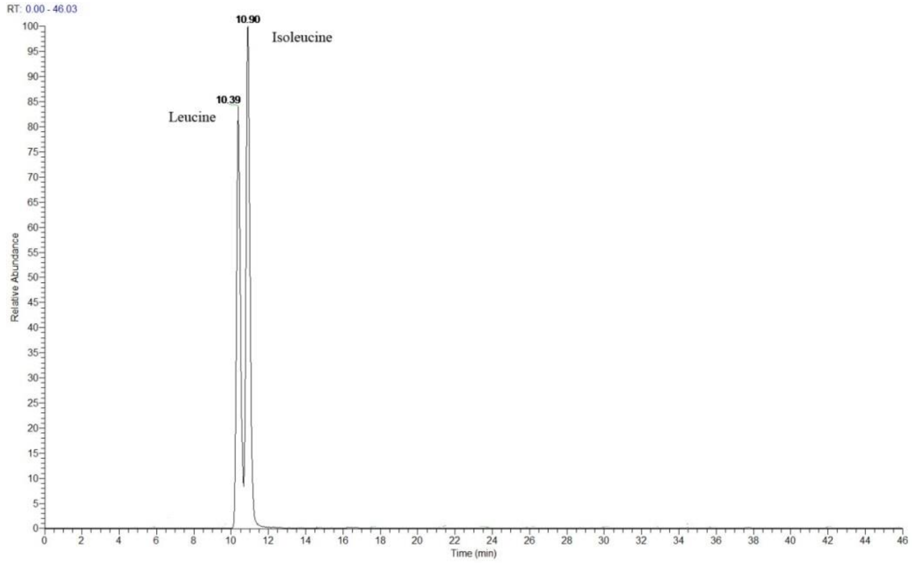

Figure 3.13 Isoleucine and leucine on LNCaP cell extract sample on a ZICpHILIC column. Conditions as in section 2.3.2.

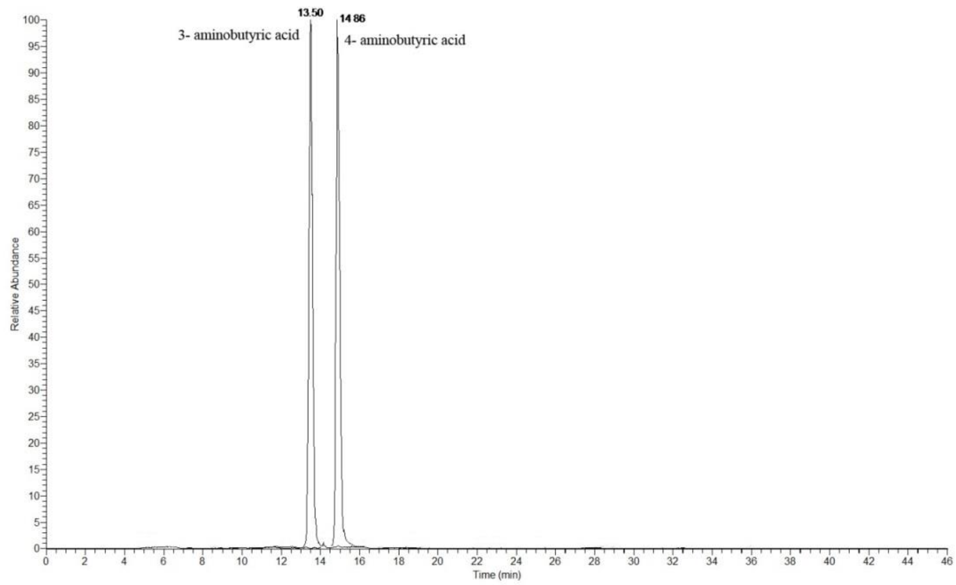

Figure 3.14 4-aminobutyric acid and 3- aminobutyric acid standards on a ZICpHILIC column. Conditions as in section 2.3.2.

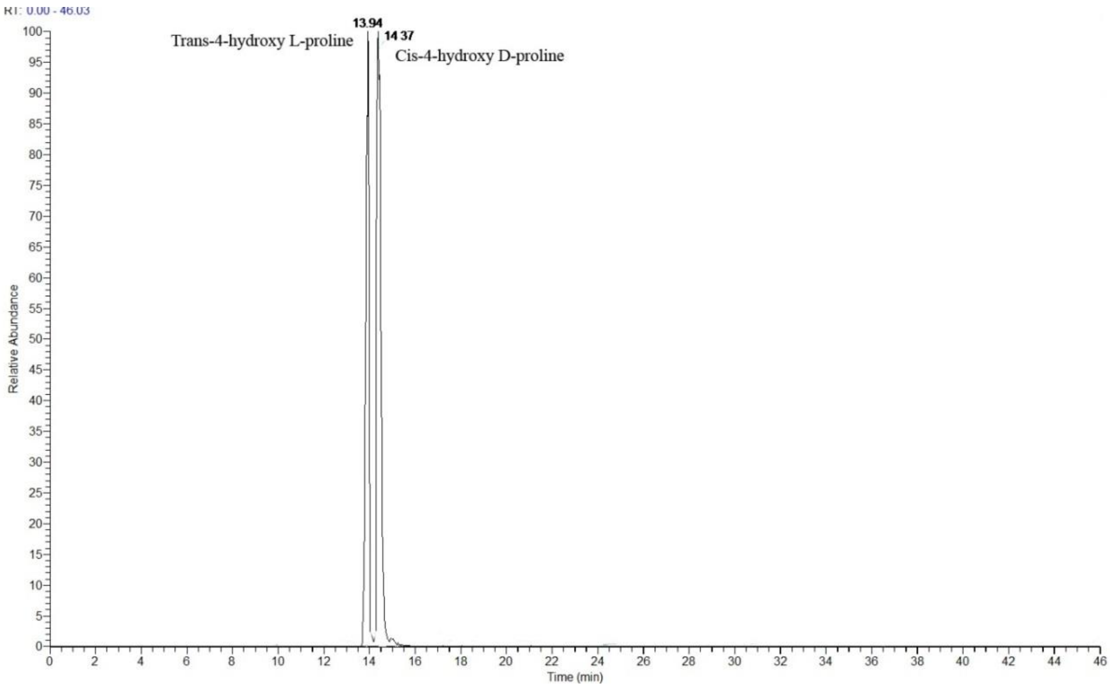

Figure 3.15 Cis-4-hydroxy D-proline and Trans-4-hydroxy D-proline standards on a ZICpHILIC column. Conditions as in section 2.3.2.

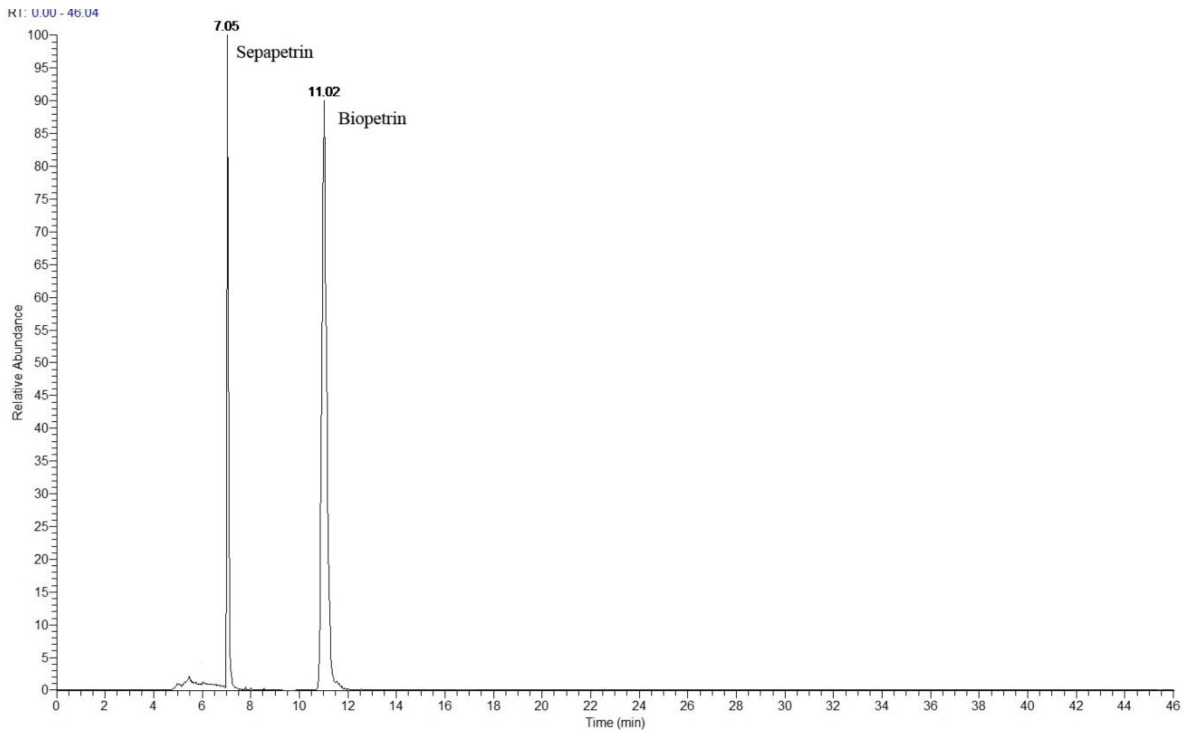

Figure 3.16 Biopetrin and sepiapetrin standards on a ZICpHILIC column. Conditions as in section 2.3.2.

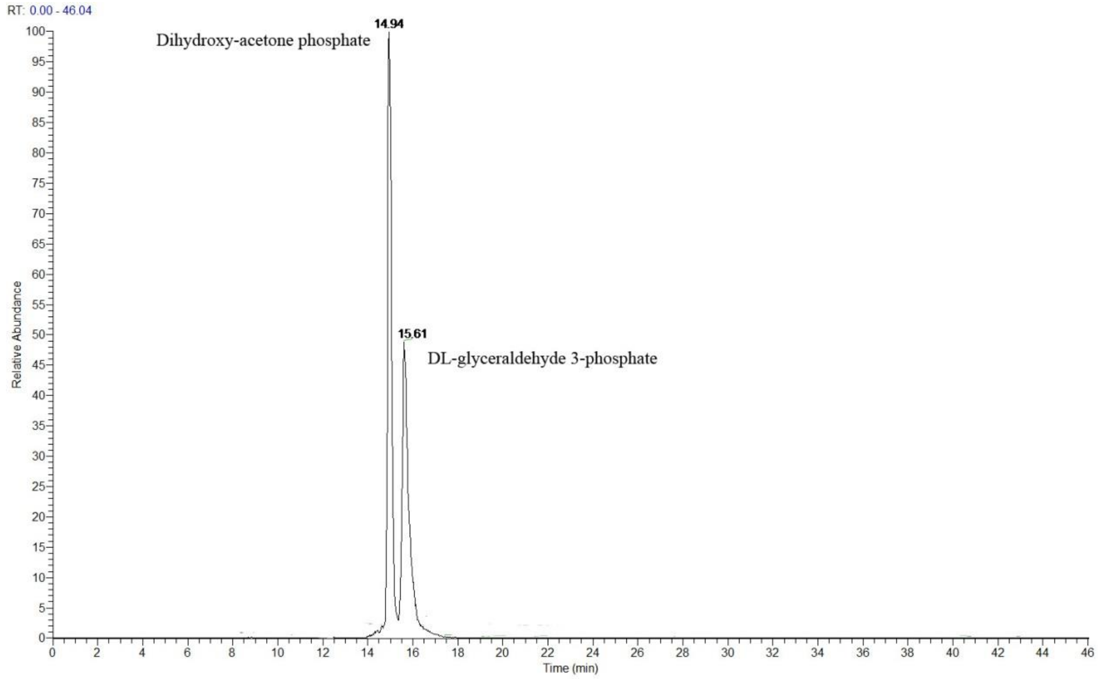

Figure 3.17 DL-glyceraldehyde 3-phosphate and Dihydroxy-acetone phosphate standards on a ZICpHILIC column. Conditions as in section 2.3.2.

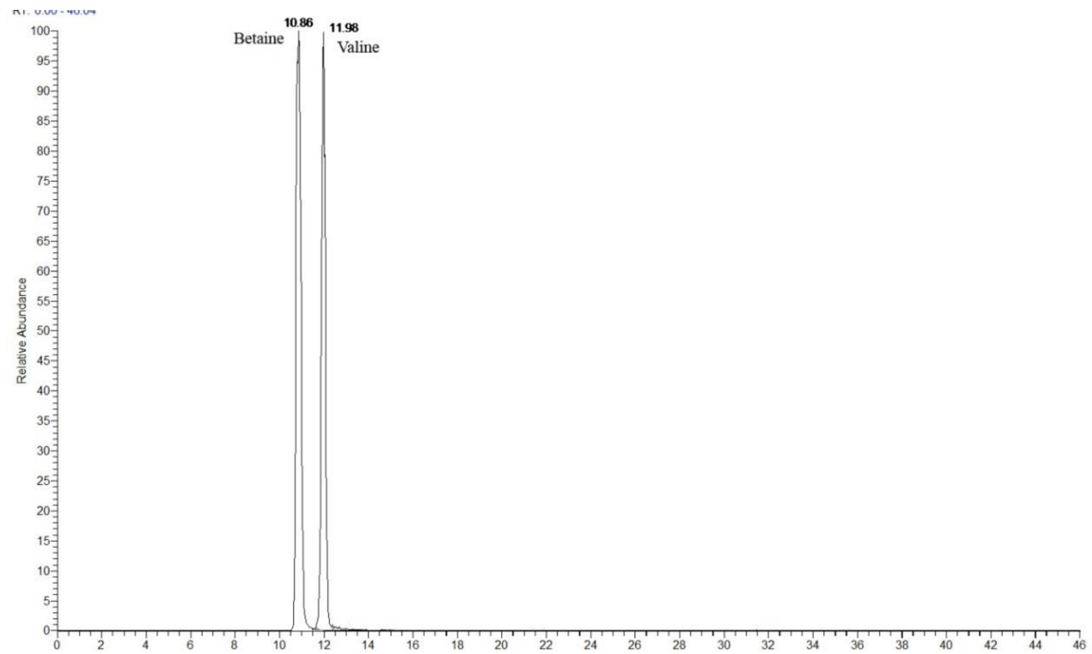

Figure 3.18 Betaine and valine standards on a ZICpHILIC column. Conditions as in section 2.3.2.

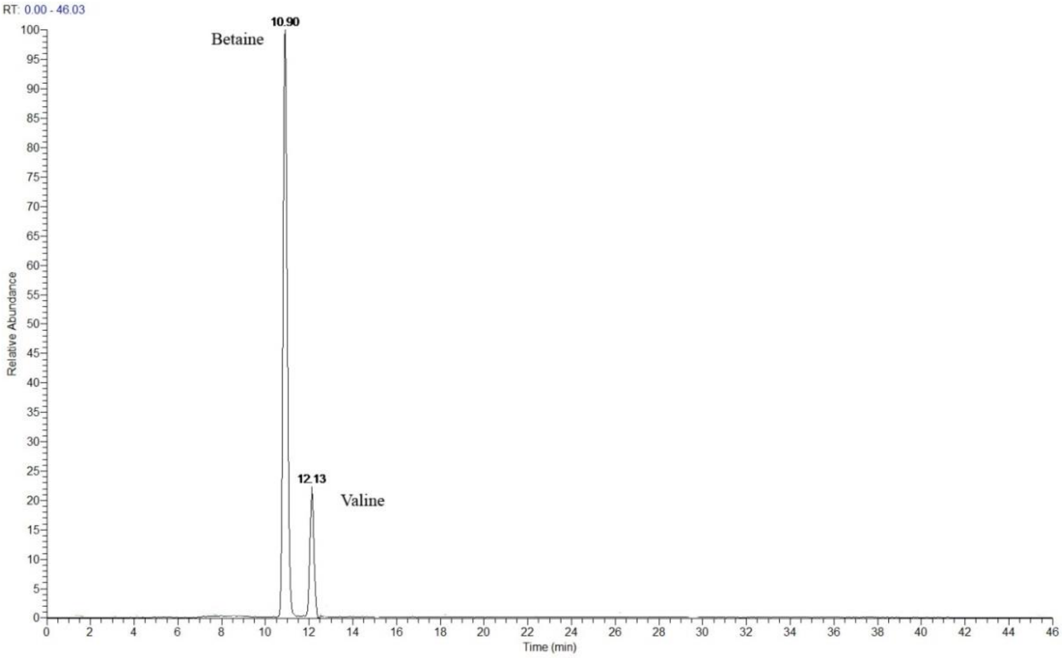

Figure 3.19 Betaine and Valine in an LNCaP cell extract sample on a ZICpHILIC column. Conditions as in section 2.3.2.

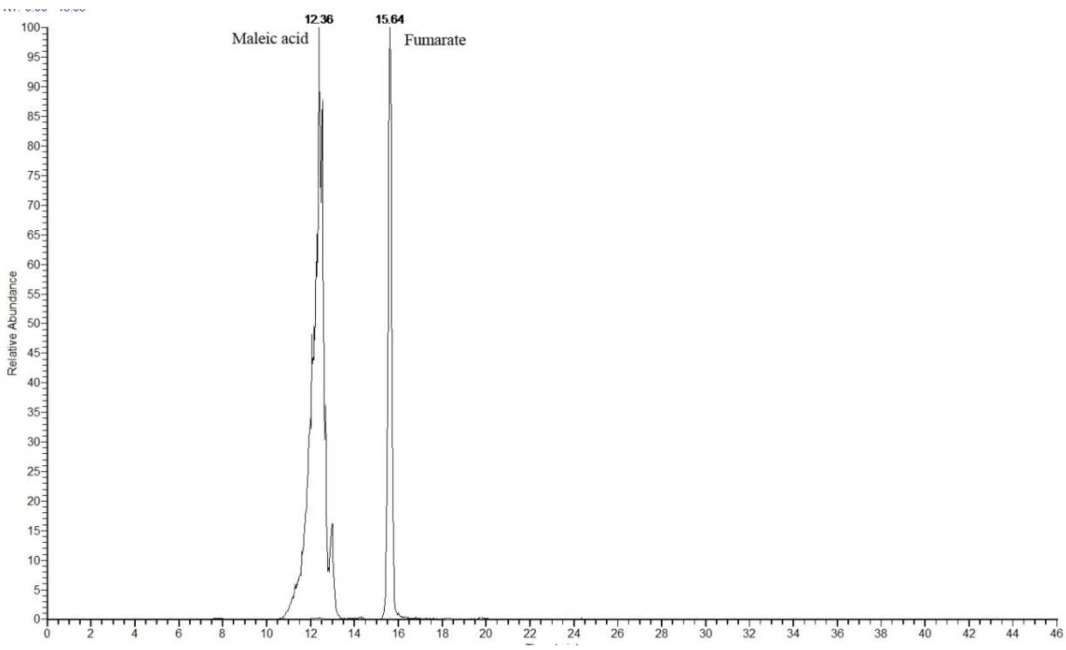

Figure 3.20 Maleic acid and Fumarate standards on a ZICpHILIC column. Conditions as in section 2.3.2.

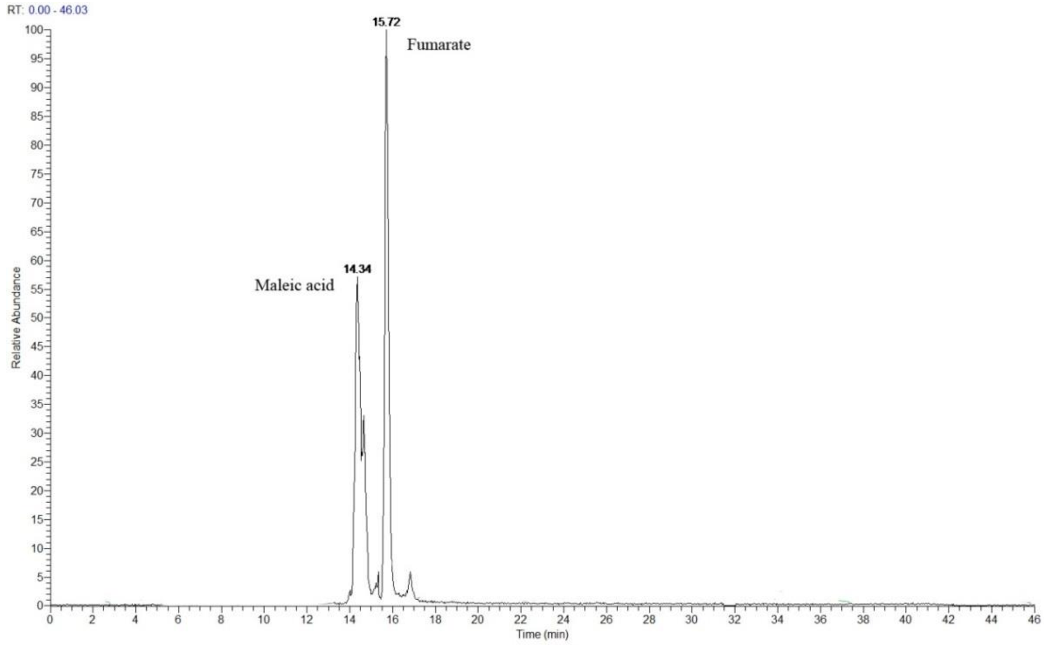

Figure 3.21 Fumarate and Maleic acid in an LNCaP cell extract sample on a ZICpHILIC column. Conditions as in section 2.3.2.

3.2.5 Testing linearity of response and limit of detection on the ZIC-pHILIC column for the metabolite standards.

In order to investigate the performance of the LC-MS method, ~ 180 metabolite standards were prepared and diluted to concentrations of (1-20000 ng/ml) from their original concentrations 1mg/ml. They were diluted with 80:20 ACN: H2O. Tables 3.3-3.11 summarise the results obtained for linear range, limit of detection, limit of quantitation and technical precision obtained for the metabolite standards. The majority of the metabolites standards showed a broad linear range according to calibration curve lines. While a few of them showed a narrow dynamic range at high concentration levels might be due to ion suppression effects such as alloxanthine, some nucleotides (CMP, GMP, AMP, NAD), sugar phosphates and ethanolamine phosphate.

3.2.6 Assessment of the technical performance of the ZIC-pHILIC LC-MS method

3.2.6.1 Limit of detection

The LOD was determined for all of the standard metabolites and it was found that the method presented here was suitable for metabolomics analysis because it had both low detection limits and a broad linear range for most analytes. However, some metabolites as CMP, alloxanthine, NAD+ have high LOD and further investigation is required to ascertain why certain metabolites appeared to perform more poorly than expected. However, overall the sensitivity was sufficient for detection of the levels of many of the metabolites expected in cell culture extracts.

3.2.6.2 Technical precision and reproducibility

The instrument precision (or chromatographic repeatability) was obtained by injecting aliquots from the same sample of one standard mixture six times in single run and calculating the relative standard deviation (RSD) of the response of standard compounds which were below 5%. The precision for each compound was determined by injecting three points (low, medium, high) of the calibration curve six times. Then RSD of the responses were calculated. Tables 3.3-3.11 show the results of metabolites standards retention time precision and mass accuracy. The precisions obtained for each analytes was good and for three points on the calibration curve RSDs were ≤ ± 5% for all of the metabolite standards at each calibration point. The summary was made by focusing on eleven chemical classes of compounds, the accurate masses of each metabolite were detected in negative and positive mode with mass accuracy < 2ppm and the reproducibility of the retention times of the metabolites were below ± 5% across runs (n=6).

Table 3.3 Linearity of response and limit of detection on the ZIC-pHILIC column of amino acids

Metabolits	Condition	Formula	Polarity	Detected m/z(accurate mass)	Delta (ppm)	Average-Rt	%RSD of Rt. reproducibility	Precision	Dynamic Range(µg/ml)	r^2	LOD (µg/ml)	LOQ (µg/ml)	n
2-Phenylglycine	pHILIC	$C_8H_9NO_2$	+	152.07071	0.68	10.52	0.431	4.5	0.05-1	0.999	0.0073	0.0245	5
beta-Alanine	HILIC	$C_3H_7NO_2$	+	90.05499	0.42	14.83	4.424	4.4	0.05-1	0.999	0.0069	0.0231	5
cis-4-Hydroxy-D-proline	pHILIC	$C_5H_9NO_3$	+	132.06558	0.47	14.31	0.792	4.8	0.01-1	0.999	0.0028	0.0094	5
Creatine	pHILIC	$C_4H_9N_3O_2$	+	132.07678	0.22	14.05	0.778	2.7	0.01-1	0.999	0.0029	0.0099	5
Ectoine	pHILIC	$C_6H_{10}N_2O_2$	+	143.08176	1.76	13.48	0.886	2.7	0.01-1	0.999	0.0027	0.0091	5
Gamma-Aminobutyric acid	pHILIC	$C_4H_9NO_2$	+	104.07067	0.63	14.83	0.580	2.6	0.05-1	0.999	0.0073	0.0244	5
Glycine	pHILIC	$C_2H_5NO_2$	+	76.03944	1.73	14.99	0.682	4.0	0.1-2	0.999	0.0233	0.0777	5
L-Alanine	pHILIC	$C_3H_7NO_2$	+	90.05490	-0.60	14.12	0.713	3.6	0.05-1	0.999	0.0059	0.0197	5
L-Arginine	pHILIC	$C_6H_{14}N_4O_2$	+	175.11900	0.29	24.62	0.546	3.3	0.05-1	0.999	0.0054	0.0182	5
L-Aspartate	HILIC	$C_4H_7NO_4$	+	134.04472	-0.45	14.71	3.047	5.0	0.01-1	0.999	0.0029	0.0098	5
L-Cystathionine	pHILIC	$C_7H_{14}N_2O_4S$	-	221.06039	1.10	16.16	0.607	2.7	0.01-1	0.999	0.0022	0.0075	5
L-Cysteine	pHILIC	$C_3H_7NO_2S$	-	120.01262	1.22	15.28	0.632	4.9	0.01-1	0.999	0.0027	0.0090	5
L-Cystine	pHILIC	$C_6H_{12}N_2O_4S_2$	-	239.01677	0.83	15.49	0.552	1.4	0.01-1	0.999	0.0026	0.0088	5

Metabolits	Condition	Formula	Polarity	Detected m/z(accurate mass)	Delta (ppm)	Average-Rt	%RSD of Rt. reproducibility	Precision	Dynamic Range(µg/ml)	r^2	LOD (µg/ml)	LOQ (µg/ml)	n
L-Glutamic acid	pHILIC	$C_5H_9NO_4$	+	148.06068	1.69	10.52	0.828	2.9	0.01-1	0.999	0.0028	0.0094	5
O-Acetyl-L-serine	pHILIC	$C_5H_9NO_4$	+	148.06047	0.25	10.41	1.114	4.3	0.05-1	0.999	0.0054	0.0182	5
L-Glutamine	pHILIC	$C_5H_{10}N_2O_3$	+	147.07643	0.09	14.36	0.777	3.3	0.05-1	0.999	0.0134	0.0448	5
L-Histidine	HILIC	$C_6H_9N_3O_2$	+	156.07672	-0.20	25.55	2.363	1.0	0.01-0.5	0.999	0.0032	0.0099	5
L-Homoserine	pHILIC	$C_4H_9NO_3$	+	120.06555	0.27	14.30	0.502	3.6	0.05-1	0.999	0.0147	0.0491	5
L-Isoleucine	pHILIC	$C_6H_{13}NO_2$	+	132.10188	-0.17	10.68	0.602	4.7	0.01-0.5	0.999	0.0027	0.0091	5
L-Kynurenine	pHILIC	$C_{10}H_{12}N_2O_3$	+	209.09212	0.23	10.19	0.581	4.7	0.01-1	0.999	0.0030	0.0100	5
L-Leucine	pHILIC	$C_6H_{13}NO_2$	+	132.10188	-0.17	10.22	0.585	3.8	0.05-1	0.999	0.0135	0.0451	5
L-Lysine	pHILIC	$C_6H_{14}N_2O_2$	+	147.11288	0.55	23.18	0.708	3.6	0.05-1	0.999	0.0142	0.0473	5
L-Methionine	pHILIC	$C_5H_{11}NO_2S$	+	150.05843	0.67	10.86	0.828	3.4	0.01-1	0.999	0.0022	0.0074	5
L-Ornithine	pHILIC	$C_5H_{12}N_2O_2$	+	133.09712	-0.24	21.89	3.451	2.8	0.01-0.5	0.999	0.0024	0.0088	5
L-Phenylalanine	pHILIC	$C_9H_{11}NO_2$	+	166.08640	0.84	9.52	0.652	3.9	0.01-0.5	0.999	0.0030	0.0100	5
L-Proline	pHILIC	$C_5H_9NO_2$	+	116.07067	0.57	12.21	0.565	4.9	0.01-0.5	0.999	0.0025	0.0086	5
L-Serine	pHILIC	$C_3H_7NO_3$	+	106.04990	0.25	15.04	3.152	0.6	0.01-0.5	0.999	0.0025	0.0084	5
L-Threonine	pHILIC	$C_4H_9NO_3$	+	120.06556	0.33	13.75	0.979	2.7	0.05-1	0.999	0.0129	0.0431	5

Metabolits	Condition	Formula	Polarity	Detected m/z(accurate mass)	Delta (ppm)	Average-Rt	%RSD of Rt. reproducibility	Precision	Dynamic Range(μg/ml)	r^2	LOD (μg/ml)	LOQ (μg/ml)	n
L-Tryptophan	pHILIC	$C_{11}H_{12}N_2O_2$	+	205.09729	0.66	11.00	0.695	1.8	0.05-1	0.999	0.0144	0.0482	5
L-Tyrosine	HILIC	$C_9H_{11}NO_3$	+	182.08113	-0.21	5.37	2.265	3.7	0.001-1	0.999	0.0002	0.0007	5
L-Valine	pHILIC	$C_5H_{11}NO_2$	+	118.08633	0.60	11.86	0.710	3.1	0.05-1	0.999	0.0128	0.0429	5
Nα-Acetyl-L-lysine	pHILIC	$C_8H_{16}N_2O_3$	+	189.12341	0.23	14.35	0.537	4.7	0.05-1	0.999	0.0148	0.0495	5
O-Acetylcarnitine	pHILIC	$C_9H_{17}NO_4$	+	204.12315	0.58	10.43	0.617	4.1	0.05-1	0.999	0.0128	0.0427	5
Pantothenate	pHILIC	$C_9H_{17}NO_5$	+	220.11806	0.49	8.31	0.408	3.4	0.01-0.1	0.999	0.0029	0.0098	5
Picolinic acid	pHILIC	$C_6H_5NO_2$	+	124.03940	0.75	8.28	1.359	3.8	0.05-1	0.999	0.0125	0.0417	5
Taurine	pHILIC	$C_2H_7NO_3S$	-	124.00714	1.34	14.28	0.703	1.9	0.01-0.5	0.999	0.0029	0.0099	5
5-Aminolevulinate	pHILIC	$C_5H_9NO_3$	+	132.06544	-0.57	12.95	0.577	4.3	0.01-0.1	0.999	0.0006	0.0020	5
Saccharopine	pHILIC	$C_{11}H_{20}N_{2O}6$	-	275.12445	2.06	15.17	0.598	3.5	0.1-2	0.999	0.0216	0.0720	5
N-Acetyl-L-aspartate	pHILIC	$C_6H_9NO_5$	+	176.05545	0.58	14.14	0.621	2.6	0.05-1	0.999	0.0129	0.0432	5
N-Acetyl-L-glutamate	pHILIC	$C_7H_{11}NO_5$	+	190.07101	0.08	13.71	0.658	4.4	0.05-1	0.999	0.0140	0.0469	5
S-Adenosyl-L-homocysteine	pHILIC	$C_{14}H_{20}N_6O_5S$	+	385.12900	0.35	12.71	1.116	2.0	0.05-1	0.999	0.0127	0.0424	5

Metabolits	Condition	Formula	Polarity	Detected m/z(accurate mass)	Delta (ppm)	Average-Rt	%RSD of Rt. reproducibility	Precision	Dynamic Range(μg/ml)	r^2	LOD (μg/ml)	LOQ (μg/ml)	n
Betaine	pHILIC	$C_5H_{11}NO_2$	+	118.08625	1.25	10.73	0.59	3.7	0.01-1	0.999	0.0029	0.0098	5
Sarcosine	pHILIC	$C_3H_7NO_2$	+	90.05499	0.42	13.40	0.737	3.2	0.05-1	0.999	0.0124	0.0415	5
B-alanine-methyl-ester	HILIC	$C_4H_9NO_2$	+	104.07066	0.49	14.39	4.764	4.8	0.1-2	0.999	0.0257	0.0859	5
2-Indolecarboxylicacid	pHILIC	$C_9H_7NO_2$	-	160.04030	-0.65	7.04	0.983	4.4	0.05-1	0.999	0.0142	0.0475	5
DL-3-aminobutyrate	pHILIC	$C_4H_9NO_2$	+	104.07072	1.07	13.38	0.602	5.1	0.01-0.1	0.999	0.0006	0.0020	5
N(pi)-Methyl-L-histidine	pHILIC	$C_7H_{11}N_3O_2$	+	170.09248	0.47	12.08	1.075	5.0	0.05-1	0.999	0.0132	0.0443	5
trans-4-Hydroxy-L-proline	pHILIC	$C_5H_9NO_3$	+	132.06560	0.59	13.88	0.713	4.3	0.05-1	0.999	0.0132	0.0441	5
(R)-S-Lactoylglutathione	pHILIC	$C_{13}H_{21}N_3O_8S$	+	380.11240	0.49	12.88	0.853	1.9	0.05-1	0.999	0.0149	0.0499	5
Glutathione	HILIC	$C_{10}H_{17}N_3O_6S$	-	306.07693	1.33	14.65	5.000	4.1	0.05-1	0.999	0.0133	0.0443	5

Table 3.4 Linearity of response and limit of detection on the ZIC-pHILIC column of Sugars

Metabolits	Condition	Formula	Polarity	Detected m/z(accurate mass)	Delta (ppm)	Average-Rt	%RSD of Rt. repreducebility	Precision	Dynamic Range(µg/ml)	r2	LOD (µg/ml)	LOQ (µg/ml)	n
D-Fructose	pHILIC	$C_6H_{12}O_6$	-	179.05634	1.25	13.93	1.101	4.81	0.05-1	0.999	0.0160	0.0353	5
D-Galactose	HILIC	$C_6H_{12}O_6$	-	179.05640	1.59	14.28	1.388	3.34	0.1-2	0.999	0.0305	0.1018	5
D-Mannose	pHILIC	$C_6H_{12}O_6$	-	179.05658	2.62	13.42	0.604	4.29	0.2-2	0.999	0.044	0.146	5
Maltose	pHILIC	$C_{12}H_{22}O_{11}$	-	341.10895	0.04	15.40	1.620	4.5	0.5-10	0.999	0.145	0.485	5
D-Xylose	HILIC	$C_5H_{10}O_5$	-	149.04576	1.44	11.95	2.514	3.57	0.2-5	0.999	0.061	0.205	5
D-Glucosamine	pHILIC	$C_6H_{13}NO_5$	+	180.08662	-0.14	14.40	3.031	2.90	0.5-5	0.999	0.0961	0.230	5
N-Acetyl-D-glucosamine	pHILIC	$C_8H_{15}NO_6$	+	222.09727	0.28	11.20	0.615	3.21	0.05-2	1	0.0106	0.0335	5
D-Glucose	pHILIC	$C_6H_{12}O_6$	-	179.05626	0.83	14.12	0.696	2.17	0.1-2	0.999	0.026	0.087	5
Cis-Aconitate (Dehydroascorbic acid)	pHILIC	$C_6H_6O_6$	-	173.00890	1.38	18.40	2.608	4.10	0.05-1	0.999	0.0161	0.0538	5
N-Acetyl-D-mannosamine	pHILIC	$C_8H_{15}NO_6$	+	222.09720	-0.07	11.62	0.650	4.65	0.05-2	0.999	0.0183	0.0613	5

Table 3.5 Linearity of response and limit of detection on the ZIC-pHILIC column of Carboxylic Acids

Metabolits	Condition	Formula	Polarity	Detected m/z(accurate mass)	Delta (ppm)	Average-Rt	%RSD of Rt. reproducibility	Precision	Dynamic Range(µg/ml)	r2	LOD (µg/ml)	LOQ (µg/ml)	n
(R)-Malate (Malic acid)	pHILIC	$C_4H_6O_5$	-	133.01440	1.19	15.57	0.574	3.0	0.5-10	0.999	0.145	0.484	5
Phthalate	pHILIC	$C_8H_6O_4$	+	167.03386	-0.16	13.38	1.024	5.0	0.5-5	0.999	0.146	0.487	5
2-Hydroxybutanoic acid	pHILIC	$C_4H_8O_3$	-	103.04016	0.91	7.75	1.639	5.0	0.05-2	0.999	0.0116	0.0387	5
2-Oxoglutarate	pHILIC	$C_5H_6O_5$	-	145.01450	1.72	15.18	0.612	4.0	0.1-2	0.999	0.0331	0.1104	5
4-Coumarate	pHILIC	$C_9H_8O_3$	-	163.04030	1.42	8.60	0.335	2.4	0.5-10	0.999	0.074	0.249	5
4-hydroxylphenylacetate	pHILIC	$C_8H_8O_3$	-	151.04021	0.92	8.69	0.202	4.7	0.05-2	0.999	0.0147	0.0491	5
Ascorbate	HILIC	$C_6H_8O_6$	-	175.02490	0.52	10.26	2.809	4.2	0.1-2	0.999	0.0273	0.0912	5
Caffeate	pHILIC	$C_9H_8O_4$	-	179.03513	0.80	11.30	1.622	4.7	0.5-10	0.999	0.0947	0.3159	5
Citramalate	pHILIC	$C_5H_8O_5$	-	147.03012	1.53	14.65	0.729	4.7	0.5-10	0.999	0.0662	0.2207	5
Diethyl 2-oxoglutarate	pHILIC	$C_9H_{14}O_5$	-	201.07733	2.41	3.94	1.458	4.8	0.05-1	0.999	0.0129	0.0431	5
Fumarate	pHILIC	$C_4H_4O_4$	-	115.00386	1.55	15.60	0.817	5.1	0.5-10	0.999	0.1374	0.4580	5
Gallate	pHILIC	$C_7H_6O_5$	-	169.01440	0.93	17.29	2.096	5.0	0.05-1	0.999	0.0139	0.0466	5
Isocitrate	pHILIC	$C_6H_8O_7$	-	191.01982	0.50	18.02	0.576	3.4	0.5-10	0.999	0.4590	0.1377	5

Metabolits	Condition	Formula	Polarity	Detected m/z(accurate mass)	Delta (ppm)	Average-Rt	%RSD of Rt. reproducibility	Precision	Dynamic Range(µg/ml)	r^2	LOD (µg/ml)	LOQ (µg/ml)	n
Isonicotinic acid	pHILIC	$C_6H_5NO_2$	+	124.03941	0.87	7.42	1.211	4.6	0.1-2	0.999	0.0266	0.0887	5
Itaconate	pHILIC	$C_5H_6O_4$	-	129.01955	1.66	14.63	0.832	4.3	0.05-2	0.999	0.0168	0.0560	5
Maleic acid	pHILIC	$C_4H_4O_4$	-	115.00328	1.02	12.44	1.055	4.1	0.05-2	0.999	0.0149	0.0497	5
Malonate	pHILIC	$C_3H_4O_4$	-	103.00327	0.70	15.27	0.508	3.2	0.5-10	0.999	0.1395	0.4650	5
Mesaconate	pHILIC	$C_5H_6O_4$	-	129.01880	1.54	14.98	0.506	4.8	0.05-1	0.999	0.0144	0.0482	5
Methylmalonate	pHILIC	$C_4H_6O_4$	-	117.01889	1.25	14.46	0.620	5.0	0.05-2	0.999	0.0136	0.0456	5
Oxalate	pHILIC	$C_2H_2O_4$	-	88.98804	0.06	17.19	0.334	4.0	0.5-5	0.999	0.1138	0.3794	5
Pyruvate	pHILIC	$C_3H_4O_3$	-	87.00877	0.07	16.32	0.454	2.0	0.5-5	0.999	0.1154	0.3848	5
Succinate	pHILIC	$C_4H_6O_4$	-	117.01904	1.18	14.78	0.544	3.7	0.1-2	0.999	0.0258	0.0861	5
D-Glucuronate	pHILIC	$C_6H_{10}O_7$	-	193.03493	1.55	15.64	0.747	3.9	0.5-10	0.999	0.1587	0.5292	5

Table 3.6 Linearity of response and limit of detection on the ZIC-pHILIC column of Nucleosides & Nucleotides

Metabolits	Condition	Formula	Polarity	Detected m/z(accurate mass)	Delta (ppm)	Average-Rt	%RSD of Rt. reproducibility	Precision	Dynamic Range(µg/ml)	r2	LOD (µg/ml)	LOQ (µg/ml)	n
5'-Methylthioadenosine	pHILIC	$C_{11}H_{15}N_5O_3S$	+	298.09677	-0.22	7.55	5.000	2.9	0.5-10	0.999	0.1281	0.4272	5
Adenosine	pHILIC	$C_{10}H_{13}N_5O_4$	+	268.10403	0.01	8.47	0.353	3.9	0.5-10	0.999	0.1459	0.4864	5
Cytidine	pHILIC	$C_9H_{13}N_3O_5$	+	244.09370	2.72	11.34	0.752	2.0	0.05-1	0.999	0.0118	0.0393	5
Guanosine	pHILIC	$C_{10}H_{13}N_5O_5$	+	284.09982	3.09	12.00	0.972	3.5	0.5-10	0.999	0.1107	0.3691	5
Inosine	pHILIC	$C_{10}H_{12}N_4O_5$	+	269.08795	-0.35	10.35	0.696	4.1	0.1-2	0.999	0.0190	0.0634	5
Thymidine	pHILIC	$C_{10}H_{14}N_2O_5$	-	241.08250	0.50	6.98	0.883	4.5	0.5-10	0.999	0.1068	0.3562	5
IMP (inosine monophosphate)	pHILIC	$C_{10}H_{13}N_4O_8P$	-	347.04053	2.03	14.96	0.762	4.3	0.5-10	0.999	0.1350	0.4500	5
Allantoin	pHILIC	$C_4H_6N_4O_3$	-	157.03690	1.16	13.36	0.392	1.6	0.5-10	0.999	0.1027	0.3424	5
CMP	pHILIC	$C_9H_{14}N_3O_8P$	-	322.04420	1.93	15.30	0.673	4.9	1-15	0.999	0.3017	1.005	5
UMP	pHILIC	$C_9H_{13}N_2O_9P$	-	323.02810	1.34	14.66	0.628	3.0	0.5-10	0.999	0.1252	0.4175	5
AMP	pHILIC	$C_{10}H_{14}N_5O_7P$	+	348.07050	0.39	13.18	1.028	4.8	1-10	0.999	0.2401	0.8003	5
dAMP	pHILIC	$C_{10}H_{14}N_5O_6P$	+	332.07693	2.48	12.20	1.129	2.5	1-15	0.999	0.1484	0.4949	5
GMP	pHILIC	$C_{10}H_{14}N_5O_8P$	+	364.06537	0.26	16.14	0.690	3.5	1-15	0.999	0.1975	0.6584	5
NAD+	pHILIC	$C_{21}H_{27}N_7O_{14}P_2$	+	664.11700	0.91	13.53	0.691	4.0	1-15	0.999	0.6178	0.1853	5

Table 3.7 Linearity of Response and limit of detection on the ZIC-pHILIC Column of Purines & Pyrimidines

Metabolits	Condition	Formula	Polarity	Detected m/z(accurate mass)	Delta (ppm)	Average-Rt	%RSD of Rt. reproducibility	Precision	Dynamic Range(µg/ml)	r2	LOD (µg/ml)	LOQ (µg/ml)	n
Adenine	pHILIC	$C_5H_5N_5$	-	134.04742	1.54	9.05	0.261	3.1	0.5-5	0.999	0.1040	0.3468	5
Guanine	pHILIC	$C_5H_5N_5O$	+	152.05736	2.42	11.74	0.361	1.3	0.1-2	0.999	0.0192	0.0642	5
Hypoxanthine	pHILIC	$C_5H_4N_4O$	-	135.03146	1.70	9.66	0.563	3.5	0.1-2	0.999	0.0247	0.0826	5
1,7-DimethylXanthine (Paraxanthine)	pHILIC	$C_7H_8N_4O_2$	-	179.05745	0.00	7.03	0.963	3.0	0.05-1	0.999	0.0113	0.0379	5
Xanthine	pHILIC	$C_5H_4N_4O_2$	-	151.02574	1.24	11.03	0.451	4.3	0.05-1	0.999	0.0099	0.0332	5
Pyridoxamine	HILIC	$C_8H_{12}N_2O_2$	+	169.09691	-1.45	26.99	3.736	3.1	0.05-1	0.999	0.0115	0.0384	5
Cytosine	pHILIC	$C_4H_5N_3O$	+	112.05057	-1.21	11.00	0.535	2.2	0.05-1	0.999	0.0096	0.0320	5
Alloxanthine	pHILIC	$C_5H_4N_4O_2$	-	151.02637	1.45	10.07	0.554	4.8	1-10	0.999	0.2373	0.7911	5

Table 3.8 Linearity of Response and limit of detection on the ZIC-pHILIC Column of Pterins

Metabolits	Condition	Formula	Polarity	Detected m/z (accurate mass)	Delta (ppm)	Average-Rt	%RSD of Rt. reproducibility	Precision	Dynamic Range(µg/ml)	r2	LOD (µg/ml)	LOQ (µg/ml)	n
Biopterin	pHILIC	$C_9H_{11}N_5O_3$	+	238.09348	-0.09	11.1	1.002	1.9	0.05-2	0.999	0.0497	0.1659	5
Dihydrobiopterin	pHILIC	$C_9H_{13}N_5O_3$	+	240.10893	-0.76	8.31	0.741	2.9	0.5-10	0.999	0.1456	0.4854	5
Riboflavin	HILIC	$C_{17}H_{20}N_4O_6$	+	377.14560	0.10	7.41	3.116	1.6	0.05-2	0.999	0.0090	0.0303	5
Sepiapterin	pHILIC	$C_9H_{11}N_5O_3$	+	238.09344	-0.09	7.04	0.883	3.0	0.05-2	0.999	0.0494	0.1648	5

Table 3.9 Linearity of Response and limit of detection on the ZIC-pHILIC Column of Amines

Metabolits	Condition	Formula	Polarity	Detected m/z (accurate mass)	Delta (ppm)	Average-Rt	%RSD of Rt. reproducibility	Precision	Dynamic Range(µg/ml)	r2	LOD (µg/ml)	LOQ (µg/ml)	n
Acetylcholine	pHILIC	$C_7H_{15}NO_2$	+	146.11772	1.14	14.88	1.074	4.9	0.01-0.5	1	0.0029	0.0097	5
4-Hydroxy-phenylacetaldoxime	pHILIC	$C_8H_9NO_2$	-	150.05609	0.26	7.12	1.346	4.7	0.05-1	0.999	0.0145	0.0484	5
Triethanolamine	pHILIC	$C_6H_{15}NO_3$	+	150.11261	0.93	8.54	0.990	4.1	0.1-2	0.999	0.0254	0.0849	5
1-Phenylethylamine	HILIC	$C_8H_{11}N$	+	122.09640	-0.23	12.54	3.339	3.7	0.01-0.5	0.999	0.0034	0.0113	5
1-(4-Hydroxyphenyl)-2-aminoethanol	HILIC	$C_8H_{11}NO_2$	+	154.08617	-0.58	15.50	1.111	3.6	0.01-0.5	0.999	0.0028	0.0096	5

Table 3.10 Linearity of Response and limit of detection on the ZIC-pHILIC Column of Sugar Phosphates

Metabolits	Condition	Formula	Polarity	Detected m/z (accurate mass)	Delta (ppm)	Average-Rt	%RSD of Rt. reproducibility	Precision	Dynamic Range(µg/ml)	r2	LOD (µg/ml)	LOQ (µg/ml)	n
D-Glucosamine 6-phosphate	pHILIC	$C_6H_{14}NO_8P$	-	258.03885	1.64	15.75	0.706	3.8	0.5-15	0.999	0.2102	0.7008	5
N-Acetyl-D-Glucosamine6-Phosphate	pHILIC	$C_8H_{16}NO_9P$	+	302.06339	-0.53	14.60	0.428	4.7	1-15	0.999	0.3125	1.041	5
D-Glucose 6-phosphate	pHILIC	$C_6H_{13}O_9P$	-	259.02267	0.90	16.31	0.691	4.9	1-15	0.999	0.2973	0.9910	5

Table 3.11 Linearity of Response and limit of detection on the ZIC-pHILIC Column of Miscellaneous Compounds

Metabolits	Condition	Formula	Polarity	Detected m/z	Delta (ppm)	Average-Rt	%RSD of Rt. reproducibility	Precision	Dynamic Range(µg/ml)	r2	LOD (µg/ml)	LOQ (µg/ml)	n
Ethanolamine phosphate	HILIC	$C_2H_8NO_4P$	-	140.01204	1.58	18.82	2.192	4.2	1-15	0.999	0.292	0.975	5
L-Metanephrine	pHILIC	$C_{10}H_{15}NO_3$	+	198.11252	0.24	16.80	0.873	4.8	0.05-2	0.999	0.0128	0.0426	5
L-Adrenaline	HILIC	$C_9H_{13}NO_3$	+	184.09686	0.23	17.45	0.587	2.5	0.05-2	0.999	0.0148	0.0496	5
L-Noradrenaline	pHILIC	$C_8H_{11}NO_3$	+	170.08125	0.49	7.96	0.377	3.2	0.05-2	0.999	0.0149	0.0499	5

3.2.7 Optimisation of Extraction and Storage of Cell Cultures

The work in the sections above allowed for the selection of the optimal column for the work in terms of producing the best chromatography for the largest number of the standards. No comprehensive evaluation of these columns had been carried out before for intracellular metabolites. The evaluation carried out in chapter 3 confirmed that for overall coverage the ZIC-pHILIC colmn was the best.The technical precision of the LC-MS method was found to be good so the next task was to check the precision for the extraction and storage of cell cultures. An extraction protocol was obtained from previous work on cell cultures (L. Zheng personal communication) and is detailed in section 2.7. Thus a protocol for assessing extraction and storage of extracts from cell cultures was carried out as detailed in section 2.7. The experiments were designed show which changes in any of the protocol parameters might affect the response of metabolites. Therefore, further validation of the method was required in our hands in order to assess the reproducibility of quenching and extraction.

3.2.7.1 Reproducibility of Quenching and Extraction

The method reproducibility was investigated using LNCaP cell extraction by repeating the whole method of extraction of LNCaP cell cultures within a day (n = 6) over 6 weeks giving a total of 36 extractions. The numbers of cells in the counting flasks for each run are shown in table 3.12. The samples were analysed using LC-MS on a ZIC-pHILIC column as detailed in section 2.3.2 and the data was extracted using mzMatch and IDEOM as described in section 2.8.2 and then modelled using SIMCA-P in order to see whether or not there were significant changes in metabolite profiles with time or with storage. The Simca P plot shown in figure 3.21 shows the PCA plot for groups of six samples extracted in six separate weeks. The closest agreement is between the six extracts in each set but between weeks the replicates also cluster quite closely except for R6. In case of R6 the cells in the flask selected for counting were probably lower than the rest of the flasks and thus a lower volume of extraction solvent was used than in the other extractions sets. Upon checking some specific metabolite levels such as glutamate, creatinine, arginine, glucosamine it was found that the levels were much higher than in the other extracts sets. Thus R6 was excluded in order to give a clearer picture of the precision of the extraction method. It is possible to use cell number to normalize the data but as can be seen in figure 3.22 this has no effect on the PCA plot separation.

The intra-day (six repetitions of fresh cell extract) and inter-day repeatability (six repetitions of fresh cell extract of five weeks) were their results summarized in tables 3.12-3.20 for each metabolite. Intra- and inter-day precision for almost all metabolites evaluated were < ±15%.

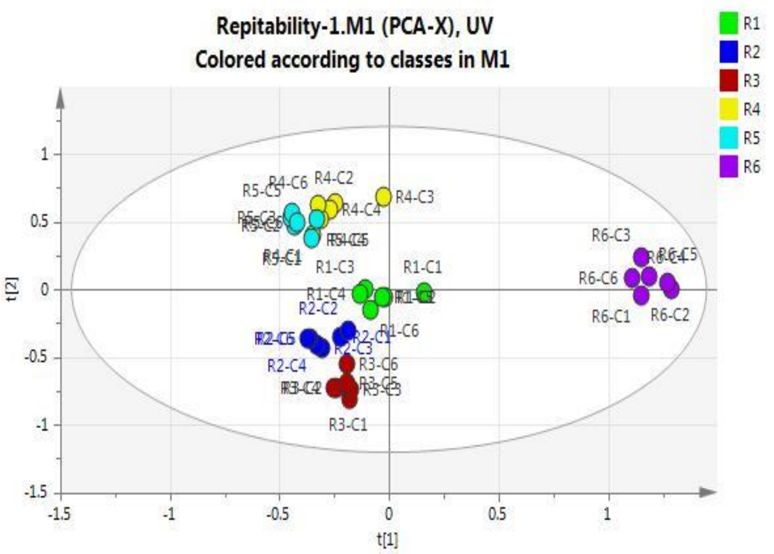

Figure 3.22 PCA plot showing variation in the total metabolite profile over six weeks with one extraction in each week. (R= week number, C=sample number), from PCA plot can see rare cluster of R6 due to misscounte in cell numbers lead to extraction variation in this set of experiment(R6).

A.

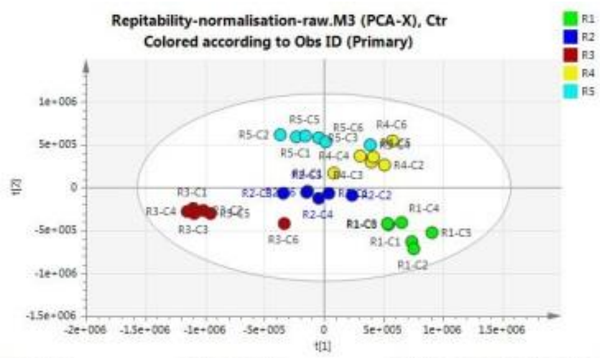

B.

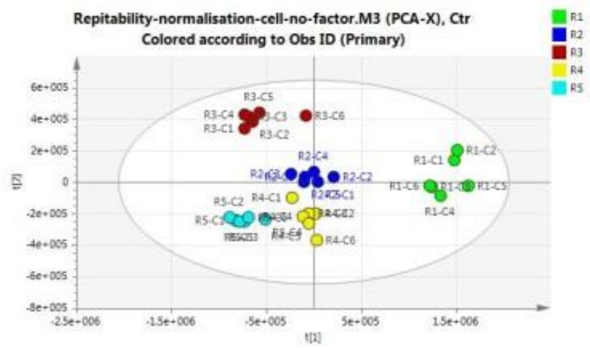

Figure 3.23 Normalization of LNCaP cell (multiply by cell no. factor) using SIMCA-P. (A. raw data, B. normalization using cell number factor).

Table 3.12 Cells in the counting flasks for the experiments R1-R6

EXP. No	Cell No.
R1	**$1.9*10^6$**
R2	**$2.7*10^6$**
R3	**$2.6*10^6$**
R4	**$3.1*10^6$**
R5	**$4.1*10^6$**
R6	**$0.22*10^6$**

3.2.7.2 Stability of Cell Extraction

The stability test was performed by analyzing (n = 5) prepared samples from the same LNCaP cell extractions and dividing them into sixty six aliquots six of them were analyzed on the same day of extraction (S1) then each week twelve extracts were analyzed six of which were stored at -20°C the other six at -80°C for an additional five weeks (S2, S3, S4, S5, S6). The PCA plot is shown in figure 3.23. The samples do not cluster into distinct groups for weeks one and two, which indicate that there were not changes upon storage and that storage temperature did not have effect on these times. While in weeks three and four show a small different cluster which indicate that were changes in metabolite with time as it was approved in section 3.2.7.3 by calculating %RSD (100 x standard deviation/mean).

The short term stability within the autosampler tray was investigated and the PCA shows that there was no change in the metabolites because the clustering of the four samples with different time 0, 4 then 24 hours in the auto injector try cluster each sample together, figure 3.24.

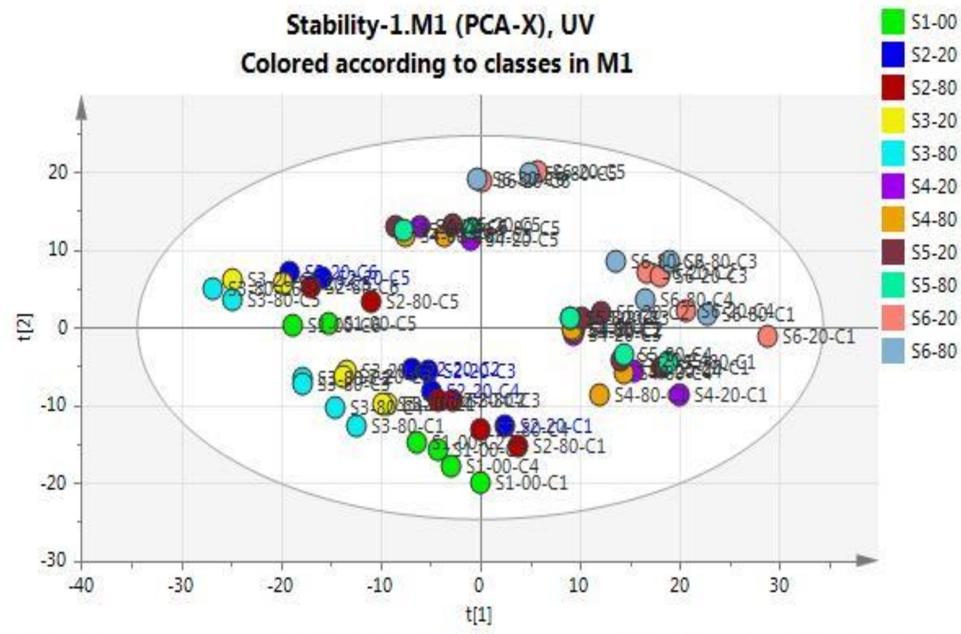

Figure 3.24 The effect of time and storage at -20°C or -80°C on the stability of extracts from LNCaP cells.

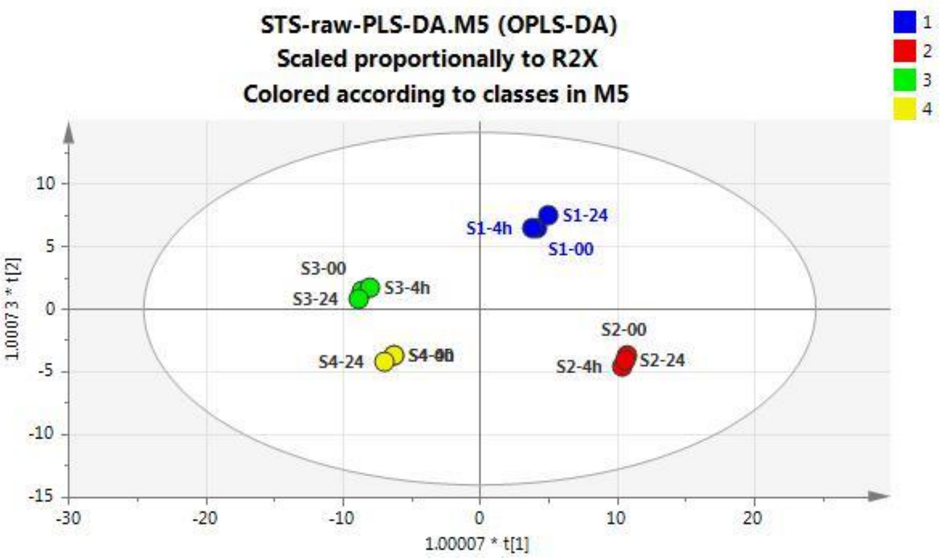

Figure 3.25 Short term stability of cell extracts, S1-4 it is the number of the samples, 00 it is the zero time, 4h it is the sample after 4 hours in the auto injector tray, 24 h it is the sample after 24 hours in the auto injector tray.

The freeze-thaw stability was investigated by using six samples which were kept at -20 °C for 24 hours then thawed at room temperature and then analyzed by LC-MS. Then this cycle was repeated two more times, and then the samples were analyzed again and compared with first run of this group. Figure 3.25 shows the PCA plot for the freeze thaw samples and it is evident that freeze thaw does not cause a significant change in these samples since there are no distinct clusters in the samples.

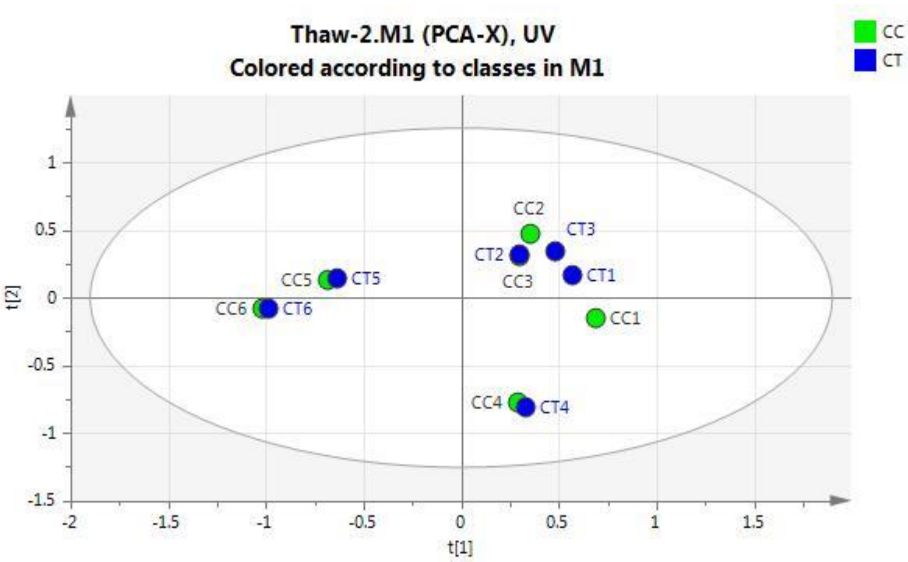

Figure 3.26 The effect of freeze thaw on sample stability of LNCaP cell extracts, CC is the samples before thaw cycle and CT is the sample after thaw cycle.

3.2.7.3 Comparison of metabolite levels of the LNCaP cell extracts stored for increasing lengths of time

Although many metabolites were affected by storage the effect on some metabolites was quite marked. In particular the responses of thiol compounds were decreased with time this observation could be due to the oxidation of these groups or the reaction of these compounds with other components in the mixture. Figure 3.27 and figure 3.28 show that levels of cystine and cysteine were decreased with time while the responses for standards were stable so the instrumental error here is not a reason for the changes in response. Adenine was increased gradually with time (figure 3.29) and this could be explained by the fact that adenine containing metabolites such as adenosine, AMP, ADP and ATP can be hydrolyzed to produce adenine. There was a decrease in glutamine with time and this might be explained by the fact that the amide group in glutamine can hydrolyze to produce glutamic acid.

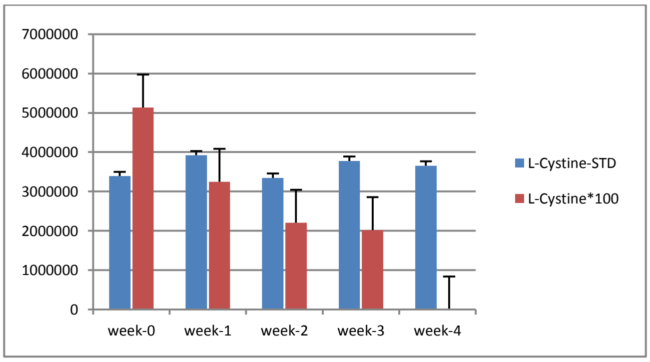

Figure 3.27 Levels of cystine standard (blue bars) and sample extract (red bars) following storage at -20°C for 0-4 week periods. Data are shown as mean ±SEM for N=6 independent experiments.

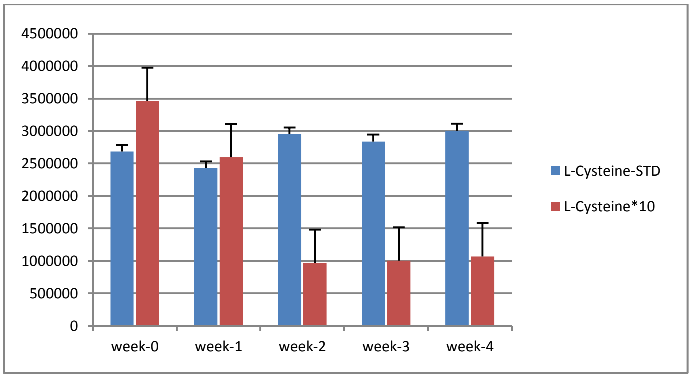

Figure 3.28 Levels of cysteine standard (blue bars) and sample extract (red bars) following storage at -20°C for 0-4 week periods. Data are shown as mean ±SEM for N=6 independent experiments.

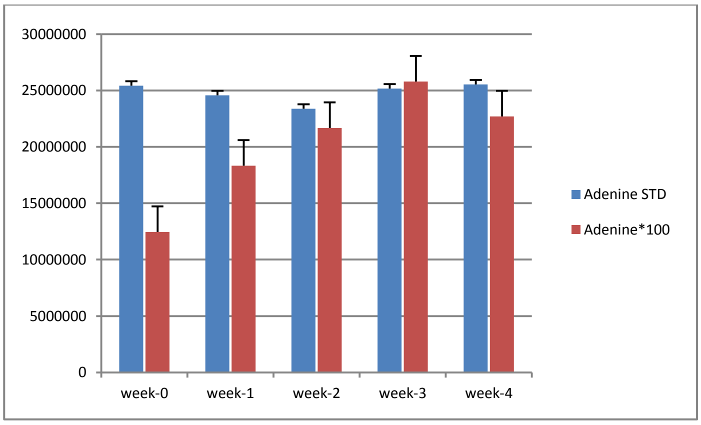

Figure 3.29 Levels of adenine standard (blue bars) and sample extract (red bars) following storage at -20°C for 0-4 week periods. Data are shown as mean ±SEM for N=6 independent experiments.

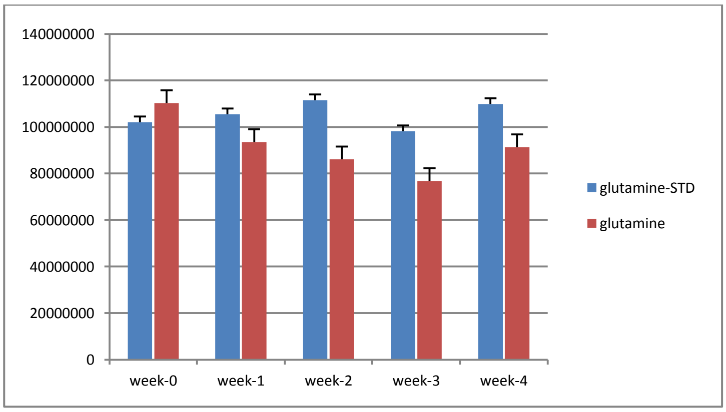

Figure 3.30 Levels of glutamine standard (blue bars) and sample extract (red bars) following storage at -20°C for 0-4 week periods. Data are shown as mean ±SEM for N=6 independent experiments.

Table 3.13 Repeatability and stability for amino acids extracted from LNCaP cultures (n=6). ǂ Compounds exhibititing storage problems.

Metabolites	Stability %RSD		Repeatability %RSD		Thaw %RSD
	2 weeks (6-samples)	4 weeks (6-samples)	Inter-day	Intra-day	
2-Phenylglycine	ND	ND	ND	ND	ND
ǂ beta-Alanine	<57.4	< 71	< 8.2	14.1	< 4.2
cis-4-Hydroxy-D-proline	< 15	< 20	< 10.5	9.9	< 8.5
Creatine	< 10.3	< 14.6	< 7.3	13.8	< 4.8
Ectoine	< 12.1	< 13.8	< 14.7	7.9	< 11.7
Gamma-Aminobutyric acid	< 11.8	< 30.2	< 13.6	13.2	< 7.5
Glycine	< 5.3	< 15	< 12.8	11.7	< 8.6
L-Alanine	< 14.7	< 7.2	< 11.6	14.5	< 3.8
ǂ L-Arginine	< 14.8	< 92.8	< 10.5	13	< 6.2
L-Aspartate	< 13.9	< 14.6	< 8	11.9	< 10.3
L-Cystathionine	< 7.4	< 6.4	< 4.2	9.1	< 4
ǂ L-Cysteine	< 96.4	< 82.9	< 14.7	11.8	ND
L-Cystine	< 22	< 37.4	< 14.7	10.7	< 3.8
ǂ L-Glutamic acid	< 13.1	< 73	< 11	13.9	< 8
O-Acetyl-L-serine	ND	ND	ND	ND	ND
L-Glutamine	< 14.6	< 28.06	< 6.3	8.7	< 4.7
L-Histidine	< 12.8	< 18.2	< 13.6	11.9	< 6.7
ǂ L-Homoserine	< 10.6	< 85.5	<10.5	9.6	< 7
L-Isoleucine	< 14	< 5.5	< 9.4	13.5	< 7
L-Kynurenine	< 7.2	< 14.8	ND	ND	ND
L-Methionine	< 14	< 20.5	< 8.8	14.7	< 5.4
L-Ornithine	< 11.4	< 14.2	< 9.3	13.9	< 9.8
L-Phenylalanine	< 12.7	< 10.5	< 13.8	14.6	< 8.5
L-Proline	< 10.6	< 11.8	< 10.9	9.8	< 5.3

ǂ L-Serine	< 6.7	< 62.9	< 14.8	12.8	< 14.5
L-Threonine	< 10.8	< 13.8	< 6.6	14.6	< 7
L-Tryptophan	< 9.4	< 12.7	< 14.7	14.5	< 9.4
L-Tyrosine	ND	ND	ND	ND	ND
L-Valine	< 13.8	< 12.2	< 14.3	12.4	< 8.3
ǂ Nα-Acetyl-L-lysine	< 73.5	< 29.6	*	*	< 5
O-Acetylcarnitine	< 11.2	< 11.8	< 7.3	15	< 8.2
ǂ Pantothenate	< 15	< 35.9	< 7.4	12.5	< 5.5
Picolinic acid	ND	ND	ND	ND	ND
Taurine	< 14	< 52.7	< 6.2	13	< 8.6
5-Aminolevulinate	<13.6	< 11.2	< 8.7	8.7	< 2.6
Saccharopine	< 12.1	< 15.2	< 14.4	11.6	< 10.8
N-Acetyl-L-aspartate	< 12.5	< 72	< 14.1	13.5	< 9
N-Acetyl-L-glutamate	< 12.1	< 91.9	< 10.4	13.1	< 13
ǂ S-Adenosyl-L-homocysteine	< 97.1	< 60.6	< 10.5	12	< 5.5
Betaine	<14.3	< 32.2	< 9.4	13.3	< 4.7
Sarcosine	< 14.5	< 7.2	< 9	6.4	< 3.8
beta;-alanine-methyl-ester	<10.5	< 7.12	< 12	14.7	< 7.5
2-Indolecarboxylicacid	ND	ND	ND	ND	ND
DL-3-aminobutyrate	< 10	< 27.6	< 12.8	9.5	< 8.3
ǂ N(pi)-Methyl-L-histidine	< 8	< 140.6	< 10.3	15	< 9.2
trans-4-Hydroxy-L-proline	< 13.6	< 11.2	< 8.7	13.4	< 5.2
(R)-S-Lactoylglutathione	ND	ND	ND	ND	ND
ǂ Glutathione	< 6.04	< 31.03	< 5.2	9.9	< 2.9

Table 3.14: Repeatability and stability for sugars extracted from LNCaP cultures (n=6).

Metabolites	Stability %RSD		Repitability %RSD		Thaw %RSD
	2 weeks (6-samples)	4 weeks (6-samples)	Inter-day	Intra-day	
D-Fructose	*	*	*	*	*
D-Galactose	*	*	*	*	*
D-Mannose	*	*	*	*	*
D-Xylose	< 12.8	< 11.5	< 14	6.7	< 4.2
D-Glucosamine	ND	ND	< 13.7	8.6	< 3.9
N-Acetyl-D-glucosamine	*	*	*	*	*
D-Glucose	*	*	*	*	*
cis-Aconitate (Dehydroascorbic acid)	<12.9	< 41.9	< 10.6	15	< 9
N-Acetyl-D-mannosamine	*	*	*	*	*

* The chromatographic separation was not good

Table 3.15 Repeatability and stability for carboxylic acids extracted from LNCaP cultures (n=6). ǂCompounds exhibiting storage problems.

Metabolites	Stability %RSD		Repitability %RSD		Thaw %RSD
	2 weeks (6-samples)	4 weeks (6-samples)	Inter-day	Intra-day	
ǂ (R)-Malate	<14.4	< 31.7	< 8.9	14.2	< 10.6
Phthalate	ND	ND	< 10.8	7.4	< 13.6
2-Hydroxybutanoic acid	< 15	< 21.3	< 13.8	8.5	< 3.8
ǂ 2-Oxoglutarate	<7.01	< 33.9	< 6.9	3	< 7.7
4-Coumarate	ND	ND	ND	ND	ND
4-hydroxylphenylacetate	ND	ND	ND	ND	ND
ǂ Ascorbate	<12.9	< 43.5	< 9.2	12.4	< 8.2
Caffeate	ND	ND	ND	ND	ND
Citramalate	< 8.1	< 17.2	< 4.2	8.9	< 1.6
Diethyl 2-oxoglutarate	< 11.5	< 40.7	< 13.9	15	< 8.1
ǂ Fumarate	< 14.05	< 42.3	< 7.6	9.2	< 2.1
Gallate	ND	ND	ND	ND	ND
Isocitrate	< 14.7	< 14.4	< 6.6	10.6	< 5.9
Isonicotinic acid	ND	ND	ND	ND	ND
ǂ Itaconate	< 14.8	< 70.1	< 11	11.5	< 8.5
Maleic acid	<15.3	< 78.6	< 7.8	10.1	< 2.1
ǂ Malonate	< 7.9	< 45.7	< 9.7	15	< 9.0
ǂ Mesaconate	< 11.8	< 70.1	< 12.8	14.1	< 9.8
ǂ Methylmalonate	< 6.11	< 32.5	< 11.5	5.7	< 5.7
ǂ Oxalate	< 6.1	< 47.1	< 8.4	12.9	< 9.7
ǂ Pyruvate	< 7.3	< 34.1	< 8.2	11.4	< 5.9
ǂ Succinate	< 7	< 32.5	< 12.1	9.3	< 5.7
D-Glucuronate	ND	ND	< 12.7	11.5	< 6.1

Table 3.16 Repeatability and stability for nucleoside & nucleotide extracted from LNCaP cultures (n=6). ǂ Compounds exhibiting storage problems.

Metabolites	Stability %RSD		Repitability %RSD		Thaw %RSD
	2 weeks (6-samples)	4 weeks (6-samples)	Inter-day	Intra-day	
ǂ 5'-Methylthioadenosine	<14.2	< 68.3	< 11.9	14.4	< 12
Adenosine	< 14.9	< 14.8	< 14.4	11.4	< 10.9
Cytidine	< 12.7	< 13.4	< 11.7	11.5	< 8.6
Guanosine	ND	ND	ND	ND	ND
Inosine	< 14.8	< 15	ND	ND	< 9.8
ǂ Thymidine	< 12.8	< 65.7	< 5.4	13.8	< 10.8
IMP	ND	ND	ND	ND	ND
Allantoin	<14.4	< 15.0	< 12.8	6	< 3.6
CMP	ND	ND	ND	ND	ND
UMP	< 11.9	< 25.7	< 11.6	11.9	< 9.2
ǂ ATP	<11.9	< 45.8	< 8.9	14.2	< 9.1
AMP	<10.1	< 56	< 9.8	7.7	< 10
dAMP	ND	ND	ND	ND	ND
ǂ GMP	< 11.6	< 46.1	< 12.1	13.6	< 7.7
GTP	< 7.4	< 14.3	< 14.7	7.5	< 6.9
ǂ NAD+	< 4.5	< 35.07	< 9.7	8.7	< 3.1

Table 3.17 Repeatability and stability for purines & pyrimidines extracted from LNCaP cultures (n=6). ǂ Compounds exhibiting storage problems.

Metabolites	Stability %RSD		Repitability %RSD		Thaw %RSD
	2 weeks (6-samples)	4 weeks (6-samples)	Inter-day	Intra-day	
ǂ Adenine	< 44.5	< 45.4	< 12.7	10.5	< 14.8
Guanine	< 6.4	< 11.4	< 10.7	6.4	< 4.6
Hypoxanthine	< 14.5	< 13.5	< 13.3	10.7	< 5.8
1,7-DimethylXanthine	ND	ND	ND	ND	ND
Xanthine	< 13.4	< 20.0	< 9.8	10.7	< 7.8
Pyridoxamine	ND	ND	ND	ND	ND
ǂ Cytosine	< 14.5	< 66.1	< 12.5	10.6	< 14.5
Alloxanthine	< 13.4	< 20.0	< 10.7	13.2	< 8

Table 3.18 Repeatability and stability for pterins extracted from LNCaP cultures (n=6). ǂ Compounds exhibiting storage problems.

Metabolites	Stability %RSD		Repitability %RSD		Thaw %RSD
	2 weeks (6-samples)	4 weeks (6-samples)	Inter-day	Intra-day	
Biopterin	ND	ND	ND	ND	ND
ǂ Dihydrobiopterin	< 13.9	< 29.8	ND	ND	< 10.5
Riboflavin	ND	ND	ND	ND	ND
Sepiapterin	ND	ND	ND	ND	ND

Table 3.19 Repeatability and stability for amines extracted from LNCaP cultures (n=6).

Metabolites	Stability %RSD		Repitability %RSD		Thaw %RSD
	2 weeks (6-samples)	4 weeks (6-samples)	Inter-day	Intra-day	
Acetylcholine	ND	ND	5.3	7.6	< 9.7
4-Hydroxyphenylacetaldoxime	ND	ND	13.8	11.2	ND
Triethanolamine	< 4.9	< 105.2	11.3	12.5	< 6.8
1-Phenylethylamine	ND	ND	ND	ND	ND
1-(4-Hydroxyphenyl)-2-aminoethanol	ND	ND	ND	ND	ND

Table 3.20 Repeatability and stability for sugar phosphates extracted from LNCaP cultures (n=6).

Metabolites	Stability %RSD		Repitability %RSD		Thaw %RSD
	2 weeks (6-samples)	4 weeks (6-samples)	Inter-day	Intra-day	
D-Glucosamine 6-phosphate	ND	ND	ND	ND	ND
N-Acetyl-D-Glucosamine 6-Phosphate	ND	ND	ND	ND	ND
D-Glucose 6-phosphate	< 11.9	< 13.2	< 9.2	10.1	< 6.5

Table 3.21 Repeatability and stability for miscellaneous compounds extracted from LNCaP cultures (n=6). ǂ Compounds exhibiting storage problems.

Metabolites	Stability %RSD		Repitability %RSD		Thaw %RSD
	2 weeks (6-samples)	4 weeks (6-samples)	Inter-day	Intra-day	
ǂ Ethanolamine phosphate	< 9.5	< 25.8	< 9.4	9.9	< 4.2
L-Metanephrine	ND	ND	ND	ND	ND
L-Adrenaline	ND	ND	ND	ND	ND
L-Noradrenaline	< 7.5	< 23.6	< 10.2	12.9	< 5.8

3.2.8 Confirmation of metabolite identity by MS^2 on the LTQ Orbitrap

In order to provide extra confirmation of identity MS^2 spectra (MS/MS) were obtained for some of the compounds in the standard mixtures of compounds in so far as it was possible to obtain good quality spectra. Figures 3.30 – 3.35 show some examples of MS^2 spectra and the table 3.21 shows some of the interpretation of the spectra.

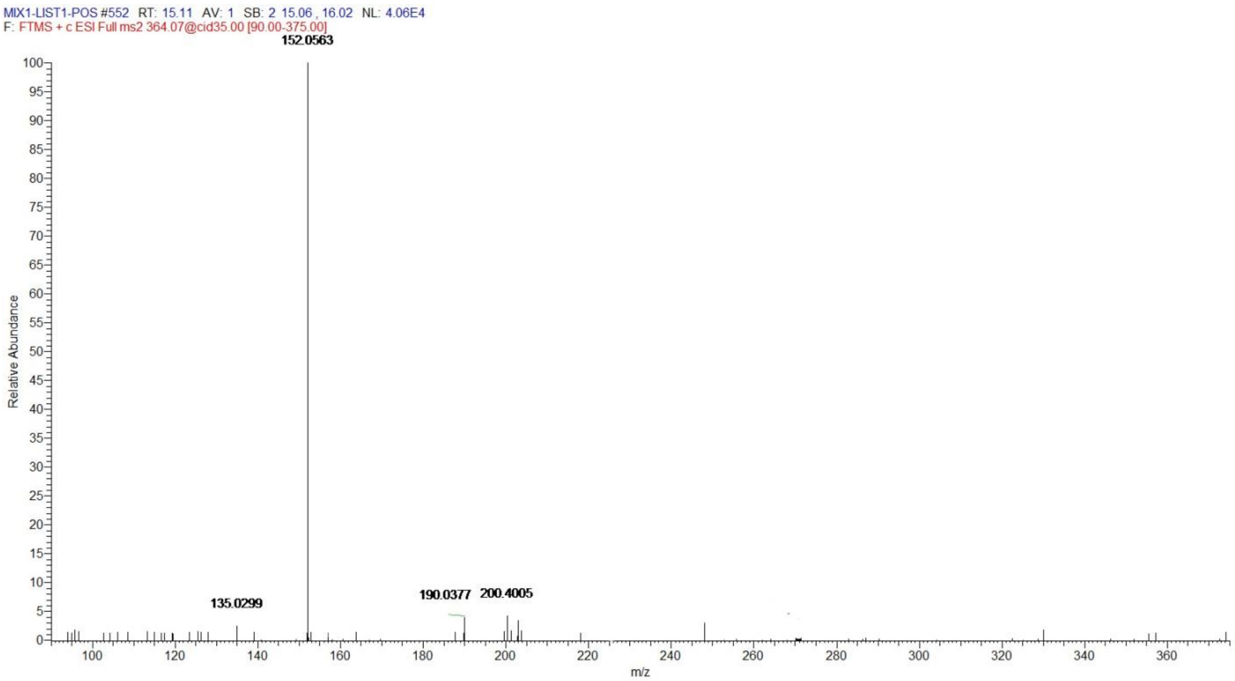

Figure 3.31 MS^2 spectrum of guanosine monophosphate (152.0563 (100% $-C_5H_8O_7P$))

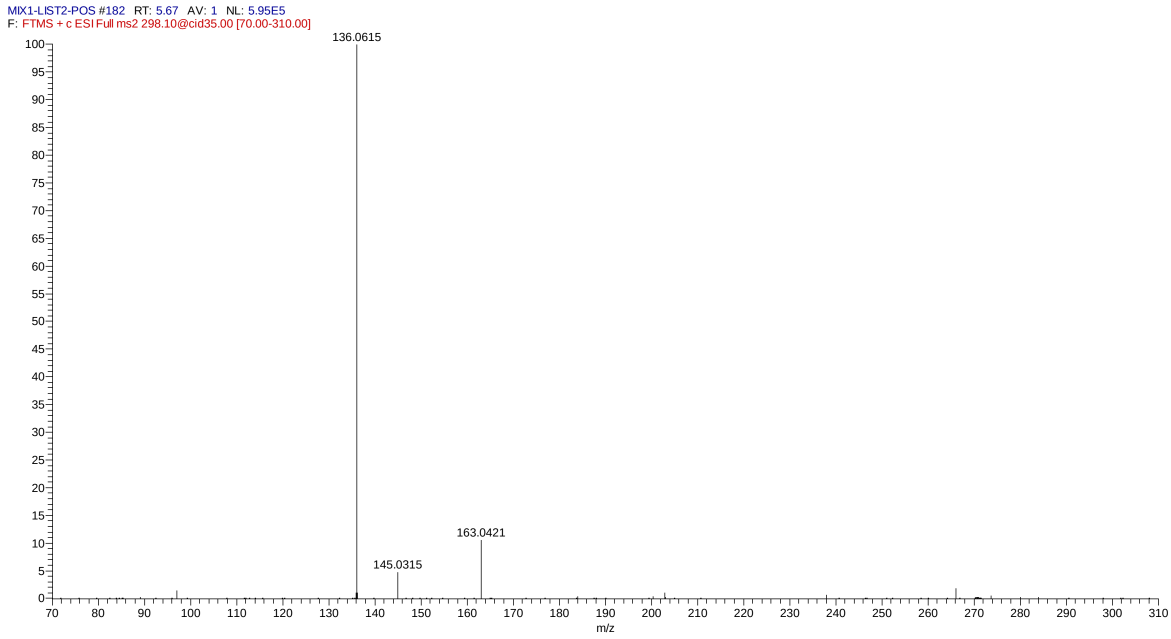

Figure 3.32 MS^2 spectrum of S-adenosyl methionine (136.0615 (100% - $C_{10}H_{19}O_5NS$)).

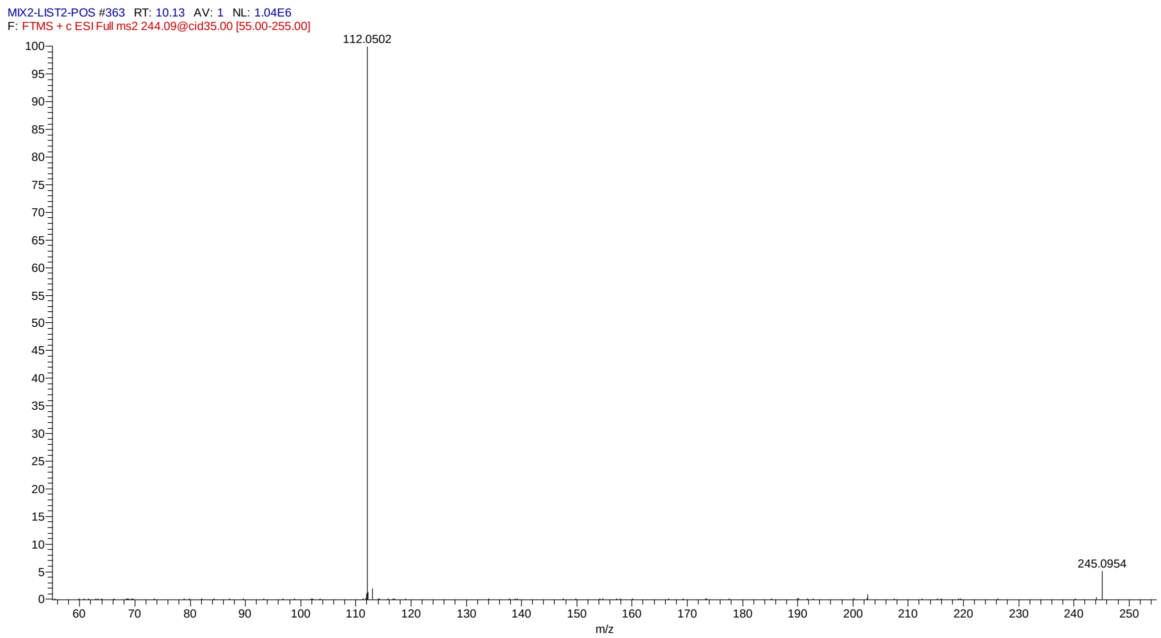

Figure 3.33 MS^2 spectrum of cytidine (112.0502 (100% - $C_5H_{10}O_4$))

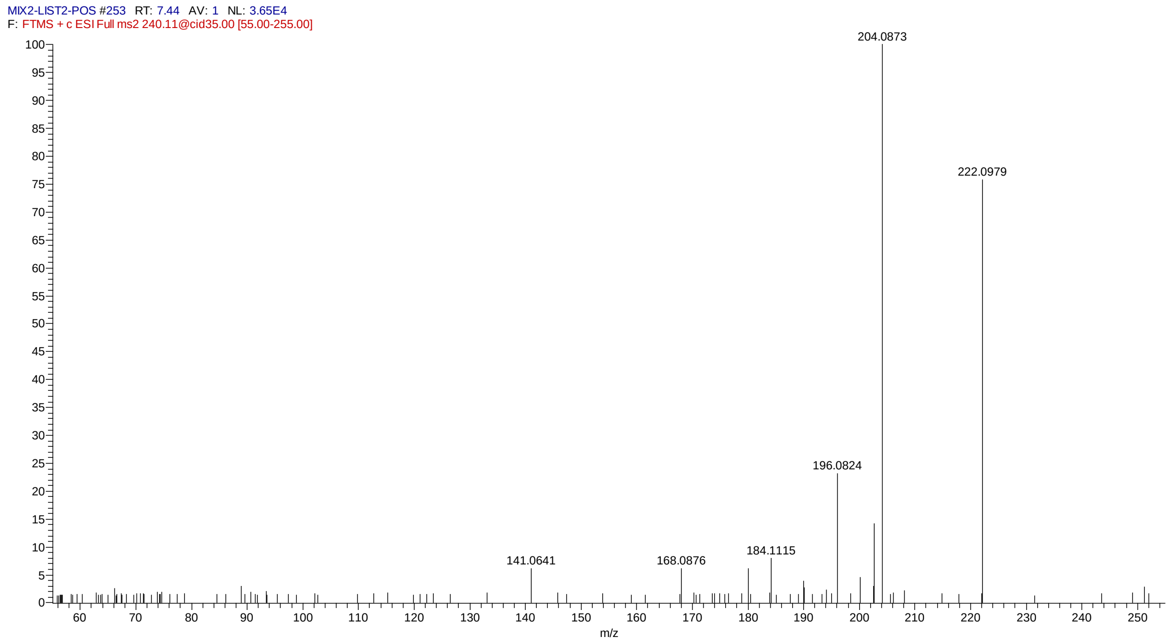

Figure 3.34 MS^2 spectrum of dihydrobiopterin (204.0873(100% - 2OH) 222.0979 (78% - H_2O))

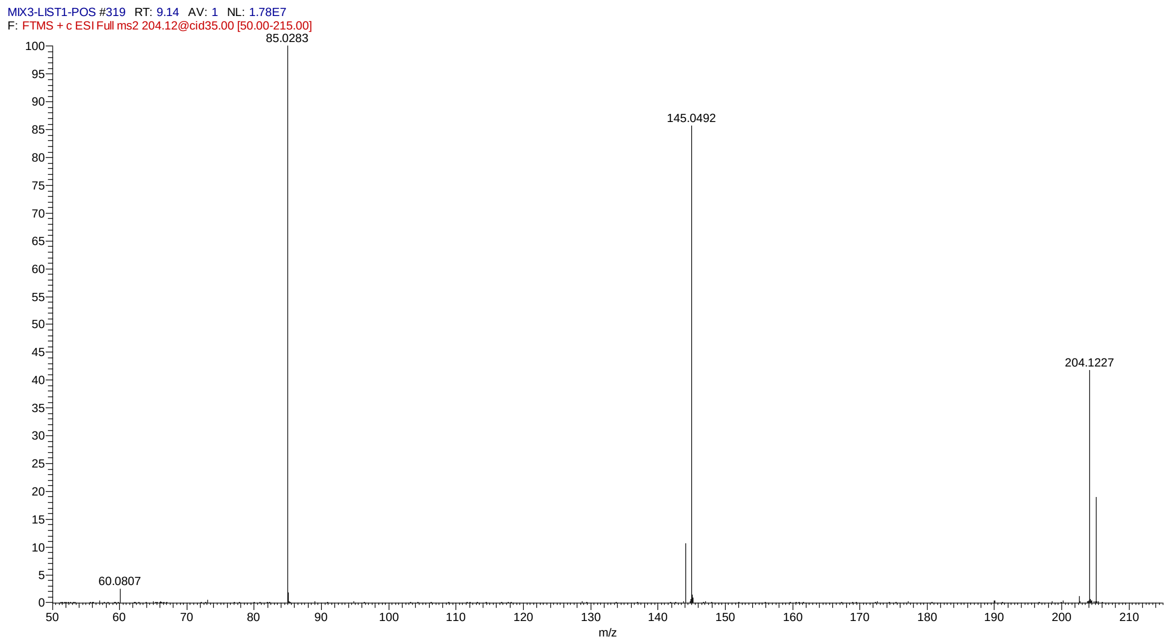

Figure 3.35 MS^2 spectrum of acetyl carnitine (85.0283 (100% -$C_5H_{12}O_2N$) 145.0492 (90% - $C_2H_2O_2$))

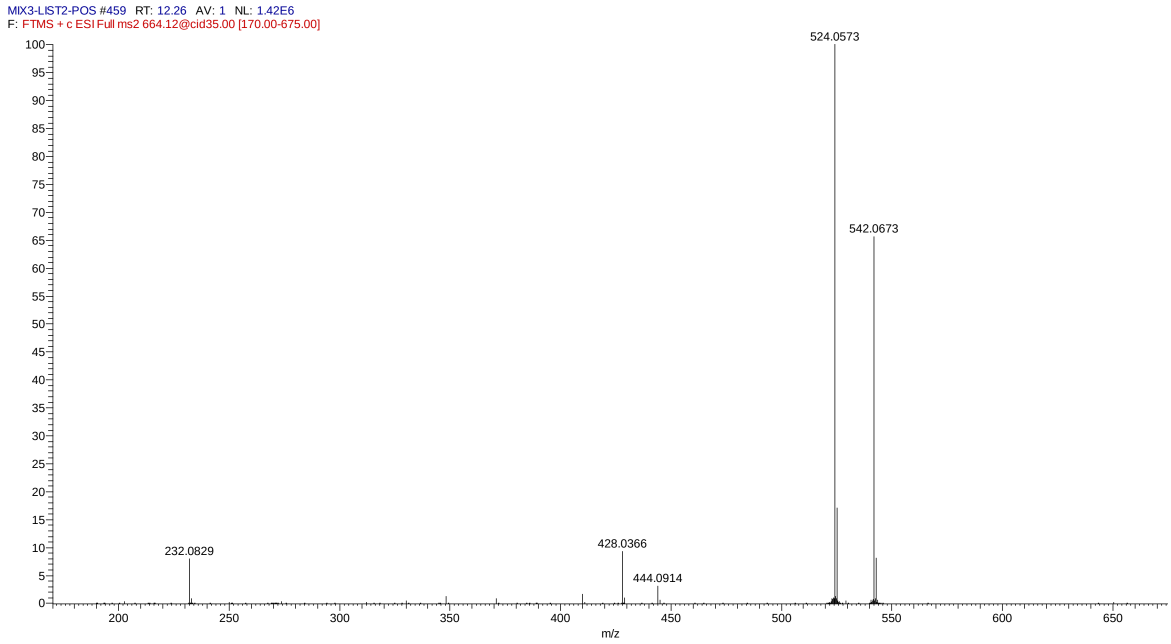

Figure 3.36 MS[2] spectrum of NAD+ (524.0573 (100% - $C_5H_8N_5$) 542.0673 (70% - $C_6H_6ON_2$) 428.0366 (13% - $C_{11}H_{11}O_4N_2$) 232.0829 (10% - $C_{10}H_{17}O_{10}N_5P_2$))

Table 3.22 Summary of MS^2 data for some of the metabolite standards.

Metabolite	Molecular Ion	Fragments
2-Phenylglycine	152.0703	135.0438 (100%-NH_2), 107.0489 (9%-COOH),106.0650 (43% -COO),79.0541 (3%-$C_2H_3O_2N$)
beta-Alanine	90.0548	73.0646 (7%-OH),72.0443 (100%-H_2O),
cis-4-Hydroxy-D-proline	132.0653	114.0548 (2%-H_2O),86.0599 (100%-COOH),68.0493 (5%-COOH-OH)
Creatine	132.0765	114.0660 (2.5% -H_2O), 90.0548 (100%- CN_2H_2)
Ectoine	143.0813	97.0759 (100%-COOH)
Gamma-Aminobutyric acid	104.0704	87.0439 (100%- NH_2),86.0600 (32%- H_2O),73.0647 (1%-OH- NH_3) ,56.0494(3%-COOH)
Glutamic acid	146.0600	102.0547 (100% -HCOOH) 74.0235 (10.3% -HCOOH-CO)
L-Glutamine	147.0761	130.0495 (100% -OH), 84.0443 (5% -HCOOH-NH_3)
L-Histidine	156.0763	112.0866 (1% -NH_2 -CO),110.0710 (100% -HCOOH),95.0602 (3% -COOH-NH_3)
L-Homoserine	120.0653	102.0548 (95% -H_2O),84.0442 (2% -OH-OH),74.0599 (100% -HCOOH),56.0494 (18% -HCOOH-OH)
L-Isoleucine	132.1016	86.0963 (100% -HCOOH),69.0698 (8% -HCOOH-NH_3)
L-Phenylalanine	166.0858	149.0549 (4% -OH),131.0489 (9% -H_2O-NH_2),120.0804 (100% -HCOOH), 103.0541 (1% -HCOOH-NH_3)
L-Proline	116.0704	70.0650 (100% -HCOOH)
L-Threonine	120.0653	102.0548 (100%-H_2O),84.0442 (4% -2H_2O),74.0599(55% -HCOOH),56.0494 (13% -HCOOH -H_2O)
L-Valine	118.0860	72.0806 (100% -HCOOH),55.0541 (6% -HCOOH-NH_3)
Nα-Acetyl-L-lysine	189.1230	171.1125 (56% -H_2O),153.1020 (23% -2H_2O),147.1126 (9% -$COCH_3$),129.1020 (100% -$HCOCH_3NH_2$),112.0756 (1% -$HCOCH_3NH_2$ -OH),101.1072 (2% - $COCH_3$ -COOH),84.0807 (11% -$HCOCH_3NH_2$ -COOH)
O-Acetylcarnitine	204.1227	,145.0492 (88% - N-3(CH_3)),85.0283 (100% -$COOCH_3$ -N-3(CH_3)), 60.0807 (3% -$C_6H_8O_4$)
Pantothenate (Pantothenic acid)	220.1174	202.1067 (100% -H_2O) ,184.0962 (43% -2H_2O) ,174.1121 (10% -HCOOH) ,166.0859 (3%-3H_2O) ,142.0860 (1% -3OH –C2H3) 116.0340 (4% -CH_2CH_2COOH-CH_3-CH_3),98.0235 (2% -CH_2CH_2COOH-CH_3-CH_3 -H_2O),90.0548 (15% -$C_6H_9O_3$)
Picolinic acid	124.0390	106.0284 (100%-H_2O),78.0336 (39% -HCOOH)
5-Aminolevulinate	132.0652	114.0547 (100% -H_2O),96.0441 (1% -2H_2O),86.0599 (15% -HCOOH)

N-Acetyl-L-glutamate	190.071	172.0599 (100% -H_2O) ,154.0496 (1% -2H_2O) ,144.0653 (4%-HCOOH) ,130.0495 (78% -$COCH_3$ -H_2O) ,116.0704 (1% -2OH-$COCH_3$), 102.0548 (1% -COOH -$COCH_3$), 84.0442 (3% -COOH -$COCH_3$ H_2O), 73.0646 (1% -COO^- -$NCOCH_3$ -O^-)
Betaine	118.0863	59.0729 (76% -N^+3CH_3),58.0651 (100% -CH_3COOH)
2-Indolecarboxylicacid	160.0401	116.0502 (100% -COOH)
N(pi)-Methyl-L-histidine	170.0920	126.1022 (97% -COOH),109.0758 (100% -COOH –NH_3),97.0759 (10% - $CHNH_2$- COOH)
(R)-Malate (Malic acid)	133.0141	115.0034 (100% -H_2O),87.0086 (3% -HCOOH),71.0136 (9% -HCOOH -OH)
4-Coumarate (Coumaric acid)	163.0398	119.0499 (100% -COOH)
Benzenesulfonate	156.9963	93.0344 (100% -SO_2)
Citramalate (Citramalic acid)	147.0297	129.0191 (63% -H_2O),111.0086 (1% -2H_2O),103.0399 (8% -COOH), 87.0086 (62% -COOH –CH_3),85.0293 (100%-COOH -OH),71.0137 (1% -CH_2COOH -OH), 57.0344 (15% -2 COOH)
Maleic acid	115.0033	71.0136 (100%-COOH)
D-Glucose ; beta-D-Glucose	179.0563	161.0453 (1% -H2O),143.0348 (12% -2H2O), 131.0346 (0.5% -COH -H2O),119.0348 (0.6% -CH2OH -COH) , 101.0242 (3% -CH_2OH –COH -H_2O),89.0242 (4.5% HO-CH_2-CH-OH -COH),71.0137 (0.9% -HO-CH_2-CH-CH-OH -COH -OH),59.0136 (1.7% - HO-CH_2-CH-OH -COH -OH)
AMP	348.0705	136.0615 (100% -$C_5H_8O_7P$),119.0350 (5% -$C_5H_8O_7P$ -NH_3)
GMP	364.0654	248.0775 (4% -PO_4 -OH),152.0565 (100%-$C_5H_8O_7P$),135.0300 (-$C_5H_8O_7P$ –NH_3)
Adenine	134.0470	107.0361 (100% -N=CH)
Cytosine	112.0503	95.0237 (31% -NH_3), 66.1405 (100% -H_2N-CH-OH)
Sepiapterin	238.0929	220.0822 (100% -H_2O) ,202.0720 (4% -2H_2O), 194.0667 (25% -HO-CH-CH_3),178.0720 (8% HO-CH-CH_3 -O^-),165.0643 (1% -$C_3H_5O_2$)
Acetylcholine	146.1172	114.0548 (1% -2CH_3),87.0439 (100%-N^+3(CH_3)),60.0807(15% -$C_4H_7O_2$)
Triethanolamine (Trolamine)	150.1122	132.1016 (100% -H_2O), 114.0912 (12% -2H_2O), 106.0862 (2% -C_2H_5O),96.0808 (1% -3H_2O),88.0756 (6% -C_2H_5O -OH),70.0650 (3% -C_2H_5O -2H_2O)
1-Phenylethylamine	122.0962	105.0697 (100% -NH_3), 79.0541 (1% -H_2N-CH-CH_3)
Inosine	269.0879	137.0543 (100% $C_5H_5N_4O$)

3.3Discussion:

The objective of the work was to select the chromatographic column which would give the best performance for the greatest number of metabolites. Four mixtures containing about 180 metabolites were run on five different columns.

The chromatographic data obtained shows examples of good chromatography on the ZIC-pHILIC column. High efficiencies were obtained on the ZICHILIC column although not far as great number of analytes as with the ZIC-pHILIC column. ZICHILIC column shows some examples of good chromatography. The C18 AR column produced sharp peaks for many analytes but this is largely as a result of a lack of chromatographic retention and lack of chromatographic retention brings with it the risk of ion suppression effects in biological extracts and also isomers cannot be resolved. The silica C column was also capable of producing good chromatographic performance for a more limited range of analytes than the ZIC-pHILIC column. Finally the BEH amide column also produced good chromatographic performance and was second in overall high quality coverage to the ZIC-pHILIC column although the ZICHILIC column complements the ZIC-pHILIC column in terms of its separation abilities. Zhang et al compared three columns (Reversed Phase, Aqueous Normal Phase and Hydrophilic Interaction Liquid Chromatography) for testing polar compounds of urine samples. They found that the ZIC-pHILIC column was very useful for extending the coverage of polar metabolites in human urine (Zhang et al., 2012).

The clearest superiority of performance of the ZIC-pHILIC column can be seen in the separations produced for acids, comparing the chromatography of four acids on the five columns no column comes close to matching the performance of the ZIC-pHILIC column. The retention of polar compounds on ZIC-pHILIC is caused by a combination of hydrophilic partitioning and electrostatic interaction of polar/ionised solutes between the mobile phase and the water-rich/zwitterionic stationary phase. Good peak shapes of acids are likely to be produced by a competition between hydrophilic partitioning and electrostatic interaction for totally ionized metabolites. That is why acidic metabolites show good peak shapes under the conditions of ZIC-pHILIC+AC (mobile phase pH 9.2). However, bad peak shapes are likely to result from a competition between hydrophilic partitioning and electrostatic interaction for partially ionized metabolites. That is why acidic metabolites show bad peak shapes under the conditions of ZIC-HILIC+FA (mobile phase pH 2.8) (Schaefercor and Dixon, 1996). The tailing on acid peaks separated with BEH Amide column at high pH which may due to strongly retained of totally ionized acids whichmay undergo electrostatic repulsion by the many free silanol groups in this column. It is notable that the ZIC-pHILIC column is based on a polymer so there are no silanol groups in the stationary phase support.

The ZIC-pHILIC method can be used for profiling analytes of interest, such as amino acids, carboxylic acids, nucleosides, nucleotides, petrins, purines, amines and sugar phosphates. The elution of polar metabolites using the ZIC-pHILIC column can be divided according to their physicochemical properties. The carboxylic acid region starts at 4 min, finishes at 18 min. Nucleosides and nucleutides region starts at 6.5 min and finishes at 18.5 min. The purines and pyrimidins region starts at 6.5 min and finishes at 12 min. The amino acids region starts at about 7 min, finishes around 17 min. The amines region starts at 7 min and finishes at 15.5 min. The pterins region starts at 7 min and finishes at 8 min. The sugars region starts at about 11 min, finishes around 18 min. The sugar phosphate region starts at 14.5 min and finishes at 16.5 min. This data can be used for the identification of metabolites that come from the LNCaP cell culture extract identified to MSI level 1 according to accurate mass and comparison of retention times with standards. The methodology should also be able to discriminate between isomeric metabolites as far as possible. In HILIC chromatography the critical solvent combination used for the mobile phase system is essential to enhance the molecular ionization in the electrospray ion source of the mass spectrometer and produce enough variation in solvent strength to distribute metabolite elution in different areas according to hydrophilicity and polarity. Indeed, different mechanisms for metabolite retention in the ZIC-pHILIC column may be due to partitioning, adsorption and even ion exchange, based on the nature of analytes and the solvent composition. Therefore, the prediction of the behavior of metabolites regarding their retention is possible according to the quantitative structure retention relationship (QSRP) model (Creek et al., 2011). Using the QSRP model can be helpful in metabolite identification of compounds that are not commercially available since a prediction of retention time can be made.

When making measurements using high resolution mass spectrometry it is possible to be confident of the elemental composition of a metabolite but where two compounds are isomers and have the same elemental composition only chromatographic separation can be used to distinguish them. The five columns can be compared for their ability to separate isomers in this study 19 pairs of isomers were used to test the separation ability of each column and their retention times. α- alanine, β- alanine and sarcosine were separated by ZIC-pHILIC and ZIC-HILIC but not by the other columns. Methylmalonate and succinate on the ZIC-pHILIC column which they were nearly separated and might be separable will be need more optimisation of the HPLC parameters while in the other columns they were not separated at all. Isoleucine and leucine were well separated by ZIC-pHILIC, Silica-C and BEH-amide but not by ZIC-HILIC. 4-aminobutyric acid and 3- aminobutyric acid were separated by ZIC-pHILIC, Silica-C and BEH-amide but not by ZIC-HILIC. Cis-4-hydroxy D-proline and Trans-4-hydroxy D-proline were separated by ZIC-pHILIC, Silica-C and BEH-amide columns but not by a ZIC-HILIC column. Biopetrin and sepiapetrin were separated by ZIC-pHILIC, Silica-C, BEH-amide and ZIC-HILIC columns. DL-glyceraldehyde 3-phosphate and dihydroxy-acetone phosphate were separated well only by a

ZIC-pHILIC column, Silica-C shows one broad peak and BEH-amide shows multiple unseparated peaks and ZIC-HILIC shows partially separated peak. Betaine and valine were separated by ZIC-pHILIC, Silica-C and ZIC-HILIC columns but not a BEH-amide column. Fumarate and maleic acid were separated only by the ZIC-pHILIC column while Silica-C shows two peaks for maleic acid and BEH-amide shows multiple peaks and bad separation for maleic acid and it was not detected by ZIC-HILIC. None of these sets of isomers could be separated on the C18 AR column but all of them separated well using ZIC-pHILIC. On other study eight isomers was separated using ZICHILIC and ZIC-pHILIC (Zhang et al., 2012).

Testing Linearity of Response and limit of detection on the ZIC-pHILIC Column

In order investigate the performance of the LC-MS method, ~ 180 metabolite standards were prepared and diluted to concentrations of (1-20000 ng/ml). The linear range, limit of detection and technical precision obtained for the metabolite standards. The majority of the metabolites standards showed a broad linear range according to calibration curve lines. The LOD and LOQ were determined for all of the standard metabolites and it was found that the method presented here was suitable for metabolomics analysis because it had both low detection limits and a broad linear range for most analytes.

Technical precision and reproducibility

The instrument precision (or chromatographic repeatability) was obtained and the relative standard deviation (RSD) of the response of standard compounds which were below 5%. The precisions obtained for each analyte was good and for three points on the calibration curve RSDs were $\leq$ 5% for all of the metabolite standards at each calibration point.

Optimisation of Extraction and Storage of Cell Cultures

An extraction protocol was obtained from previous work on cell cultures (L. Zheng personal communication). A protocol for assessing extraction and storage of extracts from cell cultures applied on ZIC-pHILIC condition. The experiments were designed show which changes in any of the protocol parameters might affect the response of metabolites. Therefore, further validation of the method was required in our hands in order to assess the reproducibility of quenching and extraction.

The method reproducibility was investigated using LNCaP cell extraction by repeating the whole method of extraction of LNCaP cell cultures within a day (n = 6) over 6 weeks giving a total of 36 extractions. The Simca P plot shows the PCA plot for groups of six samples extracted in six separate weeks. The closest agreement is between the six extracts in each set but between weeks the replicates also cluster quite closely except for R6. In case of R6 the cells in the flask selected for counting were probably lower than the rest of the flask and thus a lower volume of extraction solvent was used in the other extractions. Upon checking some specific metabolite levels such as glutamate, creatinine, arginine, glucosamine it was found that the levels were much higher than in the other extracts. Thus R6 was excluded in order to give a clearer picture of the precision of the extraction method. It is possible to use cell number to normalize the data but as can be seen in this case has no effect on the PCA plot separation.

The stability test performed by analyzing (n = 5) prepared samples from the same LNCaP cell extractions and dividing them into 66 aliquots 6 of them were analyzed on the same day of extraction (S1) then each week 12 extracts were analyzed 6 of which were stored at -20°C the other 6 at -80°C for an additional 5 weeks (S2, S3, S4, S5, S6). The PCA plot shows the samples do not cluster into distinct groups for weeks one and two, which indicate that there were no changes upon storage and that storage temperature did not have effect on these times. While in weeks three and four show a small different cluster which indicate that were changes in metabolite with time as it was proved by calculating %RSD.

The short term of stability was investigated and the PCA shows that no change in the metabolites because the clustering of the four samples with different time 0, 4 then 24 hours in the auto injector try cluster each sample together.

The freeze-thaw stability was investigated by using 6 samples. The PCA plot for the freeze thaw samples shows evident that freeze thaw does not cause a significant change in these samples since there are overlapped and has distinct clusters in the samples.

The intra-day (six repetitions of fresh cell extract) and inter-day precision (six repetitions of fresh cell extract of five weeks) for almost all metabolites evaluated were < ±15%. However, the effect of storage on some metabolites was quite marked. In particular the responses of thiol compounds were decreased with time this observation could be due to the oxidation of these groups or the reaction of these compounds with other components in the mixture as levels of cystine and cysteine were decreased with time while the standard values were stable so the instrumental error here is not a reason. Thus it is evident that length of storage and storage conditions are important for this class of compound. Generally this has not been addressed by literature and is an area for further research in order find optimum storage conditions which might include addition of a preservative. Adenine was increased gradually with time and this could be explained by the fact that adenine containing metabolites such as adenosine, AMP, ADP and ATP can be hydrolyzed to produce adenine. There was a decrease in glutamine with time and this might be explained by the fact that the amide group in glutamine can hydrolyze to produce glutamic acid.

As a conclusion for the comparison between the five columns, it is clear that the best performance is produced on the ZIC-pHILIC column. In addition, this method covers large number of polar metabolites. It is thus suitable to apply to the study of the metabolomics of a prostate cancer cell liner LNCaP as a result of good linearity, LOD, extraction stability and repeatability.

To conclude, the work within this chapter is largely complete and could be published directly without additional work being carried out. The only gap would be to recheck the limits of detection for some of the standards. Also it might be useful to apply some chemometric modelling to the different columns in order to see if it would be possible to predict the performance of each column for the different analyte classes. The work is more comprehensive that much of the current work being published in the literature.

Chapter4: Application of the Metabolomics Methodology to Study the Effect of Sphingosine Kinase Inhibitors on the Metabolome of LNCAP cells

Application of the Metabolomics Methodology to Study the Effect of Sphingosine Kinase Inhibitors on the Metabolome of LNCAP cells

4.1 Introduction

There is a considerable body of evidence showing the involvement in cancer of sphingosine 1-phosphate (S1P) and sphingosine kinase (SK), which catalyses the formation of S1P from sphingosine (Pyne and Pyne, 2010). This makes the S1P/SK pathway an interesting target for cancer chemotherapy. The sphingosine kinase inhibitor (2-(p-hydroxyanilino)-4-(p-chlorophenyl) thiazole) (Ski) was used to treat both androgen dependent and androgen resistant LNCaP cells. In AI cells the AR is thought to remain active through a variety of potential mechanisms including AR amplification, AR mutation, increased androgen sensitivity, local androgen production and growth factor activation (Wang et al., 2009). Ski inhibits both SK1 and SK2 activity (Pyne et al., 2011). In addition (R)-FTY720 methyl ether (ROME), which is a selective inhibitor of SK2 activity (Pyne et al., 2011) was used to treat the cells in order to see if specific effects could be observed from inhibition of SK2. LNCaP cells express two N-terminal variant isoforms of SK1; namely SK1a which is a 42.5 kDa protein and SK1b which is a 51 kDa protein identical to SK1a but has an 86 amino acid N-terminal extension. LNCaP cells also express SK2 (Loveridge et al., 2010). Treatment of LNCaP prostate cancer cells with Ski (10 μM, 24 h) had been found to reduce the activity of SK1a and SK1b (Loveridge et al., 2010). The elimination of SK1a and SK1b is associated with the onset of apoptosis as assessed by the cleavage of the DNA repair enzyme, polyADP ribose polymerase (PARP) (Loveridge et al., 2010). It was previously shown that Ski failed to modulate the activity of ectopically expressed SK2 in LNCaP cells thereby demonstrating specificity for inhibition of SK1. Treatment of LNCaP cells with Ski or ROME produces different effects on autophagy in LNCaP cells. Thus, Ski (10 μM, 48 h) inhibits, while

ROME (10 μM, 48 h) stimulates. It was previously shown that ROME had no effect on SK1 expression (Lim et al., 2011). Autophagy is a defensive mechanism where the cell recycles macromolecules and organelles in order to support its nutrient requirements. However, it may also result in cell death and is one marker of the effects of anti-cancer drugs. Cell death can be divided into three types: Type I is apoptosis, type II is autophagic cell death, and type III is cytoplasmic cell death. Type II is characterized by the accumulation of autophagic vacuoles. In many situations apoptosis and autophagy may both contribute to cell death and are both promoted by anti-cancer treatments.The differences between the effects of Ski and ROME results from the fact that ROME is selective for SK2 whereas Ski inhibits both SK1 and SK2 (Lavieu et al., 2006).

4.2 LC/MS Results for Treatment of LNCAP Cells with Sphingosine Kinase Inhibitors

4.2.1 Overview of Metabolite Alterations

Using the optimized extraction procedure it was possible to identify a wide range of metabolites in the polar extraction using hydrophilic interaction chromatography (HILIC & pHILIC). In this case all the samples were analyzed in order to test the alteration of any metabolic changes can be observed. Analysis of the total ion chromatograms with SIEVE demonstrated that the intensities of a large number of polar metabolites had changed in responding to treatment (264 metabolites) table 4.1 summarizes sixty eight metabolites which showed the greatest change for both the androgen dependent and androgen independent LNCaP cells from two runs on different dates with three treated and three untreated cultures in each run. SIEVE compares the intensities of each metabolite peak, in control samples against those of treated samples, calculating a p-value and ratio based on the difference between them. A significant p-value is taken as $p < 0.05$. The metabolites were primarily identified according to their accurate masses which all had less than 2ppm mass deviation, in many cases matches were within 1 ppm, deviation from the exact mass of the proposed metabolite. The metabolite database was used as a filter to exclude any other possible metabolites so according to the metabolic standards initiative (MSI- level 2) we can say that these metabolites are putatively identified at this level (Griffin et al., 2007). In practice the only possible alternative identities to those listed are isomers of the putatively identified metabolite. In many cases there was only one isomer corresponding to a particular mass. In addition standards of common metabolites were used to characterize the column and the retention times for these are shown in table A.1. An example of retention time characterization is shown in figure 4.1 for glutathione standard and glutathione in a sample. A separation of two isomeric metabolites (Glycerone phosphate and Glyceraldehyde 3-phosphate) have the same molecular weight 170 g/mol was done by using ZIC-pHILIC conditions, as it is mention in section 3.2.4, since they were not separated by the ZIC-HILIC conditions. Then a confirmation of each one was carried out by injection standards of both separately and then in comparison with the retention times of them with the retention times in the samples.

Table 4.1 list of metabolites that were found to be significantly altered in the samples of LNCaP and androgen independent LNCaP-AI cells after treated with Sphingosine Kinase Inhibitor (Ski). ND = not detected, T/C = the ratio of the mean of three treatments' intensities to the mean of three controles' intensities.

Name/Pathways	RT	m/z	LNCaP T/c -1	p-value	LNCaPAI T/C-1	p-value	LNCaP T/c -2	p-value	LNCaPAI T/C-2	p-value
Oxidative Stress										
Cystathionine	16.5	221.0747	0.18	1.4E-03	0.35	4.2E-06	0.67	4.2 E-02	0.5	2.8 E-02
Ribulose phosphate	15.6	229.0122	2.7	1.6 E-02	4.2	9.1 E-03	3.7	1.1 E-04	2.9	4.6 E-02
Phosphogluconate	17.7	275.0177	5.1	1.0 E-02	5.0	2.2 E-02	3.5	2.2 E-02	3.5	1.7 E-02
Glutathione	15.1	308.09	1.4	5.3E-02	1.97	1.8E-02	1.90	6.9 E-03	1.8	3.4E-04
(R)-S-Lactoylglutathione	12.8	380.1112	9999	1.8 E-02	50.6	2.6 E-04	13.4	1.2 E-02	21.6	4.6 E-02
Oxidized glutathione	17.5	611.1455	67.57	4.6E-02	310.01	1.2E-02	9999	2.2E-03	3540	3.2E-02
NADP+	16.8	742.0683	3.24	1.2E-02	8.10	1.4E-03	4.2	7.8 E-03	4.0	5.1 E-03
NADPH +	16.9	744.0843	0.11	2.3E-03	0.16	5.9E-04	0.21	4.4 E-03	0.21	4.4 E-03
Glycolysis										
Fumaric acid	15.1	115.0038	1.3	4.7 E-02	2.1	6.6 E-03	ND	-	2.1	1.4 E-02
Succinic acid	15.0	117.0194	ND	-	ND	-	1.6	3.6 E-02	0.77	4.0 E-02
Malic acid	15.2	133.0144	1.3	3.9 E-02	2.1	3.0 E-03	1.2	4.3 E-02	2.4	1.5 E-02
D-Glyceraldehyde 3-phosphate	16.1	168.9908	6.6	1.6 E-02	10.6	1.9 E-02	14.7	1.7 E-02	7.1	1.9E-02
Glycerone phosphate	15.4	168.9908	ND	-	16.1	6.2 E-02	ND	-	ND	-
Phosphoenol pyruvate	17.6	166.9751	1.4	2.3 E-02	4.1	1.3 E-02	1.6	7.8 E-03	2.5	3.5 E-03
Sorbitol	13.1	181.0721	3.7	3.7 E-02	ND	ND	2.2	7.1 E-03	1.3	1.1 E-02
Citric acid	18.0	191.0200	1.5	1.6 E-02	1.3	1.3 E-02	1.8	1.3 E-03	0.78	3.6 E-02

beta-D-Fructose 1,6-bisphosphate	18.0	338.989	7.5	4.1 E-05	5.9	7.7 E-03	28.8	1.1 E-02	5.1	5.7E-04
NAD+	14.0	664.1167	1.3	5.0 E-02	1.4	3.0 E-04	1.4	9.0 E-03	1.2	6.9 E-03
NADH	13.4	664.1327	5.1	7.5 E-03	6.7	3.3 E-03	4.1	1.9 E-03	6.9	3.7 E-03
Fatty acid metabolism										
L-Acetylcarnitine	11.0	204.1232	2.69	1.60E-02	1.32	1.20E-02	10.5	4.8 E-03	2.5	1.1 E-03
Propionyl-L-carnitine	13.2	218.1385	0.65	2.50E-02	1.01	8.50E-02	1.2	1.1 E-02	1.4	3.2 E-02
3-Methylbutyroylcarnitine	8.5	246.1697	0.34	1.40E-02	0.15	2.90E-02	0.11	3.8 E-03	0.084	1.9 E-02
Hydroxyisovalerylcarnitine	13.9	262.1647	0.95	7.70E-01	ND	-	2.4	5.8 E-02	ND	-
Hydroxyhexanoyl carnitine	9.6	276.1804	3.41	7.60E-03	1.5	3.60E-02	2.5	1.9 E-03	2.1	2.30E-02
CoA	13.6	768.1226	0.13	1.20E-02	0.15	1.20E-02	0.87	5.4 E-03	0.43	1.1 E-02
Acetyl CoA	12.3	810.1312	0.87	5.90E-01	0.98	8.90E-01	1.1	3.7 E-01	0.75	1.4 E-01
Hydroxisovaleryl CoA	12.1	868.1741	0.44	5.40E-03	ND	-	1.4	2.7 E-01	0.19	6.2 E-04
Lipid degradation/ biosynthesis										
Choline	15.7	104.107	2.04	3.50E-02	2.33	1.00E-01	2.6	4.1 E-02	1.4	2.3 E-02
Choline phosphate+	23.3	184.0734	1.89	1.80E-02	2.58	5.10E-03	1.6	9.4 E-03	1.79	3.7 E-02
Glycerylphosphoryl ethanolamine	17.5	216.0632	1.64	3.80E-02	1.61	3.00E-03	2.0	2.5 E-02	1.8	1.7 E-02
PE(P-16:0e/0:0)	6.7	438.2975	2.32	1.50E-02	ND	-	2.0	9.4E-03	ND	-
PE(P-16:0e/0:0)	8.1	438.2976	2.41	3.80E-02	ND	-	2.7	3.0E-02	ND	-
[PC (13:0)] 1-tridecanoyl-sn-glycero-3-phosphocholine	8.2	454.2923	2.29	3.40E-02	ND	-	2.7	6.6 E-03	ND	-
[PC (13:0)] 1-tridecanoyl-sn-glycero-3-phosphocholine	6.6	454.2926	2.12	2.70E-02	ND	-	3.1	4.0 E-02	ND	-
[PC (15:1)] 1-(1Z-pentadecenyl)-sn-glycero-3-phosphocholine	6.7	466.3292	2.16	3.90E-02	ND	-	3.3	2.1 E-02	ND	-

LysoPE(18:1(9Z)/0:0)	6.6	480.3084	1.20	6.50E-03	ND	-	1.8	1.9 E-02	ND	-
LysoPE(18:0/0:0)	6.6	482.3239	1.94	8.60E-03	ND	-	2.9	2.4 E-02	ND	-
LysoPE(18:0/0:0)	8.0	482.3241	2.16	3.10E-02	ND	-	3.0	5.3 E-02	ND	-
1-O-Hexadecyl-2-lyso-glycero-3-phosphorylcholine	10.5	482.3605	19.40	3.00E-03	10.6	3.50E-03	6.7	3.6 E-06	ND	-
[PC (10:0/18:0)] 1-decanoyl-2-octadecanoyl-sn-glycero-3-phosphocholine	8.7	678.507	2.93	1.20E-03	4.85	3.90E-02	2.5	3.8E-02	2.9	3.0 E-03
[PC (10:0/18:0)] 1-decanoyl-2-octadecanoyl-sn-glycero-3-phosphocholine	6.7	678.5072	3.99	3.80E-04	3.34	1.50E-02	ND	-	ND	-
[PC (14:2/16:0)] 1-tetradecyl-2-(9Z-hexadecenoyl)-sn-glycero-3-phosphocholine	8.4	690.5431	2.49	1.10E-02	2.40	3.10E-03	1.9	6.5 E-02	2.3	1.0 E-02
PC(o-14:0/16:0)	8.5	692.5585	4.05	2.80E-02	3.25	1.40E-02	2.1	6.0 E-02	2.6	4.7 E-03
Amino acid nutrients										
Glycine	15.1	76.03942	2.52	7.70E-04	1.70	5.40E-03	1.3	3.0 E-02	1.3	3.4 E-02
D-Alanine	14.5	90.05496	0.18	2.30E-03	0.35	1.60E-03	0.47	2.4 E-03	1.1	7.2 E-03
D-Serine	18.2	106.0499	0.79	8.40E-03	0.99	8.10E-03	0.66	1.7E-02	0.22	1.3 E-02
Proline	12.6	116.0707	2.16	3.10E-03	2.44	2.10E-04	2.1	7.0E-03	2.2	3.2 E-03
Valine	12.1	118.0863	1.74	6.40E-03	2.06	4.80E-02	2.066	6.2E-03	1.9	2.1 E-02
Threonine	13.9	120.0655	1.12	3.40E-02	1.49	2.80E-02	0.981	7.3E-03	1.2	3.8 E-02
Taurine	14.2	126.022	0.67	1.00E-02	0.43	8.70E-04	0.287	4.9E-02	0.26	5.1 E-02
1-Pyrroline-4-hydroxy-2-carboxylate	8.1	130.0499	2.17	3.20E-02	5.80	9.80E-02	3.6	8.6E-02	3.2	8.0 E-02
Leucine	10.1	132.0655	0.50	1.50E-02	2.86	4.40E-02	0.35	3.4E-02	0.24	1.4 E-04
L-Aspartic acid	14.4	134.0447	0.18	7.00E-05	0.58	3.10E-02	2.1	2.1E-03	2.2	5.6 E-04
Methionine	10.9	150.0583	1.86	5.00E-02	3.28	1.10E-01	ND	-	ND	-
L-Histidine	25.2	156.0768	2.56	4.20E-02	3.05	4.70E-02	2.3	8.2 E-04	2.4	6.5 E-04

Miscellaneous										
Phosphoric acid	18.7	98.98421	1.50	1.80E-02	1.25	2.30E-01	2.1	3.0 E-02	1.2	6.4 E-01
Creatinine	9.2	114.0662	0.66	2.20E-03	0.77	4.90E-02	1.00	4.9E-02	0.85	3.2 E-02
4-Guanidinobutanoic acid	14.9	146.0924	0.85	2.60E-02	ND	-	0.23	8.3E-03	0.21	1.4 E-05
N-Acetylaspartate+	14.1	176.0553	0.88	1.10E-02	0.97	1.50E-02	0.98	8.1 E-03	1.0	4.3 E-03
L-beta-aspartyl-L-aspartic acid	18.9	249.0715	1.93	1.40E-04	1.86	1.10E-03	2.0	3.3 E-03	1.4	2.7 E-03
saccharopine	15.3	277.1391	8.17	7.80E-03	4.72	1.60E-03	5.00	2.2 E-02	7.0	1.3 E-02
Glycerophosphoglycerol	14.9	247.0575	1.94	3.60E-03	3.05	7.70E-03	1.9	1.1 E-02	2.6	1.6 E-02
Dehydrosphinganine(Sphingosine)	7.1	300.2894	1.1	6.30E-03	0.92	2.50E-02	1.1	3.3 E-02	0.90	4.8 E-02
Diadenosine triphosphate	15.5	757.0897	2.24	7.80E-03	ND	-	2.1	6.4 E-04	ND	-
FAD	11.4	786.1650	1.10	8.90E-03	1.46	5.70E-03	2.4	3.0 E-02	2.4	1.9 E-02

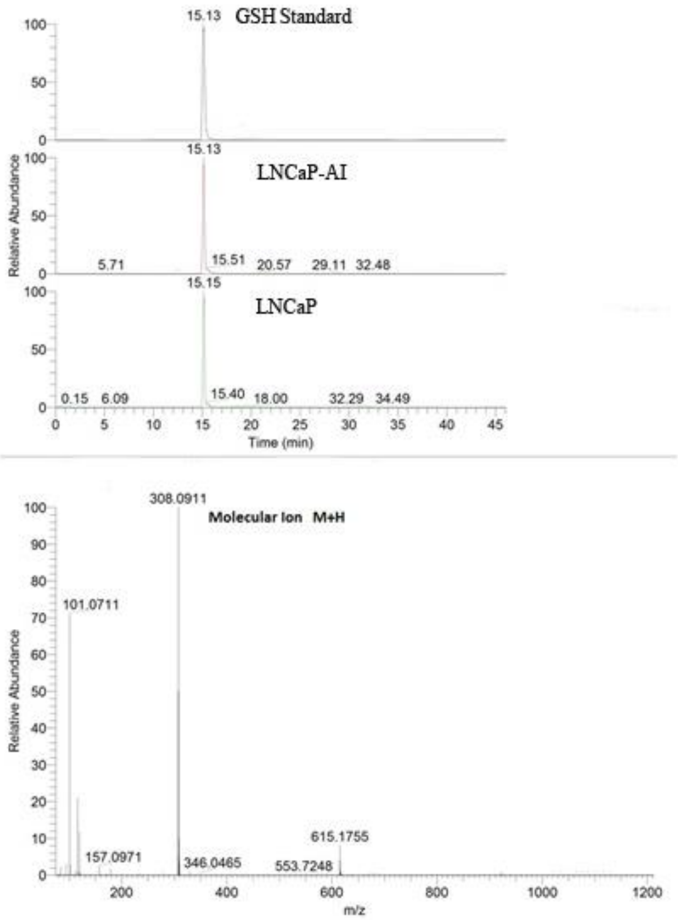

Figure 4.1 The spectrum of glutathione using ZIC-HILIC conditions indicates the same retention time for the standard and the samples.

4.2.2 The effect of a Sphingosine Kinase Inhibitor on LNCaP Cells

The effects of Ski on the androgen dependent and androgen independent cells were broadly similar so in the first instance the changes in androgen dependent cells will be discussed. Since so many metabolites were altered the metabolites have been divided so that they fall into defined pathways. The metabolites listed in table 4.2 show selected metabolites for the androgen dependent LNCaP cells which were greatly affected by the treatment and fall into a coherent pattern although there were many other metabolite changes as indicated in table 4.1.

Table 4.2 shows that the treatment of LNCaP cells with Ski (10 μM, 24 h) modulates the Warburg effect. This is indicated by the elevated levels of glycolytic metabolites and increased levels of (R)-S-lactoyl-glutathione, which is formed from methylglyoxal. Ski treatment elevates glycolytic metabolites fructose 1,6-bisphosphate, D-glyceraldehyde 3-phosphate, dihydroxy-acetone phosphate, and 3-phosphoglycerate, implying that the accumulation of these metabolites is a result of inhibition of the glycolytic pathway. Moreover, NADH levels are elevated in the Ski-treated cells, suggesting increased fatty acid oxidation. In addition, treating cells with Ski induces formation of diadenosine 5′,5′′′-*P*1,*P*3-triphosphate (Ap3A).

LNCaP cells also respond to Ski by diverting glucose 6-phosphate into the pentose phosphate pathway to provide NADPH to counter the responses to oxidative stress. NADPH is used by the glutathione (GSH) system to recycle the oxidized form, GSSG, to GSH. In this case, the protection given by NADPH toward oxidative stress is insufficient, as the levels of GSSG and pentose phosphate pathway intermediates (ribulose 5-phosphate and phosphogluconate) are increased and the NADPH level is decreased (Table 4.2). Figure 4.3 shows oxidized glutathione chromatograms in control and treated sample of LNCaP cells and mass spectrum. Also Figure 4.4 shows the difference in Dihydroxyacetone phosphate and Glyceraldehyde phosphate chromatograms for control and treated sample of LNCaP cells and mass spectrum. Figure 4.2 summarises the effects on the glycolysis pathway.

The other principal effects of Ski are on lipid metabolism, including marked changes in certain carnitines (Table 4.2), which shuttle fatty acids in and out of the mitochondria. For example, the levels of acetylcarnitine and 3-hydroxyhexanoylcarnitine are considerably elevated in LNCaP cells subsequent to treatment with Ski. In addition, free CoA also drops considerably. Ski also raised the levels of 1-O-hexadecyl-2-lyso-phosphatidylcholine (table 4.2).

Table 4.2 The main changes in LNCAP cells following treatment with Sphingosine Kinase Inhibitor (Ski). T/C = the ratio of the mean of three treatments' intensities to the mean of three controles' intensities. p-value (n=6) = Combined data from two runs (each run containing three treated and three untreated sets of cells) using Fisher's method.

	m/z	RT	LNCaP T/C	p-value (n=6)
Oxidative stress				
GSSG	611.1455	17.4	16.1	< 0.001
NADP+	742.0683	17.0	4.0	<0.001
NADPH	744.0843	17.1	0.20	<0.001
Phosphogluconate	275.0177	17.7	4.3	<0.01
Ribulose phosphate	229.0122	15.6	3.2	<0.001
Glycolysis Krebs Cycle				
Dihydroxy acetone phosphate	168.9908	15.3	11.5	<0.01
Glyceraldehyde phosphate	168.9908	16.0	9.0	<0.01
3-phosphoglyceric acid	184.9857	17.2	2.2	<0.001
Fructose 1,6, bisphosphate	338.9890	18.0	18.2	<0.001
Lactoyl glutathione	380.1112	12.5	>250	-
NADH	664.1182	13.5	4.7	<0.001
Fatty Acid Metabolism				
Acetylcarnitine	204.1232	11.2	2.5	<0.001
Butylcarnitine	232.1544	8.9	0.7	<0.01
3-methylbutyryl carnitine	246.1697	8.1	0.21	<0.001
hexanoylcarnitine	260.1853	7.7	0.77	<0.01
Hydroxyhexanoyl carnitine	276.1084	9.4	2.4	<0.001
Saccharopine	277.1391	15.9	3.6	<0.01
CoA	768.1226	13.6	0.5	<0.001
Miscellaneous				
1-O-Hexadecyl-2-lyso-glycero-3-phosphorylcholine	482.3605	10.5	13.1	<0.001
Diadenosine triphosphate	757.0897	15.5	2.2	<0.001

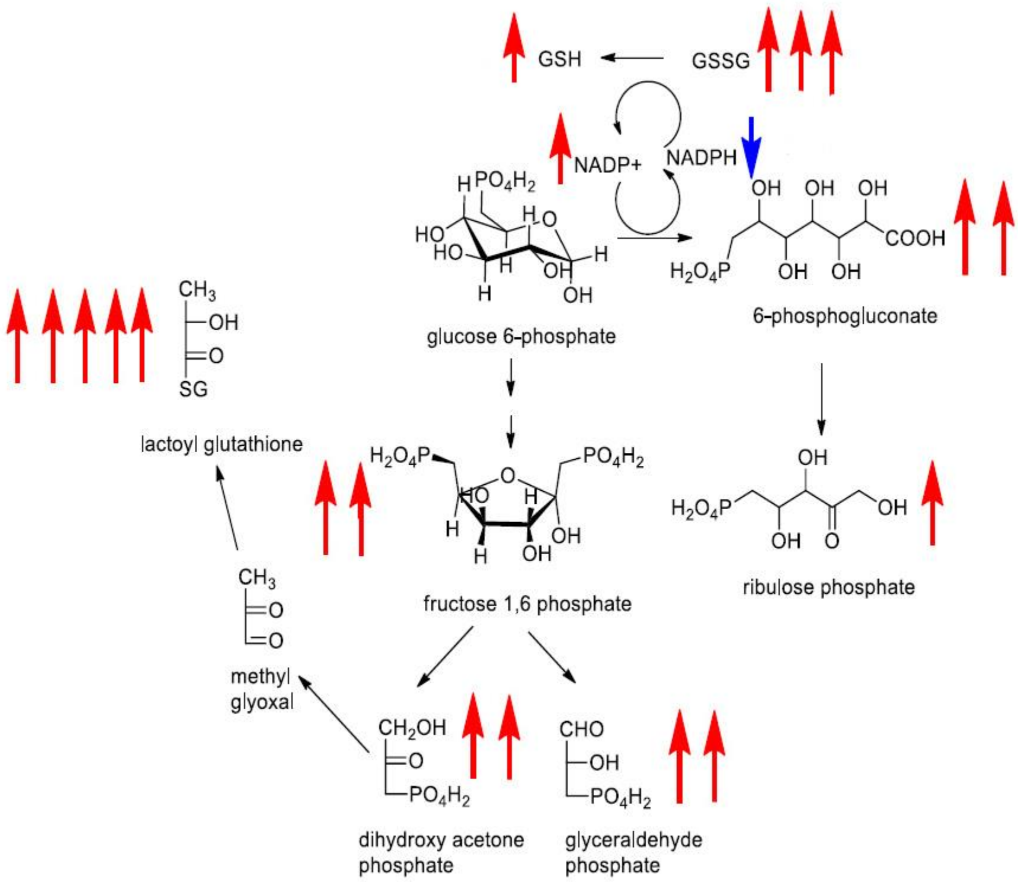

Figure 4.2 Summary of the effects of Ski on the glycolytic pathway in LNCaP cells.

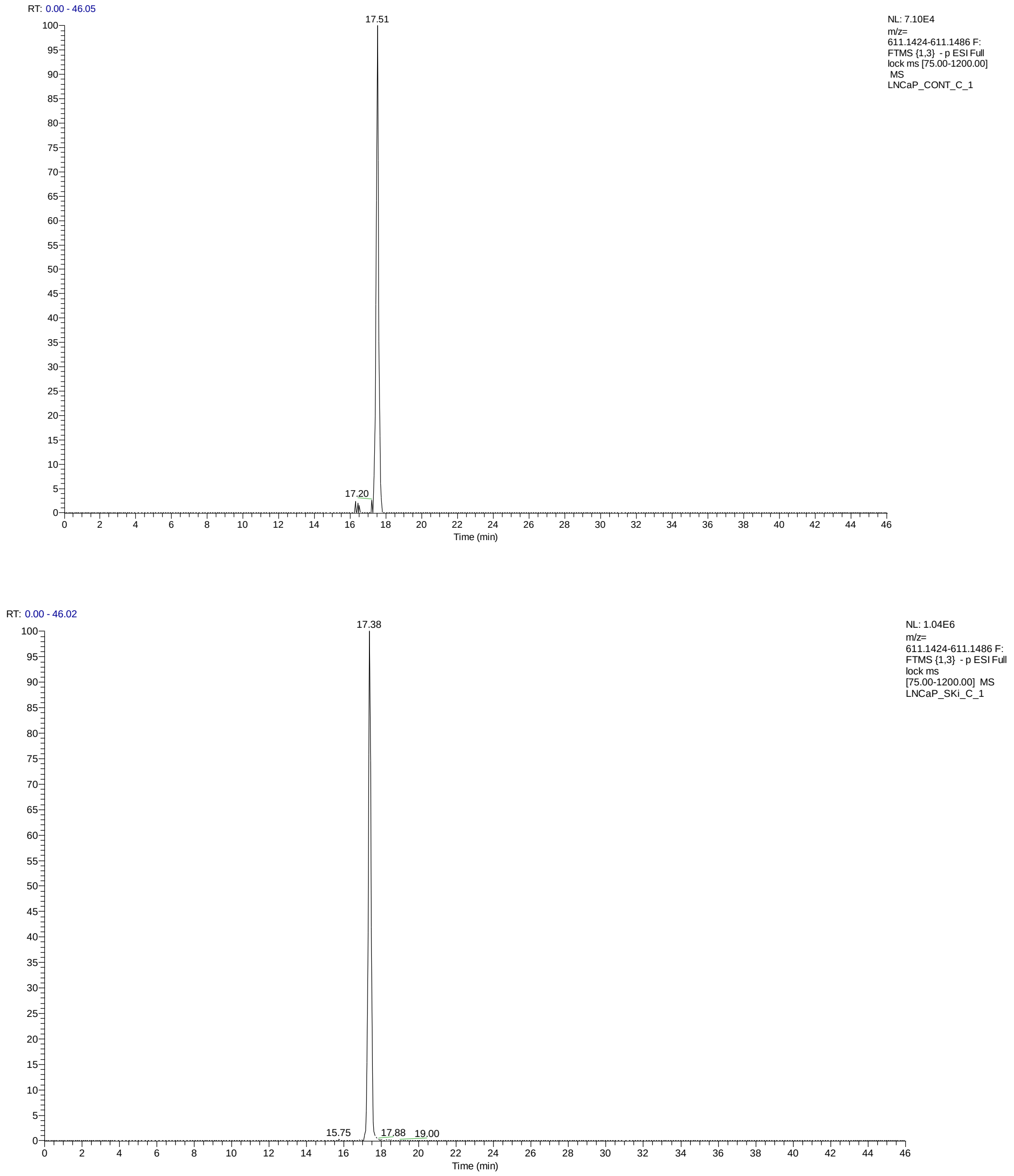

Figure 4.3 GSSG chromatograms in control and treated sample of LNCaP cells.

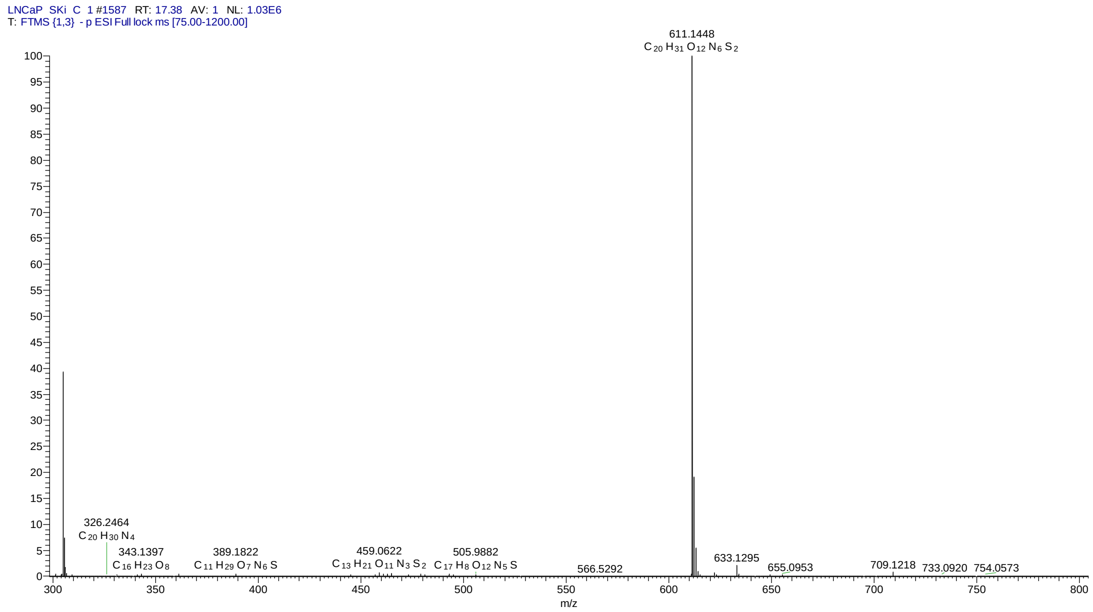

Figure 4.4 GSSG mass spectrum in treated sample of LNCaP cells.

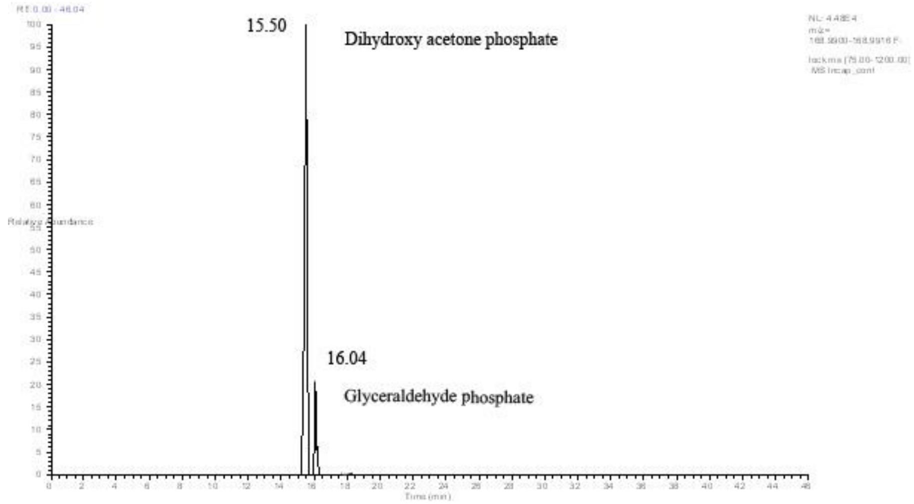

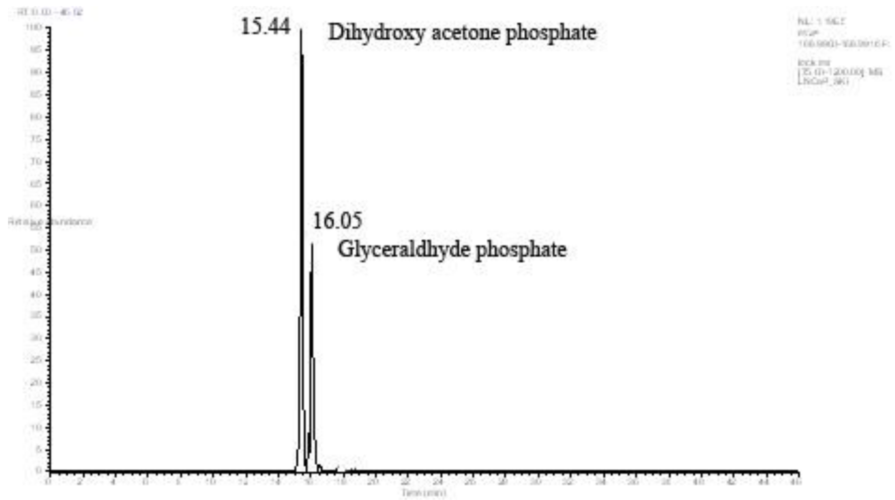

Figure 4.5 Dihydroxyacetone phosphate and Glyceraldehyde phosphate chromatograms in control and treated sample of LNCaP cells.

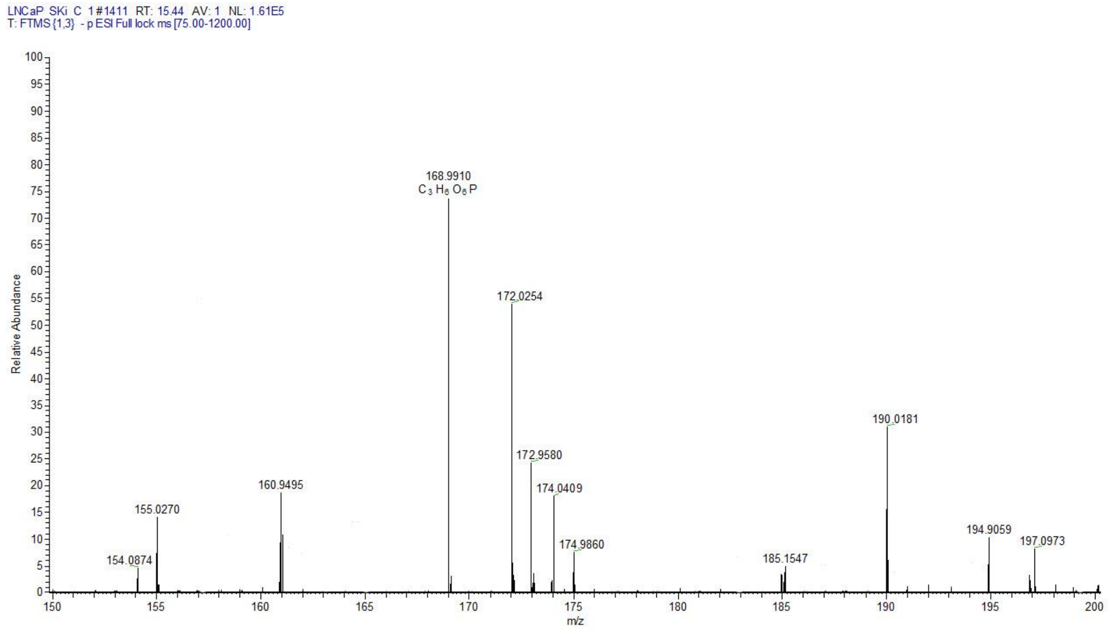

Figure 4.6 Dihydroxyacetone phosphate and Glyceraldehyde phosphate mass spectrum in treated sample of LNCaP cells.

4.2.3 Direct Detection of Methylglyoxal

The production of methylglyoxal from glycerone phosphate by methylglyoxal synthase could be elevated after Ski treatment. Since the lactoylglutathione was increased. Methylglyoxal cannot be detected by LC-MS thus it is necessary to use GC-MS to detect this metabolite. Since methylglyoxal is very reactive it is necessary to derivatise it before carrying out GC-MS. Both samples and reference materials were derivatized. After identifying the peak of a compound, its spectrum was compared to a reference material and the NIST library. Figure 4.5 shows a spectrum of methylglyoxal standard after derivatization which eluted at 6 minutes. However, this compound was not detected in the samples. The next step was to try to trap the metabolite as it was produced in the cells by using N-acetyl cysteine.

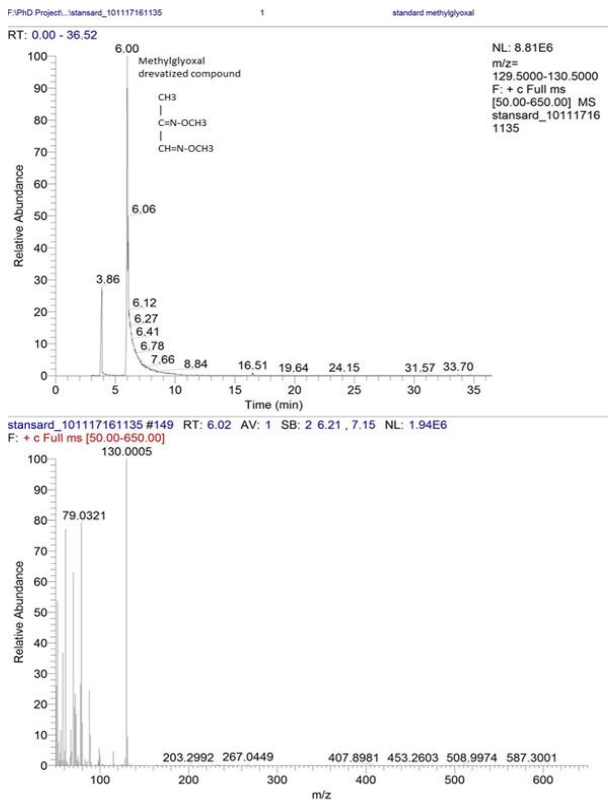

Figure 4.7 Derivative formed from a methylglyoxal standard by reaction with methoxylamine chromatogram (upper panel) and its mass spectrum (lower panel).

4.2.4 Effect of N-acetylcysteine on metabolomic changes in response to Ski

LNCaP cells were pre-treated with the reactive oxygen species scavenger N-acetylcysteine (NAC) in order to observe the influence of oxidative stress on the metabolic changes in response to Ski. From table 4.3 it can be seen that there is a decreased effect of Ski in NAC-treated cells. The changes in the levels of GSSG, NADPH, saccharopine, hydroxyhexanoylcarnitine, and glycolytic metabolites in response to Ski were reduced (compare Table 4.3 with Table 4.2). The exact mechanism whereby NAC inhibits damage to the cells is not entirely clear.

In order to examine whether or not any direct conjugates were formed between NAC and methylglyoxal the two compounds were reacted. LC-MS analysis of the products revealed formation of a thioacetal with the formula $C_8H_{13}O_5NS$ (figures 4.6, 4.8). In addition oxidized NAC was formed (figures 4.7 and 4.8). Examining cell cultures incubated in the presence of NAC and with and without Ski there was no evidence for the formation of a thioacetal conjugate in the cells and there were no differences between the levels of NAC or oxidized NAC in the cells.

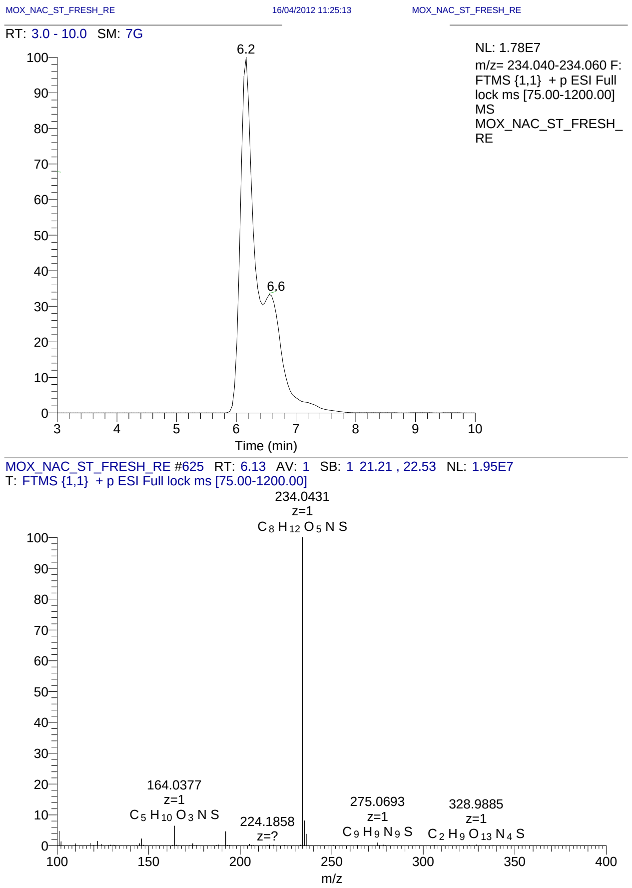

Figure 4.8 Thioacetal formed by reaction of NAC with methylglyoxal.

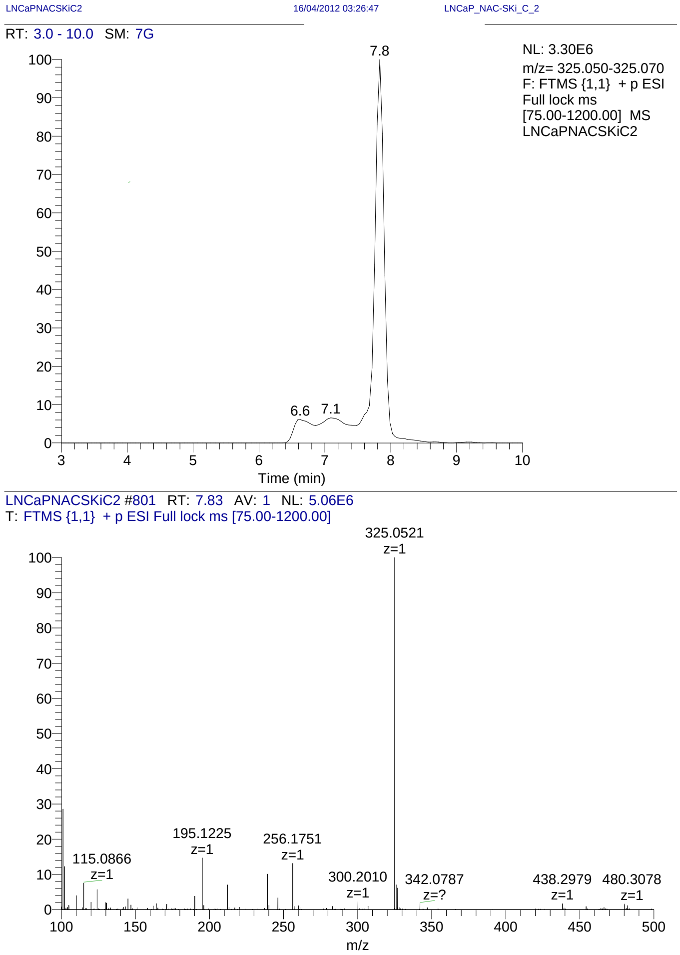

Figure 4.9 Oxidised NAC

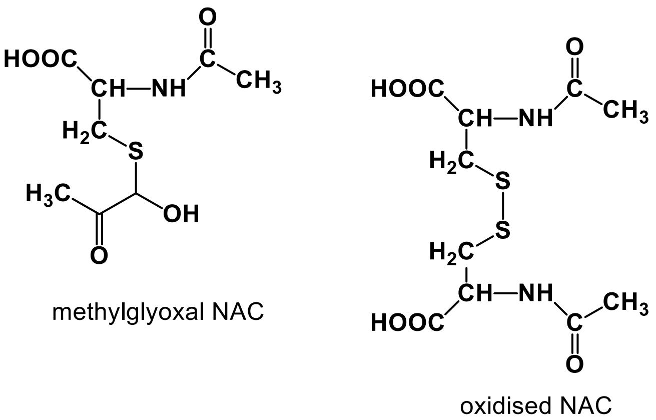

Figure 4.10 Methylglyoxal-NAC (thioacetal), and oxidized NAC.

Table 4.3 Effect of NAC on LNCaP-Ski treatment.

	m/z	RT	Ratio LNCaP-Ski/SkiNAC	p-value n=3	Ratio LNCaP/ LNCaP-NAC	p-value n=3
Oxidative stress						
GSSG	611.1455	17.8	4.4	0.0003	0.64	0.34
NADP+	742.0683	17.1	13.9	0.005	ND	-
NADPH	744.0843	17.2	0.04	0.000034	1.1	0.51
Phosphogluconate	275.0177	-	ND	-	ND	-
Ribulose phosphate	229.0122	15.4	0.41	0.054	1.1	0.7
Glycolysis Krebs Cycle						
Dihydroxy acetone phosphate	168.9908	15.4	2.1	0.032	0.81	0.022
Glyceraldehyde phosphate	168.9908	16.1	6.1	0.033	ND	-
3-phosphoglyceric acid	184.9857	17.2	2.7	0.0033	1.1	0.76
Fructose 1,6, bisphosphate	338.9890	-	ND	-	ND	-
Lactoyl glutathione	380.1112	-	ND	-	ND	-
NADH	664.1182	13.7	2.7	0.033	1.4	0.19
Fatty Acid Metabolism						
Acetylcarnitine	204.1232	11.2	2.4	0.066	0.96	0.87
Butylcarnitine	232.1544	8.9	0.24	0.00031	1.1	0.14
3-methylbutyryl carnitine	246.1697	8.1	0.03	0.0047	1.4	0.04
hexanoylcarnitine	260.1853	7.7	0.31	0.052	0.99	0.97
Hydroxyhexanoyl carnitine	276.1804	9.4	5.0	0.000007	1.3	0.019
Saccharopine	277.1391	15.9	7.2	0.0026	0.91	0.40
CoA	768.1226	14.0	0.65	0.013	ND	-
Miscellaneous						
1-O-Hexadecyl-2-lyso-glycero-3 phosphorylcholine	482.3605	10.5	14.0	0.0032	1.2	0.60
Diadenosine triphosphate	757.0914	15.3	1.1	0.53	0.77	0.15

4.2.5 The Effect of Ski on the Metabolome of LNCaP-AI cells

Table 4.1 summarises the main changes in the metabolome of LNCaP-AI cells following with Ski as detailed in section 4.2.1. Increased the levels of glycolytic metabolites that include fructose 1,6-bisphosphate, D-glyceraldehyde 3-phosphate, dihydroxyacetone phosphate, 3-phosphoglycerate and lactoyl glutathione were observed. These effects reflect inhibition of aerobic glycolysis (Warburg effect) by Ski. Thus LNCaP-AI cells also respond to Ski by diverting glucose 6-phosphate into the pentose phosphate pathway in order to provide NADPH to counter oxidative stress responses. As in the case of the androgen dependent LNCaP cells the levels of GSSG and pentose phosphate pathway intermediates (ribulose 5-phosphate and phosphogluconate) were increased and the NADPH level was reduced. These changes are also common to androgen-sensitive LNCaP cells treated with Ski as indicated by the ratios which are shown in Table 4.4 which in many cases are close to 1 and there are only a few significant differences. However, LNCaP-AI cells do not undergo apoptosis in response to Ski (Loveridge et al., 2010). From the metabolomics results the main difference between two LNCaP cell types, is the absence of diadenosine 5′,5‴-P^1,P^3-triphosphate (Ap3A) in LNCaP-AI cells.

Table 4.4 Comparison between the response of LNCaP and LNCaP AI cells to treatment with Ski.

	m/z	RT	AI/LNCaP Control	p-value n=6	AI/LNCaP treated	p-value n=6
Oxidative stress						
GSSG	611.1455	17.4	1.5	>0.1	2.1	<0.001
NADP+	742.0683	17.0	0.60	0.01	0.75	>0.1
NADPH	744.0843	17.1	0.88	>0.1	0.76	>0.1
Phosphogluconate	275.0177	17.7	0.21	0.1	0.18	<0.01
Ribulose phosphate	229.0122	15.6	0.2	0.1	0.12	>0.1
Glycolysis Krebs Cycle						
Dihydroxy acetone phosphate	168.9908	15.4	0.85	>0.1	0.59	>0.1
Glyceraldehyde phosphate	168.9908	16.1	0.78	0.1	0.65	>0.1
3-phosphoglyceric acid	184.9857	17.2	1.5	<0.1	1.8	<0.1
Fructose 1,6, bisphosphate	338.9890	18.0	0.6	<0.1	0.37	<0.1
Lactoyl glutathione	380.1112	12.5	1.2	0.1	1.6	0.1
NADH	664.1182	13.5	0.9	>0.1	1.3	>0.1
Fatty Acid Metabolism						
Acetylcarnitine	204.1232	11.2	1.2	<0.01	0.75	>0.1
Butylcarnitine	232.1544	8.9	3.9	<0.001	4.8	<0.001
3-methylbutyryl carnitine	246.1697	8.1	1.3	>0.1	0.46	<0.1
hexanoylcarnitine	260.1853	7.7	1.1	>0.1	0.48	<0.01
Hydroxyhexanoyl carnitine	276.1842	9.4	0.026	<0.0001	0.16	<0.01
Saccharopine	277.1391	15.9	0.62	<0.01	0.63	<0.01
CoA	768.1226	13.6	0.41	<0.001	0.5	<0.01
Miscellaneous						
1-O-Hexadecyl-2-lyso-glycero-3-phosphorylcholine	482.3605	10.5	1.3	>0.1	1.1	>0.1
*Diadenosine triphosphate	757.0897	15.5	1776	-	3809	-

*absent from LNCaP-AI cells

4.2.6 The effect of ROME on the metabolome of LNCaP cells

ROME had no significant effect on oxidative stress or the pentose phosphate pathway (Table 4.5). However, there was a small but significant effect on glycolysis, with glycolytic intermediates being depressed to about 50% of the levels in the controls (Table 4.5). However, examination of the lipid profile produced by ROME treatment (table 4.6) indicated that treatment of LNCaP cells with ROME increased the levels of several lysophosphatidylinositols (Lyso PI) and LPA species. Both Lyso PI and LPA are ligands for GPR55 and LPA/EDG receptors that promote proliferation and cell survival (Anavi-Goffer et al., 2012, Tigyi, 2010).

Table 4.5 effect of ROME on polar metabolites of LNCaP cells

	m/z	Retention time	LNCaP T/C	p-value n=6
Oxidative stress				
GSSG	611.1455	17.0	0.88	>0.1
NADP+	742.0683	16.8	1.3	>0.1
NADPH	744.0843	17.1	1.2	<0.001
Phosphogluconate	275.0177	-	ND	-
Ribulose phosphate	229.0122	15.6	0.74	0.1
Glycolysis Krebs Cycle				
Dihydroxy acetone phosphate	168.9908	15.4	0.43	<0.01
Glyceraldehyde phosphate	168.9908	16.1	0.47	<0.01
3-phosphoglyceric acid	184.9857	17.0	0.79	>0.1
Fructose 1,6, bisphosphate	338.9890	18.0	0.48	<0.01
Lactoyl glutathione	380.1112	-	ND	-
NADH	664.1182	13.5	0.91	0.1
Fatty Acid Metabolism				
Acetylcarnitine	204.1232	11.3	1.1	>0.25
3-methylbutyryl carnitine	246.1697	8.2	0.78	<0.05
Hydroxyhexanoyl carnitine	276.1084	-	ND	-
Saccharopine	277.1391	16.0	1.1	>0.25
CoA	768.1226	13.5	0.89	0.25
Miscellaneous				
1-O-Hexadecyl-2-lyso-glycero-3-phosphorylcholine	482.3605	-	ND	-
Diadenosine triphosphate	757.0897	15.2	0.93	>0.1

Table 4.6 lipid markers of ROME treated of LNCaP cells

	m/z	RT	LNCaP T/C	p-value n=6
NADPH	744.0843	17.1	1.2	<0.001
*Palmitoyl glucuronide	417.2861	4.2	11.2	<0.01
Lysophosphatidyl inositol 18:0	599.3210	7.5	17.9	<0.001
Lysophosphatidyl inositol 18:0	597.3051	7.6	14.3	<0.001
Lysophosphatidyl inositol 16:0	571.9893	7.6	>250	<0.001

* Marker only detected in one batch of controls vs treatment (n=3)

4.2.7 The effect of Ski on the metabolome of LNCaP-SK1b cells

LNCaP-SK1b cells in which FLAG-tagged SK1b had been over-expressed were created to investigate the effect of Ski on the metabolome of LNCaP-SK1b cells. The over-Expresssion of SK1b should protect the LNCaP-SK1b cells from the effects of the SK inhibitor (Ski). The treatment of these cells with Ski still induced an increase in dihydroxyacetone phosphate and glyceraldehyde 3-phosphate (Table 4.7), which is consistent with inhibition of SK1 and antagonism of the Warburg effect. There were also similar changes in acylcarnitine levels, but the saccharorpine level is further elevated compared with LNCaP cells (compare Table 4.7 with Table 4.2). LNCaP-SK1b cells also experience a more severe oxidative stress response, as evidenced by the almost complete conversion of GSH into GSSG and more severe changes in phosphogluconate and NADPH compared with LNCaP cells (compare Table 4.7 with Table 4.2). In addition, the accumulation of a unique sphingolipid dihydrodesmethylsphingosine in LNCaP-SK1b cells occurred, which is confirmed in chapter six by using a silica column, and table 4.8 shows comparison of LNCaP-SK1b cells and LNCaP treated with Ski in sphingolipid metabolism results.

Table 4.7 Metabolites changes in LNCaP-SK1b cells due to Ski treatment

	m/z	RT	LNCaP-SK1b T/C	p-value n=3
Oxidative stress				
GSSG	611.1455	17.8	24.3	0.00091
GSH	306.0773	14.6	0.03	0.00013
NADP+	742.0683	17.1	16.3	0.00035
NADPH	744.0843	17.4	0.04	0.00076
Phosphogluconate	275.0220	17.2	>250	-
Ribulose phosphate	229.0122	15.9	1.3	0.43
Glycolysis Krebs Cycle				
Dihydroxy acetone phosphate	168.9908	15.4	2.1	0.015
Glyceraldehyde phosphate	168.9908	16.1	7.3	0.016
3-phosphoglyceric acid	184.9857	17.3	3.5	0.00011
Fructose 1,6, bisphosphate	338.9890	-	ND	-
Lactoyl glutathione*	380.1112	-	ND	-
[a]NADH	664.1182	13.5	4.4	0.0058
Fatty Acid Metabolism				
Acetylcarnitine	204.1232	11.1	2.9	0.0074
Butylcarnitine	232.1544	8.9	0.64	0.0079
3-methylbutyryl carnitine	246.1697	8.2	0.054	0.0018
hexanoylcarnitine	260.1853	7.6	0.40	0.071
Hydroxyhexanoyl carnitine	276.1804	9.2	7.7	0.005
Saccharopine	277.1391	15.8	13.5	0.0035
CoA	768.1226	-	ND	-
Miscellaneous				
1-O-Hexadecyl-2-lyso-glycero-3-phosphorylcholine	482.3605	-	ND	-
Diadenosine triphosphate	757.089	15.4	2.3	0.03

Table 4.8 Sphingolipids changes in LNCaP-SK1b cells and LNCaP cells due to treatment with Ski

	m/z	RT	LNCaP-SK1b T/C	p-value n=3	LNCaP T/C	p-value n=3
DihydrodesmethylSP	288.2896	4.8	4.8	0.00013	1.4	0.015
Sphingosine	300.2896	4.8	1.8	0.017	1.2	0.0043
DihydromethylSP	316.3209	4.8	2.0	0.032	1.7	0.0037

4.2.8 The Effect of (S)-FTY720 Vinylphosphonate on metabolome of LNCaP and LNCaP-AI cells

The levels of Ap3A do not change in LNCaP cells treated with (*S*)-FTY70 vinylphosphonate and Ap3A was undetectable in LNCaP-AI cells. Moreover, treatment of LNCaP and LNCaP-AI cells with (*S*)-FTY70 vinylphosphonate failed to induce changes in the metabolome that would indicate oxidative stress (lactoylglutathione levels actually decreased in LNCaP cells) or antagonism of the Warburg effect (Table 4.9). Therefore, these effects are different compared with Ski. Moreover, the metabolites that were modestly changed in response to (*S*)-FTY70 vinylphosphonate were phospholipids, such as lysophosphatidylethanolamine (lyso-PE), phosphatidylserine (PS), and phosphatidic acid (PA) in LNCaP-AI cells (Table 4.9). These changes were less evident in LNCaP cells (Table 4.9). The change in PS might be linked with apoptosis of LNCaP-AI cells, indicating distinct mechanisms of apoptosis in response to (S)-FTY720 vinylphosphonate in the cell type. In addition, a clear elevation in sphingosines adds more evidence for apoptosis of both cell types. There was a > 50% decrease in Nucleobases which might be an indication of apoptosis resulting from downregulation of purine nucleoside phosphorylase through inhibition of SK1 by (S)-FTY720 vinylphosphonate.

Table 4.9 changes in metabolites of LNCaP and LNCaP-AI cells treated with (S)-FTY720 Vinylphosphonate

Compound	m/z	Rt	LNCaP-AI T/C	p-value (n=3)	LNCaP T/C	p-value (n=3)
Lipids						
PA 32:2	717.4719	3.5	2.50	3.90E-05	2.07	1.80E-02
PA 32:1	719.4885	3.5	2.39	6.60E-03	1.35	3.60E-01
PA 34:2	745.5034	3.5	2.33	3.60E-05	1.54	1.10E-01
LysoPE 18:1	478.2947	4.2	2.18	2.20E-03	0.92	6.10E-01
PS 38:6	806.4967	3.6	2.16	2.20E-03	ND	-
LysoPE 20:1	506.3259	7.1	2.10	6.90E-03	1.02	8.50E-01
LysoPE 20:2	504.3109	4.1	2.10	2.00E-03	0.97	7.80E-01
PS 32:1	732.4831	3.6	2.04	1.40E-02	ND	-
Sphingosine bases						
Dihydrosphingosine (sphinganine)	302.3051	7.1	3.86	3.70E-02	4.14	5.00E-02
Hydroxysphinganine	318.2999	7.1	3.35	4.60E-02	2.70	2.30E-02
Sphingosine	300.2896	7.1	2.35	4.80E-02	2.42	5.50E-02
Hydroxysphingosine	316.284	7.1	2.10	2.70E-02	2.50	2.40E-02
Ceramide (d18:1/16:0)	536.5056	3.6	1.9	3.40E-02	1.5	3.90E-02
Nucleobases						
hypoxanthine	137.046	9.7	0.19	4.30E-02	0.19	4.20E-02
guanine	152.0567	11.8	0.27	3.10E-02	0.51	2.50E-02
uridine	243.0624	11.4	0.458	3.30E-02	0.41	5.30E-02
Oxidative stress						
Glutathione	308.091	14.0	0.98	7.60E-01	0.75	7.50E-03
(R)-S-Lactoylglutathione	378.0983	12.6	0.97	8.3E-01	0.61	9.30E-03
Oxidized glutathione	613.1597	16.8	0.88	3.90E-01	0.58	6.20E-02
Miscellaneous						
Diadenosine triphosphate	757.089	15.4	ND	-	0.89	6.0 E-03

4.3 Discussion

4.3.1 Separation of polar metabolites

A good separation of polar compounds and improving the ionization efficiency at the mass spectrometer interface were linked with hydrophilic interaction liquid chromatography methods ZIC-HILIC or ZIC-pHILIC (Nguyen and Schug, 2008). HILIC is useful for the analysis of highly polar metabolites which are poorly retained on reversed phase columns due to the hydrophobic nature of the stationary phase (Dunn et al., 2005). The ZIC-HILIC phase is stable over the pH range of 3-7 (Dunn, 2008). While ZIC-pHILIC stable at high pH ranges. Sixty eight metabolites were found to be significantly altered in the samples. Molecular mass was used as a key factor for metabolite identification in order to check the reality of peak was used in Xcalibur software (Thermo Fisher Scientific) after SIEVE processing by adding a proton in case of positive ESI or removing proton in case of negative ESI to metabolite ions. These conditions showed a good separation of most of the metabolites in table 4.1 with a matching retention time for standard, control and samples. For instance the glutathione peak appears at 15.12 minutes in control and in the samples. Sometimes there are slight variations the retention time between samples and controls and this could be due to sample preparation or extraction protocols with other components in the sample matrix having some effect on retention time. Variations of around ± 0.3 min within batch are acceptable but outside this range there might be some doubt about the standard and analyte in the sample being the same. The variability in metabolomics study of biological samples comes from cell counts so the biological variations are greater than the analytical variations (Dunn et al., 2005). One hundred and eighty standards of common metabolites were used to characterize the column and the retention times (table A1) and RSD of retention time was calculated in chapter three.

4.3.2 The effect of Sphingosine Kinase Inhibitor on LNCaP

The treatment of LNCaP cells with Ski modulated the metabolome, with marked changes in glutathione, NADPH, pentose phosphate shunt and glycolytic metabolite levels these were indicative of a pronounced oxidative stress response and modulation in the Warburg effect; although without carrying out flux measurements it is difficult to determine whether the Warburg effect was up or down regulated. GSSG levels are elevated and it is formed by the reaction of GSH and hydrogen peroxide catalysed by glutathione peroxidase. The treatment of cells with Ski reduces NADPH levels; this is consistent with NADPH being depleted since it is required to recycle GSSG back into GSH by glutathione reductase. Another possible route for the decrease in NADPH is that Ski might activate NADPH oxidase to produce superoxide, which is then converted to hydrogen peroxide by superoxide dismutase. Indeed, knock-down of SK1 by shRNA increased levels of ROS in doxorubicin-treated carcinoma cells, resulting in increased DNA damage and apoptosis. Moreover, the treatment of these cells with the NADPH oxidase inhibitor reduced apoptosis in doxorubicin-treated SK-1 knock-down cells (Huwiler et al., 2011). Much of the NADPH is derived from the conversion of glucose phosphate into ribulose 5 phosphate in the pentose phosphate pathway and ribulose phosphate is elevated in Ski-treated cells. The changes in GSSG, NADPH and ribulose-5-phosphate suggest a failed attempt by the cells to maintain NADPH levels using the pentose phosphate pathway. Hence, LNCaP cells seem to be overwhelmed by the oxidative stress, which may explain the ensuing apoptotic response.

The other glycolytic metabolites that are elevated by Ski treatment of cells are fructose 1,6 bisphosphate and the two isomers glyceraldehyde 3-phosphate and glycerone phosphate which are derived from it, implying that the accumulation of these metabolites might be a result of inhibition of the glycolytic pathway. Lactoyl glutathione is elevated and this compound derives from methylglyoxal (a highly reactive glycolytic byproduct that is apoptotic in prostate cancer cells (Vanderluit et al., 2003)). These changes reflect accumulation of intermediates as a consequence of indirect antagonism of the Warburg effect.

NADH is greatly elevated in the Ski-treated cells and this suggests increased fatty acid oxidation, which might be consistent reduced flux through the glycolysis pathway and compensation for this through β-oxidation of fatty acids. Indeed, others have shown that apoptosis in cancer cell lines caused by ENOX2 inhibitors, such as EGCG and phenoxodiol is due to elevation of cytosolic NADH. Moreover, this results in decreased pro-survival S1P and increased pro-apoptotic ceramide, both of which may be important to initiation of the ENOX2 inhibitor-induced apoptosis (Wu et al., 2011) and suggesting close coupling between SK1 and NADPH oxidase.

The other major effects of Ski are on lipid metabolism, including marked changes in certain carnitines which shuttle fatty acids in and out of the mitochondria. The levels of acetylcarnitine and 3-hydroxyhexanoylcarnitine are considerably elevated in LNCaP cells subsequent to treatment with Ski. This response might imply and increased flux through the glycolytic pathway since acetyl carnitine provides a strategy for removing acetate from cell rather than it entering into the Krebs cycle where it could be transferred from acetyl CoA to acetyl carnitine and removed from the mitochondria. This could provide an alternative strategy to the conversion of pyruvate to lactate and would account for an elevation in NADH levels in the cells. Free CoA also drops considerably, implying that this may be a limiting factor. A function of acylcarnitines is to keep homeostatic levels of free CoA (Zammit et al., 2009). The elevated levels of carnitines indicate that LNCaP cells may compensate for overload of the CoA available. Lysine is another source of acetyl CoA (Benevenga and Blemings, 2007). Saccharopine is an intermediate of lysine degradation, is also elevated in LNCaP cells treated with Ski. This finding might suggest that this degradation pathway is unable to function properly due to a lack of CoA. However, perhaps more pertinently the pathway between saccharopine and acetate yields two molecules of NADPH and could provide an alternative route for compensating for the depletion of NADPH.

A striking difference between LNCaP and LNCaP-AI cells is the high levels of diadenosine triphosphate (Ap3A) in the LNCaP cells. Elevated levels of this compound are associated with apoptosis and it is barely detected in LNCaP-AI cells while it is elevated in the LNCaP cells in response to treatment with Ski. This is consistent with previous finding that the LNCaP cells undergo apoptosis in response to Ski, while LNCaP-AI cells are resistant (Loveridge et al., 2010).

Ski also raised the levels of 1-O-hexadecyl-2-lyso- phosphatidylcholine, a cell membrane-permeable lipid belonging to a class of alkyl-lyso phospholipids which are known to induce cancer cell apoptosis (Vanderluit et al., 2003).

4.3.3 The effect of Ski on the metabolome of LNCaP-SK1b cells

FLAG-tagged SK1b had been over-expressed to investigate the effect of Ski on the metabolome of LNCaP-SK1b cells. LNCaP-SK1b cells should be protected from the effects of the SK inhibitor (Ski) as K.Lim determined that the expression level and properties of sphingosine kinase 1 (SK1b) in prostate cancer cells reduce its sensitivity to Ski-induced proteasomal degradation (Lim et al., 2012). Surprisingly, however, over-expression of FLAG-SK1b appears to induce a more severe oxidative stress response to Ski as assessed by the almost complete loss of GSH and the substantial increase in $NADP^+$ level compared with LNCaP cells. The treatment of these cells with Ski still induced an increase in dihydroxyacetone phosphate and glyceraldehyde 3-phosphate, which is consistent with inhibition of SK1 and antagonism of the Warburg effect. There were also similar changes in acetylcarnitine levels. Moreover, the over-expression of FLAG-SK1b appears to perturb sphingolipid metabolism as evidenced by the accumulation of the novel sphingolipid, dihydrodesmethylsphingosine in response to treatment of LNCaP-SK1b cells with Ski. It remains to be determined whether this sphingolipid is responsible for the enhanced oxidative stress in LNCaP-SK1b cells in response to Ski.

4.3.4 Methylglyoxal Analysis

Methylglyoxal is the aldehyde form of pyruvic acid. It contains two carbonyl groups. It is considered as both an aldehyde and a ketone. It is a reactive aldehyde that is very toxic to cells (Lodge-Ivey et al., 2004). There are many sources of methylglyoxal but it is mainly formed from intermediates of glycolysis such as dihydroxyacetone phosphate (DHAP) by lipid peroxidation systems (Nemet et al., 2004, Desai and Wu, 2007). Since MG is highly cytotoxic, the detoxification of reactive aldehyde take place by thiol-dependent enzymes glyoxalase I S-lactoyl-glutathione which was detected at high levels in the Ski treated cells (Thornalley, 2003). A high glucose level in diabetic patients is associated with elevation of plasma methylglyoxal (Dhar et al., 2009). The derivatized methylglyoxal compound was detected at 6 minutes with m/z 130. However, it was not detected in the LNCaP and LNCaP-AI cell samples which treated by Ski. Previous work suggests that methylglyoxal is not detected in the samples probably because it is too reactive to survive within the cells. So another analytical method was tried to identify methylglyoxal as LCMS method by trapping it with N-acetylcysteine as in section 4.3.5.

4.3.5 Effect of N-Acetylcysteine on metabolomic changes in response to Ski

Knock down of SK1 using shRNA raised levels of ROS in carcinoma cells treated with doxorubicin, leading to greater DNA damage and apoptosis (Huwiler et al., 2011). Evidence of this was seen when LNCaP cells were treated by Ski in section 4.3.2 as oxidized glutathione levels are increased: a consequence of of ROS production. In addition, (Fajardo et al., 2012) showed that AR down-regulation in several prostate cancer cell lines was induced by oxidative stress. This was investigated by (Tonelli et al., 2013) and it was found that Ski (10 mM) induced down-regulation of AR, an effect that was reversed by NAC (10 mM). In this light, LNCaP cells tested to establish whether or not the effect of Ski on AR expression is mediated by a ROS-dependent pathway by pre-treatment of the LNCaP cells with the ROS scavenger NAC and then treatment of the cells with Ski. The ratio of GSSG/GSH levels in LNCaP cell treated with Ski versus LNCaP cell untreated was 19.7 compared to 5.65 for LNCaP cells pretreated with NAC (10 mM) then Ski. The GSSG/GSH ratio in LNCaP cells treated with Ski after NAC compared with LNCaP cells treated with Ski alone was 0.29. NAC rescue AR expression and inhibited the increase of oxidative stress levels in response to Ski, thus confirming that the oxidative stress response to Ski is abrogated by this compound.

In case of detection methylglyoxal by LC-MS, examination of whether or not any direct reaction was formed between NAC and methylglyoxal was carried out. LC-MS analysis of the products indicated that the reaction product was a thioacetal with the formula $C_8H_{13}O_5NS$. This compound was detected at 6.2 minutes in negative ion mode on a ZIC-pHILIC column. In addition oxidized NAC was formed at 7.8 minutes in the same condition in LNCaP cells. Examining cell cultures incubated in the presence of NAC and with or without Ski there was no evidence for the formation of a thioacetal conjugate in the cells and there were no differences between the levels of NAC or oxidized NAC in the cells. In several studies an increase in the level of methylglyoxal binding with bovine serum albumin (BSA) and decreasing in methylglyoxal free was related to increasing incubation time (Dhar et al., 2009). Methylglyoxal is behind diabetic complications due to its reversible and irreversible binding and modification of proteins (Lo et al., 1994). The high degree of binding of methylglyoxal to proteins might be the cause behind undetectable methylglyoxal either in this method or the GCMS method.

4.3.6 The Effect of Ski on the Metabolome of LNCaP-AI cells

The treatment of LNCaP-AI cells with Ski had elevated levels of glutathione, NADPH, pentose phosphate and glycolytic metabolites as for LNCaP cells, these increases indicate a response to oxidative stress. GSSG levels are elevated in both cell types as well. In addition, the treatment of cells with Ski reduces NADPH levels in both cell types. Fructose 1,6 bisphosphate and the two isomers glyceraldehyde 3-phosphate and glycerone phosphate which are derived from it, they are other glycolytic metabolites that are elevated by Ski treatment. Lactoyl glutathione is elevated which is derived from methylglyoxal that is formed from glycerone phosphate. The same elevation of NADH occurred in both cell types. Therefore the effects of Ski on the androgen dependent and androgen independent cells were broadly similar metabolome responses. However, diadenosine triphosphate is highly elevated in LNCaP while it was not detected in LNCaP-AI. Moreover, there are also effects of Ski on PE and PC lipids in LNCaP cells but not LNCaP-AI cells.

4.3.7 Diadenosine triphosphate in LNCaP cells

A striking difference between LNCaP and LNCaP-AI cells is the high levels of diadenosine triphosphate in the LNCaP cells. Elevated levels of this compound are associated with apoptosis and it is barely detected in LNCaP-AI cells while it is elevated in the LNCaP cells in response to treatment with Ski. This is consistent with previous finding that the LNCaP cells undergo apoptosis in response to Ski, while LNCaP-AI cells are resistant (Loveridge et al., 2010).

To explain the effect of increasing level of Ap3A by treatment of LNCaP cells with Ski, the Fragile Histidine Triad (FHIT) protein tumour suppressor gene product binds Ap3A to induce apoptosis. Further, FHIT is an Ap3A hydrolase, a function which could be compared to the GTPase activity of the G-protein α subunit, which terminates the GPCR-G-protein activation cycle. In addition, the intragenic alterations in the FRA3B/FHIT chromosome fragile site lead to fragile FHIT allele loss in the initial stages of the development of cancer (Ji et al., 1999). In addition, FHIT knockout mice are predisposed to tumour development, and FHIT gene therapy reduces tumour burden (Pichiorri et al., 2008). There is strong evidence to indicate that germ line variations of FHIT are involved in prostate cancer risk (Pomerantz et al., 2011). Moreover, restoration of wild-type FHIT in 3p14.2-deficient human lung cancer cells inhibits cell growth and induces apoptosis (Deng et al., 2007). Hence, it is notable that Ski induces an increase in the Ap3A level in LNCaP prostate cancer cells, as this may lead to an increase in the formation of Ap3A-FHIT complex, which in turn, may induce apoptosis. Regarding its apoptotic function, FHIT has also been demonstrated as interacting with ferridoxin reductase to produce ROS and to induce apoptosis of cancer cells (Trapasso et al., 2008). This study shows evidence for the first time for a functional link between SK1 and the cancer cell metabolome, a principal sign of cancer.

4.3.8 The effect of ROME on the metabolome of LNCaP cells

(R)-FTY720 methyl ether (ROME) had a different effect from Ski and had no significant effect on oxidative stress or the pentose phosphate pathway. However, glycolytic intermediates were decreased to about 50%. On the other hand, the lipid profile produced by ROME treatment indicated that there were increased in the levels of several lysophosphatidylinositols (Lyso PI) and LPA species. Both Lyso PI and LPA are ligands for GPR55 and LPA/EDG receptors that promote proliferation and cell survival (Anavi-Goffer et al., 2012, Tigyi, 2010). Therefore, these metabolite changes are in line with the possibility that SK2 normally functions to limit mitogenic signalling by lyso-PI and LPA. The palmitoyl glucuronide was also elevated in ROME treated cells. This metabolite might be an intermediate derived from the S1P lyase-catalysed conversion of S1P into hexedecenal and phosphoethanolamine. Hexedecenal is likely to be rapidly converted to either palmitic acid or palmitoyl alcohol. The question then is how does inhibition of SK2 and lowering of S1P (Watson et al., 2013) increase the levels of glucuronide conjugate of palmitoyl alcohol? Therefore, in the absence of functional SK2 activity in ROME-treated cells, the availability of S1P for the phosphatase might be reduced. Under these conditions, S1P becomes available to the S1P lyase. This is consistent with the reduction in S1P levels and the formation of glucuronide conjugate of palmitoyl alcohol that is observed in ROME-treated cells. Indeed, others have shown that inhibition of the S1P phosphatase decreases S1P levels and it has been proposed that under these conditions, S1P becomes accessible to S1P lyase (Siow et al., 2010).

4.2.9 The Effect of (S)-FTY720 Vinylphosphonate on metabolome of LNCaP and LNCaP-AI cells

Treatment of LNCaP and LNCaP-AI cells with (S)-FTY70 vinylphosphonate had different effects compared with Ski. The levels of Ap3A did not change in LNCaP cells and it was not detected in LNCaP-AI cells. Moreover, there were no induced changes in the metabolome that would indicate oxidative stress or antagonism of the Warburg effect. The metabolites that were modestly changed in response to (S)-FTY70 vinylphosphonate were phospholipids, such as lyso-phosphatidylethanolamine (lyso-PE), phosphatidylserine (PS), and phosphatidic acid (PA) in LNCaP-AI cells but it was less evident in LNCaP cells. The change in PS might be linked with apoptosis of LNCaP-AI cells, indicating distinct mechanisms of apoptosis in response to (S)-FTY720 vinylphosphonate in the cell type (Tonelli et al., 2010). Phosphatidylserine is formed by the reactions of phosphatidylcholine and phosphatidylethanolamine. Contrariwise, phosphatidylserine can also produce phosphatidylethanolamine and phosphatidylcholine[4]. This findings align with Eva et al, 2004 that when they used antioxidents to inhibit ROS activated key pathways of apoptosis in pancreatic cancer cells through particular cytochrome c release and effector caspase activation then stimulate inter nucleosomal DNA fragmentation and phosphatidylserine externalization (Vaquero et al., 2004).

The high levels of sphingolipid bases are evidence added to the factors lead to apoptosis of LNCaP cell types. Sphingosine and sphinganine which produce ceramide (highly bioactive apoptotic compound) through two different ways by ceramide synthase 1, they were increased more than two fold. In addition, an increasing ceramide level was detected. Moreover, hydroxysphingosine and hydroxysphinganine were elevated, these phytosphingosines induce caspase-independent cytochrome c release from mitochondria result in apoptosis in human T-cell lymphoma and cell lung cancer cells. In the presence of caspase inhibitors, phytosphingosine-induced apoptosis is completely suppressed (Park et al., 2003).

Low levels of hypoxanthine, guanine and uridine were detected in both cell types. That might be a result of downregulation of purine nucleoside phosphorylase (PNP). Purine nucleoside phosphorylase (PNP) is an enzyme that converts inosine to hypoxanthine and guanosine to guanine in purine metabolism pathway and also converts deoxyuridine to uridine in pyrimidine metabolism pathway (Roberts et al., 2004). PNP gene is highly expressed in prostate cancer cells. Inhibition of the PNP gene leads to suppression of proliferation, migration, and invasion in both PC3 and DU145 cells (Kojima et al., 2011). Kojima *el at*, 2011 showed that purine nucleoside phosphorylase was directly regulated by both miRNAs (miR-1 and miR-133a) which are significantly downregulated in prostate cancer cells compared with non- prostate cancer cells. Re-introduction of miR-1 or miR-133a in PC3 and DU145 cells detected significant inhibition of proliferation, migration, and invasion (Kojima et al., 2011). Knock-down of SK1 in ovarian cancer cells inhibit of migration and invasion by miR-124, while restoration of SK1 abrogates the suppression of motility and invasiveness induced by miR-124 in ovarian cell lines so SK1 is a direct target of miR-124 in ovarian cancer cells (Zhang et al., 2013). Another study showed that overexpression of both microRNA-124 and microRNA-1 induces apoptosis and marked decrease in glioma cell proliferation and invasiveness. This line with microRNA-124 and microRNA-1 can apply significant effect on glioma cells by inhibiting expression and activity of SK1 (Godlewski et al., 2011). These explanations consistent with our finding which is (S)-FTY720 Vinylphosphonate a selective inhibitor of SK1 and that might be upregulate miR1 and miR133a in LNCaP cells then downregulation of PNP was induced and inhibit the conversion of inosine, guanosine and deoxyuridine to hypoxanthine, guanine and uridine respectively.

These results indicated that FTY720 Vinylphosphonate is a novel selective SK1 inhibitor might be used to inhibit PNP through miR-1 and miR-133a as their target gene in both LNCaP and LNCaP-AI.

---

(4) http://lipidlibrary.aocs.org/lipids/pc/index.htm

4.4 Concluding Remarks

- An effective ZIC-pHILIC chromatographic separation method was applied on LNCaP cells treated with three sphingosine inhibitors. A large number of polar metabolites were changed in response to treatment (264 metabolites) 68 metabolites of them showed changes. Moreover, some lipids were separated well using these chromatographic conditions.
- The treatment of LNCaP cells with Ski modulated the metabolome, with marked changes in glutathione, NADPH, pentose phosphate shunt and glycolytic metabolite levels these indicative of a pronounced oxidative stress response and modulation in the Warburg effect.
- Over-expression of FLAG-SK1b appears to induce a more severe oxidative stress and antagonism of the Warburg effect in response to Ski.
- NAC rescued AR expression and inhibited the increase of oxidative stress levels in response to Ski, thus confirming that the oxidative stress response to Ski is abrogated by this compound.
- The effects of Ski on the androgen dependent and androgen independent cells were broadly similar in terms of metabolomic responses. However, diadenosine triphosphate is highly elevated in LNCaP while it was not detected in LNCaP-AI.
- The presence or absence of Ap3A in Ski-treated androgen-sensitive LNCaP cells and androgen-independent LNCaP-AI cells, respectively, might provide an explanation for the different sensitivities of these cells to the apoptotic effect of Ski. Therefore, our findings suggest that Ap3A might cooperate with the antagonism of the Warburg effect and oxidative stress to induce apoptosis of androgen-sensitive LNCaP cells. Thus the absence of Ap3A in Ski-treated androgen-independent LNCaP-AI cells might enable these cells to mitigate the

oxidative stress and antagonism of the Warburg effect, thereby escaping the apoptotic program. These findings offer motivation for the development of SK1 selective inhibitors for the abrogation of the Warburg effect in prostate cancer cells.

- A comparison between the results of 2-(p-hydroxyanilino)- 4-(p-chlorophenyl)thiazole (Ski) and (R)-FTY720 methyl ether (ROME) was used to discriminate between the effects of SK1- vs. SK2-selective inhibitors, ROME showed no effect on oxidative stress or the pentose phosphate pathway also not antagonize Warburg effect but increased in the levels of several lysophosphatidylinositols (Lyso PI).
- (S)-FTY70 vinylphosphonate did not induce changes in the metabolome that would indicate oxidative stress or antagonism of the Warburg effect. However, many change in metabolites which indicate apoptosis such as increase in phosphatidylserine (PS), Sphingosine and sphinganine, hydroxysphingosine and hydroxysphinganine. In addition, (S)-FTY720 Vinylphosphonate a selective inhibitor of SK1 and that might be upregulate miR1 and miR133a in LNCap cells then downregulation of PNP was induced and inhibit the conversion of inosine, guanosine and deoxyuridine to hypoxanthine, guanine and uridine respectively.
- To conclude these findings: SK1 can regulate aerobic glycolysis, Ap3A formation, and apoptosis of androgen-sensitive LNCaP cells, while SK2 might functionally regulate lyso-PI and LPA metabolism possibly linked with mitogenesis. This factor is therefore worthy of further study in terms of improving our understanding of how these enzymes are involved in controlling apoptosis of prostate cancer cells.

Chapter 5: Development of a Quantitative Method for the Determination of Diadenosine Triphosphate and Diadenosine tetraphosphate Using Tandem Mass Spectrometry

Development of a Quantitative Method for the Determination of Diadenosine Triphosphate and Diadenosine tetraphosphate Using Tandem Mass Spectrometry

5.1 Introduction

Diadenosine triphosphate (Ap3A) and Diadenosine tetraphosphate are members of the diadenosine polyphosphate (APnAs, n = 3-7) family which are a ubiquitous class of molecules found in prokaryotes and eukaryotes. They are a member of group formed by two adenosine molecules being linked to a specific number of phosphates. The numbers of these phosphate groups indicate the link between, diadenosine polyphosphates and their properties of vasoconstriction and vasodilatation of vascular smooth muscle cells (van der Giet et al., 1998). Diadenosine polyphosphates were discovered in the sixties by Zamecnik and his colleagues (Varshavsky, 1983). They are considered to be second messengers because they maintain and regulate vital cellular functions and they arise as intracellular and extracellular signaling molecules. They are found in the CNS, in storage vesicles in brain synaptosomes and are released in a calcium-dependent manner. They also facilitate tear secretion. Ap3A is an inhibitor of Eosinophil-derived neurotoxin (EDN) which is a catalytically proficient member of the pancreatic ribonuclease family. The interaction of FHIT protein, fragile histidine Triad which is a human tumor suppressor gene, with Ap3A is believed to inhibit tumor growth by inducing apoptosis (HMDB) [5]. The proliferative properties of diadenosine polyphosphates and their high level in platelets of patients with high-risk factors for atherosclerosis led van der Giet and his group to study their effect on vascular smooth muscle cells. They found that Ap3A and Ap4A, but not Ap5A or Ap6A; induce proliferation of VSMCs by a signaling

(5) http://www.hmdb.ca/metabolites/HMDB01211

pathway by activation of P2Y receptors and this results in the stimulation of the MAP kinases ERK1/2 (van der Giet et al., 1998). Ap4A is the only diadenosine polyphosphate that can induce a significant increase in endothelial cell Ca^{2+} (HMDB). Diadenosine polyphosphates were analyzed in 1998 by Jankowski and his colleagues, using ion-pair reversed phase perfusion chromatography to analyze the platelets from human blood. The level of diadenosine polyphosphates measured were Ap3A,192.5 nM; Ap4A, 223.8 nM; Ap5A, 100.2 nM and Ap6A, 32.0 nM (Jankowski et al., 1999). Also mass spectrometry was used for the quantification of diadenosine polyphosphates. Purification of diadenosine polyphosphates from deproteinized human plasma was carried out by affinity-, anion exchange-, and reversed phase-chromatography then homogeneous fractions were analyzed by using matrix-assisted laser desorption/ionization mass spectrometry (MALDI-MS). The concentrations detected were Ap3A 0.89, Ap4A 0.72, Ap5A 0.33, and Ap6A 0.18 (µmol/L) (Jankowski et al., 2003). Intracellular Ap3A and Ap4A were extracted and assayed to measure their level in FHIT-positive HEK293 cells which were treated with apoptosis inducers by a long and complicated method. The levels measured were 0.079 pmol/10^6 cells for Ap3A and 0.5 pmol/10^6 cells for Ap4A (Fisher and McLennan, 2008). ToF-SIMS was used to quantify Ap3A and Ap4A in HeLa cell lysates by using bismuth and argon cluster ion beams and the levels detected were 0.1mM for Ap3A and 5mM for Ap4A (Shon et al., 2014). until the current date there is no study using Triple Quadrupole LC/MS Systems thus it was of interest to develop a method to quantify Ap3A which was observed to be present in LNCaP cells and to be elevated in the presence of the the Ski sphingosine kinase inhibitor.

5.2 Materials and Methods

5.2.1 Chemicals

Quantification of the compounds was performed using commercial standards. P1,P3-Di(adenosine-5′) triphosphate ammonium salt, CAS number 102783-40-4, Sigma-Aldrich, UK. P1,P4-Di(adenosine-5′) tetraphosphate ammonium salt, CAS number 102783-36-8, Sigma Aldrich UK. Standard prepared as two stock solutions (1mg/ml) by dissolve 1.4mg of P1,P3-Di(adenosine-5′) triphosphate ammonium salt and 1.4mg of Di(adenosine-5′) tetraphosphate ammonium salt in 1.4ml of 20mM Ammonium carbonate buffer pH 9.2. Then dilute the stock solution with acetonitrile to concentrations (50µg/ml, 10µg/ml, 1µg/ml, 500ng/ml, 100ng/ml, 10ng/ml, 5ng/ml, 1ng/ml and 0.1ng/ml). All solvents and standards should be freshly prepared on the same day of the experiment.

5.2.2 LC-MS Method

Chromatographic analyses were performed on an Agilent 1200 series ultra-performance liquid chromatography system (Agilent, UK) with a quaternary pump system, a vacuum degasser and a thermostated column compartment. Separation was carried out using a ZIC®-pHiLIC column, L150 * I.d. 4.6 mm, 5µm, polymeric beads analytical column (Hichrom, Reading , UK) fitted with a guard column: ZIC®-pHILIC Guard.

Optimum separation was achieved with a binary mobile phase gradient at a flow rate of 0.2 mL/min for the MS-scan and 0.3ml/min for standard calibration. The column temperature was kept at room temperature and the injection volume was 10 µL. Solvents were (A) 20mM Ammonium carbonate buffer pH 9.2, and (B) acetonitrile. The gradient elution program for MS scan and quantification LNCaP cell extract was as follows:

Time (min)	Mobile phase A%	Mobile phase B%
0	20	80
30	80	20
31	92	8
36	92	8
37	20	80
46	20	80

While for detecting the lowest concentrations the gradient elution program was changed to the following:

Time (min)	Mobile phase A%	Mobile phase B%
0	20	80
25	70	30
26	20	80
31	20	80

Identification and quantification of Di(adenosine-5)triphosphate and Di(adenosine-5) tetraphosphate compounds was carried out by using a 6460 Series Triple Quadrupole LC/MS System equipped with an Electrospray Ionization Source (ESI) and controlled by MassHunter Workstation Software (Agilent, UK). Source working conditions were: capillary voltage 135 V, gas flow rate 3 L/min, gas temperature 300 °C and nebulizer pressure 15 psi. UK. The results obtained by using MassHunter Optimizer Software. CID was carried out by using argon as the collision gas and collision energy of 25 V.

5.3 Results

A mixture of standard solution containing 10µg/ml of Ap3A and Ap4A was injected in the LC-MS to give the full scan chromatogram and the full scan mass spectra shown in figure 5.1 and figure 5.2 respectively. The retention times with peak areas obtained from this standards solution is recorded in table 5.1 for the two analytes.

Product ion scanning revealed that the major transition for the two analytes in the case of Ap4A gave adenosine monophosphate as the major fragment ion and in the case of Ap3A gave adenosine as the major fragment ion (figure 5.3).

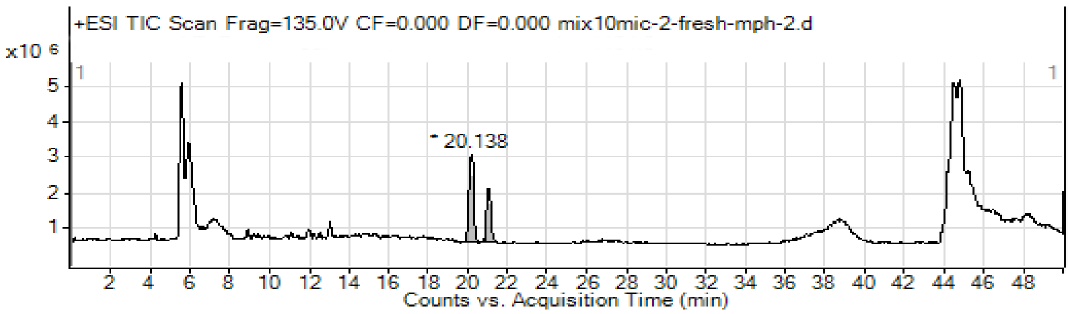

Figure 5.1 Full scan chromatogram of Di(adenosine-5)triphosphate and Di(adenosine-5)tetraphosphate standards mixture 10µg/ml using an Agilent 6460 Triple Quadrupole LC/MS system in positive ion mode.

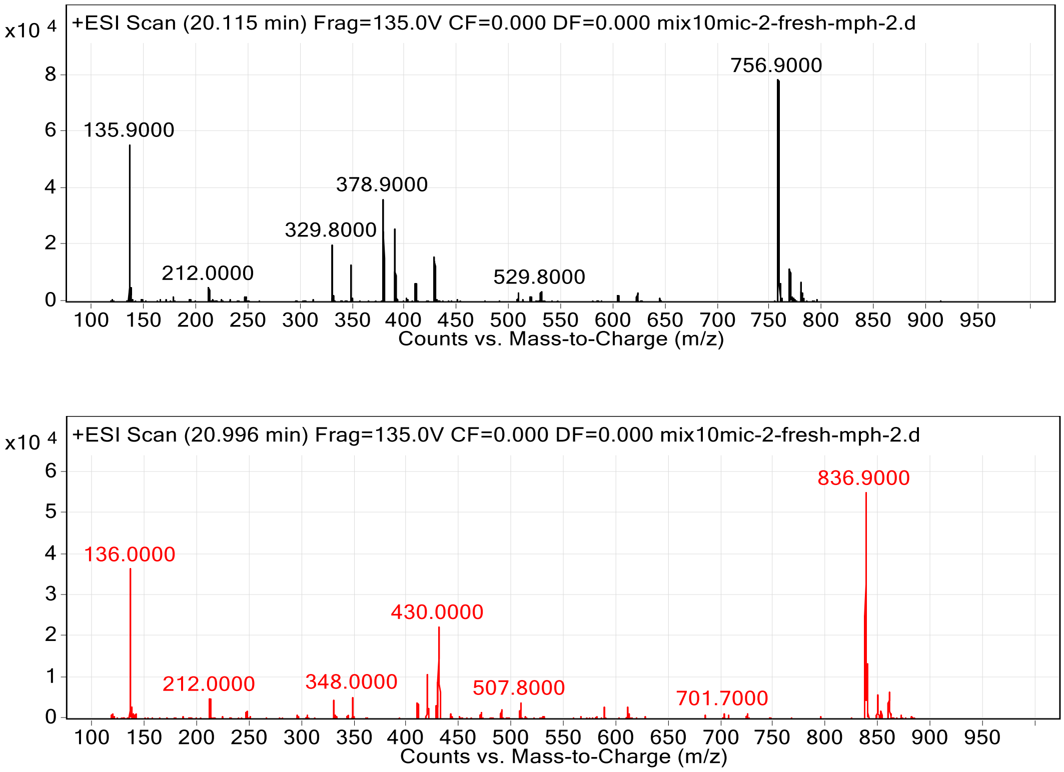

Figure 5.2 Full scan mass spectra standard solution of Ap3A (black) and Ap4A (red) obtained using an Agilent 6460 QQQ.

Table 5.1 Response for a 10μg/ml standards solution of Ap3A and Ap4A obtained using an Agilent 6460 QQQ.

Peak	RT	Height	Area
Di(adenosine-5)triphosphate	20.138	2518567.5	38386812.52
Di(adenosine-5)tetraphosphate	20.988	1486525.69	22356205.04

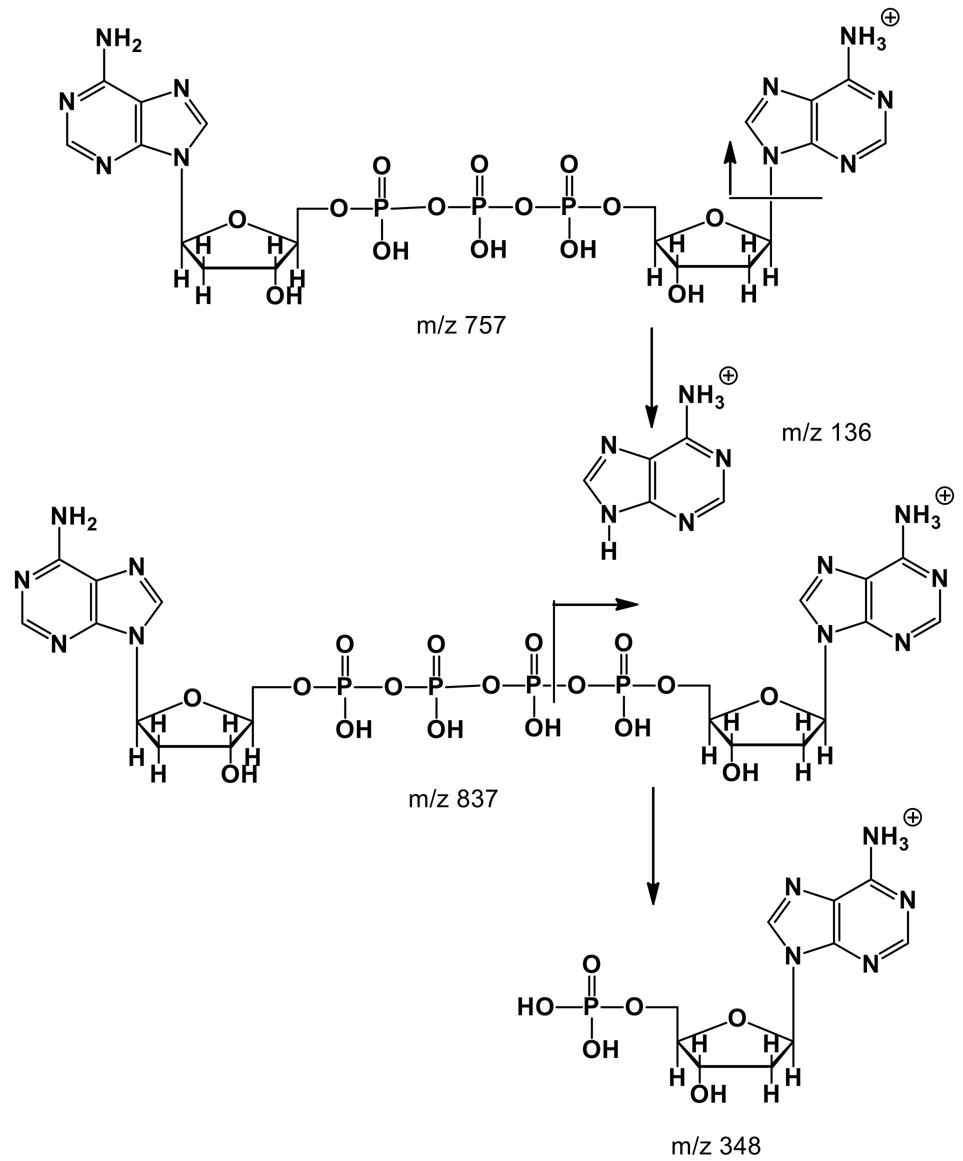

Figure 5.3 Fragmentation of Ap3A and Ap4A at 25 V with argon collision gas.

Figure 5.4 shows the traces obtained from MRM monitoring of the transitions between the molecular ions of Ap3A and Ap4A and the adenosine monophosphate fragment ions. The chromatographic conditions were adjusted to give shorter retention times and sharper peaks. The response appeared to be good with SNR values suggesting that sub nanogram per ml amounts should be detectable. Table 5.2 shows the peak areas and peak heights obtained for the two analytes at 10µg/ml. Figures 5.5-5.8 show MRM traces for the standards in the range of 0.1ng-1µg/ml. It is likely with some additional optimization that the limit of detection could be pushed lower. However, since Ap3A was observed by using the Orbitrap Exactive it was thought likely that the range shown in the figures would be sufficient to determine it in the cell cultures. Tables 5.2-5.7 summaries peak area data in the range 0.1 ng/ml to 10µg/ml. Additional points at 500 and 5 ng/ml were also determined. Calibration points in the range 5-10000 ng/ml were determined three times by plotting the peak area against concentration using a linear regression model and tables 5.8-5.9 show average areas for each calibration point for Ap3A and Ap4A respectively.

Analysis was carried out of an extract of LNCaP cells and the MRM traces obtained are shown in figure 5.9 and the peak areas are given in table 5.8. Both Ap3A and Ap4A were readily detectable in the cell extract and the calculated levels are shown in tables 5.9 and 5.10 which are 128.95ng/10^6 cells and 72.45ng/10^6 cells for Ap3A and Ap4A respectively.

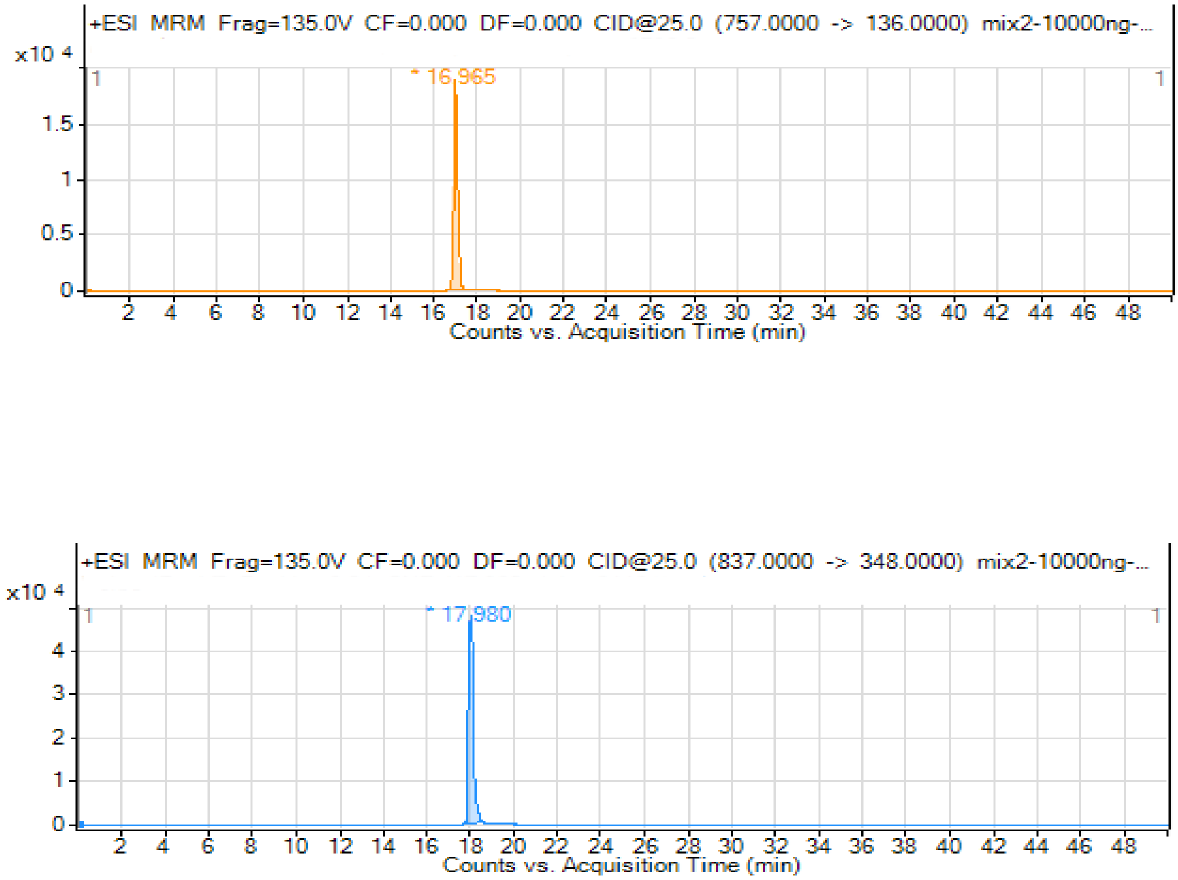

Figure 5.4 MRM traces obtained from the 10µg/ml standards solution of Ap3A (orange) and Ap4A (blue) at 25 V with argon collision gas.

Table 5.2 Peak areas obtained from MRM monitoring of Ap3A and Ap4A in the 10µg/ml standards solutions.

Peak	**RT**	**Height**	**Area**	**SNR**
Di(adenosine-5)triphosphate	16.962	18909	242372	448842
Di(adenosine-5)tetraphosphate	17.98	47852	738411	1367445

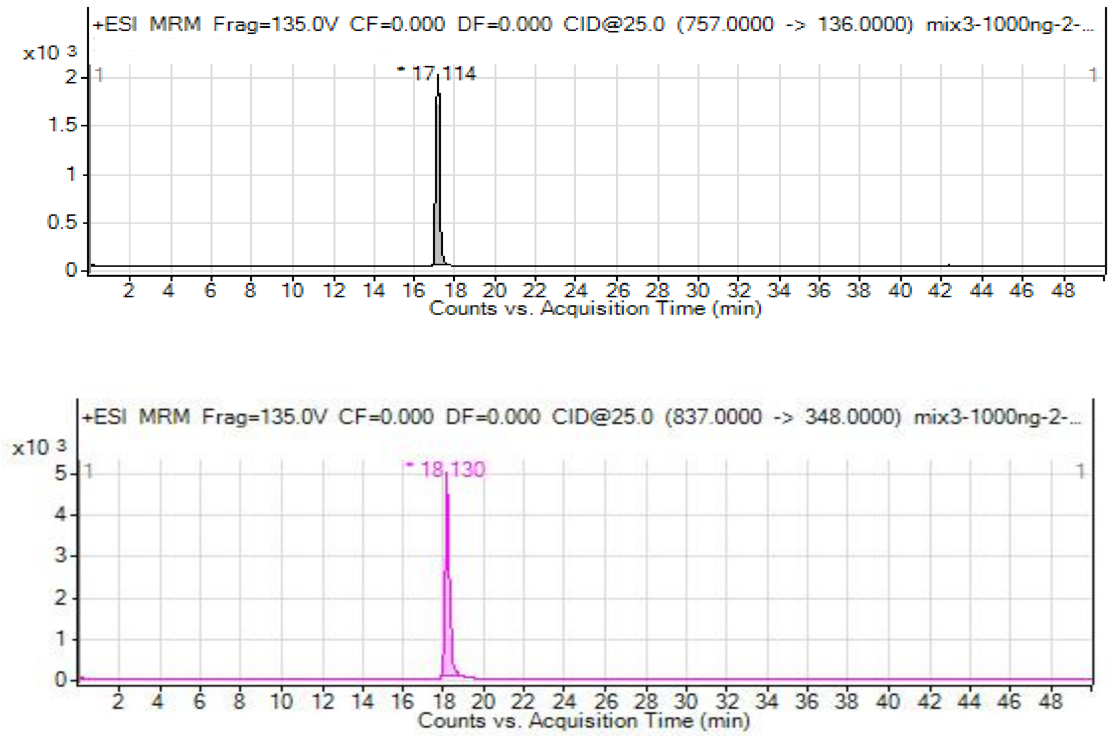

Figure 5.5 MRM traces obtained for from a 1 µg/ml standards solution of Ap3A (black) and Ap4A (purple) at 25 V with argon collision gas.

Table 5.3 Peak areas obtained from MRM monitoring of Ap3A and Ap4A in the 1µg/ml standards solutions.

Peak	**RT**	**Height**	**Area**	**SNR**
Di(adenosine-5)triphosphate	17.111	1979	25600	64000
Di(adenosine-5)tetraphosphate	18.13	4987	74553	186381

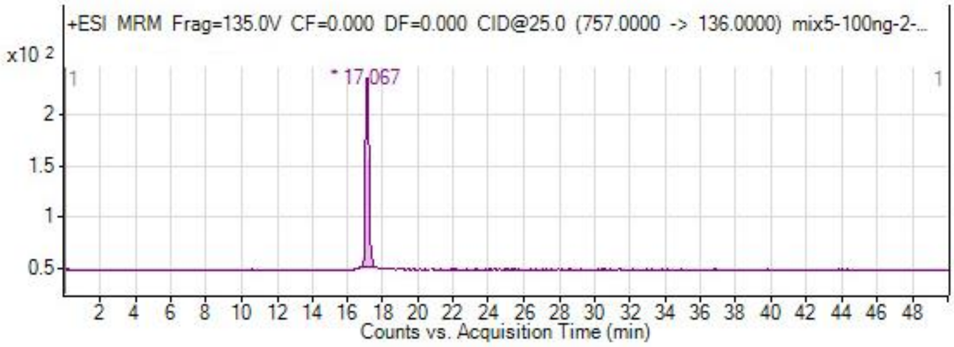

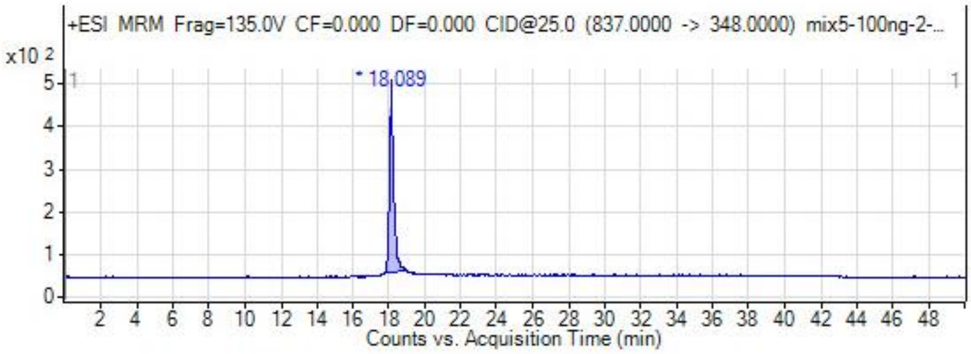

Figure 5.6 MRM traces obtained for from a 100 ng /ml standards solution of Ap3A (violet) and Ap4A (dark blue) at 25 V with argon collision gas.

Table 5.4 Peak areas obtained from MRM monitoring of Ap3A and Ap4A in the 100 ng/ml standards solutions.

Peak	RT	Height	Area	SNR
Di(adenosine-5)triphosphate	17.063	186	2443	4886
Di(adenosine-5)tetraphosphate	18.089	452	7493	14985

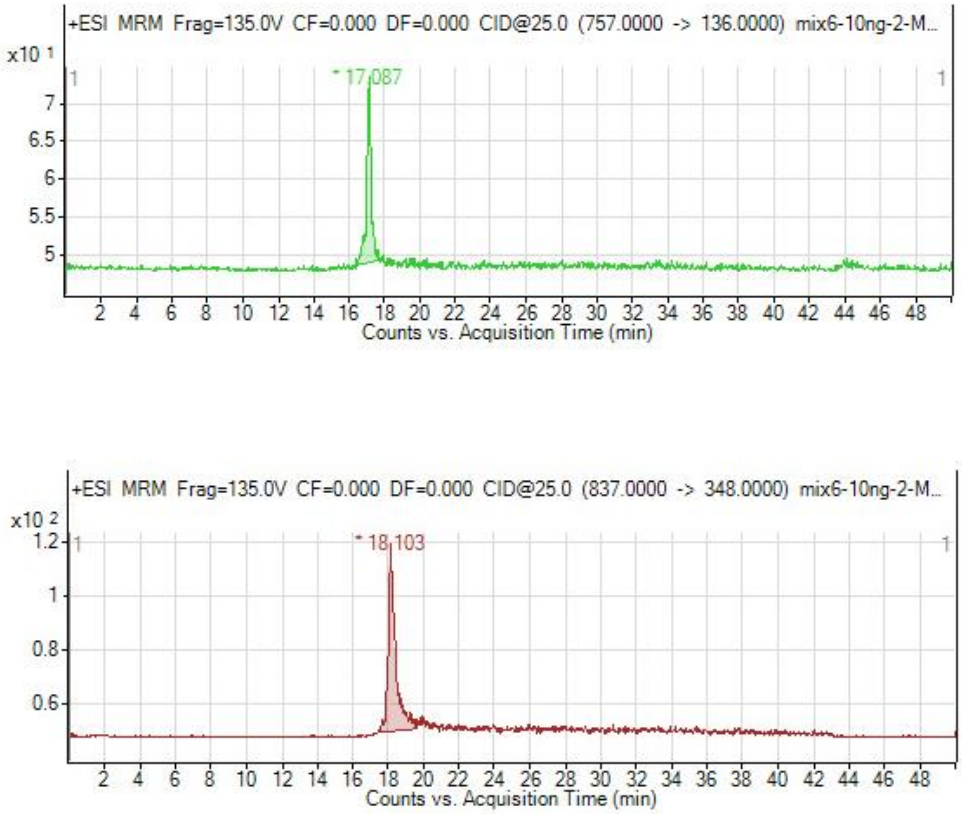

Figure 5.7 MRM traces obtained for from a 10 ng /ml standards solution of Ap3A (green) and Ap4A (brown) at 25 V with argon collision gas.

Table 5.5 Peak areas obtained from MRM monitoring of Ap3A and Ap4A in the 10 ng/ml standards solutions.

Peak	RT	Height	Area	SNR
Di(adenosine-5)triphosphate	17.084	23	330	750
Di(adenosine-5)tetraphosphate	18.103	66	1658	3767

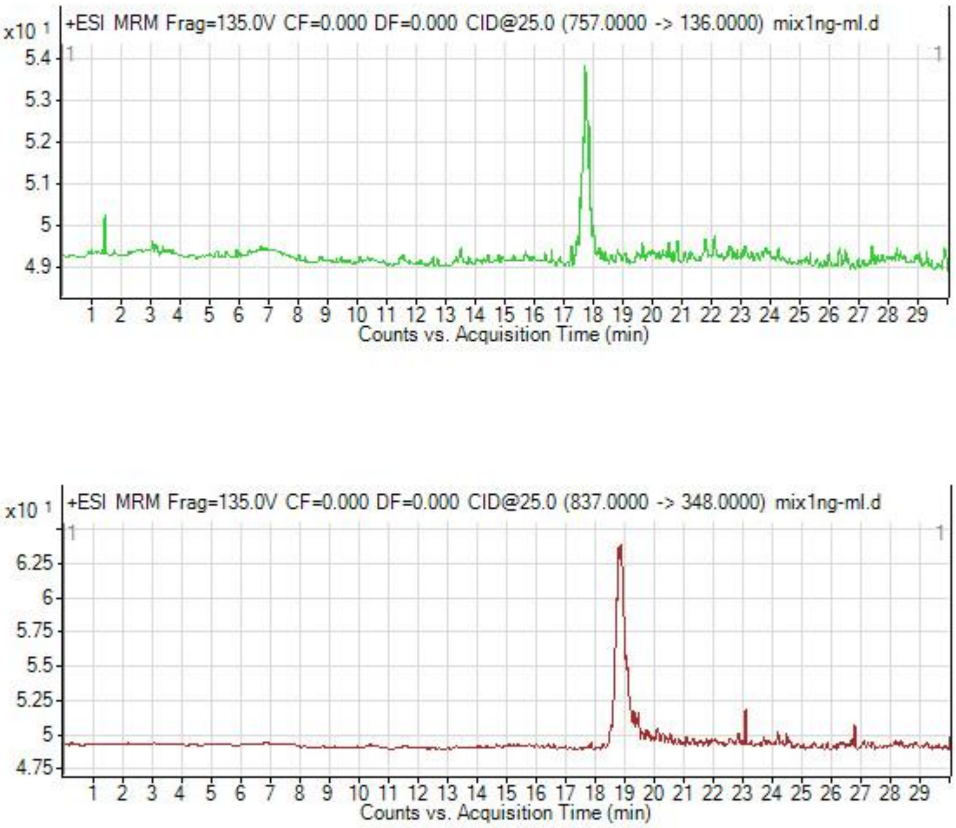

Figure 5.8 MRM traces obtained for from a 1 ng /ml standards solution of Ap3A (green) and Ap4A (brown) at 25 V with argon collision gas.

Table 5.6 Peak areas obtained from MRM monitoring of Ap3A and Ap4A in the 1 ng/ml standards solutions.

Peak	RT	Height	Area	SNR
Di(adenosine-5)triphosphate	17.688	4	63	184
Di(adenosine-5)tetraphosphate	18.836	13	268	786

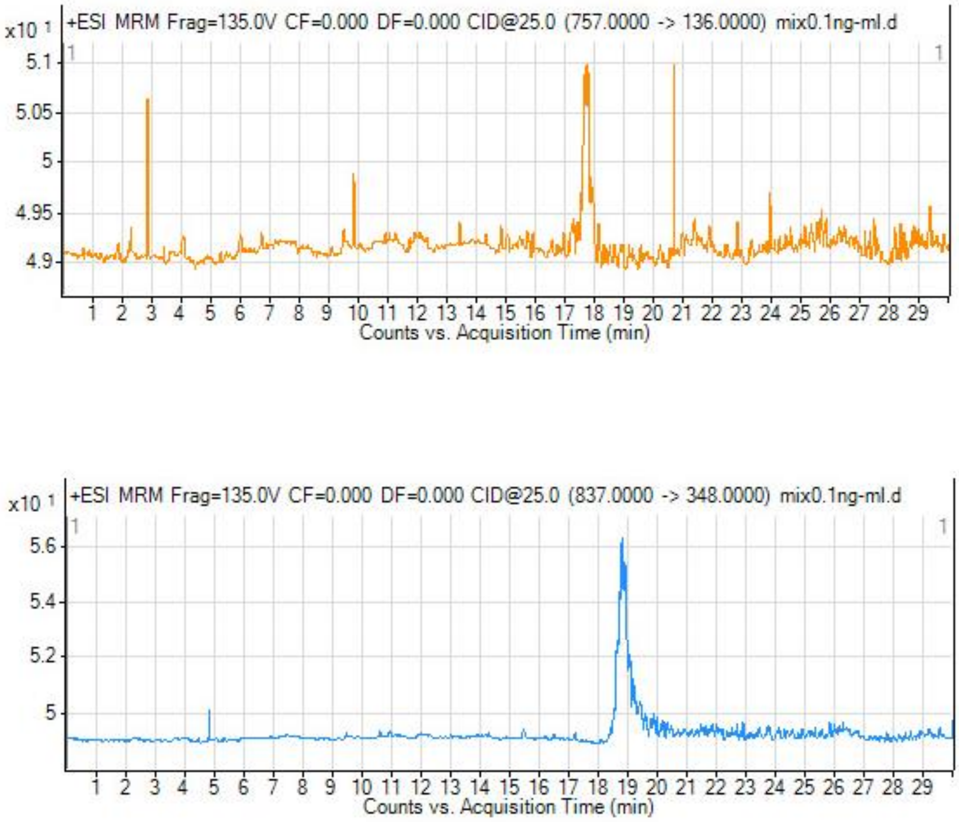

Figure 5.9 MRM traces obtained for from a 0.1 ng /ml standards solution of Ap3A and Ap4A at 25 V with argon collision gas.

Table 5.7 Peak areas obtained from MRM monitoring of Ap3A (orange) and Ap4A (blue) in the 0.1 ng/ml standards solutions.

Peak	**RT**	**Height**	**Area**	**SNR**
Di(adenosine-5)triphosphate	17.682	2	17	208
Di(adenosine-5)tetraphosphate	18.796	7	127	1590

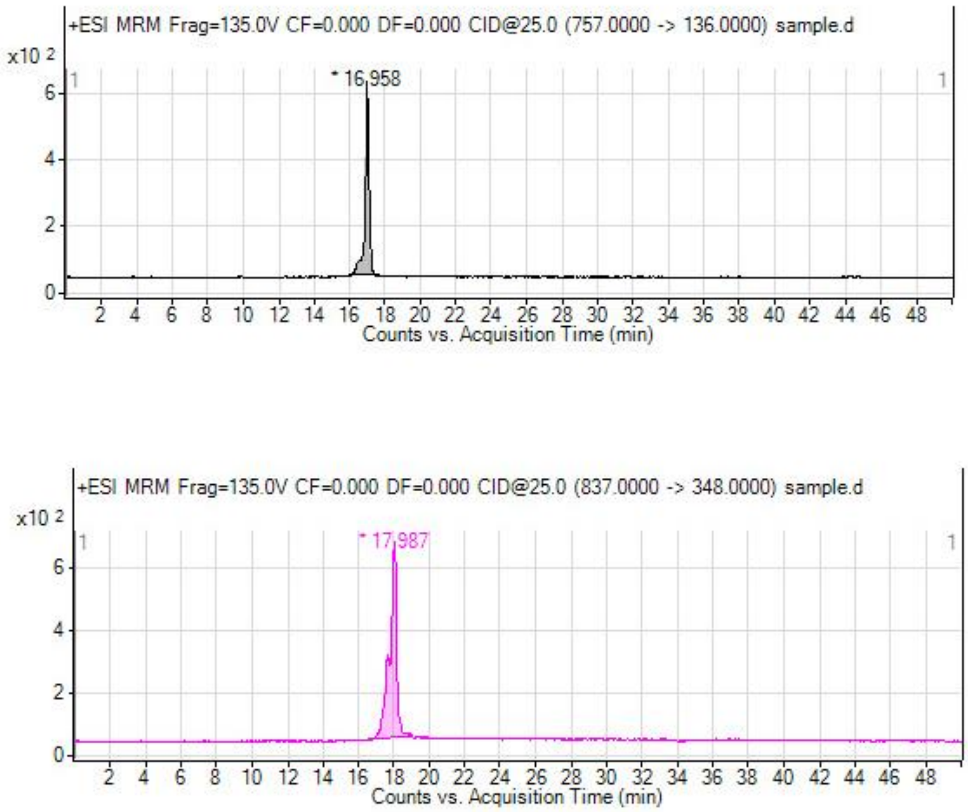

Figure 5.10 MRM traces obtained for and extract of LNCaP cells containing Ap3A and Ap4A at 25 V with argon collision gas.

Table 5.8 Peak areas obtained from MRM monitoring of Ap3A and Ap4A in LNCaP cell extract.

Peak	RT	Height	Area
Di(adenosine-5)triphosphate	16.955	528	6677
Di(adenosine-5)tetraphosphate	17.987	582	12482

Table 5.9 Average peak areas obtained from MRM monitoring of Ap3A in the range 5-1000ng/ml.

p1p3-Di(adenosine-5)triphosphate	
concentration (ng/ml)	Average area
1000	25252
500	12529
100	2404
10	318
5	198
sample	6534
Concentration of (LNCaP) cell culture extract ng/ml	257.89

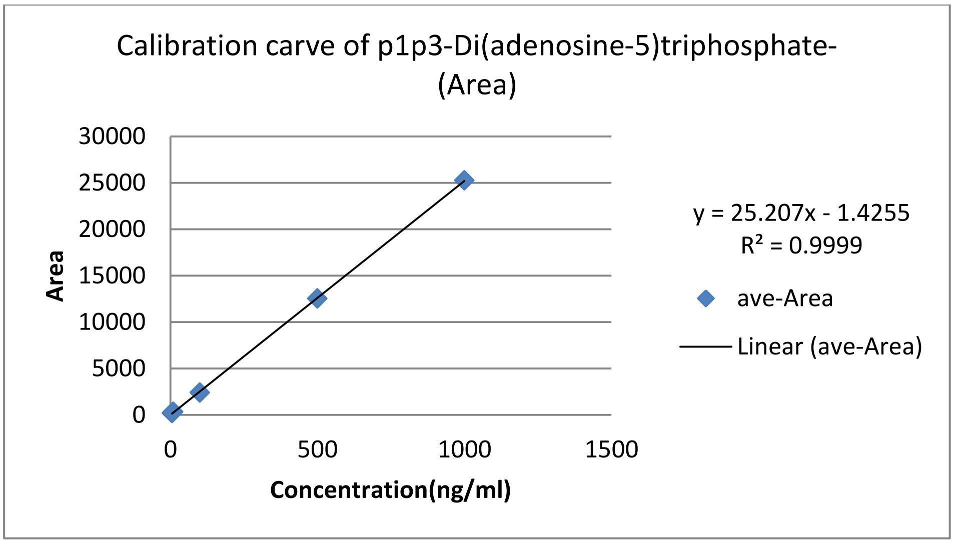

Figure 5.11 Calibration curve for Ap3A in the range 5-1000 ng/ml.

Table 5.10 Average peak areas obtained from MRM monitoring of Ap4A in the range 5-1000 ng/ml.

p1p4-Di(adenosine-5)tetraphosphate	
concentration (ng/ml)	Average areas
1000	78138
500	38121
100	7860
10	1955
5	1394
sample	12089
Concentration of (LNCaP) cell culture extract ng/ml	144.91

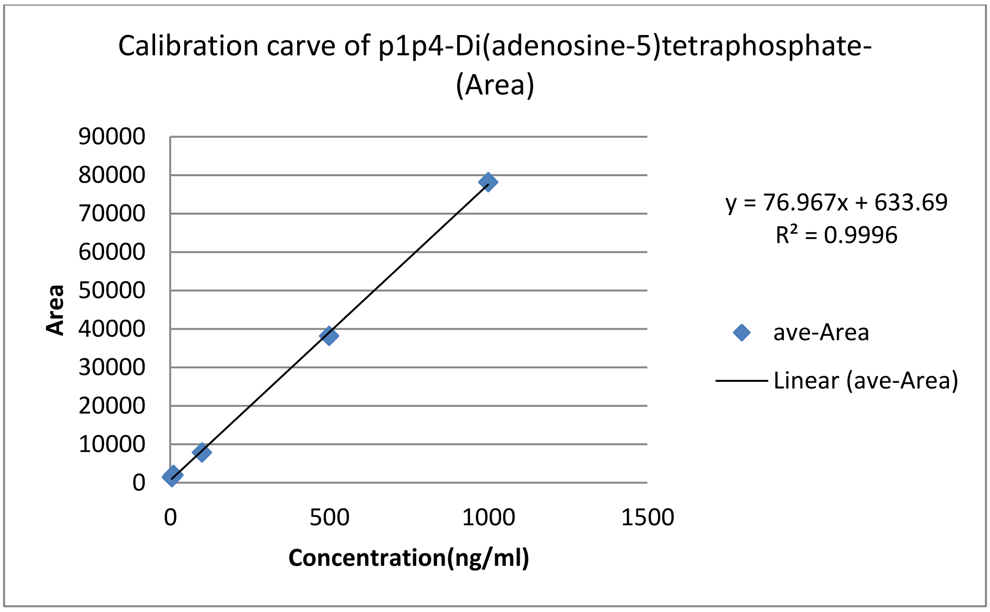

Figure 5.12 Calibration curve for Ap4A in the range 5-1000 ng/ml.

5.4 Discussion:

The extraction of Ap3A and Ap4A from LNCaP cells using the extraction solvent (methanol: acetonitrile: water –all HPLC grade – 50:30:20) gave reproducible results and using ZIC-pHILIC conditions with Tandem Mass Spectrometry provided a powerful technique for the detection of Ap3A, Ap4A.

Previously a HPLC assay for quantifying Ap3A, Ap4A content in human platelets from a 20ml blood sample was developed using an ion-pair reversed phase perfusion chromatography with very long procedure to get the result which was 145.6 ng/ml for Ap3A and 187.18 ng/ml for Ap4A (Jankowski et al., 1999). In 2003 they improved the method using the same extraction procedure but this time with MALDI, they detected 945.5 ng/ml and 752.7 ng/ml for Ap3A and Ap4A respectively (Jankowski et al., 2003).

The FHIT-positive HEK293 cells extract was analyzed using very long extraction procedure which may cause hydrolysis of the Ap3A and Ap4A to ATP. This assay will also measure nucleotides of the form Ap3N and Ap4N where N is any nucleoside that will make interference in the results. This study detected Ap3A as 0.378 ng/10^6 cells and Ap4A as 0.418 ng/10^6 cells (Fisher and McLennan, 2008). Ap3A and Ap4A molecules in HeLa (Human cervical carcinoma) cell lysates quantified in the concentration range of 7564 ng/ml to 75640 ng/ml for Ap3A, and 4181900 ng/ml and 83638000 ng/ml for Ap4A using ToF-SIMS (Shon et al., 2014).

In conclusion, this is a novel method for the quantitative analysis of Ap3A and Ap4A using tandem mass spectrometry. It was more than sensitive enough to monitor these compounds in LNCaP (which appear to contain high levels of these compounds) cells compared to the most published articles. The method could be further optimized to measure even lower levels. Since these compounds are possibly markers for potential for apoptosis they might be very significant for instance in tumour biopsies for determining the potential sensitivity of tumours to chemotherapy.

Chapter 6: Comparison of the analysis of sphingosine using two methods: ZIC-pHILIC with ammonium carbonate mobile phase and a silica column with 20% IPA mobile phase using an Agilent 6460 Triple Quadrupole LC/MS System

Comparison of the analysis of sphingosine using two methods: ZIC-pHILIC with ammonium carbonate mobile phase and a silica column with 20% IPA mobile phase using an Agilent 6460 Triple Quadrupole LC/MS Systems

6.1 Introduction

The biological significance of sphingolipids is reviewed in section 1.4.

The analysis of sphingolipids is not a new approach; it is started long time ago. In 1988, Alfred and his group analyzed sphingosine, sphinganine and phytosphingosine from liver extracts. Reverse-phase high-performance liquid chromatography was used in this study and the extraction solvent was chloroform and methanol. They used C18 columns and isocratic mobile phase (methanol: 5 mM potassium phosphate, pH 7.0 (90:10))(Merrill Jr et al., 1988). A method based on HPLC separation coupled to electrospray ionization tandem mass spectrometry (MS/MS) was used to quantify sphingosine in 2003 by Lieser's research group. The analysis of sphingosine in crude lipid extracts from cells was carried out using a mobile phase of methanol-chloroform (3:1; v/v) containing 0.1% (v) formic acid and a Thermo Hypersil Keystone Beta Basic CYANO, 3µm, 50 ×2 mm column (Lieser et al., 2003). Another study which quantified sphingolipids used a triple quadrupole mass spectrometer operating in a multiple reaction monitoring (MRM) positive ionization mode was based on calibration curves. The cells extracted into a one-phase neutral organic solvent system. A reversed phase column, BDS Hypersil C8, was used in HPLC method (Bielawski et al., 2006). Also a C18 reversed phase column was applied in a liquid chromatography–tandem mass spectrometry (LC–MS/MS) method to quantify the levels of sphingosine and sphingosine- 1-phosphate in biological samples (mouse kidney, human plasma, and HEK 293 cells treated with tumor necrosis factor and N,N-dimethylsphingosine). The mobile phase contained methanol and 0.1% formic acid

(95:5, v/v) (Lan et al., 2011). Most published studies are based on reversed phase chromatography (Scherer et al., 2010) in contrast some studies have used functionalized hydrophilic-interaction chromatography (HILIC) conditions to analyzed sphingolipids in last two years. A silica column was used in one of these studies in combination with liquid chromatography tandem mass spectrometry (LC-MS/MS) to profile sphingolipid species in plasma and in lipoprotein fractions (from tissues or blood cells) (Scherer et al., 2011). A gradient mobile phase was used with silica column and contained water with 0.2% formic acid and 200 mM ammonium formate (A) and acetonitrile with 0.2% formic acid (B) (Scherer et al., 2010). A preanalytical standardization of sphingosine-1-phosphate, sphinganine-1-phosphate and sphingosine analysis used a ZIC-HILIC column for human plasma samples. The samples were mixed with methanol to precipitate protein then injected onto the column couples to a liquid chromatography–tandem mass spectrometry system and eluted with 50 mmol/L ammonium formate in water/formic acid (100/0.2, v/v) (solvent A) and acetonitrile/solvent A/formic acid (95/5/0.2, v/v/v) (solvent B) (Ceglarek et al., 2014). In many cell signaling studies the focus is usually on single components as ceramides or sphingosine 1-phosphate (Sullards and Merrill Jr, 2001). The introduction of liquid chromatography tandem mass spectrometry in conjunction with HILIC conditions has made the analysis easier and the quantitative analysis is carried by using multiple reactions monitoring (MRM) which yields greater sensitivity.

6.2 Materials and Methods

6.2.1 Materials

Quantification of sphingosine was performed using commercial standards. D-Sphingosine, CAS number 123-78-4, SIGMA-ALDRICH, UK. The standard was prepared as stock solution (1mg/ml) by dissolving 1.7mg of sphingosine in 200µl of chloroform then adding 1500µl of methanol. Then the stock solution was diluted with (acetonitrile: water 80:20) to the concentrations 100µg/ml, 10µg/ml, 1µg/ml, 100ng/ml, 10ng/ml, 1ng/ml and 0.1ng/ml.

All solvents and standards were freshly prepared on the same day of the experiment.

6.2.2 LC-MS Analysis

Chromatographic analyses were performed on an Agilent 1200 series ultra-performance liquid chromatography system (Agilent,UK) with a quaternary pump system, a vacuum degasser and a thermostated column compartment.

Separation was carried out using a ZIC®-pHiLIC column, L150 * I.d. 4.6 mm, 5µm, polymeric beads analytical column (HiChrom, Reading, UK) and Guard column: ZIC®-pHILIC Guard PEEK 20 x 2.1 mm (HiChrom, Reading, UK) or an ACE silica gel column (3mm x 150 mm x 3 µm, HiChrom Reading U.K.)

The separation was achieved with a binary mobile phase gradient at a flow rate of 0.2 mL/min for the MS-scan and for MRM for both conditions. The column temperature was kept at room temperature and the injection volume was 10 µL for both conditions. Solvents were (A) 20mM Ammonium carbonate buffer pH 9.2, and (B) acetonitrile for the pHILIC conditions while for the silica gel column the conditions were (A) 20% IPA in 20 mM ammonium formate, and (B) 20 % IPA in acetonitrile . The gradient elution program for MS full scan was as follows:

Time (min)	Mobile phase A%	Mobile phase B%
0	20	80
30	80	20
31	92	8
36	92	8
37	20	80
46	20	80

While for MRM the gradient elution program was:

Time (min)	Mobil phase A%	Mobil phase B%
0	20	80
25	70	30
26	20	80
31	20	80

Identification and quantification of sphingosine compounds were obtained using a 6460 Series Triple Quadrupole LC/MS System equipped with an Electrospray Ionization Source (ESI) and controlled by MassHunter Workstation Software (Agilent, UK). Source working conditions were: capillary voltage 135 V, gas flow rate 3 L/min, gas temperature 300℃ and nebulizer pressure 15 psi. The results were processed by MassHunter Optimizer Software.

Identification and confirmation of Sphingosine compounds MS^2 on the LTQ Orbitrap was carried out by using ACE silica gel column (3mm x 150 mm x 3 μm, HiChrom Reading U.K.). The separation was achieved with a binary mobile phase gradient at a flow rate of

0.3 mL/min for mobile phase (A) 20% IPA in 20 mM ammonium formate, and (B) 20 % IPA in acetonitrile. The gradient elution program was as table above which was used for MS scan.

6.3 Results

6.3.1 Development of a Tandem MS Method for Quantification of Sphingosine Based on a ZIC-pHILIC column

A standard solution containing 10µg/ml of sphingosine was injected in the LC-MS to show a full scan chromatogram and the full scan mass spectra in figure 6.1. The retention times with peak area obtained from this standard solution are recorded in table 6.1.

A MRM method was set up based on the transition from 300 to 282 via the loss of water using collision energy of 25V and argon as the collision gas. The MRM trace obtained for a 1000 ng/ml solution of a standard is shown in figure 6.3 and the peak area is given in table 6.2. Figures 6.4 -6.7 show MRM traces for the range 100-0.1 ng/ml and tables 6.2-6.6 summarise the peak areas obtained. A calibration curve carried out in the range 0.1-1000 ng/ml of sphingosine standards for the method developed on the ZIC-pHILIC column (figure 6.8).

Both the linearity (r^2 = 0.9992) and range are very good. The peak shape of sphingosine is symmetric, sharp and is a high intensity peak. This indicates that the ZIC-pHILIC column has an excellent separation of sphingosine. In addition, sphingosine is eluted after 7 minutes which is a short retention time compared to the silica gel column.

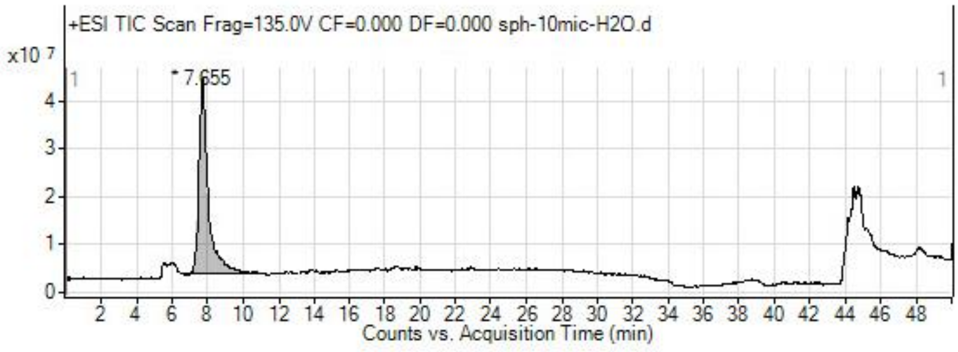

Figure 6.1 Full scan chromatogram of the sphingosine standard 10µg/ml on ZIC-pHILIC with ammonium carbonate/acetonitrile mobile phase.

Table 6.1 Peak area obtained in full scan mode for the sphingosine standard at 10µg/ml.

Peak	RT	Height	Area
1	7.655	40866402.62	1484304126

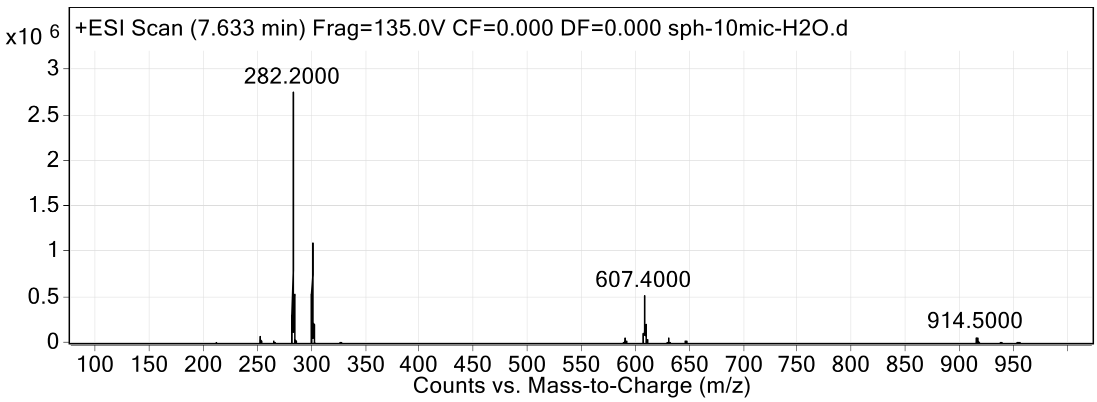

Figure 6.2 Full scan spectrum of sphingosine showing a molecular ion at m/z 300 and loss of water giving an ion at m/z 282.

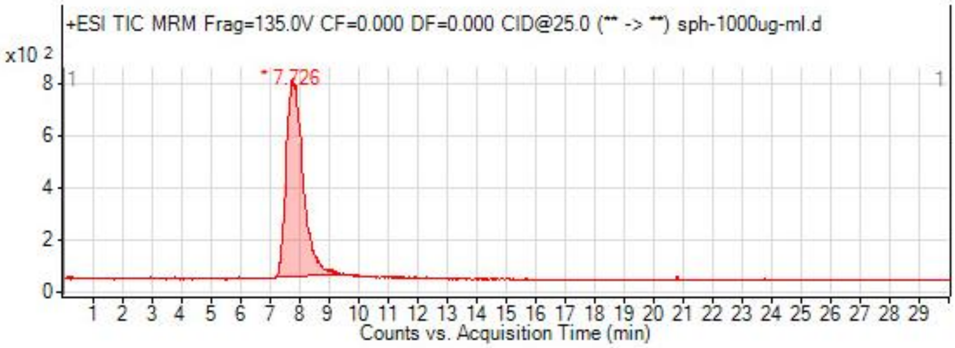

Figure 6.3 MRM trace obtained for sphingosine at 1000 ng/ml monitoring the transition from m/z 300 to m/z 282 with 25V collision energy.

Table 6.2 Peak area obtained in MRM mode for the sphingosine standard at 1000 ng/ml.

Peak	RT	Height	Area	SNR
1	7.726	760	30369	11680

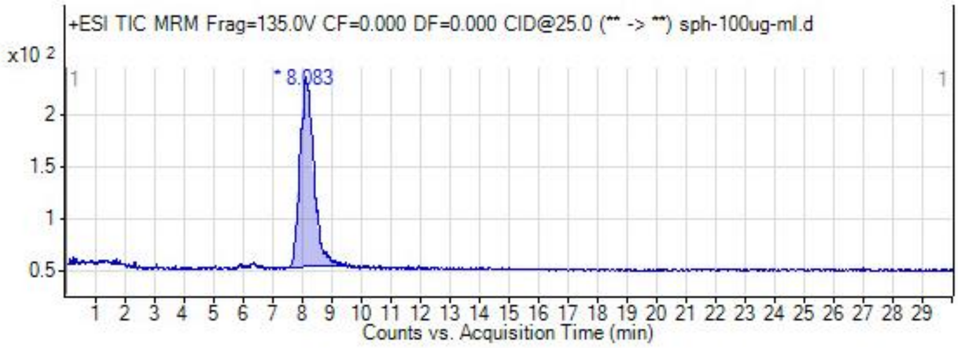

Figure 6.4 MRM trace obtained for sphingosine at 100 ng/ml monitoring the transition from m/z 300 to m/z 282 with 25V collision energy.

Table 6.3 Peak area obtained in MRM mode for the sphingosine standard at 100 ng/ml.

Peak	**RT**	**Height**	**Area**	**SNR**
1	8.083	229	4075	1180

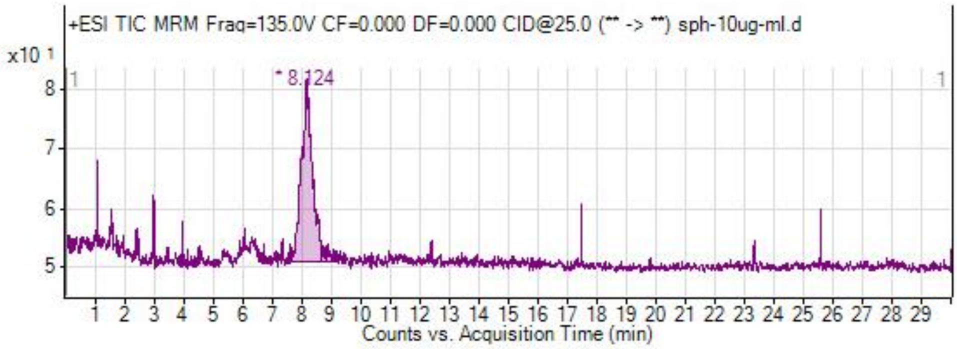

Figure 6.5 MRM trace obtained for sphingosine at 10 ng/ml monitoring the transition from m/z 300 to m/z 282 with 25V collision energy.

Table 6.4 Peak area obtained in MRM mode for the sphingosine standard at 10ng/ml.

Peak	**RT**	**Height**	**Area**	**SNR**
1	8.124	31	843	354

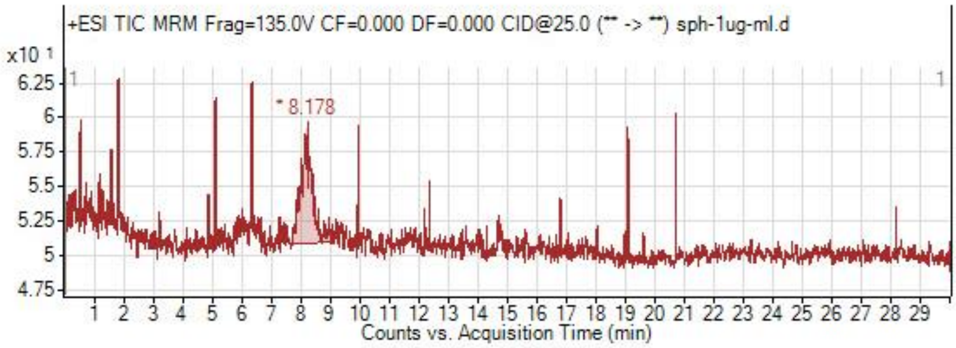

Figure 6.6 MRM trace obtained for sphingosine at 1 ng/ml monitoring the transition from m/z 300 to m/z 282 with 25V collision energy.

Table 6.5 Peak area obtained in MRM mode for the sphingosine standard at 1ng/ml.

Peak	RT	Height	Area	SNR
1	8.178	9	227	90.8

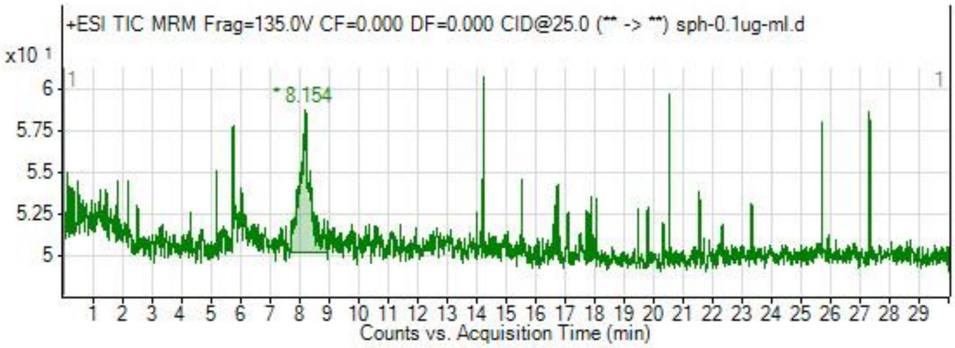

Figure 6.7 MRM trace obtained for sphingosine at 0.1ng/ml monitoring the transition from m/z 300 to m/z 282 with 25V collision energy.

Table 6.6 Peak area obtained in MRM mode for the sphingosine standard at 0.1ng/ml.

Peak	RT	Height	Area	SNR
1	8.154	9	213	67.8

Table 6.7 Summary of peak areas obtained in MRM mode for the sphingosine standards.

Concentration (ng/ml)	Area
1000	30369
100	4075
10	843
1	227
0.1	213

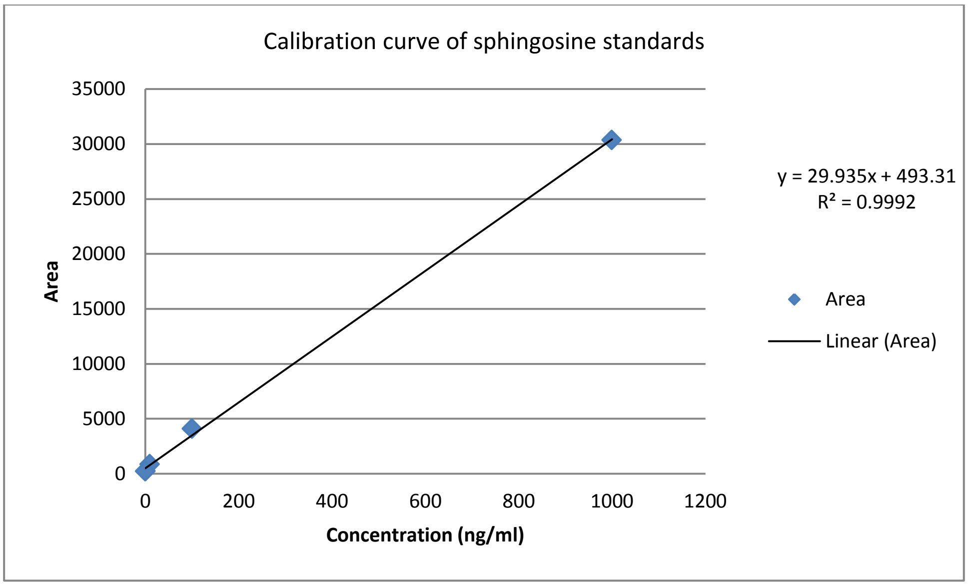

Figure 6.8 Calibration curve obtained for sphingosine standards in the range 0.1-1000 ng/ml.

6.3.2 Development of a Tandem MS Method for Quantification of Sphingosine Based on a silica gel column

An LC-MS method based on HILIC retention on the ACE silica gel column was compared with the ZIC-pHILIC method. Figure 6.9 shows the full scan chromatogram obtained for a 10µg/ml standard analyzed on an ACE silica gel column under the conditions described in section 6.2.2. The peak area is given in table 6.8.

A MRM method was used to quantify sphingosine standards in the range 0.1-1000 ng/ml. The MRM traces obtained are shown in figures 6.10-6.14 and tables 6.9-6.13 show the peak areas data. The peak areas are summarized in table 6.14 and a calibration curve based on the data is shown in figure 6.15.

Both the linearity (r^2 = 1) and range are good. The peak shape of sphingosine is symmetric but is not sharp as under the ZIC-pHILIC conditions and intensity of peak is lower than that in ZIC-pHILIC column at the same concentration. In addition, sphingosine is eluted after 13 minutes which is longer than on ZIC-pHILIC column.

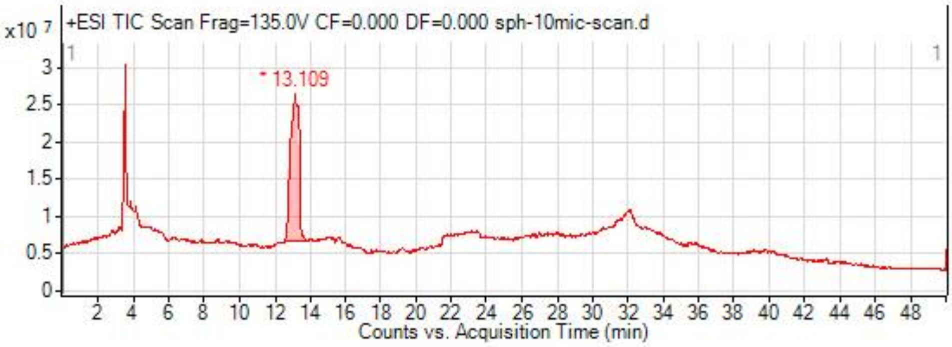

Figure 6.9 Full scan chromatogram of the sphingosine standard 10µg/ml on and ACE silica gel column with ammonium carbonate/acetonitrile mobile phase.

Table 6.8 Peak area obtained in full scan mode for the sphingosine standard at 10 µg/ml.

Peak	RT	Height	Area
1	13.109	19902101.81	677786905.3

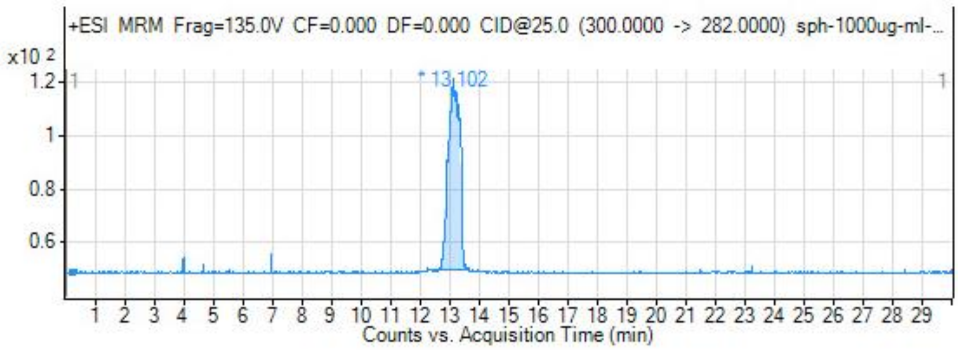

Figure 6.10 MRM trace obtained for sphingosine at 1000 ng/ml monitoring the transition from m/z 300 to m/z 282 with 25 V collision energy using a silica gel column.

Table 6.9 Peak area obtained in MRM mode for the sphingosine standard at 1000 ng/ml.

Peak	RT	Height	Area	SNR
1	13.102	71	1948	3305

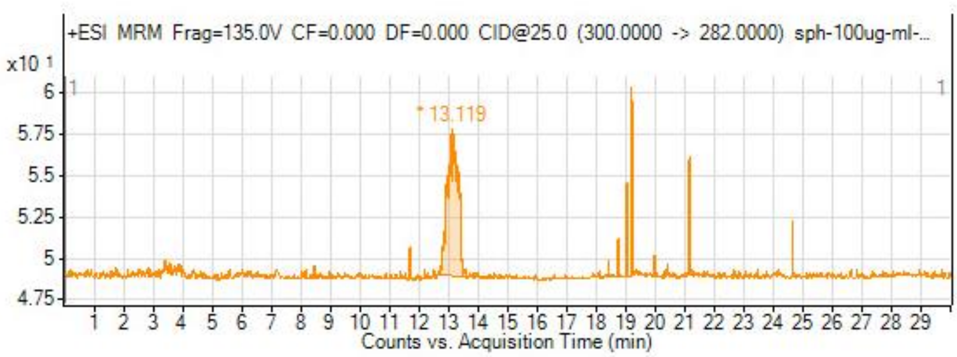

Figure 6.11 MRM trace obtained for sphingosine at 100 ng/ml monitoring the transition from m/z 300 to m/z 282 with 25 V collision energy using a silica gel column.

Table 6.10 Peak area obtained in MRM mode for the sphingosine standard at 100 ng/ml.

Peak	RT	Height	Area	SNR
1	13.119	9	220	1001

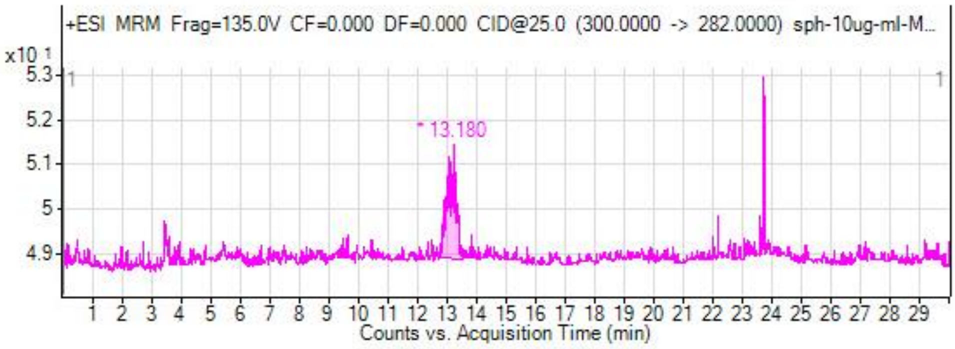

Figure 6.12 MRM trace obtained for sphingosine at 10 ng/ml monitoring the transition from m/z 300 to m/z 282 with 25 V collision energy using a silica gel column.

Table 6.11 Peak area obtained in MRM mode for the sphingosine standard at 10 ng/ml.

Peak	**RT**	**Height**	**Area**	**SNR**
1	13.18	3	49	112

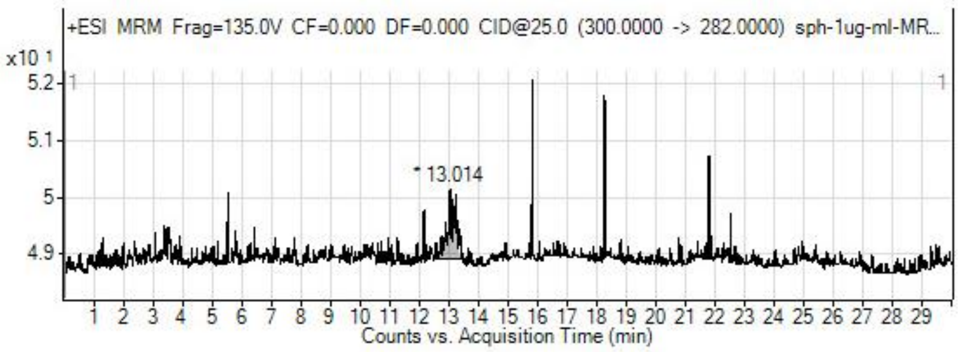

Figure 6.13 MRM trace obtained for sphingosine at 1 ng/ml monitoring the transition from m/z 300 to m/z 282 with 25 V collision energy using a silica gel column.

Table 6.12 Peak area obtained in MRM mode for the sphingosine standard at 1 ng/ml.

Peak	RT	Height	Area	SNR
1	13.014	1	25	103.5

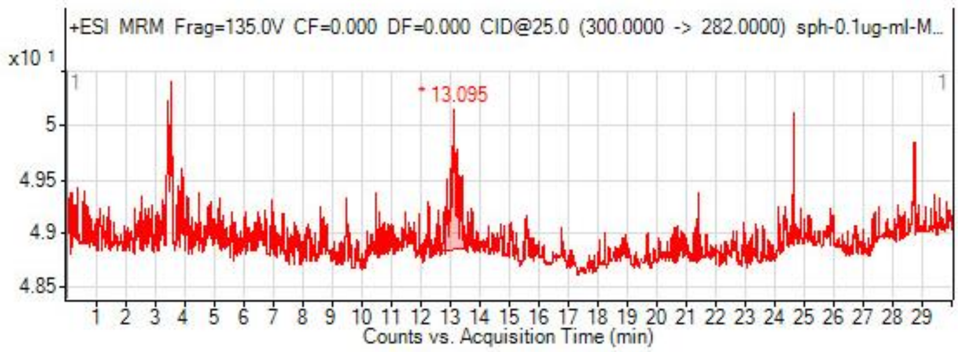

Figure 6.14 MRM trace obtained for sphingosine at 0.1 ng/ml monitoring the transition from m/z 300 to m/z 282 with 25 V collision energy using a silica gel column.

Table 6.13 Peak area obtained in MRM mode for the sphingosine standard at 0.1 ng/ml.

Peak	RT	Height	Area	SNR
1	13.095	1	20	40

Table 6.14 Summary of peak areas obtained in MRM mode for the sphingosine standard analysed on silica gel.

Concentration (ng/ml)	Area
1000	1948
100	220
10	49
1	25
0.1	20

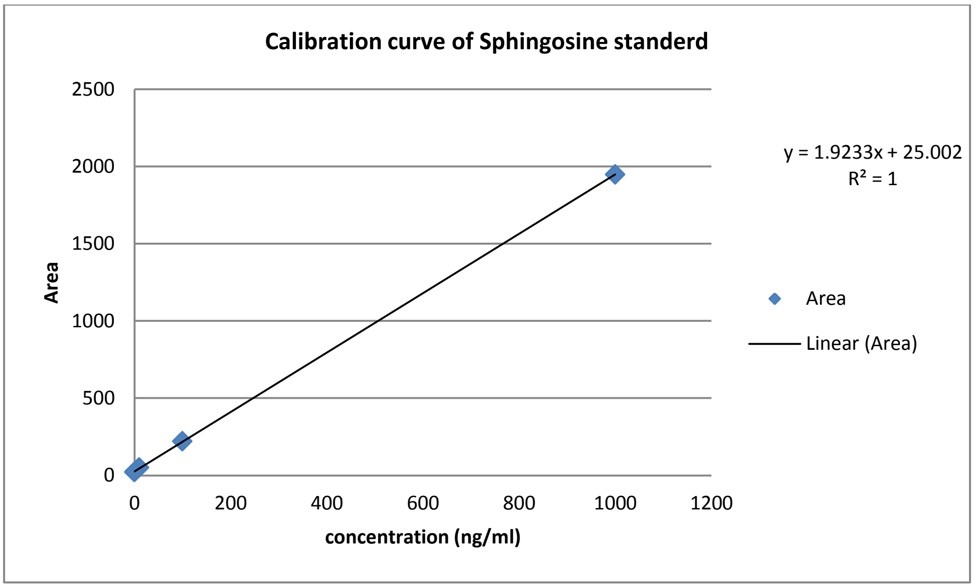

Figure 6.15 Calibration curve obtained from analysis of sphingosine standards on silica gel column 0.1-1000ng/ml.

6.3.3 Identification and confirmation of sphingosine compounds by MS^2 on the LTQ Orbitrap using a Silica gel column with a 20% IPA mobile phase

Although C18 sphingosine is the most commonly monitored sphingosine, it appeared from the general screening methods used in chapter 4 that the LNCaP cultures contained several abundant sphingosine compounds. The method for separating sphingosines based on silica gel chromatography in HILIC mode was used to characterize some of them in extracts from LNCaP cultures combination with MS^2 on the LTQ Orbitrap. Figure 6.16 shows the MS of sphingosine extracted from LNCaP cultures which gave the characteristic loss of water in MS^2 mode shown in figure 6.17.

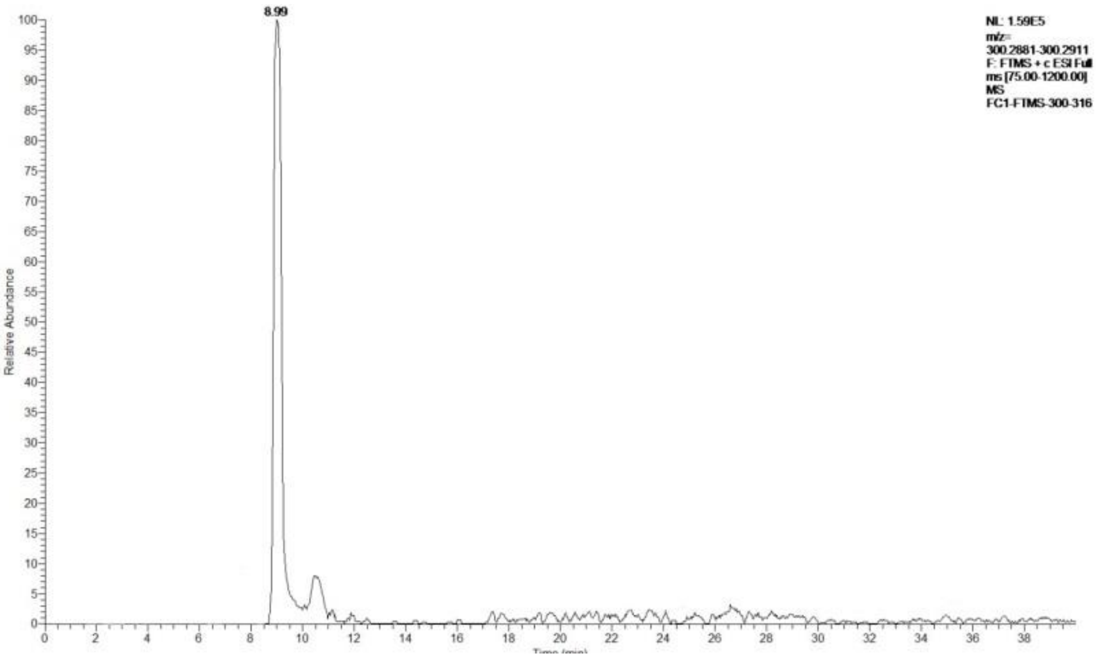

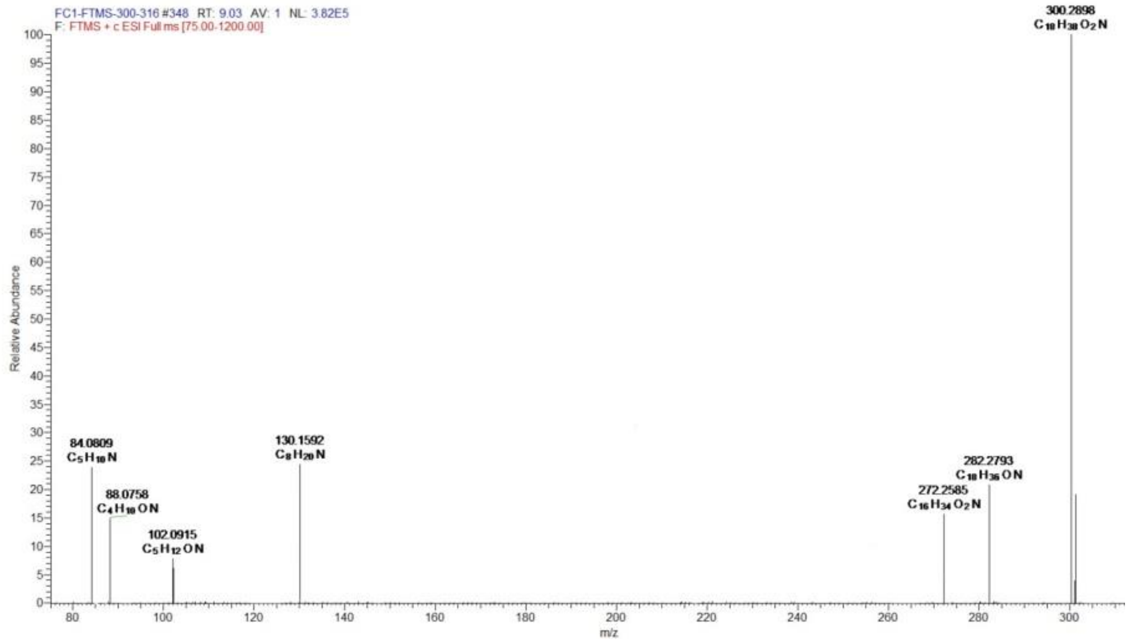

Figure 6.16 Chromatogram and spectrum of C18-Sphingosine extracted from LNCaP cultures analyzed on the LTQ Orbitrap on a silica gel column. Elemental composition $C_{18}H_{38}NO_2$.

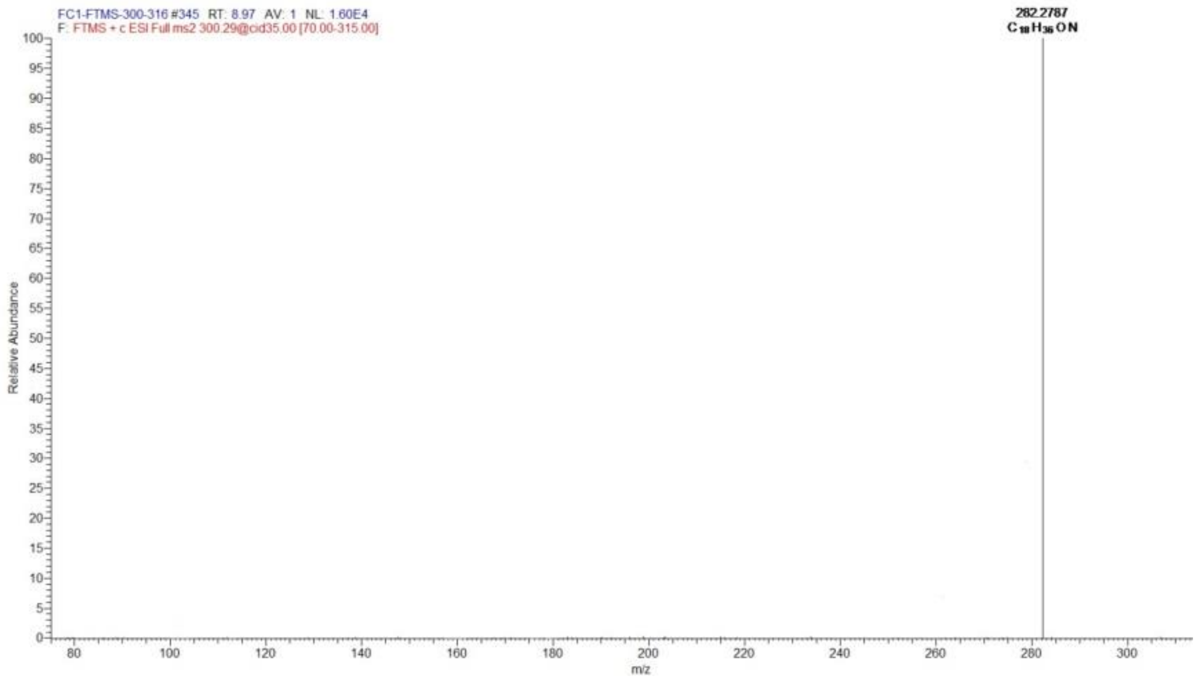

Figure 6.17 MS^2 spectrum of C18-Sphingosine extracted from LNCaP cultures analyzed on the LTQ Orbitrap on a silica gel column in MS^2 mode at 35 V. Elemental composition of fragment ion at 282.2 $C_{18}H_{36}NO$.

Another abundant sphingosine has the formula $C_{17}H_{38}NO_2$ indicating that it was a desmethyl dihydro analogue of sphingosine (Figure 6.18). The MS^2 spectrum also showed the same loss of water as was observed form sphingosine (figure 6.19). In addition it produced a small additional fragment which is typical of the proposed structure (figure 6.20).

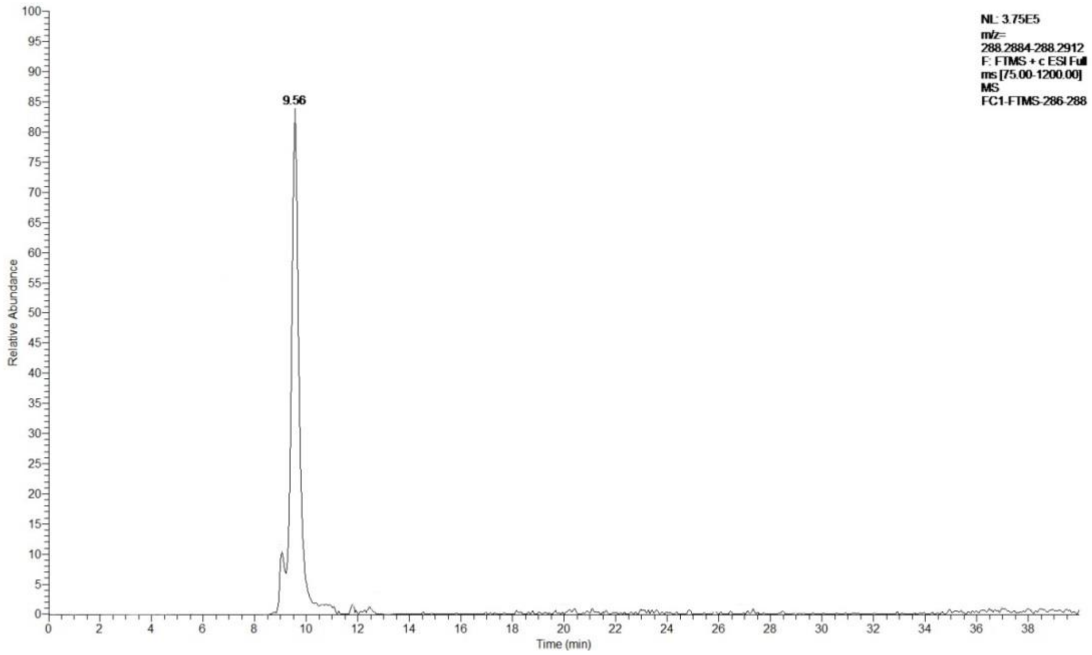

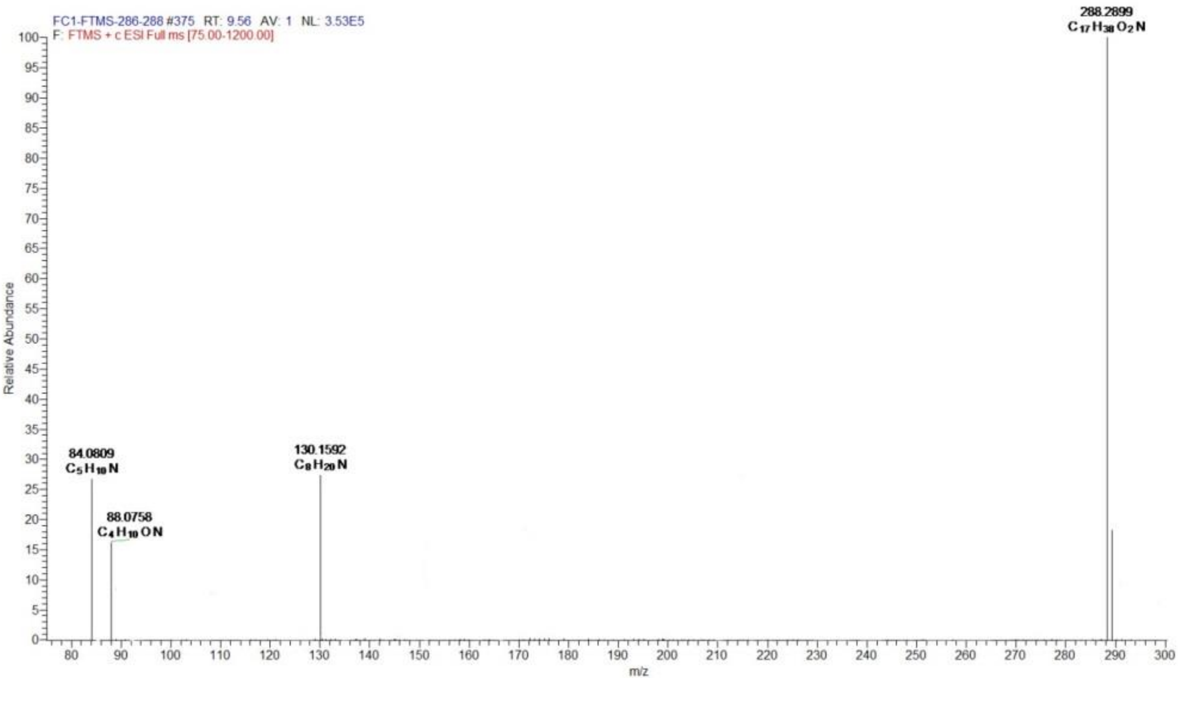

Figure 6.18 Chromatogram and spectrum of C17- Dihydro Sphingosine (Dihydrodesmethyl Sphingosine) extracted from LNCaP cultures analyzed on the LTQ Orbitrap on a silica gel column. Elemental composition $C_{17}H_{38}NO_2$.

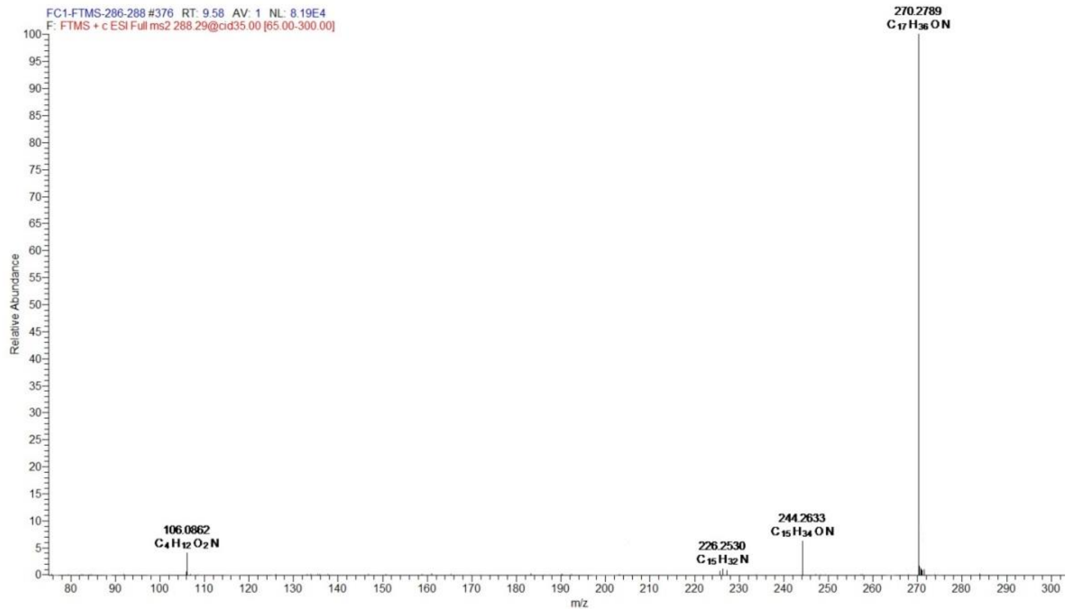

Figure 6.19 MS^2 spectrum of C17- Dihydro sphingosine extracted from LNCaP cultures analyzed on the LTQ Orbitrap on a silica gel column in MS^2 mode at 35 V. Elemental composition of fragment ion at 270.2 $C_{17}H_{36}NO$.

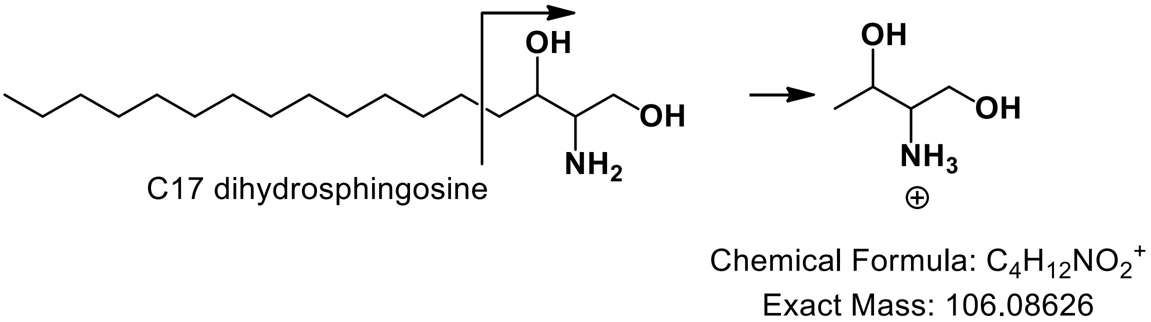

Figure 6.20 Small diagnostic fragment derived from C17-dihydrosphingosine.

Another abundant sphingosine appeared to be a methyl dihydro analogue which has an elemental composition of $C_{19}H_{42}NO_2$ (figure 6.20). The main fragment in MS^2 spectrum resulted from the loss of water (figure 6.21). Table 6.15 summarises the mass spectrometry data.

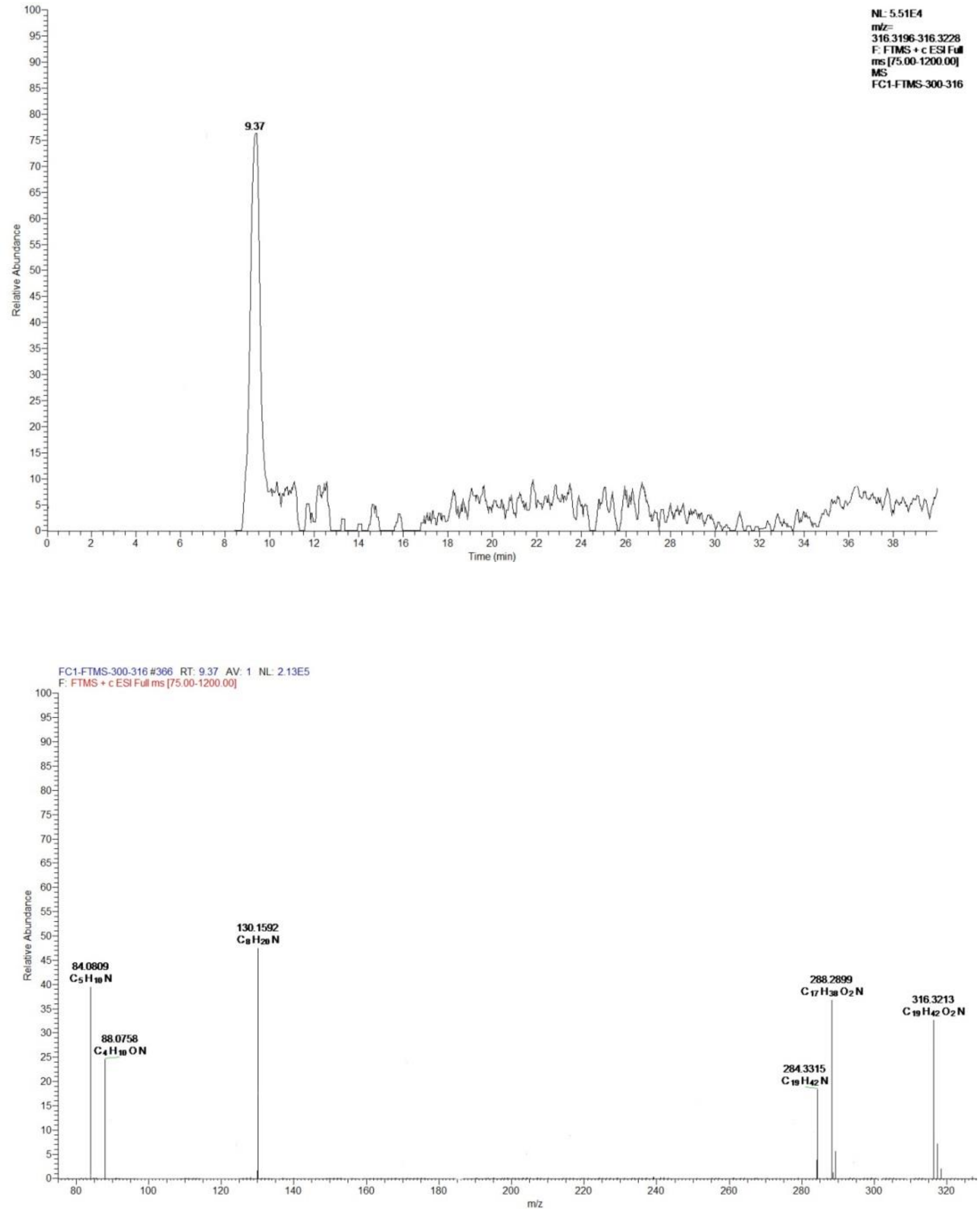

Figure 6.21 Chromatogram and spectrum of C19- Dihydro Sphingosine (Dihydromethyl Sphingosine) extracted from LNCaP cultures analyzed on the LTQ Orbitrap on a silica gel column. Elemental composition $C_{19}H_{42}NO_2$.

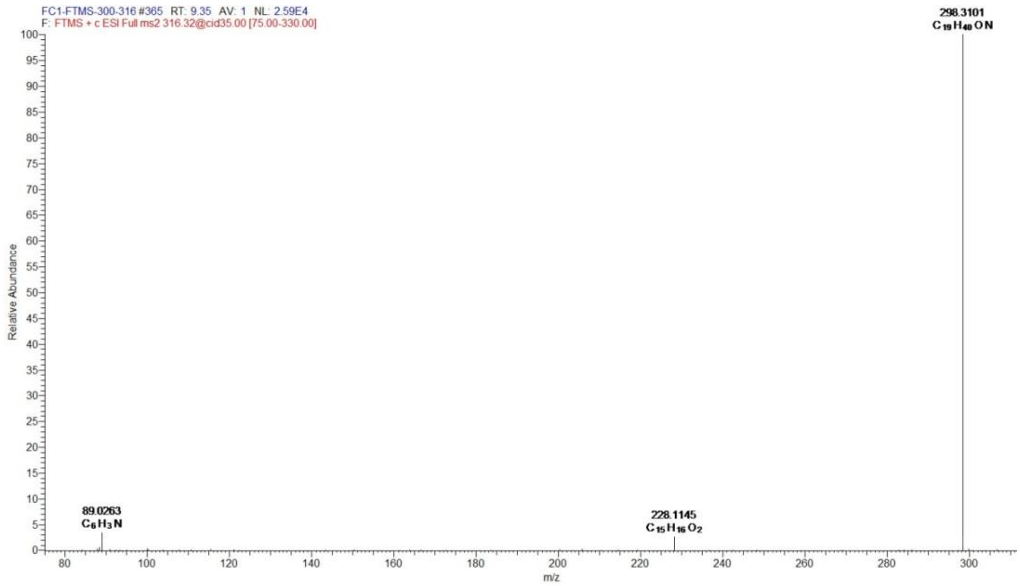

Figure 6.22 MS^2 spectrum of C19- Dihydro sphingosine extracted from LNCaP cultures analyzed on the LTQ Orbitrap on a silica gel column in MS^2 mode at 35 V. Elemental composition of fragment ion at 298.3 $C_{19}H_{40}NO$.

Table 6.15 Summary of mass spectrometry data for sphingosines extracted from LNCaP cultures.

Metabolite	**Retention time (minutes)**	**Molecular Ion**	**Fragments**
Dihydrodesmethyl Sphingosine (C17-Sphingosine)	9.56	288.2899	270.2789 (100% -H_2O), 244.2633 (10% -H_2O,CH_3), 226.2530 (2% -2.H_2O, 2.CH_3), 106.0862 (5% -$C_{13}H_{27}$)
C18-Sphingosine	8.99	300.2898	282.2787 (100% -H_2O)
Dihydromethyl Sphingosine (C19-Sphingosine)	9.37	316.3216	298.3101 (100% -H2O)

6.4 Discussion:

An explosion in bioactive sphingolipids research has occurred recently as the importance of ceramide, sphingosine and sphingosine 1-phosphate in biological systems is recognised. This has led to the development of accurate and user-friendly methods to quantify the levels of these molecules. Liquid chromatography tandem mass spectrometry ESI/MS/MS method provides qualitative analysis which is performed by a Parent Ion scan of a common fragment ion as well as quantitative analysis by multiple reactions monitoring (MRM). MRM is a robust device for increasing the efficiency and accuracy of quantitative MS/MS analyses. The first mass analyzer is set to pass a specific precursor ion m/z, and the second mass analyzer is set to pass a specific product ion m/z, thus only ions that match both precursor and product ion m/z together will be transmitted to the detector.

In contrast to most published methods based on reversed phase chromatography (Merrill Jr et al., 1988, Lieser et al., 2003, Bielawski et al., 2006, Lan et al., 2011), we developed hydrophilic interaction liquid chromatography tandem mass spectrometry (HILIC–ESI/MS/MS) methods for the specific and sensitive analysis of sphingosine which achieved good peak shapes and reasonable analysis time. The method used silica column with 20% IPA in 20 mM ammonium formate, and 20 % IPA in acetonitrile which was used to characterized sphingosine compounds (C17- sphingosine, C18- sphingosine, C19-sphingosine). Two other studies using silica column in LC-MS/MS where the eluent was water with 0.2% formic acid and 200 mM ammonium formate (A) and acetonitrile with 0.2% formic acid (B) have been published on the analysis of plasma lipid species and cultured cells (Scherer et al., 2011, Scherer et al., 2010) however, they did not separate these sphingosine compounds. Another study used a ZIC-HILIC column and a mobile phase of 50 mmol/L ammonium formate/formic acid (100/0.2) (A) and acetonitrile/eluent

A/formic acid (95/ 5/0.2) (B) on EDTA-plasma was published after our work was done. Using of a zwitterionic stationary phase because its ability to elute the analytes with their respective internal standards C17- sphingosine which is shorter than sphingosine by one methylene group (Ceglarek et al., 2014). In their method the sphingosine appeared at 2.8 min while in ZIC-pHILIC sphingosine is detected at 7 minutes because they used 500 µl/min of flow rate which is more than double the flow rate used in ZIC-pHILIC method in section 6.2.2. Also the lowest level detected in ZIC-HILIC published work was 0.5ng/ml for sphingosine but with our current ZIC-pHILIC method 0.1ng/ml was detected and less than this concentration could be detected due to high intensity of 0.1 ng/ml peak.

When compared the detection and separation of sphingosine, which is an 18-carbon amino alcohol with an unsaturated hydrocarbon chain, by two methods of HILIC-tandem mass spectrometry (HILIC–ESI/MS/MS) on a silica gel column and on a ZIC-pHILIC column some differences were observed. Both of the HILIC methods produced a good peak shape with excellent linearity and a correlation coefficient of more than 0.999. The separation in HILIC is completed by partitioning of solutes from the eluent into a hydrophilic environment. That make both hydrogen bonding (depends on the acidity or basicity of the solutes) and dipole-dipole interactions (depend on the dipole moments and polarity of the solutes) are factors leading retention. The active layer in zwitterionic sulfoalkylbetaine stationary phase is wide-pore polymer support containing both strongly acidic sulfonic acid groups and strongly basic quaternary ammonium groups separated by a short alkyl spacer so its retention will also be affected by electrostatic interactions (Buszewski and Noga, 2012). These explain high intensity sharp peak of sphingosine on the ZIC-pHILIC column combined with 20mM ammonium carbonate pH 9.2 and acetonitrile as mobile phase because the high pH makes reduces the ionization of the amine group thus weakening electrostatic interactions. The late elution of sphingosine from silica gel may be due to adding isopropanol to solvent A and B in the silica gel conditions which makes the mobile phase more viscous and less polar (Carr, 2002) than in the ZIC-pHILIC conditions . The lower intensity peak detected under the conditions used to elute the silica gel column in comparison with ZIC-pHILIC may be due to the isopropanol viscosity which makes the spray droplet less and heavier than in ZIC-pHILIC conditions making ionization less efficient and the method less sensitive (Garcia, 2005).

In conclusion, the performance of the silica gel method was comparable to that developed on the ZIC-pHILIC column and thus can provide a comparable method on a much cheaper column for the analysis of concentrations above 0.1 ng/ml.

C18 sphingosine is the most commonly analyzed sphingosine and as mention in section 6.1 and 1.3 there are diverse methods for monitoring this compound. Also C17 sphingosine (Dihydrodesmethyl Sphingosine) is usually used as internal standard in case of analyzing C18 sphingosine. However, in this study C19 sphingosine (Dihydromethyl Sphingosine) was detected and identified for first time. Moreover there is no study whch separates all of these sphingosine compounds. This study characterize them in LNCaP culture extracts using a silica gel column combined with MS^2 on the LTQ Orbitrap which gave the characteristic loss of water. This identification and confirmation of sphingosine compounds study will help researchers to differentiate between biological active sphingosine and its analogues in biological samples so there is no confusion in the monitoring C18 sphingosine.

Chapter 7: Summary and future work

Summary

7.1 Column Selection and Method optimization:

Although the Exactive (Orbitrap) mass spectrometer is an important tool in sample analysis, the other aim was to improve chromatographic selection and sample treatment. LNCaP cell lines could provide a background for a genetic screen to identify development of disease and therapy which is much less expensive than working with mice or humans. Working in LNCaP cell could allow us to build systems biology metabolic models that could predict the impact of prostate cancer causes and predict their possible therapies. It was clear that the best performance is produced on the ZIC-pHILIC column after the comparison between the five columns (ZIC-HILIC, ZIC-pHILIC, BEH amide, silica C, C18). In addition, this method covers large number of polar metabolites. It is thus suitable to apply to the study of the metabolomics of a prostate cancer cell line LNCaP as a result of good linearity, LOD, extraction stability and repeatability. Zhang et al compared three columns (Reversed Phase, Aqueous Normal Phase and Hydrophilic Interaction Liquid Chromatography) for testing polar compounds of urine samples. They found that ZIC-pHILIC column was very useful for extending the coverage of polar metabolites in human urine (Zhang et al., 2012).

7.2 The Effect of Sphingosine Kinase Inhibitors on the Metabolome of LNCaP Cells:

An effective ZIC-pHILIC chromatographic separation method was applied on LNCaP cells treated with three sphingosine inhibitors (2-(p-hydroxyanilino)- 4-(p-chlorophenyl)thiazole (Ski), (R)-FTY720 methyl ether (ROME) and (S)-FTY70 vinylphosphonate). A large number of polar metabolites were changed in response to treatment. Moreover, some lipids were separated well using these chromatographic conditions. The treatment of LNCaP cells with Ski modulated the metabolome, with marked changes in glutathione, NADPH, pentose phosphate shunt and glycolytic metabolite levels these indicative of a pronounced oxidative stress response and modulation in the Warburg effect. Surprisingly, Over-expression of FLAG-SK1b appears to induce a more severe oxidative stress and antagonism of the Warburg effect in response to Ski. On the other hand, NAC rescued AR expression and inhibited the increase of oxidative stress levels in response to Ski, thus confirming that the oxidative stress response to Ski is abrogated by this compound. In addition, the effects of Ski on the androgen dependent and androgen independent cells were broadly similar in terms of metabolomic responses. However, diadenosine triphosphate is highly elevated in LNCaP while it was not detected in LNCaP-AI.

A comparison between the results of 2-(p-hydroxyanilino)- 4-(p-chlorophenyl)thiazole (Ski) and (R)-FTY720 methyl ether (ROME) was used to discriminate between the effects of SK1- vs. SK2-selective inhibitors, ROME showed no effect on oxidative stress or the pentose phosphate pathway also not antagonize Warburg effect but increased in the levels of several lysophosphatidylinositols (Lyso PI).

(S)-FTY70 vinylphosphonate did not induce changes in the metabolome that would indicate oxidative stress or antagonism of the Warburg effect. However, many change in metabolites which indicate apoptosis such as increase in phosphatidylserine (PS), Sphingosine and sphinganine, hydroxysphingosine and hydroxysphinganine. In addition, (S)-FTY720 Vinylphosphonate a selective inhibitor of SK1 and that might be upregulate miR1 and miR133a in LNCap cells then downregulation of PNP was induced and inhibit the conversion of inosine, guanosine and deoxyuridine to hypoxanthine, guanine and uridine respectively.

So, SK1 can regulate aerobic glycolysis, Ap3A formation, and apoptosis of androgen-sensitive LNCaP cells, while SK2 might functionally regulate lyso-PI and LPA metabolism possibly linked with mitogenesis. This factor is therefore worthy of further study in terms of improving our understanding of how these enzymes are involved in controlling apoptosis of prostate cancer cells.

7.3 Using Tandem Mass Spectrometry to Identify and Quantify Some Metabolomes in LNCaP Cells:

C18 sphingosine is the most commonly analyzed sphingosine. Also C17 sphingosine (Dihydrodesmethyl Sphingosine) is usually used as internal standard in case of analyzing C18 sphingosine. However, in this study C19 sphingosine (Dihydromethyl Sphingosine) was detected and identified for first time. Moreover there is no study separate all of these sphingosine compounds. In our study we characterize them in LNCaP culture extracts using a silica gel column combined with MS^2 on the LTQ Orbitrap which gave the characteristic loss of water. This identification and confirmation of sphingosine compounds study will help researchers to differentiate between biological active sphingosine and its analogues in biological samples.

A novel method for the quantitative analysis of Ap3A and Ap4A using tandem mass spectrometry, it was done and it was more than sensitive enough to monitor these compounds in LNCaP cells compared to the most published articles (Shon et al., 2014), (Fisher and McLennan, 2008). Since these compounds are possibly markers for potential for apoptosis they might be very significant for instance in tumour biopsies for determining the potential sensitivity of tumours to chemotherapy.

Future work

- The validation of the extraction and quenching method for LNCaP cell cultures will allow this method to be extended and applied to other cell culture models.
- It was found that the formation of Ap3A from ATP, ADP, and tryptophan is catalysed by the enzyme tryptophanyl-tRNA synthetase (Vartanian et al., 1997). Further research is required to determine whether the inhibition of SK1 leads to the activation of tryptophanyl-tRNA synthetase-catalysed formation of Ap3A or the inhibition of FHIT Ap3A hydrolase activity.
- In the LNCaP cells where there was overexpression SK1b, it would be of interest to determine whether or not the elevation in sphingolipids is responsible for the enhanced oxidative stress in LNCaP-SK1b cells in response to Ski or not.
- Application of the method which was developed on Triple Quadrupole LC/MS tandem mass system for quantification of sphingosine C17 and sphingosine C19 in LNCaP cell extract could be applied quantify these sphingosines cells treated with drugs affecting sphingosine kinase.
- The metabolome of LNCaP cells could be labelled with ^{13}C-glucose in order to get a picture of the dynamic response of the metabolome to treatment with Ski.

Appendices

Table A1: Comparison of the retention times of the metabolites found in the LNCaP cells with the retention times of authentic standards for a range of different metabolite types.

Compound Name	Formula	Polarity	Standard	Actual RT	Sample	Actual RT	Detection conditions
Adenosine	C10H13N5O4	+	37460667	8.5	5134	9.0	pHILIC
AMP	C10H14N5O7P	-	5614542	13.2	37743	13.40	pHILIC& ZIC-HILIC
GMP	C10H14N5O8P	-	38433	16.2	8861	16.40	pHILIC& ZIC-HILIC
ATP	C10H16N5O13P 3	-	*	*	830021	16.27	pHILIC
GTP	C10H16N5O14P 3	-	*	*	19044	19.09	pHILIC
5'-Methylthioadenosine	C11H15N5O3S	+	51131989	7.6	834285	7.58	pHILIC
10-Phenanthroline	C12H8N2	+	*	*	*	*	*
Beta-Alanine	C3H7NO2	+	51151396	15.00	3457528	14.76	pHILIC
Allantoin	C4H6N4O3	-	5906555	13.4	8911	13.6	pHILIC& ZIC-HILIC
(R)-Malate	C4H6O5	-	55474755	15.6	8291365	15.8	pHILIC& ZIC-HILIC
β-alanine-methyl-ester	C4H9NO2	+	2668593	14.5	716483	15.00	ZIC-HILIC
Betaine	C5H11NO2	+	238684106	11.00	1144163 3	11.11	pHILIC& ZIC-HILIC
2-Oxoglutarate	C5H6O5	-	20433876	15.16	1314987	15.12	pHILIC
5-Oxoproline	C5H7NO3	-	52713543	10.54	2933565	10.31	pHILIC& ZIC-HILIC
Citramalate	C5H8O5	-	141448171	14.8	354280	15.00	pHILIC
5-Aminolevulinate	C5H9NO3	+	41947443	13.05	4152686	13.30	pHILIC
Cis-Aconitate	C6H6O6	-	18294838	17.98	253823	18.30	pHILIC& ZIC-HILIC
Benzenesulfonate	C6H6O3S	-	105798785	7.58	9744	7.52	pHILIC& ZIC-HILIC
AcetylCholine	C7H15NO2	+	26653870	14.7	640833	14.21	pHILIC& ZIC-HILIC

2-Indolecarboxylicacid	C9H7NO2	-	124549142	7.18	11703	6.96	pHILIC
4-Coumarate	C9H8O3	-	16941272	8.40	9376	8.70	pHILIC
glutethimide	C13H15NO2	+	75330	4.55	*	*	pHILIC
Glycine	C2H5NO2	+	694878	15.19	264417	15.2	pHILIC& ZIC-HILIC
Ethanolamine phosphate	C2H8NO4P	-	5486783	18.77	12162	18.52	pHILIC& ZIC-HILIC
Fumarate	C4H4O4	-	18233297	15.90	459386	15.80	pHILIC& ZIC-HILIC
L-Aspartate	C4H7NO4	-	5349762	14.89	96528	14.86	pHILIC& ZIC-HILIC
2-Hydroxybutanoic acid	C4H8O3	-	2915496	7.49	119536	7.54	pHILIC& ZIC-HILIC
Creatine	C4H9N3O2	+	213556896	14.08	5284533 3	14.02	pHILIC& ZIC-HILIC
L-Glutamine	C5H10N2O3	-	39827	14.52	515645	14.62	pHILIC& ZIC-HILIC
Itaconate	C5H6O4	-	31724756	15.00	52395	14.56	pHILIC& ZIC-HILIC
Cis-4-Hydroxy-D-Proline	C5H9NO3	+	40672522	14.5	4152686	14.32	pHILIC& ZIC-HILIC
D-Gluconic acid	C6H12O7	-	2103050	12.8	35186	13.08	pHILIC
D-Glucose 6-phosphate	C6H13O9P	-	2398680	16.5	21283	16.6	pHILIC& ZIC-HILIC
L-Arginine	C6H14N4O2	+	6956487	24.45	1074221	24.51	pHILIC& ZIC-HILIC
Isocitrate	C6H8O7	-	4483701	18.1	897233	17.98	pHILIC
Cystathionine	C7H14N2O4S	-	5475621	16.13	16810	16.29	pHILIC& ZIC-HILIC
4-Hydroxyphenylacetald oxime	C8H9NO2	+	1217014	7.63	28729	7.58	pHILIC& ZIC-HILIC
O-Acetylcarnitine	C9H17NO4	+	391533586	10.3	8103325	10.62	pHILIC& ZIC-HILIC
Pantothenate	C9H17NO5	-	52434675	8.49	249026	8.36	pHILIC& ZIC-HILIC
L-Tryptophan	C11H12N2O2	+	21650320	11.33	52509	11.28	pHILIC& ZIC-HILIC
Maltose	C12H22O11	-	745094	15.5	10014	15.54	pHILIC
Oxalate	C2H2O4	-	2125351	17.22	108660	17.35	pHILIC& ZIC-HILIC
Putrescine	C4H12N2	+	*	*	*	*	pHILIC&

								ZIC-HILIC
Pyruvate	C3H4O3	-	21355414	16.39	94007	16.46	pHILIC
Malonate	C3H4O4	-	69213195	15.26	104795	15.36	pHILIC
L-Serine	C3H7NO3	-	2527502	15.06	1657161	15.10	pHILIC& ZIC-HILIC
Methylmalonate	C4H6O4	-	112330425	14.52	254813	14.66	pHILIC& ZIC-HILIC
DL-3-aminobutyrate	C4H9NO2	+	93667365	13.48	716483	13.55	pHILIC& ZIC-HILIC
L-Homoserine	C4H9NO3	+	26526066	14.4	1027016	14.34	pHILIC& ZIC-HILIC
L-Valine	C5H11NO2	+	74018165	11.93	1144163 3	11.91	pHILIC& ZIC-HILIC
L-Methionine	C5H11NO2S	+	35853854	11.02	742117	11.11	pHILIC& ZIC-HILIC
L-Ornithine	C5H12N2O2	+	2172367	22.1	416154	22.03	pHILIC& ZIC-HILIC
Mesaconate	C5H6O4	-	11637669	15.2	52395	14.79	pHILIC
L-Proline	C5H9NO2	+	154851281	12.3	7108018 4	12.4	pHILIC& ZIC-HILIC
L-isoleucine	C6H13NO2	+	67631253	10.55	3151329	10.7	pHILIC& ZIC-HILIC
L-Lysine	C6H14N2O2	+	2975263	23.26	77434	23.3	pHILIC& ZIC-HILIC
Nicotinate	C6H5NO2	+	31483285	7.96	12432	7.94	pHILIC
L-Histidine	C6H9N3O2	+	10972236	25.5	636859	25.5	ZIC-HILIC
N-Acetyl-L-aspartate	C6H9NO5	-	48052432	14.61	9069958	14.54	pHILIC& ZIC-HILIC
N(pi)-Methyl-L-histidine	C7H11N3O2	+	16059578	12.08	8696	12.17	pHILIC
Pyridoxamine	C8H12N2O2	+	3636957	26.7	6144	26.67	HILIC
N-Acetyl-D-glucosamine 6-phosphate	C8H16NO9P	-	2808797	15.5	7011	15.62	pHILIC& ZIC-HILIC
Phthalate	C8H6O4	-	19846	13.1	9715	13.44	pHILIC
L-Phenylalanine	C9H11NO2	+	73735185	9.47	669132	9.60	pHILIC& ZIC-HILIC
Citraconate	C5H6O4	-	1918471	7.97	39426	7.98	ZIC-HILIC
4-hydroxylphenylacetate	C8H7O3	+	61311	8.48	81608	8.53	pHILIC
Amphetamine	C9H13N	+	246892836	12.42	*	*	ZIC-HILIC

Glutathione	C10H17N3O6S	-	28566	14.54	29745909	14.67	ZIC-HILIC
Homoserine lactone	C4H7NO2	+	11761324	17.67	1581992	17.59	ZIC-HILIC
Hypoxanthine	C5H4N4O	+	142139950	9.90	4951	9.81	pHILIC
D-Isoascorbic acid	C6H8O6	-	673675	6.01	58679	6.39	pHILIC
Maleic acid	C4H4O4	-	66240568	12.5	200527	12.6	pHILIC
Alloxanthine	C5H4N4O2	-	19106457	10.18	7439	10.2	pHILIC
L-Tyrosine	C9H11NO3	+	77305702	5.48	1156386	5.42	ZIC-HILIC
L-Threonine	C4H9NO3	-	13.8	12298431	14.0	437222	pHILIC& ZIC-HILIC
Succinate	C4H6O4	-	14.5	21598607	14.6	643564	pHILIC
Taurine	C2H7NO3S	-	14.19	17674268	14.27	785462	pHILIC
trans-4-Hydroxy-L-proline	C5H9NO3	+	14.0	55953980	14.10	4699879	pHILIC
Triethanolamine	C6H15NO3	+	8.66	1.29E+08	8.55	23572	pHILIC
Imidazole-4-acetate	C5H6N2O2	-	7.37	8051465	7.35	14312	pHILIC
L-Leucine	C6H13NO2	-	10.21	18071968	10.26	810859	pHILIC
Sarcosine	C3H7NO2	-	13.52	12139865	13.61	1975762	pHILIC
Sucrose	C12H22O11	-	15.61	21197	15.3	9975	pHILIC
Xanthine	C5H4N4O2	-	11.12	11170	11.16	12387	pHILIC
DL-Glyceraldehyde 3-phosphate	C3H7O6P	-	389065	16.15	26005	16.16	pHILIC
S-Lactoylglutathione	C13H21N3O8S	+	2624354	12.8	3460	12.53	pHILIC& ZIC-HILIC
D(+)2-Phosphoglyceric acid	C3H7O7P	-	3524828	17.18	12325	17.31	pHILIC
Dihydroxy acetonephosphate	C3H7O6P	-	2837780	15.38	98906	15.46	pHILIC

References

American Cancer Society. Cancer Facts & Figures 2011. Atlanta: American Cancer Society; 2011.

Anavi-Goffer, S., Baillie, G., Irving, A. J., Gertsch, J., Greig, I. R., Pertwee, R. G. & Ross, R. A. 2012. Modulation of L-α-lysophosphatidylinositol/GPR55 mitogen-activated protein kinase (MAPK) signaling by cannabinoids. *Journal of Biological Chemistry,* 287**,** 91-104.

Apakama, I., Robinson, M., Walter, N., Charlton, R., Royds, J., Fuller, C., Neal, D. & Hamdy, F. 1996. bcl-2 overexpression combined with p53 protein accumulation correlates with hormone-refractory prostate cancer. *British journal of cancer,* 74**,** 1258.

Bathen, T. F., Jensen, L. R., Sitter, B., FJÖSNE, H. E., Halgunset, J., Axelson, D. E., Gribbestad, I. S. & Lundgren, S. 2007. MR-determined metabolic phenotype of breast cancer in prediction of lymphatic spread, grade, and hormone status. *Breast cancer research and treatment,* 104**,** 181-189.

Bawazeer, S., Sutcliffe, O. B., Euerby, M. R., Bawazeer, S. & Watson, D. G. 2012. A comparison of the chromatographic properties of silica gel and silicon hydride modified silica gels. *Journal of Chromatography A,* 1263**,** 61-67.

Ben-Shlomo, Y., Evans, S., Ibrahim, F., Patel, B., Anson, K., Chinegwundoh, F., Corbishley, C., Dorling, D., Thomas, B. & Gillatt, D. 2008. The risk of prostate cancer amongst black men in the United Kingdom: the PROCESS cohort study. *European Urology,* 53**,** 99-105.

Benevenga, N. J. & Blemings, K. P. 2007. Unique aspects of lysine nutrition and metabolism. *The Journal of nutrition,* 137**,** 1610S-1615S.

Bielawski, J., Szulc, Z. M., Hannun, Y. A. & Bielawska, A. 2006. Simultaneous quantitative analysis of bioactive sphingolipids by high-performance liquid chromatography-tandem mass spectrometry. *Methods,* 39**,** 82-91.

Burton, A. J., Tilling, K. M., Holly, J. M., Hamdy, F. C., Rowlands, M.-A. E., Donovan, J. L. & Martin, R. M. 2010. Metabolic imbalance and prostate cancer progression. *International journal of molecular epidemiology and genetics,* 1**,** 248.

Buszewski, B. & Nona, S. 2012. Hydrophilic interaction liquid chromatography (HILIC)—a powerful separation technique. *Analytical and bioanalytical chemistry,* 402**,** 231-247.

Carr, D. 2002. The handbook of analysis and purification of peptides and proteins by reversed-phase HPLC. *Hesperia, CA, USA: Grace Vydac*.

Ceglarek, U., Dittrich, J., Helmschrodt, C., Wagner, K., Nofer, J.-R., Thiery, J. & Becker, S. 2014. Preanalytical standardization of sphingosine-1-phosphate, sphinganine-1-phosphate and sphingosine analysis in human plasma by liquid chromatography–tandem mass spectrometry. *Clinica Chimica Acta,* 435**,** 1-6.

Cheng, L. L., Burns, M. A., Taylor, J. L., HE, W., Halpern, E. F., Mcdougal, W. S. & Wu, C.-L. 2005. Metabolic characterization of human prostate cancer with tissue magnetic resonance spectroscopy. *Cancer research,* 65**,** 3030-3034.

Costello, L. & Franklin, R. 2008. Prostatic fluid electrolyte composition for the screening of prostate cancer: a potential solution to a major problem. *Prostate cancer and prostatic diseases,* 12**,** 17-24.

Creek, D. J., Jankevics, A., Breitling, R., Watson, D. G., Barrett, M. P. & Burgess, K. E. 2011. Toward global metabolomics analysis with hydrophilic interaction liquid chromatography–mass spectrometry: improved metabolite identification by retention time prediction. *Analytical chemistry,* 83**,** 8703-8710.

Creek, D. J., Jankevics, A., Burgess, K. E., Breitling, R. & Barrett, M. P. 2012. IDEOM: an Excel interface for analysis of LC–MS-based metabolomics data. *Bioinformatics,* 28**,** 1048-1049.

Cubbon, S., Antonio, C., Wilson, J. & Thomas-Oates, J. 2010. Metabolomic applications of hilic–lc–ms. *Mass spectrometry reviews,* 29**,** 671-684.

Čuperlovic-Culf, M., Barnett, D. A., Culf, A. S. & Chute, I. 2010. Cell culture metabolomics: applications and future directions. *Drug discovery today,* 15**,** 610-621.

Cuvillier, O., Pirianov, G., Kleuser, B., Vanek, P. G., Coso, O. A., Gutkind, J. S. & Spiegel, S. 1996. Suppression of ceramide-mediated programmed cell death by sphingosine-1-phosphate.

Danielsson, A. P., Moritz, T., Mulder, H. & Spegel, P. 2010. Development and optimization of a metabolomic method for analysis of adherent cell cultures. *Analytical biochemistry,* 404**,** 30-39.

Dejaegher, B. & Vander Heyden, Y. 2010. HILIC methods in pharmaceutical analysis. *Journal of separation science,* 33**,** 698-715.

Deng, W.-G., Nishizaki, M., Fang, B., Roth, J. A. & JI, L. 2007. Induction of apoptosis by tumor suppressor FHIT via death receptor signaling pathway in human lung cancer cells. *Biochemical and biophysical research communications,* 355**,** 993-999.

Desai, K. & Wu, L. 2007. Methylglyoxal and advanced glycation endproducts: new therapeutic horizons? *Recent patents on cardiovascular drug discovery,* 2**,** 89-99.

Dhar, A., Desai, K., Liu, J. & Wu, L. 2009. Methylglyoxal, protein binding and biological samples: are we getting the true measure? *Journal of Chromatography B,* 877**,** 1093-1100.

Dietmair, S., Timmins, N. E., Gray, P. P., Nielsen, L. K. & Kromer, J. O. 2010. Towards quantitative metabolomics of mammalian cells: Development of a metabolite extraction protocol. *Analytical biochemistry,* 404**,** 155-164.

Du, H., Wang, J., Yao, X., & Hu, Z. 2009. Quantitative structure-retention relationship models for the prediction of the reversed-phase HPLC gradient retention based on the heuristic method and support vector machine. *Journal of chromatographic science*, 47(5), 396-404.

Dunn, W. B. 2008. Current trends and future requirements for the mass spectrometric investigation of microbial, mammalian and plant metabolomes. *Physical biology,* 5**,** 011001.

Dunn, W. B., Bailey, N. J. & Johnson, H. E. 2005. Measuring the metabolome: current analytical technologies. *Analyst,* 130**,** 606-625.

Dunn, W. B., Broadhurst, D., Begley, P., Zelena, E., Francis-Mcintyre, S., Anderson, N., Brown, M., Knowles, J. D., Halsall, A., Haselden, J. N., Nicholls, A. W., Wilson, I. D., Kell, D. B. & Goodacre, R. 2011. Procedures for large-scale metabolic profiling of serum and plasma using gas chromatography and liquid chromatography coupled to mass spectrometry. *Nat. Protocols,* 6**,** 1060-1083.

Evelhoch, J., Garwoood, M., Vigneron, D., Knopp, M., Sullivan, D., Menkens, A., Clarke, L. & Liu, G. 2005. Expanding the use of magnetic resonance in the assessment of tumor response to therapy: workshop report. *Cancer research,* 65**,** 7041-7044.

Exactive PDF on World Wide Web URL: http://www.thermo.com.cn/Resources/200811/2114225422.pdf

Fajardo, A. M., Mackenzie, D. A., JI, M., Deck, L. M., Jagt, D. L. V., Thompson, T. A. & Bisoffi, M. 2012. The curcumin analog ca27 down-regulates androgen receptor through an oxidative stress mediated mechanism in human prostate cancer cells. *The Prostate,* 72**,** 612-625.

Fisher, D. I. & Mclennan, A. G. 2008. Correlation of intracellular diadenosine triphosphate (Ap< sub> 3</sub> A) with apoptosis in Fhit-positive HEK293 cells. *Cancer letters,* 259**,** 186-191.

French, K. J., Upson, J. J., Keller, S. N., Zhuang, Y., Yun, J. K. & Smith, C. D. 2006. Antitumor activity of sphingosine kinase inhibitors. *Journal of Pharmacology and Experimental Therapeutics,* 318**,** 596-603.

Futerman, A. H. & Riezman, H. 2005. The ins and outs of sphingolipid synthesis. *Trends in cell biology,* 15**,** 312-318.

Garcia, M. 2005. The effect of the mobile phase additives on sensitivity in the analysis of peptides and proteins by high-performance liquid chromatography–electrospray mass spectrometry. *Journal of Chromatography B,* 825**,** 111-123.

Glunde, K., JIE, C. & Bhujwalla, Z. M. 2004. Molecular causes of the aberrant choline phospholipid metabolism in breast cancer. *Cancer research,* 64**,** 4270-4276.

Glunde, K. & Serkova, N. J. 2006. Therapeutic targets and biomarkers identified in cancer choline phospholipid metabolism.
Godlewski, J. A., Bronisz, A., Van Brocklyn, J., Wang, Y., Lawler, S. & Chiocca, E. A. 2011. MicroRNA-124 and microRNA-1, commonly lost in glioma, coordinately target sphingosine kinase-1 in glioma cells. *Cancer Research,* 71**,** 3963-3963.
Goryński, K., Bojko, B., Nowaczyk, A., Buciński, A., Pawliszyn, J., & Kaliszan, R. 2013. Quantitative structure–retention relationships models for prediction of high performance liquid chromatography retention time of small molecules: Endogenous metabolites and banned compounds. *Analytica chimica acta*, 797, 13-19.
Greco, G. & Letzel, T. 2013. Main interactions and influences of the chromatographic parameters in HILIC separations. *Journal of chromatographic science*, 51**,** 684-693.
Griffin, J. L., Nicholls, A. W., Daykin, C. A., Heald, S., Keun, H. C., Schuppe-Koistinen, I., Griffiths, J. R., Cheng, L. L., Rocca-Serra, P. & Rubtsov, D. V. 2007. Standard reporting requirements for biological samples in metabolomics experiments: mammalian/in vivo experiments. *Metabolomics,* 3**,** 179-188.
Griffin, J. L. & Shockcor, J. P. 2004. Metabolic profiles of cancer cells. *Nature reviews cancer,* 4**,** 551-561.
Gullberg, J., Jonsson, P., Nordstrom, A., Sjostrom, M. & Moritz, T. 2004. Design of experiments: an efficient strategy to identify factors influencing extraction and derivatization of Arabidopsis thaliana samples in metabolomic studies with gas chromatography/mass spectrometry. *Analytical biochemistry,* 331**,** 283-295.
Guo, Y. & Gaiki, S. 2011. Retention and selectivity of stationary phases for hydrophilic interaction chromatography. *Journal of Chromatography A,* 1218**,** 5920-5938.
Halkidou, K., Gnanapragasam, V. J., Mehta, P. B., Logan, I. R., Brady, M. E., Cook, S., Leung, H. Y., Neal, D. E. & Robson, C. N. 2003. Expression of Tip60, an androgen receptor coactivator, and its role in prostate cancer development. *Oncogene,* 22**,** 2466-2477.
Hendriks, M. M., Eeuwijk, F. A. V., Jellema, R. H., Westerhuis, J. A., Reijmers, T. H., Hoefsloot, H. C. & Smilde, A. K. 2011. Data-processing strategies for metabolomics studies. *TrAC Trends in Analytical Chemistry,* 30**,** 1685-1698.
Horoszewicz, J. S., Leong, S. S., Kawinski, E., Karr, J. P., Rosenthal, H., Chu, T. M., Mirand, E. A. & Murphy, G. P. 1983. LNCaP model of human prostatic carcinoma. *Cancer research,* 43**,** 1809-1818.
Howe, F., Barton, S., Cudlip, S., Stubbs, M., Saunders, D., Murphy, M., Wilkins, P., Opstad, K., Doyle, V. & Mclean, M. 2003. Metabolic profiles of human brain tumors using quantitative in vivo 1H magnetic resonance spectroscopy. *Magnetic Resonance in Medicine,* 49**,** 223-232.
Huwiler, A., Kotelevets, N., XIN, C., Pastukhov, O., Pfeilschifter, J. & Zangemeister-Wittke, U. 2011. Loss of sphingosine kinase-1 in carcinoma cells increases formation of reactive oxygen species and sensitivity to doxorubicin-induced DNA damage. *British journal of pharmacology,* 162**,** 532-543.
Jacobs, I. J., Skates, S. J., Macdonald, N., Menon, U., Rosenthal, A. N., Davies, A. P., Woolas, R., Jeyarajah, A. R., Sibley, K. & Lowe, D. G. 1999. Screening for ovarian cancer: a pilot randomised controlled trial. *The Lancet,* 353**,** 1207-1210.
Jandera, P. 2011. Stationary and mobile phases in hydrophilic interaction chromatography: a review. *Analytica Chimica Acta,* 692**,** 1-25.
Jankowski, J., Jankowski, V., Laufer, U., Vander Giet, M., Henning, L., Tepel, M., Zidek, W. & Schluter, H. 2003. Identification and quantification of diadenosine polyphosphate concentrations in human plasma. *Arteriosclerosis, thrombosis, and vascular biology,* 23**,** 1231-1238.
Jankowski, J., Potthoff, W., Vander Giet, M., Tepel, M., Zidek, W. & Schluter, H. 1999. High-performance liquid chromatographic assay of the diadenosine polyphosphates in human platelets. *Analytical biochemistry,* 269**,** 72-78.
Ji, L., Fang, B., Yen, N., Fong, K., Minna, J. D. & Roth, J. A. 1999. Induction of apoptosis and inhibition of tumorigenicity and tumor growth by adenovirus vector-mediated fragile histidine triad (FHIT) gene overexpression. *Cancer research,* 59**,** 3333-3339.

Kamleh, M. A., Dow, J. A. & Watson, D. G. 2009. Applications of mass spectrometry in metabolomic studies of animal model and invertebrate systems. *Briefings in functional genomics & proteomics,* 8**,** 28-48.

Katajamaa, M., Miettinen, J. & Oresic, M. 2006. MZmine: toolbox for processing and visualization of mass spectrometry based molecular profile data. *Bioinformatics,* 22**,** 634-636.

Katajamaa, M. & Oresic, M. 2007. Data processing for mass spectrometry-based metabolomics. *Journal of Chromatography A,* 1158**,** 318-328.

Kell, D. B. 2004. Metabolomics and systems biology: making sense of the soup. *Current opinion in microbiology,* 7**,** 296-307.

Kell, D. B. 2006. Systems biology, metabolic modelling and metabolomics in drug discovery and development. *Drug discovery today,* 11**,** 1085-1092.

Kohama, T., Olivera, A., Edsall, L., Nagiec, M. M., Dickson, R. & Spiegel, S. 1998. Molecular cloning and functional characterization of murine sphingosine kinase. *Journal of Biological Chemistry,* 273**,** 23722-23728.

Kojima, S., Chiyomaru, T., Kawakami, K., Yoshino, H., Enokida, H., Nohata, N., Fuse, M., Ichikawa, T., Naya, Y. & Nakagawa, M. 2011. Tumour suppressors miR-1 and miR-133a target the oncogenic function of purine nucleoside phosphorylase (PNP) in prostate cancer. *British journal of cancer,* 106**,** 405-413.

Lan, T., Bi, H., Liu, W., Xie, X., Xu, S. & Huang, H. 2011. Simultaneous determination of sphingosine and sphingosine 1-phosphate in biological samples by liquid chromatography–tandem mass spectrometry. *Journal of Chromatography B,* 879**,** 520-526.

Lavieu, G., Scarlatti, F., Sala, G., Carpentier, S., Levade, T., Ghidoni, R., ... & Codogno, P. 2006. Regulation of autophagy by sphingosine kinase 1 and its role in cell survival during nutrient starvation. *Journal of Biological Chemistry*, 281(13), 8518-8527.

Lieser, B., Liebisch, G., Drobnik, W. & Schmitz, G. 2003. Quantification of sphingosine and sphinganine from crude lipid extracts by HPLC electrospray ionization tandem mass spectrometry. *Journal of lipid research,* 44**,** 2209-2216.

Lim, K. G., Sun, C., Bittman, R., Pyne, N. J. & Pyne, S. 2011. (R)-FTY720 methyl ether is a specific sphingosine kinase 2 inhibitor: Effect on sphingosine kinase 2 expression in HEK 293 cells and actin rearrangement and survival of MCF-7 breast cancer cells. *Cellular signalling,* 23**,** 1590-1595.

Lim, K. G., Tonelli, F., Berdyshev, E., Gorshkova, I., Leclercq, T., Pitson, S. M., Bittman, R., Pyne, S. & Pyne, N. J. 2012. Inhibition kinetics and regulation of sphingosine kinase 1 expression in prostate cancer cells: functional differences between sphingosine kinase 1a and 1b. *The international journal of biochemistry & cell biology,* 44**,** 1457-1464.

Lo, T., Westwood, M. E., Mclellan, A. C., Selwood, T. & Thornalley, P. J. 1994. Binding and modification of proteins by methylglyoxal under physiological conditions. A kinetic and mechanistic study with N alpha-acetylarginine, N alpha-acetylcysteine, and N alpha-acetyllysine, and bovine serum albumin. *Journal of Biological Chemistry,* 269**,** 32299-32305.

Lodge-Ivey, S. L., May, T., Petersen, M. K. & Strickland, J. R. 2004. Determination of methylglyoxal in ruminal fluid by high-performance liquid chromatography using fluorometric detection. *Journal of agricultural and food chemistry,* 52**,** 6875-6878.

Loveridge, C., Tonelli, F., Leclercq, T., Lim, K. G., Long, J. S., Berdyshev, E., Tate, R. J., Natarajan, V., Pitson, S. M. & Pyne, N. J. 2010. The sphingosine kinase 1 inhibitor 2-(p-hydroxyanilino)-4-(p-chlorophenyl) thiazole induces proteasomal degradation of sphingosine kinase 1 in mammalian cells. *Journal of Biological Chemistry,* 285**,** 38841-38852.

Lu, S., Tsai, S. Y. & Tsai, M.-J. 1999. Molecular Mechanisms of Androgen-Independent Growth of Human Prostate Cancer LNCaP-AI Cells 1. *Endocrinology,* 140**,** 5054-5059.

Maceyka, M., Milstien, S. & Spiegel, S. 2005. Sphingosine kinases, sphingosine-1-phosphate and sphingolipidomics. *Prostaglandins & other lipid mediators,* 77**,** 15-22.

Makarov, A. 2000. Electrostatic axially harmonic orbital trapping: a high-performance technique of mass analysis. *Analytical chemistry,* 72**,** 1156-1162.
Makarov, A. & Scigelova, M. 2010. Coupling liquid chromatography to Orbitrap mass spectrometry. *Journal of Chromatography A,* 1217**,** 3938-3945.
Mazurek, S. & Eigenbrodt, E. 2002. The tumor metabolome. *Anticancer research,* 23**,** 1149-1154.
Mcdonnell, T. J., Troncoso, P., Brisbay, S. M., Logothetis, C., Chung, L. W., Hsieh, J.-T., Tu, S.-M. & Campbell, M. L. 1992. Expression of the protooncogene bcl-2 in the prostate and its association with emergence of androgen-independent prostate cancer. *Cancer research,* 52**,** 6940-6944.
Mcgarvey, T. W., Meng, R. D., Johnson, O., El-Deiry, W. & Malkowicz, S. B. Growth inhibitory effect of p21 and p53 containing adenoviruses on transitional cell carcinoma cell lines in vitro and in vivo. Urologic Oncology: Seminars and Original Investigations, 2001. *Elsevier*, 155-162.
Merrill Jr, A. H., Wang, E., Mullins, R. E., Jamison, W. C. L., Nimkar, S. & Liotta, D. C. 1988. Quantitation of free sphingosine in liver by high-performance liquid chromatography. *Analytical biochemistry,* 171**,** 373-381.
Nawroocki, J. 1997. The silanol group and its role in liquid chromatography. *Journal of Chromatography A,* 779**,** 29-71.
Nemet, I., Varga-Defterdarovic, L. & Turk, Z. 2004. Preparation and quantification of methylglyoxal in human plasma using reverse-phase high-performance liquid chromatography. *Clinical biochemistry,* 37**,** 875-881.
Nguyen, H. P. & Schug, K. A. 2008. The advantages of ESI-MS detection in conjunction with HILIC mode separations: Fundamentals and applications. *Journal of separation science,* 31**,** 1465-1480.
Novakova, L., Kaufmannova, I. & Janska, R. 2010. Evaluation of hybrid hydrophilic interaction chromatography stationary phases for ultra-HPLC in analysis of polar pteridines. *Journal of separation science,* 33**,** 765-772.
Noworolski, Susanmoyher,.2008. Dynamic contrast-enhanced MRI and MR diffusion imaging to distinguish between glandular and stromal prostatic tissues. *Magnetic resonance imaging,* 26.8, 1071-1080.
Olivera, A. & Spiegel, S. 2001. Sphingosine kinase: a mediator of vital cellular functions. *Prostaglandins & other lipid mediators,* 64**,** 123-134.
Pandher, R., Ducruix, C., Eccles, S. & Raynaud, F. 2009. Cross-platform Q-TOF validation of global exo-metabolomic analysis: application to human glioblastoma cells treated with the standard PI 3-Kinase inhibitor LY294002. *Journal of Chromatography B,* 877**,** 1352-1358.
Park, M.-T., Kang, J. A., Choi, J.-A., Kang, C.-M., Kim, T.-H., Bae, S., Kang, S., Kim, S., Choi, W.I. & Cho, C.-K. 2003. Phytosphingosine induces apoptotic cell death via caspase 8 activation and Bax translocation in human cancer cells. *Clinical cancer research,* 9**,** 878-885.
Perry, R. H., Cooks, R. G., & Noll, R. J. (2008). Orbitrap mass spectrometry: instrumentation, ion motion and applications. *Mass spectrometry reviews,* 27(6), 661-699.
Pesek, J. J. & Matyska, M. T. 2012. A new approach to bioanalysis: aqueous normal-phase chromatography with silica hydride stationary phases. *Bioanalysis,* 4**,** 845-853.
Pichiorri, F., Palumbo, T., Suh, S.-S., Okamura, H., Trapasso, F., Ishii, H., Huebner, K. & Croce, C. M. 2008. Fhit tumor suppressor: guardian of the preneoplastic genome.
Pomerantz, M. M., Werner, L., Xie, W., Regan, M. M., Lee, G.S. M., Sun, T., Evan, C., Petrozziello, G., Nakabayashi, M. & Oh, W. K. 2011. Association of prostate cancer risk loci with disease aggressiveness and prostate cancer–specific mortality. *Cancer Prevention Research,* 4**,** 719-728.
Putluri, N., Shojaie, A., Vasu, V. T., Nalluri, S., Vareed, S. K., Putluri, V., Vivekanandan-Giri, A., Byun, J., Pennathur, S. & Sana, T. R. 2011. Metabolomic profiling reveals a role for androgen in activating amino acid metabolism and methylation in prostate cancer cells. *PLoS One,* 6**,** e21417.

Pyne, N. J. & Pyne, S. 2010. Sphingosine 1-phosphate and cancer. *Nature Reviews Cancer*, 10**,** 489-503.

Pyne, S., Bittman, R. & Pyne, N. J. 2011. Sphingosine kinase inhibitors and cancer: seeking the golden sword of Hercules. *Cancer research,* 71**,** 6576-6582.

Pyne, S. & Pyne, N. 2000. Sphingosine 1-phosphate signalling in mammalian cells. *Biochem. J,* 349**,** 385-402.

Ramautar, R., Mayboroda, O. A., Somsen, G. W., & de Jong, G. J. 2011. CE-MS for metabolomics: Developments and applications in the period 2008–2010. *Electrophoresis*, 32(1), 52-65.

Rein, B. J., Gupta, S., Dada, R., Safi, J., Michener, C. & Agarwal, A. 2011. Potential markers for detection and monitoring of ovarian cancer. *Journal of oncology*, 2011.

Roberts, E. L., Newton, R. P. & Axford, A. T. 2004. Plasma purine nucleoside phosphorylase in cancer patients. *Clinica chimica acta,* 344**,** 109-114.

Roberta, M. J., Schirra, H. J., Lavin, M. F. & Gardiner, R. A. 2011. Metabolomics: a novel approach to early and noninvasive prostate cancer detection. *Korean journal of urology,* 52**,** 79-89.

Rojo, D., Barbas, C. & Ruperez, F. J. 2012. LC-MS metabolomics of polar compounds. *Bioanalysis,* 4**,** 1235-1243.

Schaefercor, W. H. & Dixon, F. 1996. Effect of high-performance liquid chromatography mobile phase components on sensitivity in negative atmospheric pressure chemical ionization liquid chromatography-mass spectrometry. *Journal of the American Society for Mass Spectrometry,* 7**,** 1059-1069.

Scheltema, R. A., Jankevics, A., Jansen, R. C., Swertz, M. A. & Breitling, R. 2011. PeakML/mzMatch: a file format, Java library, R library, and tool-chain for mass spectrometry data analysis. *Analytical chemistry,* 83**,** 2786-2793.

Scherer, M., Bottcher, A., Schmitz, G. & Liebisch, G. 2011. Sphingolipid profiling of human plasma and FPLC-separated lipoprotein fractions by hydrophilic interaction chromatography tandem mass spectrometry. *Biochimica et Biophysica Acta (BBA)-Molecular and Cell Biology of Lipids,* 1811**,** 68-75.

Scherer, M., Leuthauser-Jaschinski, K., Ecker, J., Schmitz, G. & Liebisch, G. 2010. A rapid and quantitative LC-MS/MS method to profile sphingolipids. *Journal of lipid research***,** jlr. D005322.

Schroder, F. H. 2008. Progress in understanding androgen-independent prostate cancer (AIPC): a review of potential endocrine-mediated mechanisms. *European urology,* 53**,** 1129-1137.

SciFinder Scholar search, 2014 http://pubs.acs.org/

Serkova Nj, S. J., Eckhardt S G 2007. NMR-based metabolomics: translational application and treatment of cancer. *Curr Opin Mol Ther,* 9**,** 572-585.

Shon, H. K., Cho, Y. L., Lim, C. S., Choi, J. S., Chung, S. J. & Lee, T. G. 2014. ToF-SIMS analysis of diadenosine triphosphate and didadenosine tetraphosphate using bismuth and argon cluster ion beams. *Surface and Interface Analysis*.

SIEVE User Guide pdf, 2007 http://sjsupport.thermofinnigan.com/techpubs/manuals/Sieve_User.pdf

Siow, D. L., Anderson, C. D., Berdyshev, E. V., Skobeleva, A., Pitson, S. M. & Wattenberg, B. W. 2010. Intracellular localization of sphingosine kinase 1 alters access to substrate pools but does not affect the degradative fate of sphingosine-1-phosphate. *Journal of lipid research,* 51**,** 2546-2559.

Smith, C. A., Want, E. J., O'maille, G., Abagyan, R. & Siuzdak, G. 2006. XCMS: processing mass spectrometry data for metabolite profiling using nonlinear peak alignment, matching, and identification. *Analytical chemistry,* 78**,** 779-787.

Snyder, L. R., Kirkland, J. J. & Dolan, J. W. 2011. *Introduction to modern liquid chromatography*, John Wiley & Sons.

Spiegel, S. & Milstien, S. 2002. Sphingosine 1-phosphate, a key cell signaling molecule. *Journal of Biological Chemistry,* 277**,** 25851-25854.

Spiegel, S. & Milstien, S. 2003. Sphingosine-1-phosphate: an enigmatic signalling lipid. *Nature Reviews Molecular Cell Biology,* 4**,** 397-407.

Spratlin, J. L., Serkova, N. J. & Eckhardt, S. G. 2009. Clinical applications of metabolomics in oncology: a review. *Clinical Cancer Research,* 15**,** 431-440.

Sreekumar, A., Poisson, L. M., Rajendiran, T. M., Khan, A. P., Cao, Q., Yu, J., Laxman, B., Mehra, R., Lonigro, R. J. & Li, Y. 2009. Metabolomic profiles delineate potential role for sarcosine in prostate cancer progression. *Nature,* 457**,** 910-914.

Stanwell, P., Gluch, L., Clark, D., Tomanek, B., Baker, L., Giuffre, B., Lean, C., Malycha, P. & Mountford, C. 2005. Specificity of choline metabolites for in vivo diagnosis of breast cancer using 1H MRS at 1.5 T. *European radiology,* 15**,** 1037-1043.

Sullards, M. C. & Merrill JR, A. H. 2001. Analysis of sphingosine 1-phosphate, ceramides, and other bioactive sphingolipids by high-performance liquid chromatography-tandem mass spectrometry. *Science Signaling,* 2001**,** pl1.

Swanson, M. G., Zektzer, A. S., Tabtabai, Z. L., Simko, J., Jarso, S., Keshari, K. R., Schmitt, L., Carroll, P. R., Shinohara .K. & Vigneron, D. B. 2006. Quantitative analysis of prostate metabolites using 1H HR-MAS spectroscopy. *Magnetic resonance in medicine,* 55**,** 1257-1264.

Tainsky, M. A. 2009. Genomic and proteomic biomarkers for cancer: a multitude of opportunities. *Biochimica et Biophysica Acta (BBA)-Reviews on Cancer,* 1796**,** 176-193.

Teahan, O., Bevan, C. L., Waxman, J. & Keun, H. C. 2011. Metabolic signatures of malignant progression in prostate epithelial cells. *The international journal of biochemistry & cell biology,* 43**,** 1002-1009.

Thornalley, P. 2003. Glyoxalase I-structure, function and a critical role in the enzymatic defence against glycation. *Biochemical Society Transactions,* 31**,** 1343-1348.

Tigyi, G. 2010. Aiming drug discovery at lysophosphatidic acid targets. *British journal of pharmacology,* 161**,** 241-270.

Tomlins, S. A., Rubin, M. A. & Chinnaiyan, A. M. 2006. Integrative biology of prostate cancer progression. *Annu. Rev. Pathol. Mech. Dis.,* 1**,** 243-271.

Tonelli, F., Alossaimi, M., Williamson, L., Tate, R. J., Watson, D. G., Chan, E., Bittman, R., Pyne, N. J. & Pyne, S. 2013. The sphingosine kinase inhibitor 2-(p-hyroxyanilino)-4-(p-chlorophenyl) thiazole reduces androgen receptor expression via an oxidative stress-dependent mechanism. *British journal of pharmacology,* 168**,** 1497-1505.

Tonelli, F., Lim, K. G., Loveridge, C., Long, J., Pitson, S. M., Tigyi, G., Bittman, R., Pyne, S. & Pyne, N. J. 2010. FTY720 and (< i> S</i>)-FTY720 vinylphosphonate inhibit sphingosine kinase 1 and promote its proteasomal degradation in human pulmonary artery smooth muscle, breast cancer and androgen-independent prostate cancer cells. *Cellular signalling,* 22**,** 1536-1542.

Trapasso, F., Pichiorri, F., Gaspari, M., Palumbo, T., Aqeilan, R. I., Gaudio, E., Okumura, H., Iuliano, R., Dileve, G. & Fabbri, M. 2008. Fhit interaction with ferredoxin reductase triggers generation of reactive oxygen species and apoptosis of cancer cells. *Journal of Biological Chemistry,* 283**,** 13736-13744.

Umetrics, SIMCA-P
http://www.umetrics.com/

Van Der Giet, M., Jankowski, J., Schluter, H., Zidek, W. & Tepel, M. 1998. Mediation of the vasoactive properties of diadenosine tetraphosphate via various purinoceptors. *Journal of hypertension,* 16**,** 1939-1943.

Vanderluit, A., Budde, M., Verheij, M. & Vanblitterswijk, W. 2003. Different modes of internalization of apoptotic alkyl-lysophospholipid and cell-rescuing lysophosphatidylcholine. *Biochem. J,* 374**,** 747-753.

Vaquero, E. C., Edderkaoui, M., Pandol, S. J., Gukovsky, I. & Gukovskaya, A. S. 2004. Reactive oxygen species produced by NAD (P) H oxidase inhibit apoptosis in pancreatic cancer cells. *Journal of Biological Chemistry,* 279**,** 34643-34654.

Varshavsky, A. 1983. Diadenosine 5′, 5. *P1, P4-tetraphosphate: a pleiotropically acting alarmone***,** 711-712.

Vartaniian, A., Prudovsky, I., Suzuki, H., Dal Pra, I. & Kisselev, L. 1997. Opposite effects of cell differentiation and apoptosis on Ap3A/Ap4A ratio in human cell cultures. *FEBS letters,* 415**,** 160-162.

Wallstrom, P., Bjartell, A., Gullberg, B., Olsson, H. & Wirfalt, E. 2009. A prospective Swedish study on body size, body composition, diabetes, and prostate cancer risk. *British journal of cancer,* 100**,** 1799-1805.

Wang, H. Q., Yang, B., Xu, C. L., Wang, L. H., Zhang, Y. X., Xu, B., Ji, J. T. & Sun, Y. H. 2010. Differential phosphoprotein levels and pathway analysis identify the transition mechanism of LNCaP cells into androgen-independent cells. *The Prostate,* 70**,** 508-517.

Wang, Q., Li, W., Zhang, Y., Yuan, X., Xu, K., Yu, J.& Brown, M. 2009. Androgen receptor regulates a distinct transcription program in androgen-independent prostate cancer. *Cell,* 138(2), 245-256.

Watson, D. 2010. The potential of mass spectrometry for the global profiling of parasite metabolomes. *Parasitology,* 137**,** 1409-1423.

Watson, D. G., Tonelli, F., Alossaimi, M., Williamson, L., Chan, E., Gorshkova, I., Berdtshev, E., Bittman, R., Pyne, N. J. & Pyne, S. 2013. The roles of sphingosine kinases 1 and 2 in regulating the Warburg effect in prostate cancer cells. *Cellular signalling,* 25**,** 1011-1017.

Wu, L.-Y., De Luca, T., Watanabe, T., Morre, D. M. & Morre, D. J. 2011. Metabolite modulation of HeLa cell response to ENOX2 inhibitors EGCG and phenoxodiol. *Biochimica et Biophysica Acta (BBA)-General Subjects,* 1810**,** 784-789.

Wu, Z., Li, D., Meng, J. & Wang, H. 2010. Introduction to SIMCA-P and Its Application. *Handbook of Partial Least Squares.* Springer.

Zammit, V. A., Ramsay, R. R., Bonomini, M. & Arduini, A. 2009. Carnitine, mitochondrial function and therapy. *Advanced drug delivery reviews,* 61**,** 1353-1362.

Zhang, H., Wang, Q., Zhao, Q. & Di, W. 2013. MiR-124 inhibits the migration and invasion of ovarian cancer cells by targeting SphK1. *J Ovarian Res,* 6**,** 84.

Zhang, T., Creek, D. J., Barrett, M. P., Blackburn, G. & Watson, D. G. 2012. Evaluation of coupling reversed phase, aqueous normal phase, and hydrophilic interaction liquid chromatography with Orbitrap mass spectrometry for metabolomic studies of human urine. *Analytical chemistry,* 84**,** 1994-2001.

Zhou, J. R., Yu, L., Zerbini, L. F., Libermann, T. A. & Blackburn, G. L. 2004. Progression to androgen-independent LNCaP human prostate tumors: Cellular and molecular alterations. *International journal of cancer,* 110**,** 800-806.